

Book of Abstracts

(Unprinted version)

1st European Symposium on Nanofluids

8-10 October 2017, Lisboa, Portugal

Organized by:

Centro de Química Estrutural

Faculdade de Ciências, Universidade de Lisboa, Portugal

Editors:

**S M Sohel Murshed
Carlos Nieto de Castro
José Enrique Julia**

©2017 Faculdade de Ciências da Universidade de Lisboa
1749-016 Lisbon, Portuga

**This unprinted version of BoA is customized only for
COST Action- NanoUptake(CA15119).**

PREFACE

It is our pleasure to warmly welcome all the delegates and guests to the 1st European Symposium in Nanofluids (ESNf2017) and to welcome you to Lisbon.

This symposium is organized under the auspices of the European Cooperation in Science and Technology (COST) Action “NANOUP TAKE - Overcoming Barriers to Nanofluids Market Uptake (CA15119)”. In addition to build research and development cooperation among the participants of this COST Action, the symposium provides a platform for strong collaboration and exchange of research and ideas as well as to bring together other researchers, scientists and engineers from Europe and around the world, who are working on nanofluids and related areas. Numbers of related companies were invited and have participated in the symposium. This symposium featured plenary and invited lectures as well as regular oral and flash presentations. This “Abstracts Collection” contains the extended abstracts of the contributions accepted.

All submitted papers were carefully reviewed and then classified under different topics mostly based on NanoUptake work groups’ topics such as nanofluids in heating, cooling, storage, boiling and solar in addition to optical and other properties, and numerical simulations. Apart from main single sessions for plenary and some invited lectures, there were total 13 sessions and most of the sessions started with an invited lecture. Besides on plenary lectures, there were 10 invited lectures, 54 regular presentations and 2 flash presentations.

We are very pleased with the responds and outcomes so far achieved and as planned a set of high quality papers from the symposium will be published in special issues of two international journals- Journal of Nanofluids and Journal of Thermal Analysis and Calorimetry.

Finally, we would like to thank to the authors, reviewers, and FCIENCIAS.ID teams for their support and contribution to make this event possible and successful.

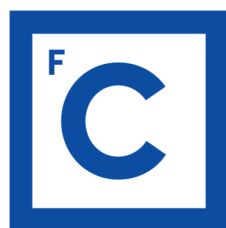
We hope you will enjoy your stay in Lisbon.

The Organizing Committee

ESNf2017 Lisbon

FCUL, 8-10 October 2017

ORGANIZATIONS



Ciências
ULisboa



ORGANIZING COMMITTEE

Carlos Nieto de Castro (Chair)

CQE, Faculdade de Ciências da Universidade de Lisboa, Portugal

José Enrique Julia (Chair)

Dep. Ingeniería Mecánica y Construcción, Universitat Jaume I, Castellón de la Plana, Spain

S M Sohel Murshed (Co-chair)

CQE, Faculdade de Ciências da Universidade de Lisboa, Portugal

Members:

Isabel Gimenez Garcia

Dept. d'Enginyeria Mecànica i Construcció, Universitat Jaume I de Castelló, Spain

Fernando J.V. Santos

CQE, Faculdade de Ciências da Universidade de Lisboa, Portugal

Manuel L.M. Lopes

CQE, Faculdade de Ciências da Universidade de Lisboa, Portugal

Maria J. Lourenço

CQE, Faculdade de Ciências da Universidade de Lisboa, Portugal

António L Moreira

IST, Universidade de Lisboa, Portugal

Xavier Paredes

CQE, Faculdade de Ciências da Universidade de Lisboa, Portugal

Salomé I.C. Vieira

CQE, Faculdade de Ciências da Universidade de Lisboa, Portugal

ABOUT THE SYMPOSIUM AND NANOUPTAKE

ESNf2017

The European Symposium on Nanofluids (ESNf) will be a series of international conferences to be organized in Europe and this very first one (1st ESNf) is taking place in Lisbon, Portugal during 8-10 October 2017. This symposium series will be organized under the auspices of the European Cooperation in Science and Technology (COST) Action-NANOUPTAKE. In addition to build research and development cooperation among the participants of this COST Action the symposium will provide a platform for strong collaboration and exchange of research and ideas as well as to bring together other researchers, scientists and engineers from Europe and around the world, who are working on nanofluids and related areas. Related companies were invited to participate in the symposium for potential discussions and collaborations. This symposium features plenary and invited lectures as well as oral and flash presentations.

ESNf2017 Topics:

The symposium will concentrate mainly on fundamentals and applications of nanofluids and liquid-based nanocomposites which include following topics:

- Nanofluids- heating and cooling
- Nanofluids- thermal storage
- Nanofluids- boiling and solar energy
- Preparation and Properties of nanofluids
- Applications of nanofluids
- Molten salts based nanosystems
- NanoPCM
- Ionanofluids
- Other areas of nanofluids

NANOUPTAKE

Nanouptake – Overcoming Barriers to Nanofluids Market Uptake (COST Action CA15119) aims to create a Europe-wide network of leading Research, Development and Innovation institutions, and of key industries, to develop and foster the use of nanofluids as advanced heat transfer/thermal storage materials to increase the efficiency of heat exchange and storage systems.

Having enhanced thermophysical and heat transfer properties nanofluids can improve the efficiency of heat exchange and thermal energy storage systems and they are specifically mentioned in the Strategic Energy Technology Plan and the Materials Roadmap to enable Low-Carbon Technologies as potential elements to improve the efficiency of heat exchange and thermal energy storage systems.

By developing of nanofluids up to higher Technological Readiness Levels (TRL) and overcoming commercial application barriers, Nanouptake will contribute to achieve the European Horizon 2020 Energy and Climate objectives (Societal Challenges 3: Secure, efficient and clean energy; and 6: Climate action, environment, resource efficiency and raw materials). In addition, nanofluids fall within one of the Key Enabling Technologies (KET) supported by the European Commission. Details of this COST action can be found on its website (www.nanouptake.eu).

ESNF2017 PROGRAM AT A GLANCE

Time/Date	8 th Oct 2017	9 th Oct 2017	10 th Oct 2017
9:00		Session 2 (Topic: General) [Hall: Sala de Conferência]	Session 5A (Storage) [Sala de Conferência]
		Session 5B (Boiling and Solar) [Sala de Doutoramentos]	
		Tea-Coffee	Tea-Coffee
13:00		Session 3A (Heating) [Sala de Conferência]	Session 3B (Cooling) [Sala de Doutoramentos]
13:00		Session 6A (Others) [Sala de Conferência]	Session 6B (Boiling and Solar) [Sala de Doutoramentos]
13:30		Lunch	Lunch
14:30		Session 4A (Others) [Sala de Conferência]	Session 4B (Cooling) [Sala de Doutoramentos]
14:30		Session 7A (Others) [Sala de Conferência]	Session 7B (Numerical) [Sala de Doutoramentos]
16:30		Session 8-Closing of ESNf2017 [Sala de Conferência]	
16:30	[Hall: Salão Nobre]	Tea-Coffee	Tea-Coffee
18:30	-Check-in -Inauguration -Session 1 (General) -Welcome drinks	NanoUptake meeting (Heating & Cooling)	NanoUptake meeting (Storage & Boiling and Solar)
20:00			Gala Dinner

CONTENTS

Sessions 1-2: Plenary and Invited Lectures

The interactions between nanoparticles: direct measurement and simplified theories	2
<i>Paul F. Luckham</i>	
Current trends in nanofluids research	4
<i>José Enrique Juliá</i>	
Understanding the influence of nanotubes and graphene interactions with ionic liquids on heat transfer	8
<i>Carlos A. Nieto de Castro</i>	
Numerical investigation on heat transfer enhancement of Fe₃O₄/water nanofluids in presence of a magnetic field	9
<i>B. Buonomo, D. Ercole and <u>O. Manca</u>*</i>	
Superior cooling with nanofluids: Hype and reality.....	15
<i>S M Sohel Murshed</i>	
Heat transfer in nanofluids: An appraisal.....	17
<i>G.J. Tertsinidou¹, M.J. Assael¹ and <u>W.A. Wakeham</u>^{2*}</i>	
MAGENTA: Magnetic nanoparticle based liquid energy materials for thermoelectric applications.....	19
<i>Sawako Nakamae</i>	
Thermal energy storage using composite phase change materials– the role of nanofluids in performance enhancement.....	21
<i>Yulong Ding</i>	
State of the art of heat transfer of heat pipes and thermosyphons employing nanofluids as working fluid	22
<i><u>M.H. Buschmann</u>^{1*}, A. Huminic², S. Mancin³ and R.R. Riehl⁴</i>	
How to validate nanofluids?	23
<i>M. J. Lourenço</i>	
Issues in convection modeling of pure and enhanced PCM.....	26
<i>Gennady Ziskind</i>	

Session 3A: Heating

Transport properties of water-based nanofluids with dispersion of graphene-oxide nanoparticles.....	28
<i>L. Fedele* and S. Bobbo</i>	
Rheological properties and surface tension of stable graphene oxide and reduced graphene oxide aqueous nanofluids	34
<i>D. Cabaleiro¹, P. Estellé^{2,*}, H. Navas³, A. Desforges³ and B. Vigolo³</i>	
Nanofluids analysis model - basis for comparison and prediction	40
<i>E.W. Marcelino, D. de O. Silva and R.R. Riehl*</i>	
A new analytical model for the effective thermal conductivity of nanofluids	46
<i>T.M. Koller*, K.N. Shukla, M.H. Rausch and A.P. Fröba</i>	
Metal oxide nanofluids for enhancing thermal properties through an experimental and theoretical perspective	51
<i>A. Sánchez-Coronilla^{1*}, J. Navas^{2*}, E.I. Martín³, T. Aguilar², R. Gómez-Villarejo², J.J. Gallardo², P. Martínez-Merino², R. Alcántara² and C. Fernández-Lorenzo²</i>	
Measurement of electrokinetic mobility of colloidal particles close to solid-liquid interface using evanescent waves.....	54
<i>K. Shirai^{1*}, S. Kaji², T. Kawanami³ and S. Hirasawa²</i>	

Session 3B: Cooling

Assessing the flow characteristics of nanofluids during turbulent natural convection	60
<i>K. Kouloulis^{1*}, A. Sergis and Y. Hardalupas</i>	
An experimental setup for flow heat transfer investigation of nanofluids	66
<i>A. Nikulin* and A.L.N. Moreira</i>	
Natural convection from a pair of differentially-heated horizontal cylinders aligned side by side in a nanofluid-filled inclined square enclosure.....	70
<i>A. Quintino, E. Ricci*, E. Habib, and M. Corcione</i>	
Nanoengineered wettability for heat transfer enhancement in spray cooling	75
<i>A.S Moita*, M. Maly and A.L.N. Moreira</i>	
Possible application of nanofluids to improve performance of wet cooling towers	79
<i>V. Mijakovski*, T. Geramitcioski and V. Mitrevski</i>	

Session 4A: Heating and Others

Thermophysical Characteristics of Nanofluids and Transport Processes Mechanisms.....	85
<i>V. Rudyak</i>	
Experimental study on rheological properties, thermal conductivity and dielectric properties of TiN-EG nanofluids	89
<i>G. Żyła^{1*}, J. Fal¹ and P. Estellé²</i>	
Temperature-compensated 3ω hot wire for quasi-isothermal thermophysical properties measurement of inhomogeneous fluids.....	92
<i>M. Chirtoc[*], J.-F. Henry and N. Horny</i>	
Experimental characterization and theoretical modelling of Cu, Ni and Ag-nanofluids: a comparative study of their thermal properties	95
<i>R. Gómez-Villarejo^{1,*}, E. I. Martín², J. Navas¹, A. Sánchez-Coronilla³, M. Teruel¹, T. Aguilar¹, J. J. Gallardo¹, R. Alcántara¹, D. de los Santos¹ and C. Fernández-Lorenzo¹</i>	
Preparation of performant copper-based nanolubricant for automotive application	100
<i>A. Gondolini^{1*}, E. Mercadelli¹, V. Zin², S. Barison² and A. Sanson¹</i>	
Ferronematics- a special class of nanofluids.....	103
<i>P. Kopcansky^{1*}, N. Tomasovicova¹, V. Gdovinova¹, J. Majorosova¹, M. Timko¹, N. Eber², T. Toth-Katona² and J. Jadzyn³</i>	

Session 4B: Cooling and Others

Thermophysical profile and heat transfer performance of dispersions of functionalized graphene nanoplatelets in an industrial coolant	109
<i>J. P. Vallejo^{1,2}, E. Álvarez-Regueiro^{1,2}, D. Cabaleiro¹, J. Fernández-Seara², J. Fernández³ and L. Lugo^{1*}</i>	
Performance investigation of a miniature plate heat exchanger with graphene nanoplatelet based EG/water nanofluids	114
<i>Z. Wang, Z. Wu and B. Sundén*</i>	
Laminar forced convection in flat tubes with Al₂O₃-water mixture for automotive applications.....	119
<i>B. Buonomo¹, D. Ercole¹, O. Manca^{1*}, A. Minea² and S. Nardini¹</i>	
Thermal performance of suspensions of graphene nanoplatelets in plate heat exchanger	125
<i>F.E.B. Bioucas, M.L. Matos Lopes*, S.M.S. Murshed and C.A. Nieto de Castro</i>	
Aspect ratio effect on the effectiveness of a single phase natural circulation mini loop	130
<i>S. Doğanay¹, M. Alaboud², Z.H. Karadeniz^{3*} and A. Turgut⁴</i>	
Thermal enhancement using nanofluids on high heat dissipation electronic components.....	135
<i>R.R. Riehl</i>	

Session 5A: Storage

- On the use of nano-encapsulated phase change materials for thermal-oil and molten salt-based nanofluids .142**
N. Navarrete¹, A. Gimeno-Furio¹, R. Mondragon¹, L. Hernandez¹, L. Cabedo², E. Cordoncillo³ and J.E. Julia^{1}*
- The influence of Al_2O_3 nanoparticles on the heat capacity of isopropanol146**
I. Motovoy^{}, V. Zhelezny and T. Lozovsky*
- An influence of Al_2O_3 nanoparticles on the heat capacity of isopropyl alcohol in metastable and solid phase .151**
I. Motovoy^{}, V. Zhelezny and T. Lozovsky*
- Solar salt with SiO_2 nanoparticles for thermal energy storage high temperature applications: scale up of the synthesis procedure156**
A. Solé¹, M. Liu², F. Bruno², J.E. Julià¹ and L.F. Cabeza^{3,}*

Session 5B: Boiling

- An experimental study of heat transfer coefficient and internal characteristics of nucleate pool boiling of nanaofluid R141b/ TiO_2162**
O. Khliyeva^{1}, A. Nikulin², T. Gordeychuk¹, N. Lukianov¹ and Y. Semenyuk¹*
- Experimental study of pool boiling heat transfer on nanoparticle-deposited surfaces.....166**
Z. Cao, Z. Wu, S. Abood and B. Sunden^{}*
- Nanofluids as working fluid in thermosyphon.....172**
A. Wlzlak¹, B. Zajaczkowski¹, S. Barison², F. Agresti², L.M. Wilde³, M.H. Buschmann^{3}*
- Nanoparticulate deposition during Cu-water nanofluid pool boiling on roughened copper surfaces178**
S. Mancin^{1}, L. Doretti², T. P. Allred³ and J. A. Weibel³*

Session 6A: Optical Properties and Others

Paraffin-based nano-encapsulated PCM prepared from solvent-assisted emulsions in water	183
<i>F. Agresti¹, S. Barison^{1*}, L. Fedele², S. Rossi², S. Mancin³</i>	
Nonlinear optical properties of carbon nanohorn-based aqueous nanofluids.....	186
<i>E. Sani^{1*}, N. Papi¹, L. Mercatelli¹, S. Barison², F. Agresti², C. Pagura³, S. Bobbo⁴ and S. Rossi⁴</i>	
Effect of nanoparticles on fluid transport in ultraconfined capillary	191
<i>X. Wang, S. Xiao, Z. Zhang and J. He*</i>	
Dielectric properties of graphite/diamonds mixture nanoparticles suspended in ethylene glycol	194
<i>J. Fal* and G. Żyła</i>	
Linear and nonlinear optical properties of graphite/diamond nanosuspensions	198
<i>E. Sani^{1*}, N. Papi¹, L. Mercatelli¹ and G. Żyła²</i>	
Optical properties of functionalized graphene nanoplatelet-nanofluids	202
<i>E. Sani^{1*}, N. Papi¹, J. P. Vallejo², D. Cabaleiro² and L. Lugo²</i>	

Session 6B: Solar

Molten salt-based nanofluids with ceramic nanoparticles for concentrated solar power application	208
<i>A. Palacios¹, Z. Jiang¹, E. Mura², M.E Navarro¹, G.Qiao² and Y. Ding¹</i>	
Mouromtseff number analysis on nanofluid based systems: Flat plate solar collectors	212
<i>A. M. Genc¹, M. A. Ezan² and A. Turgut^{2*}</i>	
Nanofluids as direct solar energy absorbers.....	217
<i>A. Gimeno Furió^{1*}, J.E. Juliá¹, S. Barison², F. Agresti², M.H. Buschmann³ and C. Friebe³</i>	
Nanofluids with enhanced thermal properties based on metallic nanoparticles for Concentrating Solar Power: a theoretical and experimental perspective	222
<i>J. Navas^{1*}, A. Sánchez-Coronilla^{2*}, R. Gómez-Villarejo¹, E. I. Martín³, P. Martínez-Merino¹, T. Aguilar¹, J. J. Gallardo¹, R. Alcántara¹ and C. Fernández-Lorenzo¹</i>	
Influence of high temperature exposure in thermal and optical properties of thermal oil-based solar nanofluid	225
<i>A. Gimeno-Furio, N. Navarrete, R. Martínez-Cuenca, J.E. Julia* and L. Hernandez</i>	
Synthesis of Tin/Ethylene Glycol solar nanofluid by a femtosecond laser-assisted technique.....	227
<i>R. Torres Mendieta¹, R. Mondragón², V. Puerto Belda^{1*}, O. Mendoza Yero¹, J. Lancis¹, G. Mínguez Vega¹ and J. E. Juliá²</i>	

Session 7A: Stability, Thermal Conductivity and Others

Aqueous based Boron Nitride nanofluids for thermal management applications: formulation, stabilization and characterization	232
<i>G. Zhang, M.E. Navarro and Y. Ding*</i>	
Effects of agitation and ultrasonication on dispersion and thermal conductivity of aqueous TiO₂ nanofluids..	237
<i>K. Cacia^{1,2}, F.E.B. Bioucas³, S.M.S. Murshed^{3*}, M.J.V. Lourenço³, F.J.V. Santos³ and C.A. Nieto de Castro³</i>	
Re-dispersion ability of MWCNT within oils	244
<i>A. Alasli¹ and A. Turgut^{2*}</i>	
The preparation of Cu@Al₂O₃ nanofiber by organometallic technique and its application in the nanofluid systems	249
<i>A. Bulut, M Yurderi, I.E. Ertas and M. Zahmakiran*</i>	
Effect of manufacturing processes on thermophysical properties and characteristics of water/ethylene glycol-based Al₂O₃ nanofluids.....	254
<i>T.J. Choi, M.S. Park and S.P. Jang*</i>	
Comparison of thermal conductivity measurement techniques of metallic nanocolloids.....	257
<i>S. Puupponen^{1*}, S. Feja², M.H. Buschmann² and A. Seppälä¹</i>	

Session 7B: Numerical and Others

NANOROUND – a proposal for a numerical round robin test for simulation of nanofluids.....	264
<i>A. A. Minea¹, A. Huminic², G. Huminic², J. Tibaut³ and J. Ravnik^{3,*}</i>	
Development of the boundary element method for simulation of nanofluids	270
<i>J. Ravnik* and J. Taibaut</i>	
Nanofluid thermal boundary layer	273
<i>J.T.C. Liu*, D. Hopper, D. Jaganathan, J.L. Orr, J. Shi, F. Simeski and M. Yin</i>	
Tailoring the properties of nanoparticles by ALD nanocoatings	278
<i>D. Valdesueiro*, A. Goulas and B. van Limpt</i>	
Environmental assessment of advanced heat management solutions	282
<i>J. Krupanek^{1*}, B. Michaliszyn¹, Ł. Lelek² and J. Kulczycka²</i>	
Graphene nanofluids – new and interesting results in a solar thermal collector	286
<i>F.E.B. Bioucas, S. Vieira, M.J.V. Lourenço*, F.J.V. Santos and C.A. Nieto de Castro</i>	
Magnetic nanofluids for electric power engineering applications	290
<i>M. Rajnak^{1,3}, M. Timko^{1*}, P. Kopcansky¹, T. Tobias¹, K. Paulovicova¹, J. Kuchta², M. Franko², J. Kurimsky², B. Dolnik², and R. Cimbalá²</i>	

Abstracts

SESSIONS 1-2: PLENARY AND INVITED LECTURES

THE INTERACTIONS BETWEEN NANOPARTICLES: DIRECT MEASUREMENT AND SIMPLIFIED THEORIES

Paul F. Luckham

Department of Chemical Engineering

Imperial College London

SW7 2BY, UK

Email: p.luckham01@imperial.ac.uk

Abstract:

The interactions between surfaces have received considerable interest since the 1950's when people first attempted to measure them directly [1]. The early attempts, although ingenious, were not successful due to the fact that the surfaces were rough, at least at the molecular level and it was not until the 1970's that Tabor and co-workers used mica, which is molecularly smooth [2]. The early experiments were in air, but Israelachvili extended the technique [3], which has now become known as the surface forces apparatus, to liquids, and in many respects experiments in liquids turn out to be simpler. Experiments have been performed in water, non-polar media and when the surfaces bear an adsorbed layer of surfactant or polymer [4] and recently ionic liquids [5]. Typical results and how they compare to simple theoretical models will be presented.

The drawback of the surface forces apparatus (and the advantage) is that it uses mica as a substrate. However, the development of atomic force microscopy, AFM overcomes this issue. In the imaging mode of an AFM a very sharp tip is attached onto a cantilever spring and the deflection of the spring as it is scanned over a surface is recorded, giving the topography of the surface, and by raster scanning over the surface and with appropriate software an image of the surface can be obtained. In another mode however the interaction between the tip and the surface can be obtained. Since the tip is small in comparison to the mica surface forces apparatus, roughness is less of an issue. It has now become almost routine to attach a particle onto an AFM cantilever and measure the interaction between that particle and either another particle or a flat surface of the same material as the particle [6]. In this presentation a range of different systems will be presented, together with how these interactions affect the bulk properties of fluids (rheology) in which these suspensions are dispersed.

References

1. P.F. Luckham, B.A.D. Costello, Recent developments in the measurement of interparticle forces, *Adv. Colloid. Interfac* 44(1993)183-240.
2. J.N. Israelachvili, D. Tabor, Measurement of vanderwaals dispersion forces in range 1.5 to 130 Nm. *Proc R Soc Lon Ser-A* 1972, 331(1584)19-38.

3. J.N. Israelachvili, G.E. Adams, Measurement of forces between 2 mica surfaces in aqueous-electrolyte solutions in range 0-100 Nm, *J. Chem. Soc. Farad. T* 1 74(1978)975-1001.
4. P.F. Luckham, Measurement of the interaction between adsorbed polymer layers - the steric effect, *Adv. Colloid. Interfac.* 34 (1991)191-215.
5. L.R. Griffin, K.L. Browning, S.M. Clarke, A.M. Smith, S. Perkin, M.W.A. Skoda, S.E. Norman, Direct measurements of ionic liquid layering at a single mica-liquid interface and in nano-films between two mica-liquid interfaces, *Phys. Chem. Chem. Phys.* 19 (2017) 297-304.
6. H.J. Butt, B. Cappella, M. Kappl, Force measurements with the atomic force microscope: Technique, interpretation and applications. *Surf. Sci. Rep.* 59 (2005)1-152.

About the Speaker:



Paul Luckham studied for his PhD in Bristol University under the guidance of Brian Vincent and Dr Tharwat Tadros and the PhD investigated the possibility of aggregating colloidal particles by using differently charged particles and investigated how rheological measurements could be used to monitor the effect. He then did a post doc in the Cavendish laboratories of Cambridge University under the direction of Jacob Klein and David Tabor where he learnt the technique which later became known as the mica surface forces apparatus. In Cambridge a fundamental investigation into how adsorbed polymers affect the interaction between mica surfaces was undertaken. In 1983 he

moved to the Chemical Engineering department of Imperial College, where he has been ever since. At Imperial College he has merged these two streams of research, rheology and surface forces and applied it to understand how controlling the interactions between particles, controls their rheology. Initially the surface forces apparatus was used, but for the last 25 years atomic force microscopy (or modifications of AFM) has been used to measure the interactions between colloidal sized particles. He has applied these skills in various areas of colloid and nano- science, including paints, inks, personal products, oil exploration, pesticides, photography, detergents *etc.* As well as using these methods to understand the interactions between colloidal systems, he has also used the methodology to understand the interactions in biological systems, being one of the first to measure specific interactions which are present in cell recognition processes for example.

It was by understanding the interactions between colloidal systems that he was able to develop with a fashion designer, Manel Torres, various formulations that can be used to form fabrics by direct spraying which has led to the formation of Fabrican, a spin-off company that is developing various applications of this technology.

CURRENT TRENDS IN NANOFUIDS RESEARCH

José Enrique Juliá

Departamento de Ingeniería Mecánica y Construcción,

Universitat Jaume I

12071-Castellón de la Plana, Spain

Email: enrique.julia@emc.uji.es

Introduction: Nanofluids are defined as engineered colloidal suspension of nanometer-sized particles with applications in thermal sciences. Since the “nanofluid” term was coined by S.U.S Choi in 1995, there has been an exponential increase in the number of indexed journal publications (see Figure 1) whose limit is very difficult to predict due to its strong multidisciplinary nature and that it will depend on, among other factors, the number of industrial applications that scientists are able to find.

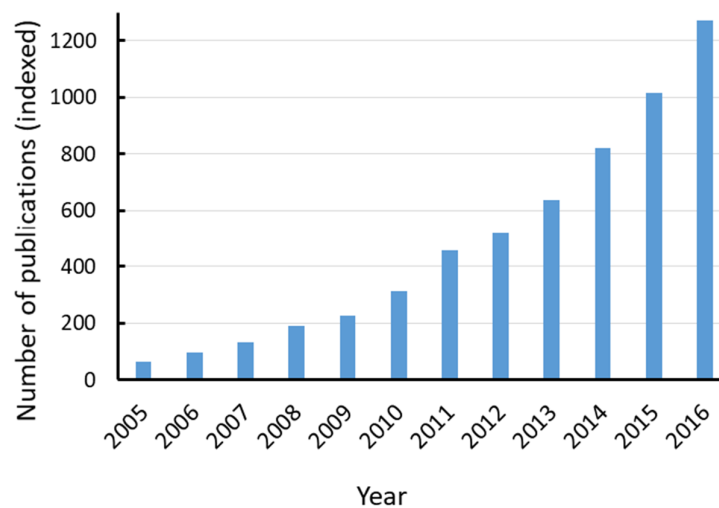


Figure 1. Number of publications in JCR indexed journals with the term “nanofluids” as topic (source: ISI web of Science).

Important changes have been produced in the nanofluid research community in the last decade. The most important one is related with the location of the research groups with active research activities in this field. Nanofluid research started in the USA and EU; however, emerging Asian nations, such as Iran, India and China, are making huge efforts in this research field and have surpassed EU countries in recent years (Figure 2).

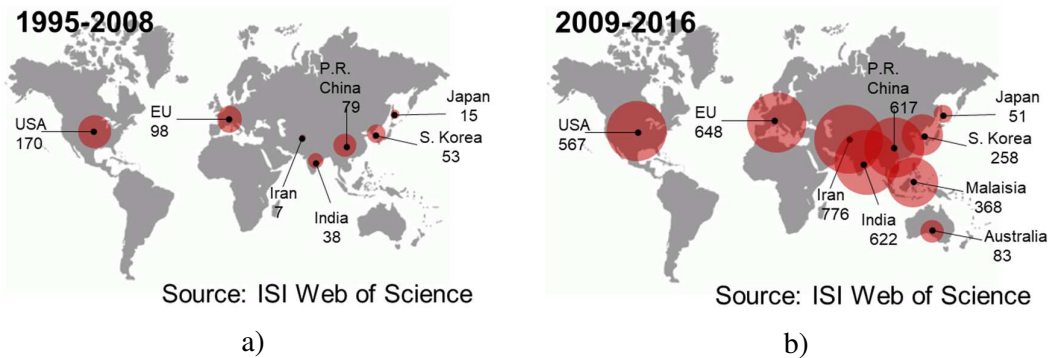


Figure 2. Number of publications in JCR indexed journals with the term “nanofluids” by country (source: ISI web of Science).

If all the nanofluids related papers published in JCR indexed journals are considered (Figure 3) it is possible to observe that most of publications are linked with the thermal conductivity measurement and/or modelling of water-based nanofluids. This fact can be explained by the importance of water as heat transfer fluid, the relative easy dispersion of nanoparticles by the control of the pH value and the working temperatures.

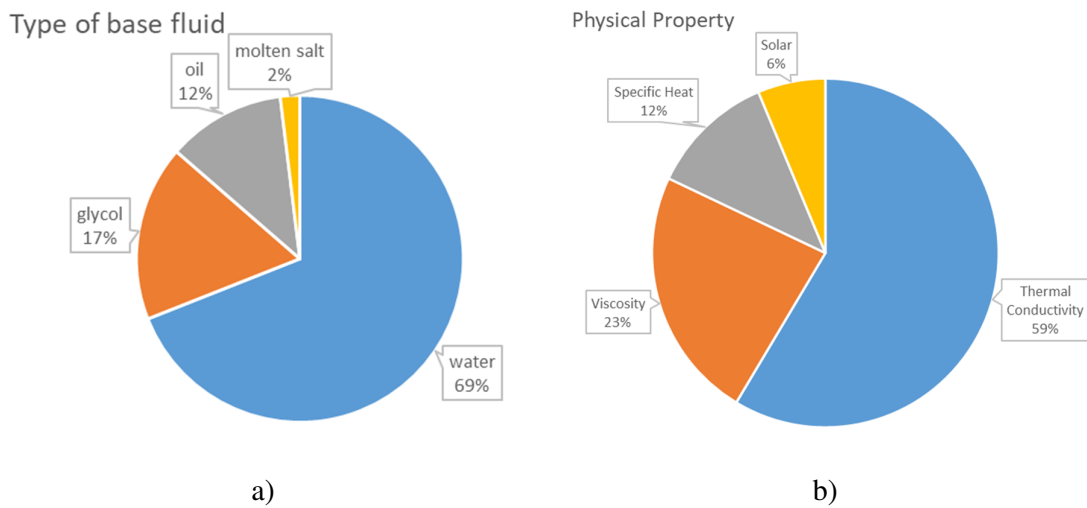


Figure 3. Percentage of publications in JCR indexed journals with the term “nanofluids” by: a) Base Fluid; b) Physical Property.

However, if we focus on the publications of the last 3 years and compare them with the previous ones, it is possible to observe that, although water remains the most popular base fluid, medium and high temperature heat transfer fluids are gaining attention. The change in the current trends is more evident in the case of the physical properties. Thermal conductivity and

boiling phenomena are losing some of the attention. The case of thermal conductivity can be explained by the huge number of previous publications about this topic and the boiling by the difficulties found in controlling the nanoparticle deposition process in the hot surface. It is worth mentioning the case of “solar” property, referred in this work to the use of solar nanofluids as solar direct volumetric absorbers. In this case, the important increment observed in the last graph of Figure 4 is partially explained by the late appearance of this type of nanofluids (first paper in 2009) and its direct use in the emerging solar thermal renewable energy sources.

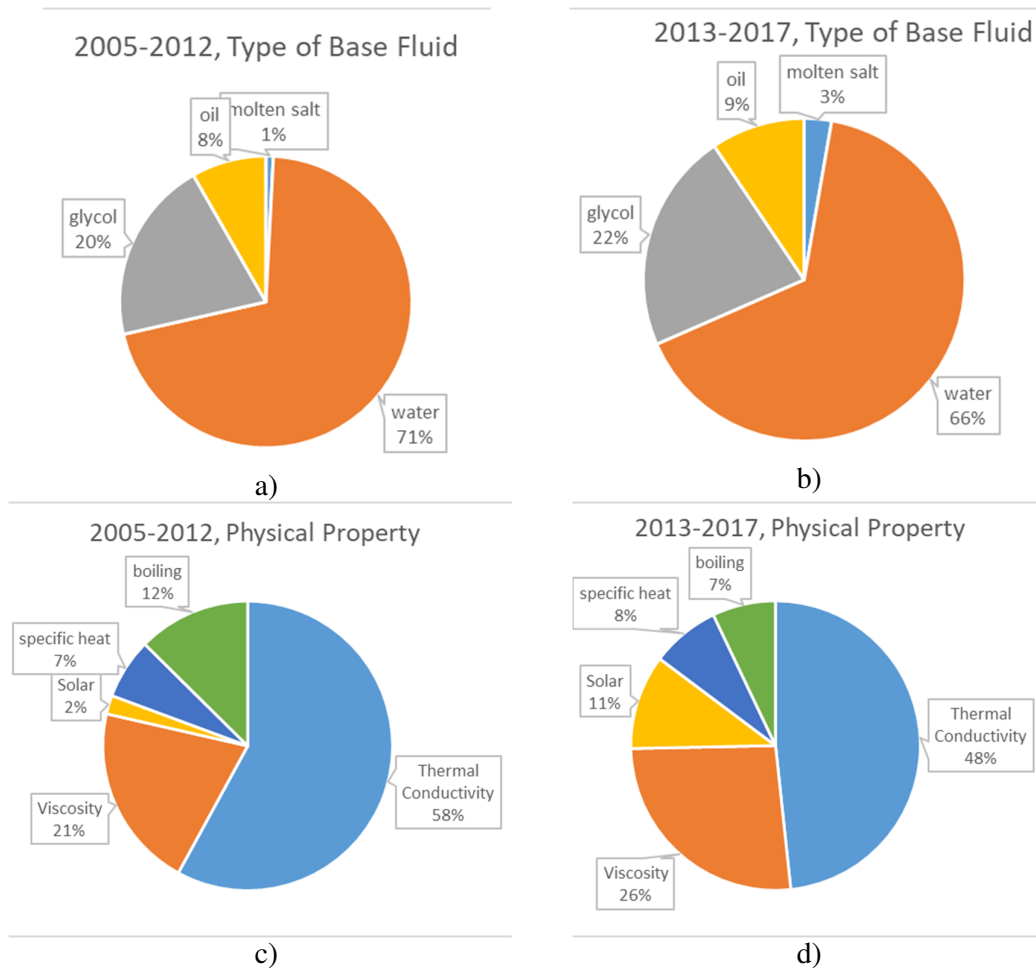


Figure 4. Comparison of percentage of publications in JCR indexed journals with the term “nanofluids” by: a and b) Base Fluid; c and d) Physical Property.

Summary:

- Water-based nanofluids and thermal conductivity measurement/modelling are the most important research topics in the nanofluids research field.
- However, new trends can be observed in the last three years with more research papers focused on medium and high temperature heat transfer and storage fluids and physical properties based on solar applications.
- It is expected that this trends will be accentuated in the future. However, it will be difficult to beat the water as heat transfer fluid due to its important practical applications and facility in obtaining the nanofluids.

References:

1. S. Choi, Enhancing thermal conductivity of fluids with nanoparticles, *ASME Fluids Engineering Division* 231 (1995) 99.
2. H. Masuda, A. Ebata, K. Teramae and N. Hishinuma, Alteration of thermal conductivity and viscosity of liquid by dispersing ultrafine particles (dispersion of gamma-al₂o₃, sio₂ and tio₂ ultrafine particles) *Netsu Bussei* 4 (1993) 227–233.

UNDERSTANDING THE INFLUENCE OF NANOTUBES AND GRAPHENE INTERACTIONS WITH IONIC LIQUIDS ON HEAT TRANSFER

Carlos A. Nieto de Castro

Centro de Química Estrutural

Faculdade de Ciências, Universidade de Lisboa

Campo Grande, 1749-016 Lisboa, Portugal

Email: cacastro@ciencias.ulisboa.pt

Abstract:

The development of nanofluids in the last 20 years led to many attempts to apply efficiently the discovered enhancements in thermal conductivity caused by the presence of nanoparticles in the common heat transfer liquids, from low to moderate temperatures. However, the need to obtain data for several systems led the authors to many artificial conclusions that differ from laboratory to laboratory and, sometimes, in the same laboratory.

The main problems are the preparation of the nanofluids, the characterization of the nanomaterials particles employed, and the instrumentation used to measure thermal conductivity. In addition, the understanding of the structure of nanofluid, namely the interaction of the nanoparticle with the bulk base fluid is fundamental, the interface size (extension in space), as the most significant theories of heat transfer in nanofluids are strongly dependent on it.

Ionic Liquids have proved to be a very promising type of base fluids, due to their specific interactions with the nanoparticles/nanotubes. Our efforts in studying these nanofluids led to several conclusions that make IoNanofluids a very sustainable type of heat transfer agents, namely for solar applications.

It is the purpose of this paper to analyse the current status of our knowledge of IoNanofluids preparation, behaviour and properties, with specially emphasis in the heteromolecular interactions and its influence on the thermal conductivity of nanofluids. A detailed analysis of the most adequate methods for the measurement of this property in nanofluids will also be presented.

NUMERICAL INVESTIGATION ON HEAT TRANSFER ENHANCEMENT OF Fe_3O_4 /WATER NANOFLUIDS IN PRESENCE OF A MAGNETIC FIELD

B. Buonomo, D. Ercole and Q. Manca*

Dipartimento di Ingegneria Industriale e dell'Informazione, Università degli Studi della Campania, Via Roma 29, Aversa (CE), 81031, Italy

*Email: oronzio.manca@unicampania.it

Introduction: The suspension of nanoparticles in conventional fluids are usually called nanofluids [1]. They were designed to improve the thermal conductivity of the basic coolant fluids. For example the water is the most utilized coolant fluid for convectional applications but it has a thermal conductivity of more of one order of magnitude lesser than the metals. Therefore using the suspension of solids is a good option to increase the thermal conductivity. This idea was just conceived by Maxwell a century ago when he presented an elementary model to calculate the effective thermal conductivity of a suspension. Nevertheless these suspensions are made by micro or macro particles and they presented many drawbacks as sedimentation, erosion of pipelines, clogging of the flow channels, increase of pressure drop. Therefore, the rise of nanofluids is recent [2] because now there is the technology to produce nanoparticles with few nanometres of diameter. The nanoparticles are suitable for suspension in fluid because they do not have the same disadvantages of macro suspensions. In fact they present: large surface area, indispensable to increase the heat transfer; low weight that leads to more stability given that the sedimentation is less and the mobility of the nanoparticles is increased for Brownian effects. Among the various classes of nanofluid, the ferrofluid could be an innovative heat transfer media for industrial applications. They are stable colloidal suspension of sub-domain magnetic particles in a carrier liquid, as water or oils [3]. They could be controlled by an external magnetic field, in fact the magnetization of nanofluids is dependent on the magnetic field and any variation induce a change of body force distribution in the ferrofluid. The ferrofluids have been the subject of several studies in literature. Ganguly et al. [4] numerically investigated two-dimensional laminar flow of ferrofluid in a channel under a constant magnetic field. The results show that the magnetic field induces the production of local vortex improving the heat transfer and the Nusselt number is increased as the magnetic field strength increases. Ghasemian et al. [5] numerically investigated the laminar forced convection of a ferrofluid in a minichannel in presence of constant and alternating magnetic field using a line dipole for different Reynolds numbers. By the results the heat transfer enhancement with a constant magnetic field is up to 16.5% while for alternating magnetic field the value could be increased up to 27.7%.

This work numerically investigated the heat transfer characteristics of water-based ferrofluid with magnetite nanoparticles (Fe_3O_4) under different values of magnetic field strength and for

different Reynolds number. A solenoid is utilized to create a magnetic field over a region of the domain. The single phase model is employed to simulate the behaviour of the ferrofluid. A body force is added to momentum equation in order to take into account the magnetic field strength.

Discussion and Results: The geometrical configuration is a circular pipe with a diameter of 3 mm and the length of 600 mm in which the ferrofluid flows. A 40mm-length solenoid is put in the centre of the pipe (between 280 mm and 320 mm from the inner surface) as showed in fig.1. The ferrofluid has a 3% of volume concentration of 20 nm-Fe₃O₄ nanoparticles and the single-phase model is applied. The fluid is electrically non-conducting in order to do not induce an electromagnetic current inside of it.

To estimate the thermal properties of the nanofluids for the single-phase model, the following equations are used [6-8]:

$$\rho_{nf} = (1 - \phi) \rho_{bf} + \phi \rho_p \quad (1)$$

$$c_{p,nf} = \frac{(1 - \phi) \rho_{bf} c_{p,bf} + \phi \rho_p c_{p,p}}{\rho_{nf}} \quad (2)$$

where the subscripts nf, bf, p indicate respectively the nanofluid, the base fluid and the nanoparticles. ϕ indicates the volume concentration of the nanoparticles in the base fluid, defined as the ratio between the volume of the nanoparticles and the total volume of the domain. The dynamic viscosity and the thermal conductivity is [8]:

$$\mu_{nf} = \frac{1}{(1 - \phi)^{2.5}} \mu_{bf} \quad (3)$$

$$\frac{k_{nf}}{k_{bf}} = \frac{k_p + 2k_{bf} + 2(k_p - k_{bf})\phi}{k_p + 2k_{bf} - (k_p - k_{bf})\phi} \quad (4)$$

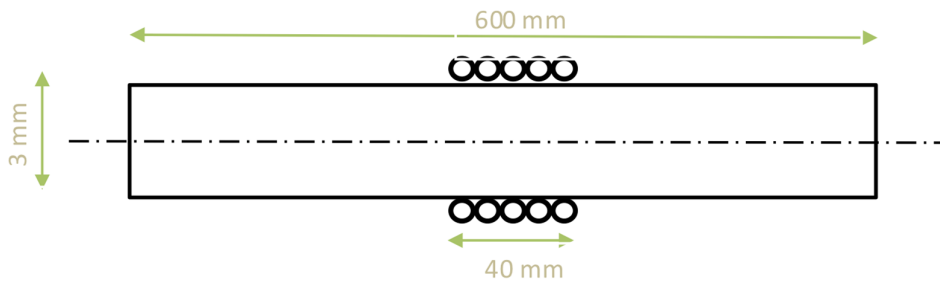


Figure 1. Sketch of the geometrical model

The Nusselt and Reynolds number are defined using the characteristics length D of 3 mm:

$$Nu = \frac{qD}{k_{nf}(T_0 - T_m)} \quad (5)$$

$$Re = \rho_{nf}VD \quad (6)$$

Where q is the wall heat flux, k_{nf} is the thermal conductivity of the ferrofluid, T_0 is the wall temperature and T_m is the mean temperature. About the boundary condition, at the inner surface the flow enters with an assigned Reynolds and a temperature of 303.16 K while the axial surface of the pipe is an isothermal wall at 313.16 K in order to have a ΔT of 10 K.

The thermal properties of the Fe_3O_4 are showed in Table 1.

Table 1. Properties of the Magnetite nanoparticles

Density [kg m ⁻³]	Specific heat [J kg ⁻¹ K ⁻¹]	Thermal conductivity [W m ⁻¹ K ⁻¹]
5200	670	8

The governing equations are the following:

Mass equation:

$$\frac{\partial \rho}{\partial t} + \bar{\nabla} \cdot (\rho \bar{V}) = 0 \quad (7)$$

Momentum equation:

$$\frac{\partial (\rho \bar{V})}{\partial t} + \bar{\nabla} \cdot (\rho \bar{V} \bar{V}) = 0 = -\bar{\nabla} p + \bar{\nabla} \cdot \bar{\tau} + (\bar{M} \cdot \bar{\nabla}) \bar{B} \quad (8)$$

Energy equation:

$$\frac{\partial (\rho c_p T)}{\partial t} + \bar{\nabla} \cdot (\rho c_p T \bar{V}) = \bar{\nabla} \cdot (k \bar{\nabla} T) \quad (9)$$

In the momentum equation the last term on the right side of the equation is the Kelvin body force. It represents the magnetic force generated by the interaction between the external magnetic field and the ferrofluid.

The validation of the model is established by the work of Ganguly et al. [4]. Using the same Reynolds numbers, a comparison of the convective heat transfer coefficient on the axial surface between the experimental setup and the numerical model is depicted in fig.2.

The results are presented for different values of the Reynolds number at laminar regime and for different strength of the magnetic fields. In fig. 3 are reported the convective heat transfer coefficient h and the Nusselt number vs Reynolds number.

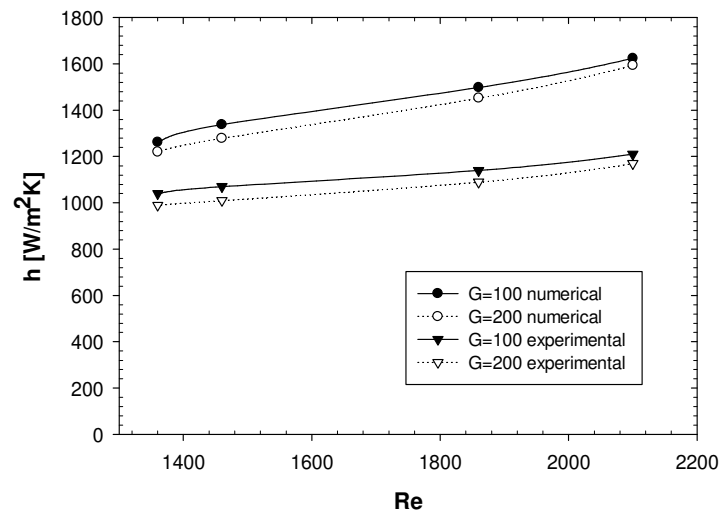


Figure 2. Validation of the model

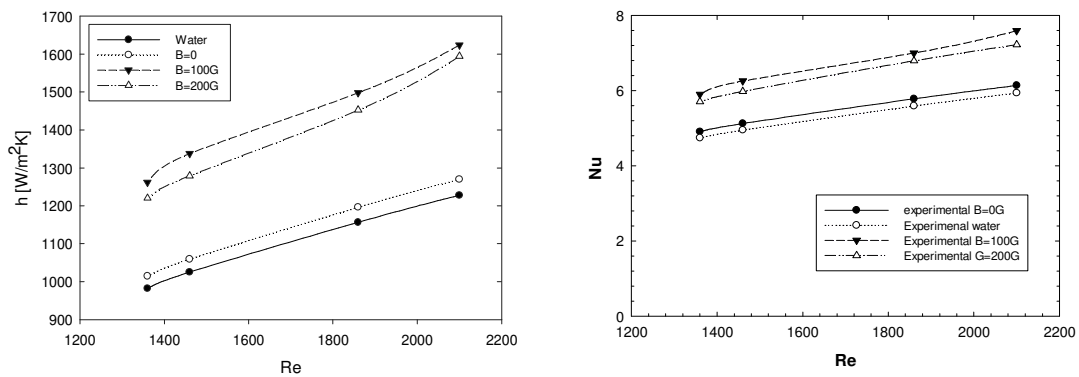


Figure 3. convective heat transfer coefficient and Nusselt number for different Reynolds number for pure water and for ferrofluid at different values of magnetic fields

It is possible to note that the presence of an external magnetic field improve the heat transfer coefficient, even that for higher magnetic field strength there is a lower value of h , so the phenomenon is not linear. In fig. 4 is reported the pressure losses for different Reynolds and magnetic strength.

The pressure losses increase for higher Reynolds and for higher magnetic field strength, even that there is a slight difference for $B=100\text{G}$ and $B=200\text{G}$

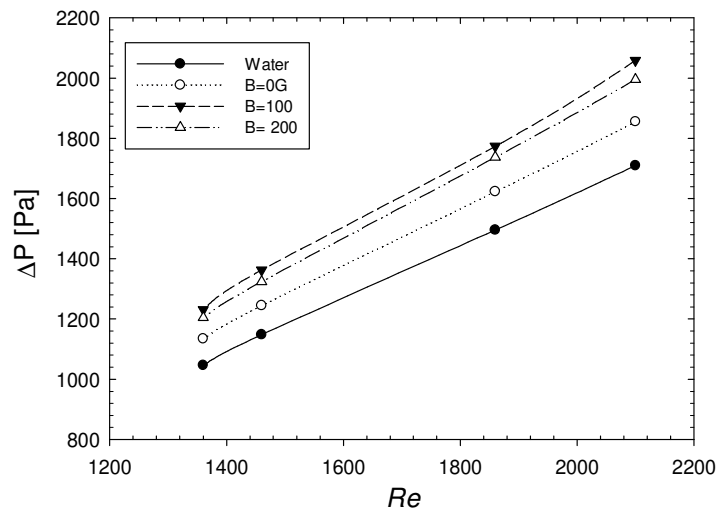


Figure 4. pressure losses for different Reynolds number for pure water and for ferrofluid at different values of magnetic fields

Conclusions: A laminar forced convection in a pipe of a ferrofluid is accomplished. The ferrofluid is affected by the presence of the magnetic field but not in linear way. Higher Nusselt number means that in the ferrofluid arise turbulent vortex that improve the heat transfer exchange. Obviously more works are necessary to understand the thermal behaviour of the ferrofluid and in which case the magnetic field is more effective on the heat transfer augmentation.

References:

1. Vincenzo Bianco, Oronzio Manca, Sergio Nardini, Kambiz Vafai, *Heat Transfer Enhancement with Nanofluids*, CRC Press, New York 2015.
2. S.U.S. Choi and J. A. Eastman, Enhancing thermal conductivity of fluids with nanoparticles, *ASME International Mechanical Engineering Congress and Exposition Proceedings*, San Francisco, CA (1995) 99-105
3. R.E. Ronsenzweig, *Ferrohydrodynamics*, Dover Publications, Mincola, New York, 1997.
4. R. Ganguly, S. Sen, I.K. Puri, Heat Transfer augmentation using a magnetic fluid under the influence of a line dipole, *Journal of Magnetism and Magnetic Materials* 271(2004)63-73.
5. M. Ghasemian, Z. Najafian Ashrafi, M. Goharkhah, M. Ashjaee, Heat transfer characteristics of Fe₃O₄ ferrofluid flowing in a mini channel under constant and alternating magnetic fields, *Journal of Magnetism and Magnetic Materials* 381 (2015) 158-167
6. B.C. Pak and Y.I. Cho, Hydrodynamic and Heat Transfer Study of Dispersed Fluids with Submicron Metallic Oxide Particles, *Experimental Heat Transfer* 11 (1998) 151–170.
7. A S.Q. Zhou, R. Ni, Measurement of the specific heat capacity of water-based Al₂O₃ nanofluid, *Applied Physics Letters* 92 (2008) 093123.
8. M. Corcione, Empirical correlating Equations for predicting the Effective Thermal Conductivity and Dynamic Viscosity of Nanofluids, *Energy Conversion and Management* 52 (2011) 789-793.

SUPERIOR COOLING WITH NANOFUIDS: HYPE AND REALITY

S M Sohel Murshed

Centro de Química Estrutural

Faculdade de Ciências da Universidade de Lisboa

1749-016 Lisboa, Portugal

Email: smmurshed@ciencias.ulisboa.pt

Abstract:

Based on the reported anomalous thermal conductivity and substantially high cooling features such as convective heat transfer coefficient and critical boiling heat flux of nanofluids compared to pure based fluids [1], nanofluids are considered as the coolants of next generation to many researchers. Although huge numbers of studies have been conducted on experimental and theoretical determination of effective thermal conductivity of nanofluids, results from different researchers are widely scattered. Regardless of inconstancy of data, any increase in thermal conductivity of nanofluids indicates their superior cooling capability compared to pure base fluids. On the other hand, most of the application of coolants are in flowing systems and thus in order to evaluate the cooling performance of nanofluids, their convective heat transfer performance in various conditions are of great importance. Compared to studies and focus on thermal conductivity, much less research have been performed on assessing the convective heat transfer performance of nanofluids in various systems and conditions related to flow and nanoparticles. Literature results on this convection heat transfer are also scattered and many issues are not yet conclusive. While a large number of researchers reported very high enhancement of convective heat transfer coefficient, others showed moderate to low enhancement. Nevertheless, results reveal that nanofluids can perform better than their base fluids in convection heat transfer [2]. One issue is critical for convection cooling performance is the pressure drop, which leads to high power consumption, and this is mainly due to substantially high viscosity of nanofluids. Thus the real cooling performance of nanofluids should be the trade off between the enhanced convection heat transfer and the viscosity in addition to other issues like the deposition of nanoparticles to channel surface. Nevertheless, high demand of coolants with superior performance particularly for modern thermal management systems and high-tech devices [3-4] and results of high thermal features of nanofluids led researchers to be ambitious and sometimes-hype-building. In this talk, convective cooling performance of nanofluids in various experimental systems such as mini and microchannel, heat pipes and other exchangers as well as in proto-type commercial systems will be analyzed. The future challenges and needs of nanofluids in cooling applications will be

discussed and nanofluids real cooling situation will be presented in order to distinguish hype and reality around cooling with this hot research-fluids.

References:

1. S.M.S. Murshed and C.A. Nieto de Castro, *Nanofluids: Synthesis, Properties and Applications*, New York: Nova Science Publishers. 2014.
2. S.M.S. Murshed, C.A. Nieto de Castro, M.J.V. Lourenço, M.L.M. Lopes, FJV Santos, *A review of boiling and convective heat transfer with nanofluids*, *Ren. Sust. En. Rev.* 15 (2011) 2342-2354.
3. S.M.S. Murshed, *Electronics Cooling*, Rijeka: INTECH, 2016.
4. S.M.S. Murshed and C.A. Nieto de Castro, *A critical review of traditional and emerging techniques and fluids for electronics cooling*, *Ren. Sust. En. Rev.* 78 (2017) 821–833.

HEAT TRANSFER IN NANOFUIDS: AN APPRAISAL

G.J. Tertsinidou¹, M.J. Assael¹ and W.A. Wakeham^{2*}

¹Chemical Engineering Department, Aristotle University, Thessaloniki 54636, Greece

²Chemical Engineering Department, Imperial College London, London SW7 2BY, U.K.

*Email: W.A.Wakeham@soton.ac.uk

Abstract:

Enhancing the apparent thermal conductivity of a base fluid by the addition of solid particles of a different material has been an attractive idea for more than a century. Stimulated by a paper of Choi *et al.* [1] in 1995 and the ready availability of a wide range of solid particles of a variety of materials with sizes of the order of a few nanometres there has been an explosion of interest in what have been designated nanofluids and a concomitant explosion in publications in the field. The ostensible reason for this explosion has been the claim by Choi and his collaborators [1] as well as by many other subsequent authors that it is possible to secure enhancements of the thermal conductivity of the base fluid in which the solid particles are suspended of as much as a factor of two. The first part of the talk considers how and why this explosion evolved and led to a situation of absolute chaos in the literature of the field.

The second part of the talk will use a critical evaluation of the work conducted in the last two decades to disentangle fact from fiction, and from hope. This critique by Tertsinidou *et al.* [2,3] takes three forms; an examination of the experiments conducted; a brief discussion of the theories put forward to explain the observations and finally an examination of heat transfer in any practical engineering context using such fluids.

The third element of the discussion then sets out the experimental work [4] we have conducted [2] on heat transfer in carefully-characterised fluids, separating those consisting of near spherical particles from those containing nanotubes that may form interconnected networks. The experimental work has been validated in a number of ways and demonstrates that the enhancement of the apparent thermal conductivity of the base fluid in the presence of nanoparticles is essentially that predicted by Maxwell's model of heat conduction in a solid substrate containing distributed particles of another material so that there is no anomalous enhancement. Using these results, in conjunction with viscosity measurements on the same fluids [3], it is possible to consider practical heat transfer design problems using nanofluids. Examples will illustrate that for most circumstances the disadvantageous increase in the viscosity of the base fluid outweighs the advantageous increase in the apparent thermal conductivity and no net benefit is derived from the use of nanofluids. However, under some very special circumstances there can be a modest benefit.

The final part of the talk makes the case for a calm, rational approach to the problem of heat transfer that might originally have been posed, but which was lost in the fever of enthusiasm that surrounded a ‘discovery’. The question posed is :**Is there a mechanism whereby heat transfer can be enhanced by the addition of nanoparticles to a base fluid?**

Three answers to this question are hypothesised none of which have really been addressed by the work conducted to date, it is suggested that the testing of these hypotheses (and possibly others) by careful modelling followed by even more careful experiments would be a sensible next step.

References:

1. S.U.S. Choi, J.A. Eastman, Pres. ASME Congress, San Francisco, USA, Nov. (1995)
2. G.J. Tertsinidou, M.J. Assael, W.A. Wakeham, *Int. J. Thermophys.* **36**:1367-1395 (2015).
3. G.J. Tertsinidou, Ch. Tsolakidou, M. Pantzali, M.J. Assael, L. Colla, L. Fedele, S. Bobbo, W.A. Wakeham, *J. Chem. Eng. Data* Editor’s Choice OpenAccess (2016).
4. K.D. Antoniadis, G.J. Tertsinidou, M.J. Assael, W.A. Wakeham, *Int. J. Thermophys.* **37**:78-100 (2016).

MAGENTA: MAGNETIC NANOPARTICLE BASED LIQUID ENERGY MATERIALS FOR THERMOELECTRIC APPLICATIONS

Sawako Nakamae

SPEC, CEA, CNRS, Université Paris-Saclay
CEA Saclay 91191 Gif-sur-Yvette Cedex, France

Email: sawako.nakamae@cea.fr

Keywords: Thermoelectricity, Ferrofluids, Ionic Liquids, Energy applications

Background: Thermoelectric (TE) materials that are capable of converting heat into electricity have been considered as one possible solution to recover the low-grade waste-heat (from industrial waste-stream, motor engines, household electronic appliances or body-heat). Solid semiconductor-based TE-modules were the first to enter the commercial application, and they still dominate the TE-market today. Despite their technical robustness including long life-time, simple use involving no moving parts, TE-technology has long been limited to low-power applications due to their poor efficiency. Closely following the rise of ‘nanotechnology’ in the 1980’s - 90’s, there has been a huge increase in the TE materials research for the past 20 years, which has led to some remarkable improvements in thermal-to-electric energy conversion capacity. However, even the most “promising” materials have not yet reached the minimum ZT requirements [1]. Furthermore, solid TE-materials suffer from a variety of practical obstacles such as small sizes, substantial production costs and the use of scarce and/or toxic raw materials, precluding them from wide-scale applications. Clearly, a technological breakthrough in TE-materials research is needed in order to make the thermoelectric technology environmentally friendly and economically viable for its future use.

Project Description: MAGENTA [2] is a 4-year research & innovation project that aims to explore the magneto-thermoelectric property of ionic-liquid (IL) based magnetic nanofluids, also known as ‘ferrofluids’. In energy applications, nanofluids have been widely considered as cooling agents for their superior thermal transfer properties; however, their ability to convert heat into electricity is only recently been reported [3]. Ionic liquids (IL), on the other hand, are enjoying substantial attention in several areas of energy research including thermoelectricity in recent decades [4, 5]. As a thermoelectric material, ILs present many promising features such as high electrical conductivity, large temperature and electrochemical windows, low vapour pressure and toxicity, and raw material abundance [6]. In MAGENTA, we combine unique and tuneable properties of both ILs and magnetic nanoparticles to bring paradigm change in the TE technology.

Presentation Summary: In this presentation, I will discuss existing examples of thermoelectric liquids and nanofluids that have led to the creation of MAGENTA, followed by the project’s

structure, methodologies and goals; i.e., 1) to provide founding knowledge of novel MTE phenomena in IL based ferrofluids, and 2) to build application-specific prototypes with tailor-made IL-FFs for their use in targeted industrial sectors.

References:

1. For thermoelectric devices to be competitive against other renewable energy technology (e.g., geothermal), ZT values greater than 4 are considered mandatory. See, for example: C. B. Vining, "An inconvenient truth about thermoelectrics," *Nat. Mater.* 8 (2009), 83.
2. MAGENTA project has received funding from the European Union's Horizon 2020 research and innovation programme under grant agreement No. 731976
3. T. Salez et al., "Can charged colloidal particles increase the thermoelectric energy conversion efficiency?" *Phys. Chem. Phys.*, 19 (2017) 9409.
4. D. R. MacFarlane et al., "Energy applications of ionic liquids," *ENERGY & ENVIRONMENTAL SCIENCE*, 7 (2014) 232.
5. A. Khan, et al., "Oxygen Reduction Reaction in Ionic Liquids: Fundamentals and Applications in Energy and Sensors" *Sustainable Chem. Eng.*, 5 (2017), 3698.
6. M. F. Dupont et al., "Thermo-electrochemical cells for waste heat harvesting – progress and perspectives," *ChemCom* (2017), DOI: 10.1039/c7cc02160g.

THERMAL ENERGY STORAGE USING COMPOSITE PHASE CHANGE MATERIALS– THE ROLE OF NANOFUIDS IN PERFORMANCE ENHANCEMENT

Yulong Ding

Birmingham Centre for Energy Storage & School of Chemical Engineering, University of Birmingham, Birmingham B15 2TT, UK

Email: Y.Ding@bham.ac.uk

Abstract:

Thermal energy storage (TES) refers to a collection of technologies that store energy in the forms of heat, cold or their combination, which accounts for a significant portion of global non-pumped hydro storage installations. TES can be sensible, latent or thermochemical heat based. The work to be presented here concerns TES using latent heat storage materials, often called phase change materials (PCMs). PCMs can be liquid-solid, solid-solid, gas-solid and gas-liquid. This work will focus on solid-liquid PCMs, particularly inorganic salts based PCMs. Two key challenges for the use of such materials are chemical incompatibility and low thermal conductivity. The use of composite materials provides an avenue to meeting the challenges. A typical composite PCM contains a structural supporting material and a thermal conductivity enhancer. Such a structure, combined with liquid-solid phase change, gives very complex flow and heat transfer behavior during repeated charge (heating) and discharge (cooling) processes. This presentation will report our recent progress in the fundamental understanding in the role of nanofluids in enhancing the thermal properties of composite PCMs. This will include molecular modelling based nanofluids formulation, to the incorporation of the nanofluids into the composite structure, and to the prediction and experimental validation of the thermal conductivity of the composite PCM.

STATE OF THE ART OF HEAT TRANSFER OF HEAT PIPES AND THERMOSYPHONS EMPLOYING NANOFLUIDS AS WORKING FLUID

M.H. Buschmann^{1*}, A. Huminic², S. Mancin³ and R.R. Riehl⁴

¹Institut für Luft- und Kältetechnik Dresden, 01309 Dresden, Germany

²Transilvania University of Brasov, Mechanical Engineering Department, 29 Bulevardul Eroilor Street, 500036, Brasov, Romania

³Department of Management and Engineering, University of Padova, Str.lla S. Nicola 3, 36100, Vicenza, Italy

⁴National Institute for Space Research – INPE - Space Mechanics and Control Division- DMC, Av dos Astronautas 1758, 12227-010 – São José dos Campos, SP – Brazil

*Email: Matthias.Buschmann@ilkdresden.de

Abstract:

The key note gives a short overview on the use of nanofluids in thermosyphons and heat pipes. The presentation starts with an analysis of possible mechanism how nanofluids / nanoparticle could act within such devices. It is shown experimentally, that no nanoparticles are transported with the gaseous phase of the working fluid. Moreover, it is argued that an increase of the thermal conductivity of the working fluid has only a minor effect on the experimentally observed improvement of the thermal performance of thermosyphons and heat pipes.

Experimental results from four independent research groups support the theoretical analysis. The experiments clearly indicate that nanofluids can enhance the amount of heat transferred with thermosyphons. Heat pipes seem to be more complicated. Mechanism are different here and an improvement of thermal performance is not to expect in any case / any nanofluid employed as working fluid.

The presentation finishes with recommendations for further research.

HOW TO VALIDATE NANOFUIDS?

M. J. Lourenço*

Centro de Química Estrutural

Faculdade de Ciências da Universidade de Lisboa

Campo Grande, 1749-016 Lisboa, Portugal

*Email: mjlourenco@ciencias.ulisboa.pt

Keywords: Nanofluid, validation, standardization, stability, thermal properties

Introduction: The International Organization for Standardization defines the term "nanomaterial" as "material with any external dimensions in the nanoscale or having internal structure or surface structure in the nanoscale". The term "nanoscale" is defined as size range from approximately 1 nm to 100 nm *"The increasing use of nanomaterials in industry and society means that their utility, risks and benefits throughout their life-cycle are important topics for discussion"* [1].

What about nanofluids? Nanofluids are not simply mixtures of nanomaterials in fluids. The simpler nanofluids are bi-phasic systems with a solid phase dispersed in a liquid phase to be stable over a long period of time with different properties from those of the base fluids. These useful nanofluids can replace, with advantages, fluids used in many engineering applications. The results show that good and coherent experimental results can be obtained when well planned experiments are used, demonstrating that nanofluids can be used in many applications with success [2]. Until now the published results on nanofluids exhibit several problems about the characterization of nanomaterials used, preparation and short/long term stability of the prepared dispersions, and the adequacy of the experimental techniques used to measure the thermophysical properties, namely thermal conductivity, due to the scatter/availability of published data. However, optical properties have considerable contribution to heat absorbance in nanofluids. Simple light absorption measurements in UV-Vis may be used to follow the stability of nanofluids using just the dispersion of light caused by the nanomaterial, even for systems that do not have any absorption bands in the visible range. The experimental results revealed that the transmittance of nanofluids has indirect relation with nanoparticle size, volume fraction, and path length [3]. Overall, results of various elements showed that the presence of large particles and particle agglomerates leads to significant amount of scattered light.

It is fundamental to be aware of the difference between agglomerate and aggregate. An agglomerate is defined as a collection of weakly or medium strongly bound particles where the

resulting external surface area is similar to the sum of the surface areas of the individual components (the forces holding an agglomerate together are weak forces, for example van der Waals forces or simple physical entanglement). An aggregate is defined as particles comprising strongly bonded or fused particles where the resulting external surface area is significantly smaller than the sum of surface areas of the individual components (the forces holding an aggregate together are strong forces, for example covalent or ionic bonds, or those resulting from sintering or complex physical entanglement, or otherwise combined former primary particles) [1].

The special case of IoNanofluid defined by C. A. Nieto de Castro et al.[4] as a nanomaterial stable dispersion in an ionic liquid have an enormous potential for many applications, due to their properties, namely HTF's. *The fundamental is to achieve kinetically stable dispersions.* Two-step methods and sonication probes are the most convenient techniques for its preparation. The toxic effect of the system ionic liquid /nanomaterial *in biota* is a challenging endeavour. The use of surfactants or any other additives to stabilize the nanofluids should be avoid. Understanding the molecular interactions cation/anion/nanomaterial is critical. There are other special and essential requirements, for example, the durability of the suspension, the prevention of agglomeration and/or aggregation, and the constancy of the fluid chemistry [5].

Conclusions: This contribution presented a broad view for the preparation of nanofluids and alert for the need to establish a known methodology for their preparation and stability testing, accordingly to its intended use. The main objective is alert for the intelligent use of greener nanofluids, as the correct use of nanoparticles saves a lot of resources and produces smaller quantities of CO₂. Aspects such as legislation, manipulation and toxicity are briefly referred [2]. In addition, selected systems, with all these properties determined and stability validation tests, must be proposed for reference nanofluids, with associated certified thermophysical data for industrial users, namely for high temperature applications.

If it is possible to select the more functional nanofluids, i.e., those in which their properties increase the overall performance of equipment/systems, without environmental contamination effects, we can state that researchers and science areas involved are fit for the beginning of a new era of research: the nano-ecological and economic research (the term economic here only attaches to the resource savings that nanomaterials can ensure in the very near future). In nanosciences, some impurity contamination may damage the stability and durability of a nanofluid.

References:

1. SOURCE: ISO/TS 80004-1:2015, 2.4, modified; Nanotechnologies — Plain language explanation of selected terms from the ISO/IEC 80004 series*
2. M. J. Lourenço and S. I. Vieira, Nanofluids Preparation Methodology”, Chapter 1 in *Nanofluids: Synthesis, Properties and Applications*”, S. M. Sohel Murshed, C. A. Nieto de Castro, Eds., NOVA Science Publishers, Inc., New York, ISBN 978-1-63321-677-8, (2014)

3. Suying Yan, Feng Wang, ZhiGuo Shi, Rui Tian, “Heat transfer property of SiO₂/water nanofluid flow inside solar collector vacuum tubes”, Applied Thermal Engineering 118 (2017) 385–391
4. C.A. Nieto de Castro, M.J.V. Lourenço, A.P.C. Ribeiro, E. Langa, S. C. Vieira, P. Goodrich, C. Hardacre, J. Chem. Eng. Data, (2010), 55 (2), 653–661
5. Carlos Nieto de Castro, Xavier Paredes, Salomé Vieira, Sohel Murshed, Maria José Lourenço and Fernando Santos, “IoNanofluids: Innovative Agents for Sustainable Development”, in Nanotechnology for Energy Sustainability, Volume 3, Part IV, Eds Baldev Raj, Marcel Van de Voorde, Yashwant Mahajan, WILEY-VCH Verlag GmbH & Co. KGaA, Weinheim, (2017)

**This document offers explanations (including examples) of selected nanotechnology terms and is intended to facilitate an understanding of the use and applications of nanotechnology. Its target audience is those who need to make decisions about the use of nanotechnology. The specific aim is to promote consistent usage and reduce misinterpretation of terms among users; and facilitate communication and understanding in developing or commercializing applications of nanotechnologies.*

ISSUES IN CONVECTION MODELING OF PURE AND ENHANCED PCM

Gennady Ziskind

Department of Mechanical Engineering

Ben-Gurion University of the Negev

Beer-Sheva, Israel

Email: gziskind@bgu.ac.il

Abstract:

This talk includes a comprehensive review and discussion regarding modelling of solid-liquid phase change processes where convection is involved. We focus on the enthalpy method and its variants that are considered today as the most prominent and effective way for numerical solution of solid-liquid phase change problems. Special attention is dedicated to the enthalpy-porosity approach, which has become one of the main tools used for the analysis of latent-heat-based systems in computational fluid dynamics (CFD) software packages. This approach is based on an apparent analogy between the partially liquid material in the mushy zone and the fluid flow through a porous medium. Obviously, it is applied when the liquid medium is treated as such, i.e., is allowed to flow. Accordingly, a complete system of governing conservation equations, i.e., continuity, momentum and energy, is solved. This might be done incorporating the associated volume change or, in a simplified manner, under the assumption that this volume change is neglected and convection in the melt is taken into account by the Boussinesq approximation.

It is well-known that materials with high latent heat usually have a low thermal conductivity. Different solutions for this problem have been suggested in the past, and are still under extensive research. Among these are dispersing highly conductive particles in the phase-change materials (PCM), impregnating PCM in a porous matrix made of a conductive material, and others. This talk discusses the convection-related issues in enhanced PCM that utilize nanoparticles for thermal conductivity enhancement. Some historical and recent works in the field are reviewed. It appears that for melting processes, the increased effective dynamic viscosity may suppress natural convection that should be the dominant heat transfer mode in some configurations. The increased viscosity can also be a problem for close-contact melting (CCM) configurations, as the highly viscous flow in the thin molten layer can increase its thickness considerably and reduce the melting rate. For solidification processes, where convection effects can mostly impede the phase-change rate, the use of nano-enhanced PCM is promising to some reasonable extent because of their increased effective thermal conductivity, although care should be taken regarding the reduced effective latent heat that is significant especially for high nanoparticle volume fractions. Finally, we discuss in brief PCM slurries, in which the phase-change material particles are dispersed in a liquid medium, water-based or other.

Abstracts

SESSION 3A: HEATING

TRANSPORT PROPERTIES OF WATER-BASED NANOFUIDS WITH DISPERSION OF GRAPHENE-OXIDE NANOPARTICLES

L. Fedele* and S. Bobbo

Istituto per le Tecnologie della Costruzione, Consiglio Nazionale delle Ricerche

Corso Stati Uniti, 4 - Padova, I-35127, Italy

Email: laura.fedele@itc.cnr.it

Keywords: Nanofluids, Graphene-oxide, Thermal conductivity, Viscosity

Introduction

Enhancement of thermal properties of heat transfer fluids is presently the most promising way to increase the performance of heat exchangers and in general of systems where heat transfer is a significant part of the energy flow. Nanofluids, dispersions of solid nanoparticles in a common fluid like water, glycol or oil, are widely studied due to their possibility to increase strongly the thermal properties of the base fluid [1]. However, the results available in the literature are still controversial and several problems (e.g. nanoparticles stability inside the fluid) need to be overcome [2]. Among the possible materials for nanoparticles, carbon nanostructures seem to exhibit the highest potential with respect to other materials, such as metal oxides or metals [3]. In particular, graphene, a graphite carbon allotrope, is one of the most interesting due to its remarkable mechanical, structural, thermal, and electrical properties [4, 5, 6]. Nonetheless, being graphene hydrophobic, it cannot be dispersed in polar solvents directly. Thus, the hydrophilic graphene oxide (GO), even if characterised by lower thermal conductivity, is a good alternative to graphene as additive in nanofluids based on polar fluids, such as water or ethylene-glycol. Only few works are available in the literature on nanofluids based on GO nanoparticles, showing significant thermal conductivity enhancements with respect to the base fluids [7] and thus interesting potentiality to apply these nanofluids as efficient heat transfer fluids. However, significant additional work is necessary to fully understand their thermal properties. Here, commercial nanofluids based on graphene-oxide (GO) nanostructure have been considered as potential substitutes for water as heat transfer fluids in ground source heat pumps (GSHP). Stability along time have been evaluated and transport properties (thermal conductivity and viscosity) have been measured as a function of temperature.

The study has been performed within the research activities of the European Project “Cheap and efficient application of reliable Ground Source Heat exchangers and Pumps” Cheap – GSHPs Grant Agreement Number 657982.

Experimental

Materials: two commercial nanofluids provided by Sigma Aldrich have been used for the experiments. Both fluids are based on water and graphene-oxide platelets, but with two different concentrations of nanoparticles: 1 mg/ml (WG1) and 2 mg/ml (WG2). Nanoparticles are constituted by a structure formed by 15-20 sheets of graphene, edge-oxidized at 4-10%. No information are available about the presence of dispersants.

Nanofluids Stability Characterization: nanoparticles stability in the dispersion has been evaluated applying a method based on the Dynamic Light Scattering (DLS) using a Zetasizer Nano ZS (Malvern) [8]. A sample of fluid is put into a proper cell, which is illuminated by a laser and the particles scatter the light which is measured using a detector. The particles move randomly and their speed is used to determine the particles dimension. The particle size measured in a DLS instrument is the diameter of the ideal sphere that diffuses at the same rate of the considered particle. This instrument can detect particle size from 0.6 nm to 6 μm using the DLS process, with a declared accuracy better than $\pm 2\%$. All size measurements were made at 25 $^{\circ}\text{C}$ with a scattering angle of 173 $^{\circ}$. In order to verify the dependency of the diameter size from the concentration of the solution, each nanofluid was sonicated and the nanoparticle size was measured three times.

Thermal Conductivity apparatus: the thermal conductivity measurements were performed using a TPS 2500 S (Hot Disk), an instrument based on the hot disk technique which can measure thermal conductivity and thermal diffusivity of several materials [9]. The main parts of the instrument are the sensor, made of a double spiral of thin nickel wire that works as a continuous plane heat source and as a temperature sensor, a proper box containing the sensor and the fluid and a thermostatic bath to reach the test temperature. The conductivity data were measured at ambient pressure and in a temperature range between 10 and 70 $^{\circ}\text{C}$. The power supplied for each measurement was 30 mW and the time of the power input was 4 s. The declared instrument uncertainty is 5%.

Dynamic Viscosity apparatus:

dynamic viscosity data were measured by means of an AR-G2 rheometer (TA Instruments), a rotational rheometer with magnetic bearing which permits ultra-low nanotorque control [10]. A plate-cone geometry with a 1 $^{\circ}$ cone and diameter of 40 mm was employed and a proper device (Upper Heated Plate) was used to stabilize the measurement temperature. A constant quantity of sample, about 0.34 mL, was considered optimal for the analysis. Before the measurements, the rheometer was carefully calibrated at each temperature, as fully described

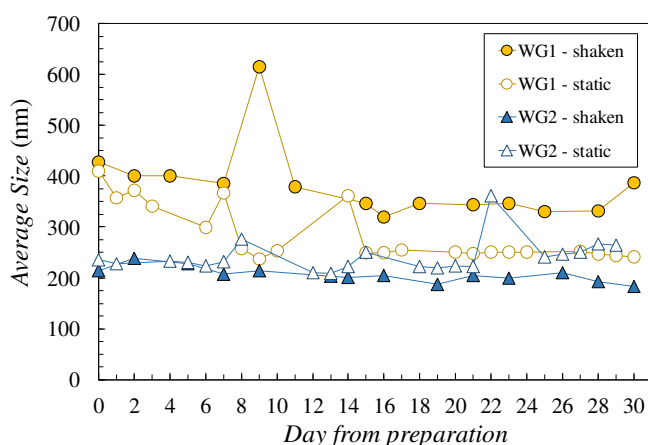


Figure 1. Variation along time of GO nanoparticles mean diameters.

in Bobbo et al. The dynamic viscosity data were measured at ambient pressure and in a temperature range between 10 and 70°C, with steps of 10°C. All the measurements were performed at constant temperature and variable shear rate. The declared instrument uncertainty is 5%.

Discussion and Results

Stability analysis: mean values of the nanoparticles nominal diameters at the starting time were 428 nm and 214 nm for WG1 and WG2, respectively. With the purpose to determine the tendency of the particles in suspension to settle down along time, two samples of the fluid were put in two different measurement cuvettes. The first sample was measured almost every day for thirty days, without shaking the fluid, to evaluate the changes in size distribution due to natural sedimentation. The second sample was measured almost every day for thirty days after sonication of the fluid to evaluate the changes in size distribution after mechanically removing the sedimentation [8]. The variations along time of the GO nanoparticles mean diameters are shown in Figure 1. The shaken WG1 sample average size slowly decrease along time stabilizing after 15 days at around 350 nm, while the static WG1 sample, after a quite fast decrease along the first 15 days, stabilizes at around 250 nm. This probably means that agglomerates with size over 250 nm are not stable and can be partially re-dispersed only after sonication. The starting average diameter of WG2 is below 250 nm and this is probably the reason why both shaken and static samples showed a quite constant size, in the range between 190 and 250 nm for all the thirty days of analysis. In any case, for both WG1 and WG2, no micrometric

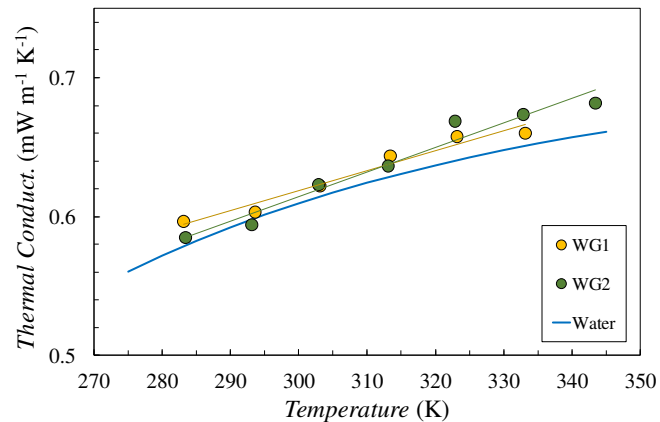


Figure 2: Thermal conductivity of the nanofluids as a function of temperature

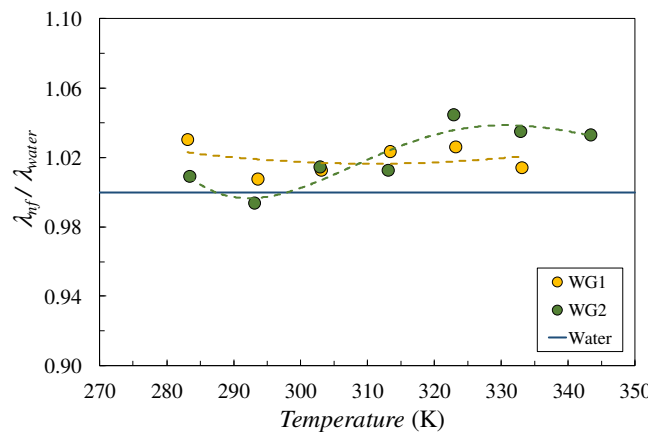


Figure 3: Thermal conductivity ratio between WG1 and WG2 nanofluids and water as a function of temperature

peaks were recorded in the period considered, suggesting there is no tendency of nanoparticles to further agglomerate.

Thermal Conductivity (λ): thermal conductivity data of the two nanofluids, measured from 283 to 333 K and 343 K for WG1 and WG2 respectively, are represented in Figure 2 and compared with the thermal conductivity of water, calculated with the database Refprop 9.1 [10]. For both nanofluids the thermal conductivity increases with temperature, as expected, and is very similar for both nanofluid, thus suggesting a very weak dependence on GO nanoparticles concentration. The fluctuation of λ with temperature are probably due to some instability of the nanofluids and anyway the differences shown by the two nanofluids are within the measurements uncertainties. Moreover, the increments with respect to water, more evident at the highest temperatures, are very moderate and do not suggest any special effect due to the presence of solid nanoparticles inside the base fluid. This is clearly represented in Figure 3, that shows the ratio ($\lambda_{nf}/\lambda_{water}$) between the thermal conductivities of the nanofluids and water. The ratio is practically constant for WG1 and weakly dependent on temperature for WG2, but in any case never exceeds 1.04, *i.e.* the maximum observed increment of thermal conductivity is 4%.

Viscosity (μ): the viscosity of the two nanofluids, measured from 283 to 313 K and 323 K for WG1 and WG2 respectively. Viscosity data are represented in Figure 4 and compared with the viscosity of water, calculated with the database Refprop 9.1 [11]. As shown, the viscosity of WG1 was close to that of water up to 303, with a more significant increase at 313 K, while the viscosity of WG2 is generally higher especially at the lowest and the highest temperatures. Figure 5

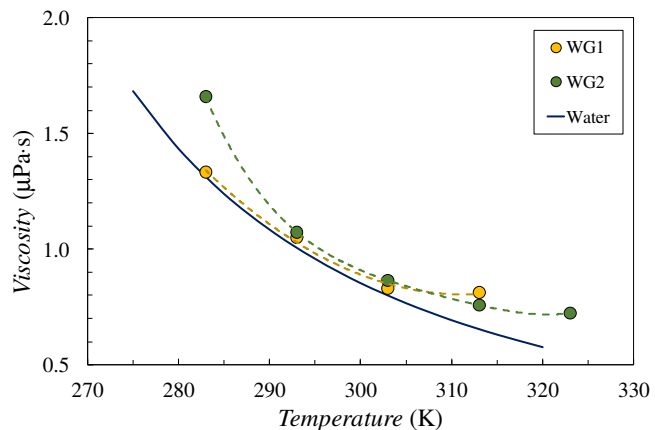


Figure 4: Viscosity of the nanofluids as a function of temperature in comparison with water

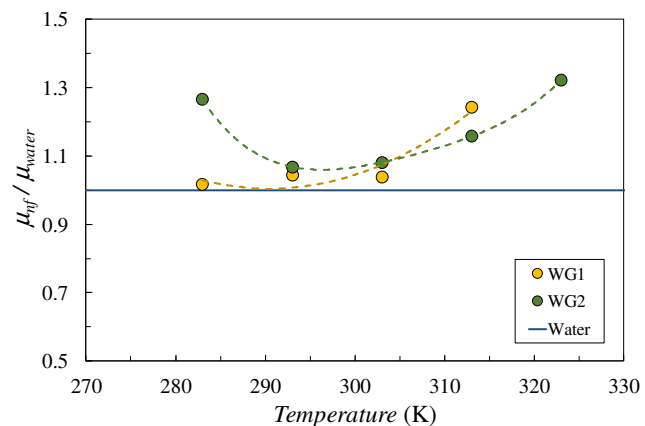


Figure 5: Viscosity ratio between WG1 and WG2 nanofluids and water as a function of temperature

shows the viscosity ratio (μ_{nf}/μ_{water}) between the viscosities of the nanofluids and water. The ratio for WG1 is almost constant and below 1.04 in the range of temperatures between 283 and 303 K, but suddenly increases to 1.24 at 313 K. For WG2, the ratio tends to increase with temperature from 293 and 323 K, ranging from 1.07 to 1.32, while an unexpected increase to 1.26 is obtained at the lowest temperature (283 K).

Conclusions: Stability, dynamic viscosity and thermal conductivity for two commercial nanofluids (named WG1 and WG2) formed by water and graphite-oxide nanoparticles at two different concentrations (1 mg/ml and 2 mg/ml) were analysed as a function of temperatures. Even if the nanofluids shown to be quite stable at ambient temperature along time, measured thermal conductivity and viscosity behaviour do not suggest any potentiality of the nanofluids to enhance the heat transfer efficiency of the nanofluids with respect to water: thermal conductivity is similar or only slightly higher than that of water in all the temperature range for both nanofluids, despite the very high thermal conductivity of graphene-oxide; at the same time, dynamic viscosity enhancement is negligible for WG1 but suddenly increases by 24% at 313 K, while it is quite significant for WG2, increasing from 7% to 32 % from 283 to 323 K, while is anomalously high (32) at the low temperature of 283 K.

References:

1. S. Choi and J.A. Eastman, Enhancing thermal conductivity of fluids with nanoparticles, *ASME International Mechanical Engineering Congress & Exposition*, San Francisco, CA, November 12-17, 1995.
2. M. Gupta, V., Singh, R. Kumar and Z. Said, A review on thermophysical properties of nanofluids and heat transfer applications, *Renewable and Sustainable Energy Review* 74 (2017) 638-670.
3. E.J. Park, S.D. Park, I.C. Bang, Y.B. Park and H.W., Park, Critical heat flux characteristics of nanofluids based on exfoliated graphite nanoplatelets (xGnPs). *Materials Letters* 81 (2012) 193–197.
4. C. Lee, X. Wei, J.W. Kysar, J. Hone, Measurement of the elastic properties and intrinsic strength of monolayer graphene. *Science* 321 (2008) 385–358.
5. B. Sun, B. Wang, D. Su, L. Xiao, H. Ahn, G. Wang, Graphene nanosheets as cathode catalysts for lithium-air batteries with an enhanced electrochemical performance. *Carbon* 50 (2012) 727–733.
6. A.A. Balandin, S. Ghosh, W. Bao, I. Calizo, D. Teweldebrhan, F. Miao and C.N. Lau, Superior thermal conductivity of single-layer graphene, *Nano Letters* 8 (2008) 902–907.
7. A.K. Rasheed, M. Khalid, W. Rashmi, T.C.S.M. Gupta, A. Chan, Graphene based nanofluids and nanolubricants – Review of recent developments, *Renewable and Sustainable Energy Reviews* 63 (2016) 346–362.
8. L. Fedele, L. Colla, S. Bobbo, S. Barison and F. Agresti, Experimental stability analysis of different water-based nanofluids, *Nanoscale Research Letters* 6 (2011) 300
9. L. Fedele, L. Colla, and S. Bobbo, Viscosity and thermal conductivity measurements of water-based nanofluids containing titanium oxide nanoparticles, *International Journal of Refrigeration* 35 (2012) 1359–1366.
10. S. Bobbo, L. Fedele, A. Benetti, L. Colla, M. Fabrizio, C. Pagura and S. Barison Viscosity

of water based SWCNH and TiO₂ nanofluids, *Experimental Thermal and Fluid Science* 36 (2012) 65–71.

11. E.W. Lemmon, M.L. Huber, M.O. McLinden, *NIST Standard Reference Database 23, Reference Fluid Thermodynamic and Transport Properties (REFPROP), version 9.1*, National Institute of Standards and Technology, Gaithersburg, MD, 2010.

RHEOLOGICAL PROPERTIES AND SURFACE TENSION OF STABLE GRAPHENE OXIDE AND REDUCED GRAPHENE OXIDE AQUEOUS NANOFUIDS

D. Cabaleiro¹, P. Estellé^{2,*}, H. Navas³, A. Desforges³ and B. Vigolo³

¹Dpto. Física Aplicada, Faculdade de Ciências, Universidade de Vigo, 36310 Vigo, Spain

²MTRhéo, LGCGM, Université Rennes 1, 35704 Rennes, France

³Institut Jean Lamour, CNRS-Université de Lorraine, BP 70239, 54506 Vandœuvre-lès-Nancy, France

*Corresponding author: patrice.estelle@univ-rennes1.fr

Keywords: Graphene, Nanofluid, Surface Tension, Rheological Behavior

Background: The improvements in thermal conductivity reported for nanofluids over the last two decades have evidenced the great potential of these new nanostructured materials to enhance the heat transfer performances of thermal installations. However, an efficient design and subsequent control of heat transfer facilities also require an accurate characterization of thermal or physical properties necessary to define the flow and dynamic wetting behavior of nanofluids, especially for microfluidic systems [1]. Thus, dynamic viscosity does not only influence flow regime but also affects pressure drop and consequent pumping power, while surface tension plays a major role in boiling and two-phase heat transfer flows, and in critical heat flux phenomena or heat pipes, for example [2;3].

Among the different nanomaterials used in the literature to design nanofluids, graphene is receiving increasing attention for its exceptional thermal properties, with ideal thermal conductivities higher than those of carbon nanotubes or diamond [4]. Unfortunately, pristine graphene (G) is hydrophobic and thus it tends to agglomerate in the presence of most of solvents and particularly in water, the most common thermal medium [5]. Alternatively, covalent functionalized graphene oxide (GO) contains hydroxyl and epoxy groups, which makes the material hydrophilic [6]. Nevertheless, the thermal conductivity of GO is considerably lowered compared to that of pristine graphene since the oxidation process destroys the sp^2 conjugated carbon structure of graphene. A controlled reduction of graphene oxide can restore part of graphene structure with a moderate decrease in hydrophilicity. The possibility of reaching a compromise between the advantages of G and GO confers to reduced graphene oxide (rGO) a great potential in the preparation of dispersions with improved thermal properties and long-term stabilities [7].

Tesfai et al. [8] and Kamatchi et al. [7] analyzed the rheological behavior of water-based nanofluids prepared at nanoadditive concentrations between 0.05 and 0.5 g/L of GO and between 0.01 and 0.3 g/L of rGO. Both studies reported non-Newtonian shear thinning behaviors at shear rates lower than 200 s^{-1} in the case of Tesfai et al. [8] and lower than 60 s^{-1} in

the case of Kamatchi et al. [7]; the phenomena being more pronounced as nanoadditive loading increases. Mehrali et al. [9] also carried out flow curve tests for graphene aqueous dispersions prepared using nanoadditives with three different specific surface areas and the authors found a pseudoplastic behavior at low shear rates for some nanofluids. As regards previous works on surface tension, Kamatchi et al. [7] and Zheng [10] studied rGO/water nanofluids and reported increases in this property with rGO concentration up to 3%. In addition, Ahammed et al. [11] experimentally investigated graphene/water nanofluids stabilized with SDBS and observed that surface tension decreases with nanoadditive concentration up to 13.8%.

The present study aims to analyze the effect that nanoparticle loading and graphene functionalization have on rheological behavior and surface tension of graphene aqueous nanofluids. Three different nanofluid sets based on GO and two different rGO at six nanoparticle volume fractions ranging from 0.0005 to 0.1% were studied.

Experimental Method:

The derived Hummers' method was used to prepare GO [12]. Briefly, 2.5 g graphite powder (SFG₆ Primary Synthetic Graphite from Timcal Inc.) and 1.9 g of NaNO₃ are added to 85 mL of sulfuric acid and 12.5 g of potassium permanganate at temperature below 20°C. After 2 h at 35°C under stirring, 125 mL of deionized water are slowly added to the above solution and followed by the addition of 10 mL of oxygenated water. GO is then rinsed several times with 10 vol.% hydrochloric acid and water. rGO was prepared by reduction of GO (0.2 vol.%) with various amounts of a 2 vol.% sodium borohydride (NaBH₄) solution. Typically, for the nanofluid series studied, concentrations of NaBH₄ are 0.2 vol.% (rGO_0.2) and 0.1 vol.% (rGO_0.1). Introduction of oxygen containing groups at the GO surface and also at rGO surface since the chemical reduction is never complete is responsible for a dramatic hydrophobicity reduction. This improved affinity of graphene with water induces a facile dispersion of GO/rGO without any use of surfactant. The GO/rGO solutions were simply homogenized with a low power sonication bath for a few minutes. Flow curve experiments were performed at temperatures of 20 and 30°C by using a Malvern Kinexus Pro rheometer (Malvern instruments, UK) working with a cone-plate geometry with a diameter of 60 mm, a cone angle of 1° and a gap of 0.03 mm, appropriate for studying low-viscosity colloidal dispersions. Tests were performed in steady-state regime at shear stress logarithmically increasing from 0.01 to 2 Pa with at least 7 points per decimal, necessary to cover the range of shear rates between 10 and 1000 s⁻¹. The estimated uncertainty of this device is less than 4% within the studied shear rate range [13]. Surface tension measurements were carried out at room temperature with a Drop Shape Analyzer DSA-30 (KRÜS, Germany) based on the pendant drop technique. This device records and digitally analyzes the shape of sample drop formed at the end of a vertical syringe just in the moment when the drop snaps from the apex of the needle. Surface tension is obtained from a drop shape analysis through a balance of internal and external forces acting on the drop from Young-Laplace equation with an accuracy better than 0.3 mN/m as given by supplier device. In this study a 15-gauge needle with an outer diameter of 1.83 mm was utilized to produce drops with a volume of around 30 μm. Studies were carried out taking special care to capture the image of the pendant drop as soon as it was formed in order to limit possible perturbations due to air currents and ambient humidity.

Discussion and Results: Stability of the prepared nanofluids was followed by both optical microscopy and visual observation of the solutions over time as shown by Figure 1 which evidences the stability of produced nanofluids. The rheological behaviors of the base fluid and the different nanofluid sets were investigated at temperature of 20 and 30°C. Results obtained for distilled water exhibit absolute average deviations lower than 1.5% with previous literature [14]. Figure 2 shows the flow curves obtained at 30°C for different concentrations of the GO and rGO_0.2 nanofluid sets. The result found for the rGO_0.1 are similar to the current presented for rGO_0.2. As it can be observed, nanofluids prepared at volume concentrations lower than or equal to 0.01% follow a Newtonian behavior within the studied shear rate range while a shear-thinning behavior was observed for higher concentrations.

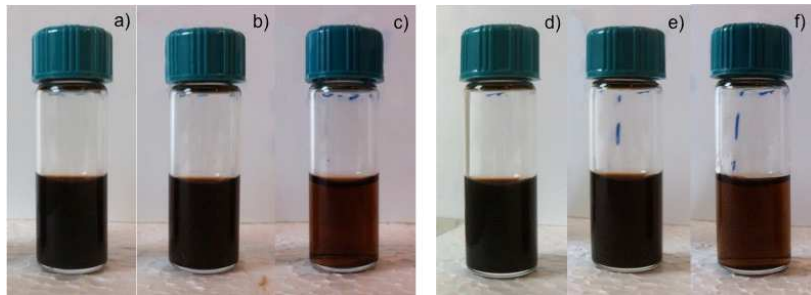


Figure 1. Photographs of rGO_0.1 (a, b and c) and rGO_0.2 (d, e and f) nanofluids one month after their preparation for different nanoparticle volume concentrations: 0.1 (a, d), 0.05 (b, e) and 0.01% (c, f)

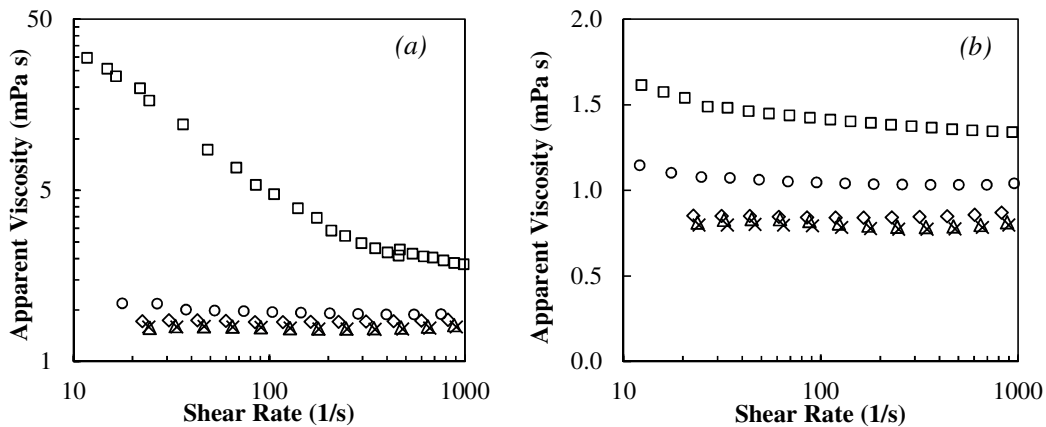


Figure 2. Flow curves of GO (a) and rGO_0.2 (b) nanofluid sets at 30°C and different nanoparticle volume concentrations: (×) Base Fluid, 0, (△) 0.0005, (◇) 0.01, (○) 0.05 and (□) 0.1 Vol.%.

Figure 3 presents the relative viscosity values of the three nanofluids sets obtained at a shear rate of about 900 s^{-1} and a temperature of 20°C . The figure shows that relative viscosity increases with nanoparticle concentration. However, chemical reduction does not have a strong influence on the dynamic and relative viscosity increases, except for the highest nanoparticle concentration for which the rise in this property is considerably higher in the case of GO than for rGO nanofluid sets. Comparing the two studied temperatures, increases in dynamic viscosity at 0.1% volume fraction are higher at 30°C than at 20°C , while the variations are within experimental uncertainty for the rest of concentrations. As expected viscosity of nanofluids decrease with the increase in temperature. Also, the evolution of relative viscosity at higher temperature of 30°C is quite similar to 20°C . Finally, relative viscosity appears to be quite independent of tested temperature whatever the nanoparticle content.

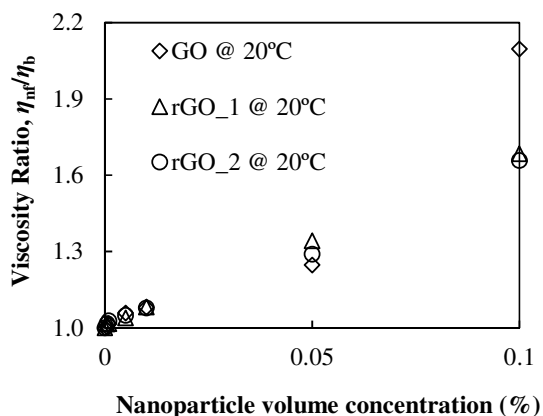


Figure 3. Relative viscosity vs. nanoparticle volume concentration at 20°C and 900 s^{-1} for:

(◇) GO, (△) rGO_0.1 and (○) rGO_0.2 nanofluid sets.

With the aim of checking the calibration and the followed procedure for measurements, surface tension was first studied for distilled water, ethylene glycol, and toluene at room temperature. A good agreement between literature values and our experimental results was found, with deviations lower than 1.3%. Afterwards, the influence of the nanoadditive concentration on the surface tension of the three sets was analyzed. As an example, captures of the drops obtained for three concentrations of the rGO_0.1 nanofluid set are shown in Figure 3. It was observed that surface tension decreases as graphene loading increases, with a maximum reduction of about 3% for the highest volume fractions, 0.1 vol.%, and without a clear effect of the chemical reduction.

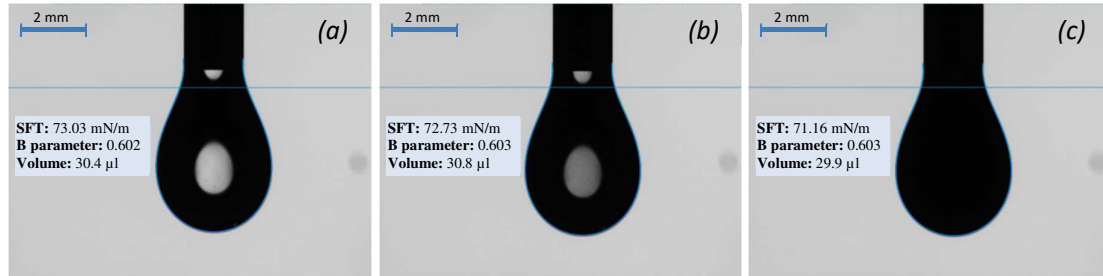


Figure 4. Pendant drop images of rGO_0.1 nanofluids at: (a) 0.0005, (b) 0.005, and (c) 0.1% volume concentrations.

Conclusions: Rheological and surface tension properties of stable reduced graphene nanofluids were experimentally studied. A Newtonian behavior was observed in the analyzed shear rate range for graphene volume fractions lower or equal to 0.01% while nanofluids with higher concentrations exhibit a shear-thinning behavior. Dynamic viscosities for the GO nanofluid are higher than that of rGO ones at 0.1 vol.% while differences in this property are similar to experimental uncertainty when comparing the three nanofluid sets at the other concentrations. These results show the influence of chemical treatment on the dispersion state and stability of graphene nanofluids for high concentration considered. Surface tension decreases as graphene loading increases, with maximum reductions of about 3% for the highest volume fractions and without a clear effect of the graphene functionalization process.

Acknowledgements: D. Cabaleiro acknowledges EU COST for the STMS grant ref. COST-STSM-CA15119-34906 as well as the Spanish Ministry of Economy and Competitiveness and EU FEDER Program for his research contract within the Project ENE2014-55489-C2-2-R. P. Estellé acknowledges the European Union through the European Regional Development Fund (ERDF), the Ministry of Higher Education and Research, the French region of Brittany and Rennes Métropole for the financial support related to surface tension device used in this study.

References:

1. S.M.S. Murshed, S.H. Tan and N.T. Nguyen, *Journal of Physics D: Applied Physics* 41 (2008) 085502.
2. J. Chinnam, D.K. Das, R.S. Vajjha and J.R. Satti, *International Journal of Thermal Sciences* 98 (2015) 68-80.
3. S.M.S. Murshed and P. Estellé, *Renewable and Sustainable Energy Reviews* 76 (2017) 1134-1152.
4. D. Cabaleiro, L. Colla, S. Barison, L. Lugo, L. Fedele and S. Bobbo, *Nanoscale Research Letters* 12 (2017) 53.

5. E.J. Kim, A. Desforges, L. Speyer, J. Ghanbaja, J. Gleize, P. Estellé and B. Vigolo, *Journal of Nanofluids* 6 (2017) 603-613.
6. P. Bansal, A.S. Panwar and D. Bahadur, *Journal of Physical Chemistry C* 121 (2017) 9847–9859.
7. R. Kamatchi, S. Venkatachalapathy and B. Abhinaya Srinivas, *International Journal of Thermal Sciences* 97 (2015) 17-25.
8. W. Tesfai, P. Singh, Y. Shatilla, M.Z. Iqbal, A.A. Abdala, *Journal of Nanoparticle Research* 15 (2013) 1989.
9. M. Mehrali, E. Sadeghinezhad, S.T. Latibari, S.N. Kazi, M.N.B.M. Zubir and H.S.C. Metselaar, *Nanoscale Research Letters* 9 (2014) 15.
10. Z. Zheng, *Advanced Materials Research* 1082 (2015) 297-301.
11. N. Ahammed, L.G. Asirvatham and S. Wongwises, *Journal of Thermal Analysis and Calorimetry* 123 (2016) 1399-1409.
12. W.S. Hummers Jr., R.E. Offeman, *Journal of the American Chemical Society* 80 (1958) 1339-1339.
13. S. Halefadi, P. Estellé, B. Aladag, N. Doner and T. Maré, *International Journal of Thermal Sciences* 71 (2013) 111-117.
14. E.W. Lemmon, M.L. Huber, M.O. McLinden, *Reference Fluid Thermodynamic and Transport Properties (REFPROP); NIST Standard Reference Database; National Institute of Standards and Technology*, Gaithersburg, MD, USA, 2010.

NANOFLUIDS ANALYSIS MODEL - BASIS FOR COMPARISON AND PREDICTION

E.W. Marcelino, D. de O. Silva and R.R. Riehl*

National Institute for Space Research, INPE/DMC,
Av dos Astronautas 1758, São José dos Campos, 12227-010 SP Brazil

*Corresponding author: roger.riehl@inpe.br

Keywords: Thermal enhancement, Viscosity, Statistical model, Nanofluids

Abstract: With current increase on the application of nanofluids to enhance the heat transfer capabilities of systems, there is a challenge to accurately compare the available nanofluid results from different authors. Researches show several experimental data using Al_2O_3 (alumina) and CuO (copper oxide) nanofluids, which lead to potentially applying them in several areas, especially industrial and aerospace. However, when comparing the results obtained by different authors, discrepancies are observed even for the same nanoparticle material and size used to form the nanofluid, which directly impact the results related to thermal conductivity, viscosity and density. Therefore, this study has the objective to evaluate some available results in the literature for CuO-water nanofluids comparing the obtained thermal enhancement results with the nanoparticle sizes used, as well as the direct influence on their viscosities. The objective is to provide some statistical trends through the reviewed data by using CuO-water nanofluid based on their particular characteristics.

Introduction:

The study of nanofluids has increased since Choi [1] established the term "nanofluids". Several nanofluid thermophysical properties and their characteristics have been experimentally tested and studied such as viscosity, density and thermal conductivity. Thermal conductivity is the most studied nanofluid property due to the fact that it is related to the increase on the nanofluid thermal enhancement levels obtained when compared to the base fluids. The most used base fluids for preparing the nanofluid are water, ethylene glycol and engine oil, which can be widely applied to several industrial, aerospace and automotive needs. The study of nanoparticle size and its influence on thermal conductivity has been of great interest for several authors [2]. In general, theoretical and experimental studies included the impact of nanoparticles sizes in their models. It is common to find in the literature the average nanoparticle sizes through statistical data over a range of nanoparticle size distribution. However, it is unusual to obtain the same nanoparticle size and shape over the volume concentration (vol.%) of nanoparticles used in any nanofluid.

Thermal conductivity and viscosity models related to nanoparticle sizes:

A review on the literature was performed to evaluate the results obtained for CuO-water nanofluid, related to the thermal conductivity and viscosity models. Tables 1 and 2 summarize

the investigated models and demonstrate how each one consider the nanoparticle size influence on the thermal conductivity or thermal enhancement ratio [3]. The thermal conductivity determination depends on other parameters besides nanoparticle sizes, such as volume fraction, temperature and sonication time. It is clear that even using the same CuO nanoparticle sizes, volume fractions and sonication times different results were obtained by different authors. This is directly related to differences on the nanoparticle purity and preparation from one study to another, as well as differences on nanoparticle shape and average sizes. Following the same trend, Table 3 shows the viscosity models available as well as their considerations on the direct impact on the nanofluid [3]. Since the nanoparticle addition on the base fluid directly changes the nanofluid's dynamic viscosity, the pumping power required to drive the nanofluid throughout the system may present higher levels than those predicted previously.

Table 1. A summary of thermal conductivity models.

Author	Model	Comments
Maxwell [4]	$k_{eff} = k_p + 2k_f + 2\phi_p(k_p - k_f)$ $k_f = k_p + 2k_f - \phi_p(k_p - k_f)$	Based on spherical particles, random suspensions which must be under conduction solution theory through stationary conditions
Hamilton [5]	$k_{eff} = \frac{k_p + (n-1)k_f + (n-1)\phi_p(k_p - k_f)}{k_p + (n-1)k_f - \phi_p(k_p - k_f)}$	For high concentrations of spherical particles under conditions of differential effective medium (DEM) theory
Prasher et al. [6]	$k_{eff} = (1 + AR e^m Pr^{0.333} \phi_p) \left[\frac{k_p + 2k_f + 2\phi_p(k_p - k_f)}{k_p + 2k_f - \phi_p(k_p - k_f)} \right] k_f$	Obtained from Maxwell model and included the effects of correction generated by the Brownian motion
Koo and Kleinstreuer [7]	$k_{eff} = k_{static} + k_{Brownian}$ $k_{static} = \frac{k_p + 2k_f + 2\phi_p(k_p - k_f)}{k_p + 2k_f - \phi_p(k_p - k_f)}$ $k_{Brownian} = 5 \times 10^4 \beta \phi_p \rho_p c_p \sqrt{\frac{k_B T}{\rho_p D}} (T, \phi_p)$	Considers the effects of surrounding liquid motion with random nanoparticles movement. Based on static Maxwell theory and dynamic effect of Brownian motion
Yu and Choi [8]	$k_{eff} = \frac{k_p + 2k_f + 2\phi(k_{pe} - k_f)(1 + \beta)^3}{k_{pe} + 2k_f - \phi(k_{pe} - k_f)(1 + \beta)^3} k_f$ $k_{pe} = \frac{2(1 - \gamma) + (1 + \beta)^3(1 + 2\gamma)\gamma}{-(1 - \gamma) + (1 + \beta)^3 + (1 + 2\gamma)} k_p$	It was based on Maxwell model but additionally taking into account the effects of nanolayer thickness and thermal conductivity parameters

Even with the gain obtained with the increase on the thermal conductivity and on the overall heat transfer capability may not be worth applying the nanofluid, due to the increase on the pumping power and the direct impact on the increase of the energy required to run the cycle. Therefore, the entire system would require to be redesigned increasing its hydraulic diameter to compensate the increase on the pressure drop. However, the tradeoff must be carefully considered and most often, redesigning the system will be well paid off due to the increase on the overall heat transfer compared to the drawback caused by the increase on the pressure drop.

Table 2. Different nanoparticle sizes applied in CuO-water nanofluid and their respective thermal enhancement ratios.

Author	CuO Nanoparticle Size (nm)	Thermal Enhancement Ratio	Volume Fraction (vol.%)	Temperature (°C)	Sonication Time (h)
Karthikeyan et al [9]	8.0	1.020	0.020	20	0.5
	8.0	1.080	0.090	20	0.5
	8.0	1.130	0.100	20	0.5
	8.0	1.190	0.300	20	0.5
	8.0	1.250	0.800	20	0.5
	8.0	1.316	1.000	20	0.5
Nemade et al [10]	33.0	1.197	0.500	55	1
	42.0	1.134	0.500	55	0.75
	46.0	1.124	0.500	55	0.5
	53.5	1.087	0.500	55	0.25
Khedkar et al [11]	25.0	1.050	0.010	26	1.5
	25.0	1.120	0.020	26	1.5
	25.0	1.130	0.030	26	1.5
	25.0	1.160	0.040	26	1.5
	25.0	1.170	0.050	26	1.5
	25.0	1.320	0.075	26	1.5
Wang et al [12]	42.5	1.080	0.020	25	not informed
	42.5	1.100	0.040	25	
	42.5	1.110	0.100	25	
	42.5	1.125	0.150	25	
	42.5	1.160	0.400	25	
Pryia et al [13]	50.0	1.020	0.004	28	6
	50.0	1.060	0.008	28	6
	50.0	1.100	0.012	28	6
	50.0	1.130	0.016	28	6
	50.0	1.050	0.004	50	6
	50.0	1.160	0.008	50	6
	50.0	1.250	0.012	50	6
	50.0	1.320	0.016	50	6
	50.0	0.950	0.004	55	6
	50.0	1.240	0.008	55	6
	50.0	1.330	0.012	55	6
	50.0	1.430	0.016	55	6

Table 3. Viscosity models.

Author	Model	Comments
Einstein [14]	$\mu_{eff} = (1 + 2.5\phi_p)\mu_f$	Based on phenomenological hydrodynamic equation for infinitely diluted suspensions of spheres with no interaction between spheres. Works well for maximum volume concentration of 2%
Brinkman [15]	$\mu_{eff} = \frac{1}{(1 + 2.5\phi_p)^{2.5}}\mu_f = (1 + 2.5\phi_p + 4.375\phi_p^2 + \dots)\mu_f$	Extended Einstein's model by considering the effect of addition of one solute molecule to an existing solution.
Buongiorno [16]	$\mu_{eff} = (1 + 39.11\phi_p + 533.9\phi_p^2)\mu_f$ $\mu_{eff} = (1 + 5.45\phi_p + 108.2\phi_p^2)\mu_f$	Curve fitting from experimental data of Al2O3-water nanofluid
Nguyen et al. [17]	$\mu_{eff} = \mu_f 0.904e^{0.148\phi_p}$ $\mu_{eff} = (1 + 0.025\phi_p + 0.015\phi_p^2)\mu_f$	Curve fitting from experimental data of Al2O3-water nanofluid
Chen et al. [18]	$\mu_{nf} = \mu_{bf} [1 + 10.6\phi_p + (10.6\phi_p)^2]$	Adjusted model for experimental versus theoretical data by considering the rheological effects of shear-rate
Kulkarni et al. [19]	$\ln(\mu_{eff}) = A\left(\frac{1}{T}\right) - B$ $A = 20587\phi_p^2 + 15857\phi_p + 1078.3$ $B = -107.12\phi_p^2 + 53.54\phi_p + 2.8715$	Curve fitting from experimental CuO-water: 5% < ϕ_p < 15% dp=29 nm; 278 < T(K) < 323; shear rate = 100 l/s
Namburu et al. [20]	$\log(\mu_{eff}) = Ae^{-BT}$ $A = -0.29956\phi_p^3 + 6.738\phi_p^2 - 55.444\phi_p + 236.11$ $B = -6.4745\phi_p^3 + 140.03\phi_p^2 - 1478.5\phi + 20341$	Curve fitting from experimental data of Al2O3-ethylene-glycol nanofluid: 1% < ϕ_p < 10%; dp=53 nm; 278<T (K)<323
Adedijan et al. [21]	$\mu_{nf} = \frac{\mu_{bf}}{\left(1 - \frac{5}{2}\phi_p\right)}$	Extention of Einstein's equation for obtaining good agreement in volume concentration ranges of up to 18-20% in suspension system non-interacting with spherical particles.
Meybodi et al. [22]	$\mu_{nf} = \mu_{bf} \frac{A_1 + A_2 \exp\left(\frac{\phi_p}{S}\right) + A_3 \left[\exp\left(\frac{\phi_p}{S}\right)\right]^2 + A_4 \left[\exp\left(\frac{\phi_p}{S}\right)\right]^3}{A_5 + A_6 \frac{\ln(S)}{T} + A_7 \frac{[\ln(S)]^2}{T}}$ $A_1 = 1.3354064976 \times 10^2$ $A_2 = -3.4382413843 \times 10^2$ $A_3 = 2.9011804759 \times 10^2$ $A_4 = -78993120761 \times 10^1$ $A_5 = 9.1161630781 \times 10^{-1}$ $A_6 = 3.2330142333 \times 10^1$ $A_7 = -1.1732514460 \times 10^1$	Model obtained from experimental data, which takes into account volume concentration, nanoparticles size and temperature

Conclusions:

The following conclusions can be derived from this study:

- Nanoparticle size can vary according to sonication time;

- As nanoparticle sizes increases, the thermal conductivity decreases;
- Further investigation is necessary for better understanding the impacts over each size percentage of the statistical nanoparticle size distribution versus thermal and pressure drop enhancement ratios;
- The addition of solid nanoparticles in the base fluid directly cause the increase on the nanofluid's viscosity, which impacts on the increase of the overall pressure drop. Proper consideration on the tradeoff related to the enhancement of the overall thermal capability of the system compared to the increase of the pumping power must be done in order to better evaluate the application of nanofluids.

Better evaluation regarding the nanofluid design and application needs to be performed, in order to better predict their thermal behavior, along with the impact on the overall pressure drop. A statistical model that considers the most important aspects of a nanofluid can highly contribute to this purpose.

References

1. S.U.S Choi, Enhancing thermal conductivity of fluids with nanoparticles, *ASME FED* 231 99–105 1995.
2. S.K. Das, S.U.S Choi, W. Yu, T. Pradeep, *Nanofluids Science and Technology*, John Wiley & Sons Inc., New Jersey, 2008.
3. E.W. Marcelino, D. Silva, R.R. Riehl, A review on the influence of nanoparticle size in thermal management of CuO-water nanofluids and their characteristics, *Heat Powered Cycles Conference*, Nottingham, UK, June 27-29, 2016.
4. J.C. Maxwell, *A Treatise on Electricity and Magnetism*, Clarendon Press, 2^a Ed., Oxford, UK, 1881.
5. R.L. Hamilton, Thermal conductivity of heterogeneous two-component systems, *Ind Eng Chem Fundam* 1 (1962)182-191.
6. R. Prasher, P. Bhattacharya, P.E. Phelan, Thermal conductivity of nanoscale colloidal solutions (nanofluids), *Phys Rev Lett.* 94 (2005)1-4.
7. J. Koo, C. Kleinstreuer, Laminar nanofluid flow in microheat-sinks, *Int J Heat and Mass Transfer* 48 (2005) 2652-2661.
8. W. Yu, S.U.S. Choi, The role of interfacial layers in the enhanced thermal conductivity of nanofluids: a renovated Maxwell model, *J. Nanoparticle Research* 5 (2003) 167-171.
9. N.R. Karthikeyan, J. Philip, B. Raj, Effect of clustering on the thermal conductivity of nanofluids, *Material Chem. Phys.*, 109 (2008) 50–55.
10. K. Nemade, S. Waghuley, A novel approach for enhancement of thermal conductivity of CuO/H₂O based nanofluids, *Applied Thermal Eng.* 95(2016)271-274.
11. R.S. Khedkar, S.S. Sonawane, K.L. Wasewar, Influence of CuO nanoparticles in enhancing the thermal conductivity of water and monoethylene glycol based nanofluids, *Int Comm in Heat and Mass Transfer* 39(2012)665-669.
12. X.J. Wang, X.F. Li, Influence of pH on nanofluids' viscosity and thermal conductivity, *Chin Phys Lett* 26(2009)056-061.

13. K.R. Priya, K.S. Suganthi, K.S. Rajan, Transport properties of ultra-low concentration CuO–water nanofluids containing non-spherical nanoparticles, *Int J of Heat and Mass Transfer* 55(2012)4734-4743.
14. A. Einstein, Eine neue bestimmung der moleküldimensionen, *Ann Phys* 324(1906)289–306.
15. H. Brinkman, The viscosity of concentrated suspensions and solutions, *J Chem Phys* 20 (1952) 571–571.
16. J. Buongiorno, Convective transport in nanofluids, *Journal of Heat Transfer* 128(2006)240-250.
17. C.T. Nguyen, F. Desgranges, G. Roy, N. Galanis, T. Mafe, S. Boucher, H.A. Mintsa, Temperature and particle-size dependent viscosity data for water-based nanofluids - hysteresis phenomenon, *Int J Heat Fluid Flow* 28(2007)1492-156.
18. H. Chen, Y. Ding, C. Tan. Rheological behaviour of nanofluids, *New Journal of Physics* 9 (2007) 367.
19. D.P. Kulkarni, D.K. Das, S.L. Patil, Effect of temperature on rheological properties of copper oxide nanoparticles dispersed in propylene glycol and water mixture, *J Nanoscience Nanotechnology*, 7(2007)2318-2322.
20. P.K. Namburu, D.K. Das, K.M. Tanguturi, R.S. Vajjha, Numerical study of turbulent flow and heat transfer characteristics of nanofluids considering variable properties, *Int J Therm Science* 48(2009)290-302.
21. B. Abedian, M. Kachanov, On the effective viscosity of suspensions, *Int J Eng Sci* 48(2010)962–5.
22. M.K. Meybodi, A. Daryasafara, M.M. Koochia, J. Moghadasia, R.B. Meybodib, A.K. Ghahfarokhia, A novel correlation approach for viscosity prediction of water based nanofluids of Al₂O₃, TiO₂, SiO₂ and CuO, *Journal of Taiwan Institute of Chemical Engineers* 58(2015)19-27.

A NEW ANALYTICAL MODEL FOR THE EFFECTIVE THERMAL CONDUCTIVITY OF NANOFLUIDS

T.M. Koller*, K.N. Shukla, M.H. Rausch and A.P. Fröba

Erlangen Graduate School in Advanced Optical Technologies (SAOT),

Friedrich-Alexander-University Erlangen-Nürnberg (FAU),

Paul-Gordan-Straße 6, D-91052 Erlangen, Germany

*Corresponding author: thomas.m.koller@fau.de

Keywords: Effective thermal conductivity, Modeling, Nanofluids, Nanoparticles

Introduction: Dispersions of nanometer-sized particles in liquids, usually called nanofluids, have been reported to possess substantially higher thermal conductivities than anticipated from Maxwell's classical theory [1]. A large number of experimental results have claimed an anomalous increase in the thermal conductivity of nanoparticle suspensions [2], which would make them very attractive as potential heat transfer fluids for many applications. However, results from other experiments have not shown any anomalous increase in thermal conductivity [2,3]. This has triggered controversy regarding the actual value of the thermal conductivity of nanofluids and the reliability of the experimental methods.

The aim of the present study is to develop a new analytical model for the effective thermal conductivity of macroscopically static nanofluids taking into account the heat transfer mechanisms caused by convection as well as thermal conduction of the particles and the base fluid. It should enable the prediction of the temperature-dependent effective thermal conductivity of nanofluids as a function of volume fraction, diameter, and shape of the nanoparticles. The main information on our developed model [4] is given below.

Description of the model: In the presented analytical model, the thermal resistances of the base fluid and the nanoparticles as well as of convection induced in the fluid due to Brownian motion of the nanoparticles are determined. It is assumed that N nanoparticles of spherical shape with diameter d_p are uniformly suspended in a volume V of the nanofluid. By this, a corresponding volume fraction of the nanoparticles φ is given. The volume V is divided into N equal parts such that each nanoparticle is located in a cube with a side of length L . Fig. 1a depicts a three-dimensional sketch of such a nanoparticle-cube system.

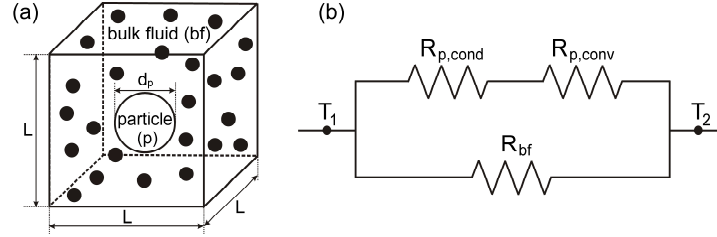


Fig. 1: (a) Conceptual three-dimensional sketch of a cube with length L containing a spherical nanoparticle of diameter d_p and bulk fluid molecules. (b) Circuit diagram for the thermal resistances of the bulk fluid due to conduction and of the nanoparticle due to conduction and convection associated with Brownian motion.

The basic idea of the present modeling approach is to treat the heat transfer problem in connection with nanofluids by the analysis of the thermal resistances present in such systems. In Fig. 1b, the corresponding circuit diagram for the total thermal resistance of the nanofluid R_{eff} subjected to a temperature difference between the hot temperature T_1 and cold temperature T_2 is illustrated based on the cube shown in Fig. 1a. The thermal resistance of the base fluid, R_{bf} , is considered to be parallel to the thermal resistance of the nanoparticle, R_p . Thus, R_{eff} can be expressed by

$$\frac{1}{R_{eff}} = \frac{1-\varphi}{R_{bf}} + \frac{\varphi}{R_p}. \quad (1)$$

Arranging the resistances of the bulk fluid and the particles in parallel is reasonable because a heat flux can be either conducted through the base fluid or through the particle along a one-dimensional temperature gradient. The key for a realistic description of the thermal resistance of the nanofluid is that the base fluid as a continuum fluid phase is analogously treated as a continuum resistance. To account for the volumes in which the resistances of the two phases are present, the inverse values of the thermal resistances R_{bf} and R_p are weighted in Eq. (1) by the corresponding volume fractions $(1-\varphi)$ and φ .

R_{eff} and R_{bf} are related to the thermal conductivities k_{eff} and k_{bf} , respectively, and the cube geometry. The thermal resistance caused by heat transfer between the nanoparticles and the boundary layer is modeled by the resistance of the sphere due to thermal conduction, $R_{p,cond}$, and by that due to convection at its surface, $R_{p,conv}$, in series. The term $R_{p,conv}$ depends on the surface area of the particle A_p and the convective heat transfer coefficient h . The latter can be expressed by a corresponding correlation for the Nusselt number Nu for creep flow around nanoparticles. In connection with A_p , the sphericity of a particle can be used which is the ratio of the surface area of a sphere, $A_{p,sph}$, having the same volume as the particle, V_p , to the surface area of the particle, A_p . Decreasing sphericity of the particles ($\psi < 1$) results in an increasing surface area and a decreasing value for $R_{p,conv}$.

The final simple expression for the dimensionless effective thermal conductivity k_{eff}/k_{bf} of nanofluids containing spherical or non-spherical particles

$$\frac{k_{\text{eff}}}{k_{\text{bf}}} = (1 - \varphi) + \pi \left(\frac{6}{\pi} \right)^{1/3} \varphi^{4/3} \left[\frac{1 + 0.5 \left(\frac{6\varphi}{\pi} \right)^{1/3}}{2} \left(\frac{k_{\text{bf}}}{k_{\text{p}}} \right) + \frac{\psi}{Nu} \right]^{-1} \quad (2)$$

contains three contributions. The first term $(1 - \varphi)$ considers the influence of the bulk fluid while the second term is related to the nanoparticles. In the latter term, the brackets include the contributions from conduction through the particles (associated with the thermal conductivity of the particle k_{p}) and from convective heat transfer between the particles and the bulk fluid (given by ψ/Nu).

Discussion and Results: To analyze the quality of our model for the effective thermal conductivity of nanofluid systems by Eq. (2), we selected the four simple systems $\text{Al}_2\text{O}_3/\text{H}_2\text{O}$, $\text{TiO}_2/\text{H}_2\text{O}$, $\text{Al}_2\text{O}_3/\text{EG}$, and TiO_2/EG , containing the liquids water (H_2O) and ethylene glycol (EG) as well as the particles aluminum oxide (Al_2O_3) and titanium dioxide (TiO_2). Data for the thermophysical properties of the nanoparticles and base fluids at atmospheric pressure were employed from literature.

In Fig. 2a, the percentage enhancement factor $(k_{\text{eff}}/k_{\text{bf}} - 1)$ calculated according to Eq. (2) is shown as a function of the volume fraction φ of spherical particles for the two systems $\text{Al}_2\text{O}_3/\text{EG}$ and $\text{TiO}_2/\text{H}_2\text{O}$ at a temperature of $T = 300$ K. Regarding the influence of convection, the enhancement found on basis of our model, which includes the effect of convection due to Brownian motion, is compared with a "theoretical" enhancement which does not account for this effect. The system related to the latter enhancement would consist of static particles suspended in the liquid, neglecting any thermal resistance in the boundary layer where heat is transferred from the liquid to the solid particle. In this case, $R_{\text{p,conv}} = 0$ which is equivalent to omitting the term ψ/Nu in Eq. (2). Neglecting the thermal resistance contribution from the convective heat transfer between particles and base fluid results in much larger enhancement factors because the thermal resistance of the nanoparticle is significantly reduced to only the resistance of conduction through the particle $R_{\text{p,cond}}$. Of course, an enhancement of the convective heat transfer with, e.g., increasing Nu numbers decreases the corresponding resistance, but this effect is rather small with respect to k_{eff} . This is caused by the almost stagnant flow behavior of nanoparticles in the fluid. These findings valid for nanofluids with spherical particles are in contradiction to the widely spread opinion in the literature [5,6] that convection associated with Brownian motion of the particles is mainly responsible for the enhancement of the effective thermal conductivity of nanofluids.

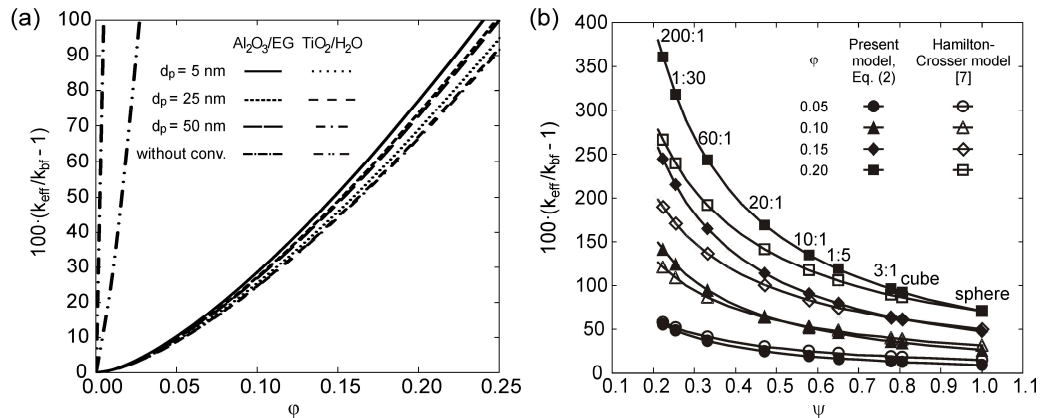


Fig. 2: (a) Percentage enhancement factor ($k_{\text{eff}}/k_{\text{bf}} - 1$) on the basis of Eq. (2) as a function of the volume fraction ϕ for different diameters d_p of spherical particles at $T = 300$ K for the nanofluids $\text{Al}_2\text{O}_3/\text{EG}$ and $\text{TiO}_2/\text{H}_2\text{O}$. (b) Percentage enhancement factor as a function of the sphericity of the particle ψ at $T = 300$ K for the nanofluid $\text{Al}_2\text{O}_3/\text{H}_2\text{O}$ containing volume-equivalent (diameter 30 nm) nanoparticles of different shape calculated by the present model (Eq. (2)) and the Hamilton-Crosser model [7] for various ϕ values.

Fig. 2a also shows that the effective thermal conductivity increases with increasing ϕ . Mainly due to the about eight times larger k_p/k_{bf} ratio for $\text{Al}_2\text{O}_3/\text{EG}$ than for $\text{TiO}_2/\text{H}_2\text{O}$, enhancement in the effective thermal conductivity is stronger for $\text{Al}_2\text{O}_3/\text{EG}$ for a given particle size. For $\phi = 0.25$ and $d_p = 5$ nm, a difference in the enhancement of about 11% is found for the two nanofluids. For all the systems studied, $k_{\text{eff}}/k_{\text{bf}}$ decreases with increasing particle size. The influence of temperature on the effective thermal conductivity enhancement of nanofluids is even less pronounced for various ϕ and d_p values.

Due to the obscure situation of experimental data in the literature [2], we preferred to check our model by comparing with other common models in the literature. Here, the effective medium model of Hamilton and Crosser [7] is considered to be one of the most reliable ones. For all the nanofluid systems tested, very good agreement between our model and the continuum model of Hamilton and Crosser [7] for various particle volume fractions is found. Regarding the enhancement factors, the relative deviations between the continuum model and ours are less than 8% for volume fractions between 0 and 0.25 for the studied conditions. Also for varied temperatures and particle diameters, this deviation is not exceeded. The very good agreement of the Hamilton-Crosser model [7] with our model indicates that the convective heat transfer associated with the Brownian motion of the nanoparticles needs to be considered for the heat transfer in nanofluids.

In Fig. 2b, the enhancement of the thermal conductivity ($k_{\text{eff}}/k_{\text{bf}} - 1$) modeled according to our prediction from Eq. (2) is exemplarily shown as a function of the sphericity of the particle ψ for the nanofluid $\text{Al}_2\text{O}_3/\text{H}_2\text{O}$ containing particles with $d_p = d_{p,\text{eq}} = 30$ nm at $T = 300$ K and different volume fractions ϕ . Spherical particles are compared with cubic particles as well as seven cylindrical particles with varying aspect ratios, i.e., the ratio of length to diameter, which are specified in Fig. 2. While prolate cylindrical particles have aspect ratios larger than 1, they are smaller for oblate particles.

Also for systems with non-spherical nanoparticles, our modeled data and those predicted by Hamilton and Crosser [7] agree well for the various particle geometries. Both models show that decreasing sphericity of the nanoparticles goes along with a distinct increase in the effective thermal conductivity. For example, our model predicts that the enhancement for cylinders with an aspect ratio of 10:1 ($\psi = 0.58$) is already twice as large as that for spherical particles ($\psi = 1$). The reduced convective heat transfer resistance caused by the larger specific surface area of non-spherical particles compared to spherical particles seems to reasonably account for the increased enhancement factors in our developed model. Furthermore, the trends regarding the distinct influence of the volume fraction and the negligible influences of temperature as well as particle diameter on the enhancement of the thermal conductivity found for systems containing spherical particles can also be observed for the corresponding systems containing non-spherical particles.

Conclusions: A new analytical model for the effective thermal conductivity in fluids containing well-dispersed spherical and non-spherical nanoparticles is presented. It reveals the significant role of the convective heat transfer resistance in reducing the effective thermal conductivity of a nanofluid compared with a theoretical nanofluid showing no thermal contact resistance between particle and base fluid. The convective heat transfer resistance turned out to control the achievable thermal conductivity enhancement. For four typical nanofluid systems, very good agreement was found between our calculation results and the commonly recommended model from Hamilton and Crosser [7]. In accordance with this continuum model, our model does also not show any anomalous enhancement of the effective thermal conductivity of nanofluids for low volume fractions of spherical nanoparticles as it is often reported in the literature. The present model also suggests that a stronger enhancement in the effective thermal conductivity of nanofluids is found using non-spherical particles due to their larger volume-specific surface areas. A further reduction of the convective heat transfer restrictions can be expected by the formation of rows of nanotubes having a large surface to volume ratio.

References:

1. J.C. Maxwell, *A Treatise on Electricity and Magnetism*, Clarendon, Oxford, 1892.
2. G. Tertsinidou, M.J. Assael, and W.A. Wakeham, The apparent thermal conductivity of liquids containing solid particles of nanometer dimensions: A critique, *Int. J. Thermophys.* 36 (2015) 1367-1395.
3. P. Keblinski, J.A. Eastman, and D.G. Cahill, Nanofluids for thermal transport, *Mater. Today* 8 (2005) 36-44.
4. K.N. Shukla, T.M. Koller, M.H. Rausch, and A.P. Fröba, Effective thermal conductivity of nanofluids – A new model taking into consideration Brownian motion, *Int. J. Heat Mass Transf.* 99 (2016) 532-540.
5. S.P. Jang and S.U.S. Choi, Role of Brownian motion in the enhanced thermal conductivity of nanofluids, *Appl. Phys. Lett.* 84 (2004) 4316-4318.
6. J. Koo and C. Kleinstreuer, A new thermal conductivity model for nanofluids, *J. Nanopart. Res.* 6 (2004) 577-588.
7. R.L. Hamilton and O.K. Crosser, Thermal conductivity of heterogeneous two-component systems, *Ind. Eng. Chem. Fundam.* 1 (1962) 187-191.

METAL OXIDE NANOFUIDS FOR ENHANCING THERMAL PROPERTIES THROUGH AN EXPERIMENTAL AND THEORETICAL PERSPECTIVE

A. Sánchez-Coronilla^{1*}, J. Navas^{2*}, E.I. Martín³, T. Aguilar², R. Gómez-Villarejo², J.J. Gallardo², P. Martínez-Merino², R. Alcántara² and C. Fernández-Lorenzo²

¹Departamento de Química Física, Universidad de Sevilla, Spain

²Departamento de Química Física, Universidad de Cádiz, Spain

³Departamento de Ingeniería Química, Universidad de Sevilla, Spain

*Corresponding authors: antsancor@us.es; javier.navas@uca.es

Keywords: Nanofluid, Concentrating Solar Power, Heat Transfer Fluid, Thermal Conductivity

Introduction: Concentrating Solar Power (CSP) is one of the most interesting options as renewable energy today. In plants based on parabolic mirrors, a thermal fluid flowing through a tube covered with a coating capable of absorbing radiation is used. The absorbed radiation heats the thermal fluid. One option in order to improve the efficiency of the plants is to enhance the thermal properties of the heat transfer fluid (HTF) by using nanofluids. Suspending nanoparticles in an HTF has been shown to improve properties such as the thermal conductivity, the heat transfer coefficient or the isobaric specific heat [1-4]. A typical HTF used in CSPs is a eutectic mixture of biphenyl (C₁₂H₁₀) and diphenyl oxide (C₁₂H₁₀O). In the present work we have used this eutectic mixture as base fluid in the preparation of NiO nanofluids with benzalkonium chloride (BAC) and 1-octadecanethiol (ODT) as surfactants. The stability of the nanofluid was analysed using techniques as UV-vis spectroscopy, particle size measurements using the dynamic light scattering technique and ζ potential measurements. Properties as density, viscosity, heat capacity, and thermal conductivity were characterized. The NiO nanofluids improved the thermal properties and the heat transfer coefficient compared with the HTF. In addition, we also report a molecular dynamics study of the NiO nanofluids described before. The structural properties of these systems were determined by analysing their radial distribution function (RDF) and spatial distribution function (SDF). The significant thermal properties such as the isobaric specific heat and thermal conductivity were obtained theoretically and were shown to follow the same tendency as values obtained experimentally, which validates the theoretical study method proposed. From the theoretical results the interactions between the NiO nanoparticles and the oxygen from the diphenyl oxide of the base fluid were shown to play a key role in the structural disposition of the fluid around the metal. That structural disposition can explain the improvement of the thermal properties and the heat transfer coefficient of the NiO-nanofluids compared with the HTF.

Discussion and Results: Our results show that a high proportion of BAC is necessary for improving the stability of nanofluids as compared with the presence of ODT. The presence of

phenyl groups from BAC may be stabilised with the base fluid molecules. In this sense, the theoretical analysis agree with those results. As an example, Figure 1 shows the SDF for the nanofluid. In this Figure, the red lobes are the oxygen atoms and the blue sky ones, the C atoms from the diphenyl oxide molecules that are distributed around the NiO (yellow colour). There are 7 diphenyl oxide molecules around the metal oxide. The BAC molecules are depicted in green (C atoms) and violet colour (N atoms). An increase in the values of both isobaric specific heat and thermal conductivity as compared with the base fluid are observed experimentally for the experimental proportions that are also theoretically assessed.



Figure 1. SDF from the NiO nanofluid.

Conclusions: The addition of NiO nanoparticles in the HTF fluid increases thermal properties of the nanofluid considerably. Thus, an enhancement of the conductivity is observed experimentally for this metal oxide nanofluid as compared with the values from the base fluid. The theoretical results agree with the experimental tendency for isobaric specific heat and thermal conductivity values. Our results indicate the interactions between the metal oxide and the oxygen from the base fluid play a key role in the structural disposition of the fluid around the metal oxide. This disposition may be involved in the increase of the thermal properties of the NiO-nanofluid compared with the base fluid.

References:

1. D.H. Yoo, K.S. Hong and H.S. Yang, Study of thermal conductivity of nanofluids for the application of heat transfer fluids, *Thermochimica Acta* 455 (2007) 66-69.

2. S.M.S. Murshed and C.A. Nieto de Castro, *Nanofluids: Synthesis, Properties and Applications*, Nova Science Publishers Inc., New York, 2014.
3. S. Lee, S. Choi, S. Li and J.A. Eastman, Measuring thermal conductivity of fluids containing oxide nanoparticles, *Journal of Heat Transfer-T. Asme* 11 (1999) 280-289.
4. W.H. Yu, D.M. France, J.L. Routbort and S. Choi, Review and comparison of nanofluid thermal conductivity and heat transfer enhancements, *Heat Transfer Engineering* 29 (2008) 432-460.

MEASUREMENT OF ELECTROKINETIC MOBILITY OF COLLOIDAL PARTICLES CLOSE TO SOLID-LIQUID INTERFACE USING EVANESCENT WAVES

K. Shirai^{1*}, S. Kaji², T. Kawanami³ and S. Hirasawa²

¹Shibaura Institute of Technology, 3-7-5, Toyosu, Koto, 135-8548, Tokyo, Japan

²Kobe University, Kobe 657-8501, Japan

³Meiji University, Kanagawa 214-8571, Japan

*Corresponding author: kshirai@shibaura-it.ac.jp

Keywords: Thermal transport colloid, Nanofluids, Phase-change emulsion, Electrokinetic mobility, Measurement technique, Evanescent wave

Introduction: Thermal transporting colloids receive higher attentions in thermal engineering. Colloidal solutions containing nanometer-sized solid particles are called as nanofluids. They are widely investigated to clarify the possibilities of heat transfer enhancement since they have been reported to exhibit higher thermal conductivities compared to the mixture ratios. Another thermal transport colloid is emulsion made of phase-change materials [2] for thermal storage. The latent heat at the solid-liquid phase change can effectively store thermal energy compared to its volume.

In the solvent of colloidal solution, solute particles are dispersed by repulsive forces originating from electrical charges of their surface. When an electric field is induced to colloid, solute particles move according to the surface charge state and the induced field. The particles of thermal transporting colloid exhibit complex motion under heat transfer at a solid-liquid interface because of additional electrokinetic forces also coming from the charged surface of the solid wall. Hence, it is important to know the movement of the colloidal particles in the vicinity of a solid wall under heat transfer.

We developed a measurement system for investigating the complex mobility of colloidal particles near a solid wall. The principle is based on laser Doppler technique, which provides the mobility of colloidal particles in a direction parallel to the interfacial plane. We use

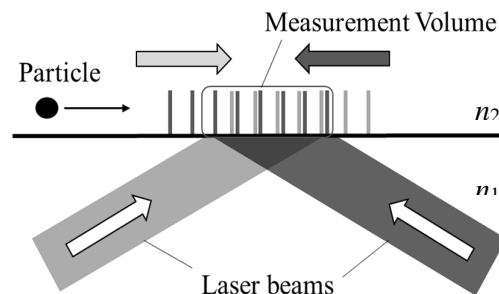


Fig. 1 Schematic of the laser-Doppler velocimetry using evanescent waves. The measurement volume is created by interference of two evanescent waves generated by total internal reflection of laser beams.

evanescent waves to realize the laser Doppler measurement. The measurement volume automatically restricted to the vicinity of a solid wall, because an evanescent wave has a very short penetration depth in the range of a few hundred nanometers at a solid-liquid interface. The measurement method had not been applied for electrokinetic studies of colloids since it was first proposed by Yamada [3]. Evanescent waves are also used in imaging techniques such as totally-internally reflected fluorescent microscopy, but they suffer from deteriorated image quality from nanometer-sized particles.

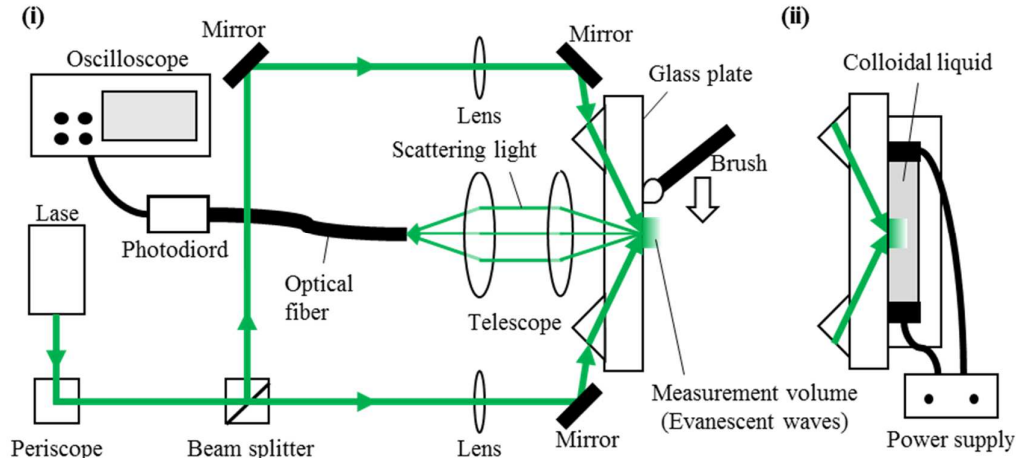


Fig. 2. Schematic overview of the measurement system: (i) scratching experiment on the glass surface with the Al_2O_3 particles and (ii) electrophoresis experiment of the Al_2O_3 particles. The optical setup was identical for both cases until the glass plate.

In the following, we report on the measurement system and its applications. We present the measurement principle and experimental results of submicrometer-sized particles.

Principle: We use evanescent waves created at the interface between colloidal liquid and a solid glass. An evanescent wave is generated at a total internal reflection of light incident at an angle beyond the critical value. The penetration depth of the evanescent wave is within a few hundred nanometers from the glass surface [4]. In the measurement, a pair of evanescent waves originated from a single-mode coherent laser source. The evanescent waves are intentionally created at a single point on the test surface so that they create an optical interference at the surface as Fig. 1. The interference pattern forms a fringe pattern perpendicular to the surface within the penetration depths of the evanescent waves. Colloidal particles passing through the measurement volume scatter the light and the resulting signals have modulation frequencies depending on the velocities of the colloidal particles in the direction perpendicular to the fringes. The velocity is measured through

$$u = f \cdot d, \quad (1)$$

with v , d , and f being the velocity, fringe spacing, and Doppler frequency. The fringe spacing d is derived as

$$d = \lambda / (2n_1 \sin \theta_i), \quad (2)$$

where λ , n_1 , θ_i are the wavelength, refractive index of the colloid, and the incident angle of the laser at the interface of the solid and liquid. Hence, the mobility of the colloidal particles is obtained by measuring the Doppler frequencies of the scattering light.

Experimental Setup: We developed a measurement system. Fig 2 (i) schematically shows the overview of the system and (ii) the experiment with colloidal test liquid at the test section. A continuous-wave laser (wavelength: 532 nm, single longitudinal mode) was employed as the light source. The measurement volume was formed on a BK7 (refractive index 1.519 for 532 nm light) glass surface by a pair of coherent evanescent light waves. The scattering light from the measurement volume was detected by receiving optics in the backward direction. The angle of total internal reflection was set to 64.1° , and the fringe spacing derived from Eq. (2) was $d = 195$ nm. The penetration depth of the evanescent waves was estimated to be 290 nm, based on the distance defined as the location where the intensity becomes $1/e$ of the initial amplitude at the interface [4]. The details of the system should be referred to another publication from our group [5].

Experiments: We carried out the following two experiments:

- (i) The measurement volume was scratched with Al_2O_3 particles (average diameter: 300 nm) put on the tip of a paint brush. The brush was moved by a hand and the velocity was maintained in the range of $O(10^{-2})$ m/s in the direction parallel to the glass surface. The scattering signals were obtained in a digital oscilloscope and the resulting power spectrum densities were obtained.
- (ii) Then, we attached the removable test section and filled with Al_2O_3 aqueous solution. A DC electric field with 4000 V/m was induced to the test colloid through the electrode. The particles move in the cell according to the combined effects of electrophoresis and electro-osmosis. The scattering signals were observed and the power spectrum densities were calculated from the time signals.

Result and Discussion: Fig. 3 exhibits typical time signal and the resulting power spectrum density of the signal in the experiment (i). The time signal forms a low frequency component with an arch shape corresponding to the Gaussian distribution of the optical intensity in the measurement volume. The signal also contains a high frequency component, which corresponds to the Doppler frequency. The sharp frequency peak around 260 kHz leads to the velocity 5.1×10^{-2} m/s based on Eq. (1). The velocity value agrees well with the expected moving velocity of the particles with the brush.

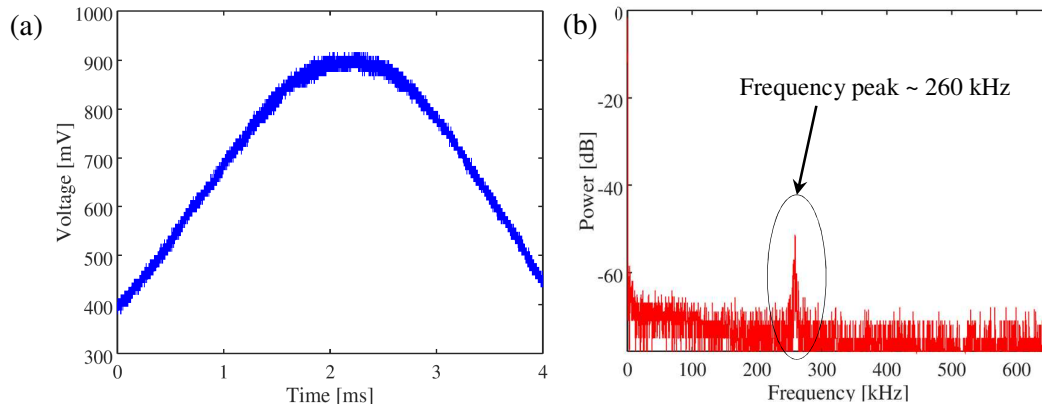


Fig. 3 Typical measurement result in the scratching experiment (i) using 300 nm Al_2O_3 particles, (a) time signal and (b) the resulting power spectrum density.

Fig. 4 shows the typical time signal and the resulting power spectrum density at the experiment (ii). The time signal oscillates with the amplitude of 1 mV and exhibits a frequency peak approximately at 130 Hz. The velocity derived from Eq. (1) becomes 2.5×10^{-5} m/s, which leads to a zeta potential of 8.8 mV through Helmholtz-Smoluchowski relation, provided that the Debye length is small compared to the flow dimension [6]. Indeed, the interpretation of the zeta potential value is not straightforward. The mobility was obtained in the vicinity of the solid wall, which should have been also electrically charged. Besides, the local flow in the cell was influenced by the combination of the electrophoresis and electro-osmosis. However, the magnitude of the zeta potential is considered to be reasonable, since the Al_2O_3 particles tended to aggregate shortly after they were mixed. Moreover, the power spectrum density in this case exhibits a peak broadened compared to the experiment (i). This is realistic because the signals are likely from multiple particles, which had slightly different velocities due to Brownian motion in the measurement volume. This feature is different from the single-particle realization of conventional laser Doppler velocimetry widely used in fluid mechanics measurements.

The above results indicate that the measurement of the particle mobility was feasible. The measured velocities obtained in the experiments were within the expected values in the same orders of magnitude. The next step is to measure the mobility of nanofluid particles. The measurement system has to be improved before the application. The photo detector has to be sufficiently sensitive to the Rayleigh scattering signals by nanometer-sized particles. The modulation depth of the scattering signals should also be improved as it affects the measurement uncertainty through the signal quality.

Summary: We developed a measurement system for investigating the complex relation between the electrokinetic mobility and heat transfer characteristics of colloids used for thermal transport applications. The system is based on laser Doppler method using a pair of evanescent waves formed at an interface between colloid and solid. The short penetration depth of the waves enables to restrict the measurements of electrokinetic mobility of colloids within a few hundred nanometers from a liquid-solid interface. We carried out two experiments and confirm the

feasibility of the measurement. In the next step, we apply the measurement system to Au nanofluids, which is undertaken at the laboratory.

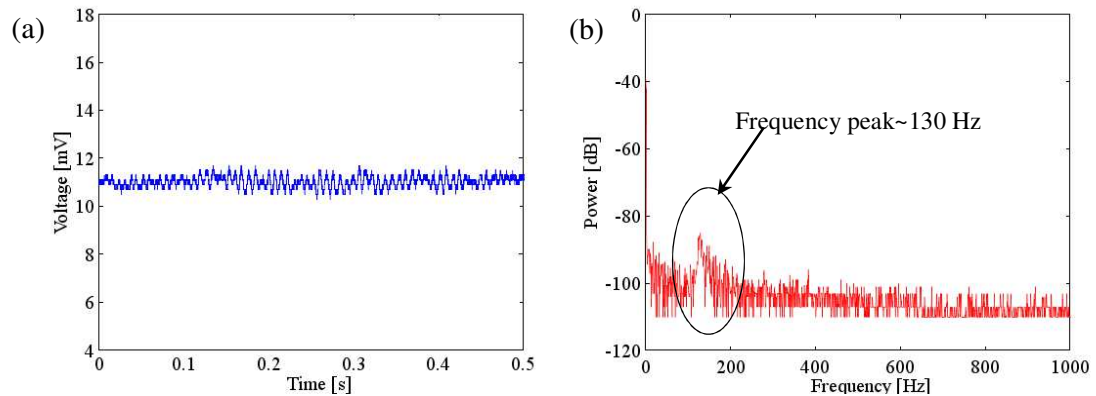


Fig. 4. Typical measurement result in the electrophoresis experiment (ii) using 300 nm Al_2O_3 particles, (a) time signal and (b) the resulting power spectrum density.

Acknowledgement: The present work was partially supported by the Tanikawa Fund Promotion of Thermal Technology, Mikiya Science and Technology Foundation, Kansai Research Foundation for Technology Promotion, TEPCO Memorial Foundation, JSPS KAKENHI (Grant Number JP17K17875) and the SIT Project Research.

References:

1. S.U.S. Choi and J.A. Eastman, Enhancing thermal conductivity of fluids with nanoparticles, *in: Development and Applications of Non-Newtonian Flows*, ASME New York, 231 (1995) 99–105.
2. T. Kawanami, K. Togashi, K. Fujimoto, S. Hirano, P. Zhang, K. Shirai, and S. Hirasawa, Thermophysical properties and thermal characteristics of phase change emulsion for thermal energy storage media, *Energy* 117 (2016) 562–568.
3. J. Yamada, Evanescent wave Doppler velocimetry for a wall's near field, *Applied Physics Letters*, 75 (1999) 1805–1806.
4. E. Hecht, *Optics*, 4th edition Pearson, Harlow, 2001.
5. K. Shirai, S. Kaji, T. Kawanami, S. Hirasawa, Development of measurement system using evanescent waves for characterizing colloidal liquids in heat transfer applications, *Int J of Comp Methods and Exp Measurements*, 5 (2017) 34–43.
6. R.F. Probstein, *Physicochemical Hydrodynamics*, 2nd edition John Wiley & Sons, Hoboken, 2003.

Abstracts

SESSION 3B: COOLING

ASSESSING THE FLOW CHARACTERISTICS OF NANOFLUIDS DURING TURBULENT NATURAL CONVECTION

K. Kouloulis^{1*}, A. Sergis and Y. Hardalupas

Imperial College London, Mechanical Engineering Department, London SW7 2AZ, UK

Corresponding author: k.kouloulis13@imperial.ac.uk

Keywords: Turbulent natural convection, Rayleigh-Benard, Nanofluids, Particle Image Velocimetry, Cooling

Introduction: Nanofluids have attracted significant attention due to their intriguing heat transfer properties under different heat transfer modes. According to an extended statistical analysis of data available in the literature, the heat transfer enhancement when nanofluids are involved is 5-9% for the conductive heat transfer, 10-14% for the mixed conductive-convective, 40-44% for pool boiling and up to 200% increase for the value of the critical heat flux [1]. Despite the reported promising heat transfer characteristics of nanofluids, the physical understanding of the underlying processes is missing and a controversy remains regarding their capability and applicability in engineering applications. This controversy arises from inconsistency in the observations of reported studies, accompanied by insufficient understanding of the physical mechanisms involved in nanofluids. For example, while heat transfer enhancement is reported for forced convection [2-5], opposing results are observed for natural convection with additional puzzling discrepancy between numerical [6-10] and experimental [11-14] natural convection studies. Two types of natural convection are distinguished based on the resulting flow conditions: laminar and turbulent. Out of those, turbulent natural convection has drawn greater attention due to the complex features associated with turbulence. In turbulent convection two discrete states have been identified according to the Rayleigh number, Ra , of the flow and the aspect ratio, Γ , of the employed cell. In cells with aspect ratios close to unity, a soft turbulent state has been observed for $Ra < 10^7$ and hard turbulence for Ra between 4×10^7 to 10^{12} [15-17], with the difference lying on the way in which the thermals and plumes are developed and traverse inside. It has been widely reported that, at the hard turbulent state, a large-scale coherent flow exists [18-20], which is self-organised by the hot rising and cold falling plumes. This flow mode is known as mean wind or large scale circulation (LSC). Up to date, the LSC remains an attractive feature to study and further analyse, as the heat transport in turbulent natural convection takes place primarily along the periphery of the cell, in the direction of the LSC [21, 22]. Therefore, the study of nanofluids under natural convection is an attractive way to assess the heat transfer properties of these new coolants and establish the underlying physical mechanisms.

Methodology: Experimental set-up: A classical Rayleigh-Benard (RB) configuration with optical access is operated in the current study. Fig. 1(a) shows a schematic drawing of the RB cell, including all the major components. A detailed description of this configuration can be found in Ref. [12], whilst a brief overview of its components is included herein. The cell consists of a

heating plate, A, at the bottom, a cooling plate, B, at the top and lateral walls, C. It incorporates four quartz windows, 2 square (40 mm x 40 mm) and 2 rectangular (10 mm x 40 mm), D, to allow laser-based visualization studies. Teflon plates, E, are inserted among all the conductive components to prevent their thermal connection. Finally, insulating pans, F and a Plexiglas cover, G are placed outside the core of the cell to eliminate the heat losses from the sides. At the same direction, a second set of heating elements, H is placed below the heating plate to prevent any heat losses downwards. The operation of the RB cell is monitored and controlled through LabVIEW software, coupled with National Instruments (NI) hardware and an in-house electrical device that is connected to the heating plates (A, H) and thermocouples placed in the cell.

Particle Image Velocimetry (PIV): A high spatial resolution (0.49 mm) flow velocimetry method, PIV, is employed for the test fluids inside the RB cell, through the available optical access. A double-pulsed Nd-Yag laser (Nano T 135-15 PIV) is used to illuminate micron-sized tracer particles (hollow glass spheres (HGS) with nominal diameter of 10 μm) dispersed in the flow. The particles are illuminated twice by the pulsed laser with fixed time interval (20 ms) on planes defined by a thin laser sheet. A charge coupled device camera (LaVision Imager Intense) is utilized to record the displacement via the change of the pattern of the intensity of the scattered light from the HGS particles during the time delay between the two laser pulses. Due to the small size of the tracers, no drift velocities are present between the liquid flow and the HGS for the timescales of the experiments. Commercial software (DaVis 8.2.2) is used to control the laser and process the recorded images. Each laser pulse pair is emitted at a rate of 0.25 Hz, while 2000 independent pairs of images of the instantaneous flow are recorded at steady state conditions. Each 2D velocity vector is calculated from an interrogation window of 32 x 32 pixels with a 75% overlap. The field of view for the PIV measurements is slightly smaller than the square windows, as the data close to the edges of the window, where light reflections could affect the reliability of the results, are neglected. In Fig. 1(b), the field of view (pink-coloured square) and the Cartesian coordinates for the analysis of the PIV results are depicted.

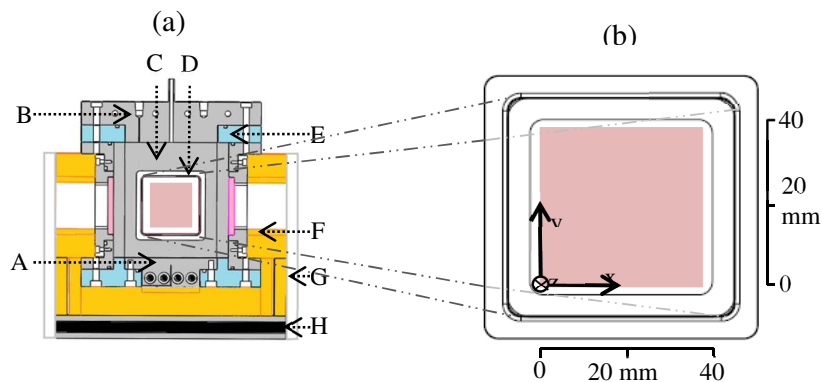


Fig. 1. Schematic drawing of the (a) Rayleigh-Benard cell [22] and (b) field of view. The marked components are explained in the text.

Experimental Procedure: Dilute Al_2O_3 -deionised (DI) H_2O nanofluids with a mean concentration of 0.00026 vol.% were synthesized, tested and compared with DI H_2O under turbulent natural convection. The employed nanoparticles were supplied by Alfa Aesar with an average particle size of 45 nm and a particle density of 3965 kg/m^3 . A constant temperature gradient between the heating and cooling plates of $DT = 63.2 \text{ }^\circ\text{C}$ and a constant temperature of $T_c = 26.4 \text{ }^\circ\text{C}$ at the cooling plate were the imposed conditions. In this way, our system had two control parameters: Rayleigh, $Ra = 4.1 \times 10^9$, and Prandtl, $Pr = 3.1$, and two response parameters: Nusselt, Nu , and temporally averaged velocities, V_{avg} . The PIV measurements were obtained at three different planes in the z direction of the coordinate system of Fig. 1(b) inside the cell, to record the impact of nanoparticles on the three dimensional flow structure and properties of the base fluid. The first plane was at the centre of the cell, $z = 0$, (central plane), the second was at an absolute distance z of $3 \pm 1 \text{ mm}$ behind the centre (back plane) and the third one was at an absolute distance z of $4 \pm 1 \text{ mm}$ in front (front plane) of the centre. The measurements on each plane were based on 2000 images to reduce the statistical uncertainties. In addition, the measurements on each plane were repeated at least four times to ensure that random uncertainties are minimised and. Therefore, in this work mean values are presented and compared for each plane. The fractional uncertainty in mean for the temporally and spatially averaged velocity $\overline{|V|}_{\text{avg}} \leq 2.6\%$ and for the Nu is $\leq 1.0\%$. Thus, the results presented herein are repeatable, reliable and precise. Finally, for the operating conditions in this study and the characteristics of the RB cell (shape and aspect ratio), the LSC is observed to develop along a diagonal of the cell. Therefore, the reported planar PIV flow measurements are projections of the diagonal flow field on the measurement plane, as seen through the square window depicted in Fig. 1.

Discussion and Results: In Table 1, the heat transfer performance, the calculated temporally and spatially averaged velocity characteristics, $\overline{|V|}_{\text{avg}}$, $Stdev$, $\delta \overline{|V|}_{\text{avg}}$ and TI for water and dilute nanofluid are presented. It is noted that the spatially averaged velocity is calculated over the applicable field of view in Fig. 1(b). At first, by comparing the general heat transport, as expressed with the Nu , for both test fluids, no clear trend can be observed. This is due to the very small concentration of nanoparticles in the base fluid, the operating conditions in this study and the associated experimental uncertainty.

Table 1. Heat transfer performance and velocity characteristics for water and dilute nanofluids at three different planes inside the RB cell.

Plane	Water				Nanofluids			
	$\overline{ V }_{\text{avg}}$	<i>Stdev</i>	<i>TI</i>	<i>Nu</i>	$\overline{ V }_{\text{avg}}$	<i>Stdev</i>	<i>TI</i>	<i>Nu</i>
	(cm/s)	(cm/s)	(%)		(cm/s)	(cm/s)	(%)	
back	0.3311	0.2604	79	76.4	0.3551	0.2651	75	76.2
central	0.3444	0.2635	77	76.1	0.3537	0.2673	76	76.2
front	0.3115	0.2578	83	76.5	0.3449	0.2662	77	77.4

The spatial distribution of the flow velocity field demonstrates differences between water and nanofluids, despite the small concentration of the nanoparticles. For instance, the temporally and spatially averaged velocity $\overline{|V|}_{\text{avg}}$ of the base fluid increases by 6.9% (on average in the planes) in the field of view when nanoparticles are employed. This trend is emphasised by examining the contours of the time-averaged mean velocity for water and nanofluids for the front plane, depicted in Fig. 2. It can be seen that the area close to the heating surface, where maximum velocities in the field of view are recorded, is notably larger for the nanofluid than for pure water. In the same figure, the direction of the velocity vectors (their length is proportional to the pixel displacement) indicates the existence of the LSC and the preferential clockwise direction. Except for $\overline{|V|}_{\text{avg}}$ the temporally and spatially averaged turbulent intensity of the velocity fluctuations, *TI*, in the field of view is consistently modified with the presence of nanoparticles in the base fluid. More specifically, *TI* for nanofluids is 4.3% (on average in the planes) smaller compared to water in the field of view. *TI* is defined as the ratio of the temporally and spatially averaged standard deviation of the turbulent velocity fluctuations to the temporally and spatially averaged velocity in the field of view.

Conclusions: This study examines the heat and mass transfer characteristics of a dilute Al_2O_3 – DI H_2O nanofluid inside a Rayleigh-Benard cell under turbulent natural convection. In this work, the behavior of nanofluids in applications where the thermal management results are only due to the density gradients in the working fluid is evaluated. Thermal studies along with a high spatial resolution velocimetry method (PIV) were conducted to assess the contribution of the addition of nanoparticles in traditional heat transfer fluids. We report that the addition of a small amount of Al_2O_3 nanoparticles, concentration of 0.00026 vol.%, to DI water alters the mass transfer behavior of the base fluid significantly. More specifically, the temporally and spatially averaged velocity

$\overline{|V|_{\text{avg}}}$ for nanofluids is higher than for water in the field of view for all three planes inside the RB cell. In addition, the temporally-averaged and spatially-averaged turbulent intensity of the velocity fluctuations, TI , in the field of view is decreased when nanoparticles are added. Finally, concerning the heat transfer performance of nanofluids, no consistent trend is observed, mainly due to the small nanoparticle concentration.

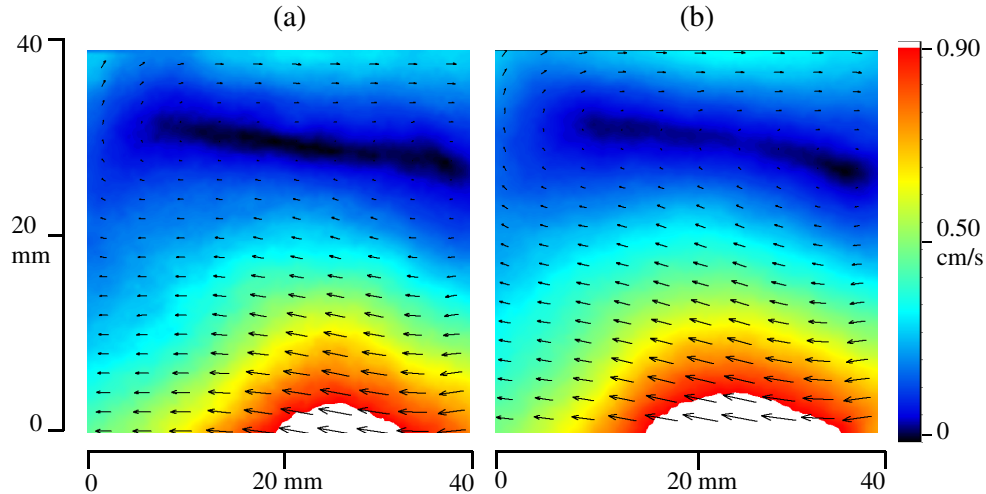


Fig. 2. Contours of the temporally averaged velocity $|V|_{\text{avg}}$ at the front plane for (a) water and (b) dilute nanofluid under $Ra = 4.1 \times 10^9$.

References:

1. A. Sergis, Y. Hardalupas, Anomalous heat transfer modes of nanofluids: a review based on statistical analysis, *Nanoscale research letters*, 6(1) (2011) 391.
2. Y. Xuan, Q. Li, Investigation on Convective Heat Transfer and Flow Features of Nanofluids, *Journal of Heat Transfer*, 125(1) (2003) 151.
3. S. Kakaç, A. Pramuanjaroenki, Review of convective heat transfer enhancement with nanofluids, *International Journal of Heat and Mass Transfer*, 52(13-14) (2009) 3187-3196.
4. A.K. Nayak, M.R. Gartia, P.K. Vijayan, An experimental investigation of single-phase natural circulation behavior in a rectangular loop with Al₂O₃ nanofluids, *Experimental Thermal and Fluid Science*, 33(1) (2008) 184-189.
5. S.E.B. Maïga, S.J. Palm, C.T. Nguyen, G. Roy, N. Galanis, Heat transfer enhancement by using nanofluids in forced convection flows, *International Journal of Heat and Fluid Flow*, 26(4) (2005) 530-546.

6. S. Savithiri, A. Pattamatta, S.K. Das, A single-component nonhomogeneous lattice boltzmann model for natural convection in Al₂O₃/water nanofluid, *Numerical Heat Transfer, Part A: Applications*, 68(10) (2015) 1106-1124.
7. M. Eslamian, M. Ahmed, M.F. El-Dosoky, M.Z. Saghir, Effect of thermophoresis on natural convection in a Rayleigh–Benard cell filled with a nanofluid, *International Journal of Heat and Mass Transfer*, 81 (2015) 142-156.
8. H. Oztop, E. Abu-Nada, Numerical study of natural convection in partially heated rectangular enclosures filled with nanofluids, *International Journal of Heat and Fluid Flow*, 29(5) (2008) 1326-1336.
9. C.J. Ho, M.W. Chen, Z.W. Li, Numerical simulation of natural convection of nanofluid in a square enclosure: Effects due to uncertainties of viscosity and thermal conductivity, *International Journal of Heat and Mass Transfer*, 51(17-18) (2008) 4506-4516.
10. F.S. Oueslati, R. Bennacer, Heterogeneous nanofluids: natural convection heat transfer enhancement, *Nanoscale research letters*, 6(1) (2011) 222.
11. C.H. Li, G.P. Peterson, Experimental studies of natural convection heat transfer of Al₂O₃/DI water nanoparticle suspensions (Nanofluids), *Advances in Mechanical Engineering*, 2010 (2010).
12. K. Kouloulias, A. Sergis, Y. Hardalupas, Sedimentation in nanofluids during a natural convection experiment, *International Journal of Heat and Mass Transfer*, 101 (2016) 1193-1203.
13. D. Wen, Y. Ding, Natural convective heat transfer of suspensions of titanium dioxide nanoparticles (nanofluids), *IEEE Transactions on Nanotechnology*, 5(3) (2006) 220-227.
14. R. Ni, S.-Q. Zhou, K.-Q. Xia, An experimental investigation of turbulent thermal convection in water-based alumina nanofluid, *Physics of Fluids*, 23(2) (2011) 022005.
15. F. Heslot, B. Castaing, A. Libchaber, Transitions to turbulence in helium gas, *Physical Review A*, 36(12) (1987) 5870-5873.
16. G. Zocchi, E. Moses, A. Libchaber, Coherent structures in turbulent convection, an experimental study, *Physica A*, 166(3) (1990) 387-407.
17. B. Castaing, G. Gunaratne, F. Heslot, L. Kadanoff, A. Libchaber, S. Thomae, X.-Z. Wu, S. Zaleski, G. Zanetti, Scaling of hard thermal turbulence in Rayleigh–Bénard convection, *Journal of Fluid Mechanics*, 204 (2006) 1-30.
18. R. Krishnamurti, L.N. Howard, Large-scale flow generation in turbulent convection, *Proceedings of the National Academy of Sciences of the United States of America*, 78(4) (1981) 1981-1985.
19. M. Sano, X.Z. Wu, A. Libchaber, Turbulence in helium-gas free convection, *Physical Review A*, 40(11) (1989) 6421-6430.
20. X.L. Qiu, P. Tong, Large-scale velocity structures in turbulent thermal convection, *Physical Review E*, 64 (2001) 036304.
21. X.D. Shang, X.L. Qiu, P. Tong, K.Q. Xia, Measured local heat transport in turbulent Rayleigh-Benard convection, *Phys Rev Lett*, 90(7) (2003) 074501.
22. K. Kouloulias, A. Sergis, Y. Hardalupas, T.R. Barrett, Measurement of flow velocity during turbulent natural convection in nanofluids, *Fusion Engineering and Design*, (2017).

AN EXPERIMENTAL SETUP FOR FLOW HEAT TRANSFER INVESTIGATION OF NANOFLUIDS

A. Nikulin* and A.L.N. Moreira

Instituto Superior Técnico, Universidade de Lisboa, IN+,
Av. Rovisco Pais 1, Lisboa, Portugal

*Corresponding author: artem.nikulin@tecnico.ulisboa.pt

Keywords: Nanofluids, heat transfer enhancement, Nanoparticles, Convective Heat Transfer

Introduction: Efficient cooling is one of the major technical challenges currently faced by energy sector. In this context, the use of nanoparticles to enhance heat exchange characteristics of working bodies and heat-carrying agents has recently attracted the close attention of researchers [1].

Many experimental studies have been reported in the literature, which suggest that the addition of nanoparticles enhance the heat transfer coefficient in the laminar and turbulent flow regime as well as during pool and flow boiling. However, the effect on heat transfer is not clear as many of these studies have also shown that nanoparticles have no effect or deteriorate heat transfer coefficient [2]. Though, in our opinion, despite the abundance of published works devoted to the study of nanofluids, the reported results on heat transfer performance still need a correct physical interpretation. Thus, it is premature to use the obtained physical data for the modeling of heat exchange processes and additional systematic experimental data on heat transfer characteristics of nanofluids is required. With this in mind, an experimental set-up is designed as a multifunction installation with the ability to study heat transfer in the laminar and turbulent regimes as well as during flow boiling in a cylindrical minichannel. The present paper is part of a major work aimed at providing careful and systematic data on the heat transfer features of nanofluids, which can contribute to the development of more rigorous physical models for convective heat transfer.

The experimental methodology: The experimental setup is shown in Fig. 1. The working fluid is pumped using the magnetically coupled vane pump 7 through a closed loop. The pump is connected to frequency converter in order to control the flow rate of the working fluid and the Coriolis mass flow meter (mini CORI-FLOW M15) 8 was used to measure mass flow rate. The flow meter allows to carry out measurements from 0.2 to 300 kg/h with the accuracy of 0.2%. Moreover, the application of this type of mass flow meter provide data on density of working fluid with the accuracy of ± 5 kg/m³.

The test section 3 is a stainless steel (AISI 321) tube 4 mm in diameter, 2.3 m long with wall thickness of 0.2 mm. A part of the tube of 0.4 m before the heating section is serve as calming

length. In order to obtain the straight and horizontal position of the test section the stretching device 10 was employed. The weight of 20 kg produce the stretching force. The stabilized power supply (HY5050EX) with the power stabilization accuracy of 0.3% was used to produce and control the heat flux supplied to the test section. This technique allows obtaining a constant wall heat flux boundary conditions. In addition, the heated area of the tube is divided into seven parts and can vary by power switch 4. Sections 2 and 11 are used for electrical insulation of the test section from the other parts of the experimental setup. To prevent heat loss to the ambient, the test section is placed in the vacuum chamber 12, where a dynamic vacuum on the order of less than 100 Pa is created by a vacuum system. All the connecting pipes are insulated by rubber insulation with the thermal conductivity less than 0.04 W/m·K.

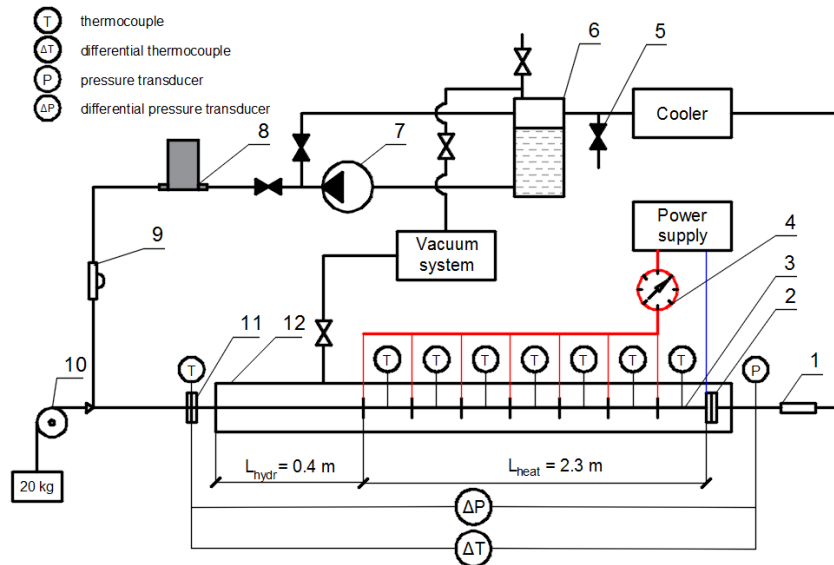


Figure 1. Schematic diagram of the experimental setup

Seven copper-constantan thermocouples fixed on the tube wall to measure the local temperature of the tube. As known [3], the heat transfer coefficient in a pipe flow greatly depends on the inlet temperature. In this context, the thermocouple is installed at the inlet of test section and the cooler serve to maintain the inlet temperature in the range of 0.2 K. Also, the differential thermocouple and differential pressure transducer (PX2300) used to control the temperature change and pressure drop along the test section. Special mixing chambers were mounted before the thermocouples at the inlet and outlet of test section, in order to obtain the mean temperature of the flow. All the thermocouples were calibrated “in situ” in turbulent flow regime using the platinum resistance thermometer installed in flow meter 8.

In addition, for carrying out the flow boiling experiments, the outlet of test section is equipped with the absolute pressure transducer (OMEGA MMA050C1B3MC0T3A6CE). The sight glasses 1 and 9 allows to study the flow boiling regimes and to control the absence of bubbles entering the test section respectively.

The filling of the experimental setup was performed through the receiver 6 and the whole loop was preliminarily evacuated by vacuum system. During the experiment on nanofluids flow heat transfer a certain amount of liquid can be sampled for further analysis by the valve 5. All electrical measurements are performed with the data acquisition system (RIGOL M300).

Preliminary tests of experimental setup using water have shown that disagreement of electric power with the heat capacity transferred to liquid is no more than 2%. Moreover, the difference of Nusselt number obtained in experiment with the calculated value by known empirical correlation $Nu = 0.021 \cdot Re^{0.8} \cdot Pr^{0.43}$ for the turbulent flow regime in the range of Reynolds number 4000 - 20000 do not exceed 4%. The reproducibility of Nusselt number in the set of three experiments agrees within 1%.

The Nusselt number was calculated as follow

$$Nu = \alpha \cdot d / \lambda \quad (1)$$

where $\alpha = G C_p (T_{out} - T_{in}) S^{-1} (T_w - \bar{T})^{-1}$ is the mean heat transfer coefficient (W/(m²·K)); G is the mass flow rate (kg/s); C_p is the specific heat of the liquid (J/(kg·K)); S is the surface area of channel (m²); T_{in} and T_{out} is the inlet and outlet temperatures of the fluid (K); \bar{T} is the mean temperature of the fluid (K); T_w is the arithmetic mean temperature of the channel wall obtained by data averaging from seven thermocouples (K); d is the diameter of the channel (m); λ is the thermal conductivity of liquid (W/(m·K)).

Preliminary results: Sigma-Aldrich isopropanol/Al₂O₃ nanofluid (Product Number 702129) with a nanoparticle concentration of 20±1 mass.% is used in this study. This nanofluid was chosen because isopropanol forms stable solutions with Al₂O₃ nanoparticles over a wide range of concentrations and temperatures. According to the manufacturer, the size of the Al₂O₃ nanoparticles is not greater than 50 nm (DLS). The test samples are prepared by diluting isopropanol/Al₂O₃ nanofluid with pure isopropyl alcohol.

Preliminary data, aimed at analyzing the influence of Al₂O₃ nanoparticles on Nusselt number for different Reynolds numbers, are shown in figure 2. The experimental data on thermal conductivity and viscosity was used [4] to calculate the Nusselt number of pure isopropanol and isopropanol/Al₂O₃ nanofluid.

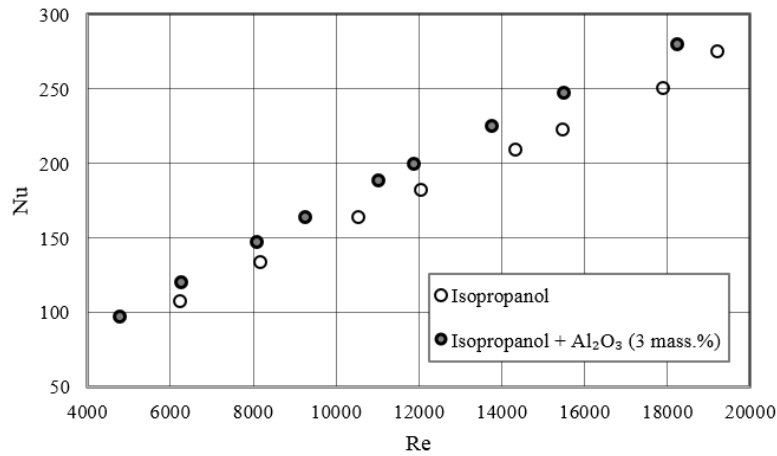


Figure 2. Nusselt number versus Reynolds number for isopropanol and isopropanol/Al₂O₃ nanofluid (3 mass.%)

The conducted test experiments indicate that the created experimental setup allows to obtain consistent and reproducible characteristics on turbulent flow heat transfer.

The preliminary results obtained shows that Al₂O₃ nanoparticles added to isopropanol lead to a significant change in heat transfer process. The average enhancement of Nusselt number depending on Reynolds number was around 10% in the range of Re number from 4000 to 20000. However, as was demonstrated in [3], the heat transfer process of nanofluids depend nonlinearly on particles concentration and size, viscosity and temperature and have to be investigated in more details.

References:

1. S.M.S. Murshed and C.A. Nieto de Castro, Nanofluids: Synthesis, Properties and Applications, *Nova Science Publishers Inc.*, New York, 2014.
2. W.Yu, D.M. France, S.U.S. Choi, J.L. Routbort, Review and assessment of nanofluid technology for transportation and other applications, *Argonne National Laboratory*, 2007.
3. A. V. Minakov, D. V. Guzei, M. I. Pryazhnikov, V. A. Zhigarev, V. Y. Rudyak, Study of turbulent heat transfer of the nanofluids in a cylindrical channel. *International Journal of Heat and Mass Transfer*, 102 (2016), 745-755.
4. V.Z. Geller, N.A. Shimchuk, S.N. Gubanov, Transport properties of nanofluids (experiment and calculation methods). *Refrigeration Engineering and Technology*, 51 (6) (2015) (72-77) (in Russian).

**NATURAL CONVECTION FROM A PAIR OF DIFFERENTIALLY-HEATED
HORIZONTAL CYLINDERS ALIGNED SIDE BY SIDE IN A NANOFLUID-FILLED
INCLINED SQUARE ENCLOSURE**

A. Quintino, E. Ricci*, E. Habib, and M. Corcione

DIAEE Sezione Fisica Tecnica - Sapienza Università di Roma, via Eudossiana 18, 00184
Rome, Italy

*Corresponding author: elisa.ricci@uniroma1.it

Keywords: Nanofluid; Natural convection; Differentially-heated horizontal cylinders; Two-phase modeling; Enhanced heat transfer; Optimal particle loading and tilting angle

Introduction: Buoyancy-induced convection of nanofluids inside adiabatic enclosures containing heated and cooled cylinders has recently gained a lot of interest. Studies on this topic were carried out numerically by Garoosi and colleagues [1,2], and Khalili et al. [3], yet a number of points have to be raised regarding these works. In fact, both studies executed by Garoosi and colleagues are based on the single-phase approach, thus neglecting the effects of the slip motion that actually occurs between the suspended nanoparticles and the base liquid. On the other hand, in the two-phase investigation performed by Khalili and co-workers, the thermophoretic velocity of the suspended nanoparticles is calculated by the way of the McNab-Meisen empirical relationship [4], whose applicability to water-based nanofluids with suspended metal oxide nanoparticles implies an underestimation of the thermophoretic velocities, as displayed by Aminfar and Haghoo [5], and thoroughly discussed by Corcione et al. [6]. Framed in this general background, a comprehensive numerical study on natural convection from a pair of differentially-heated horizontal cylinders set side by side in a nanofluid-filled adiabatic square enclosure, inclined with respect to gravity so that the heated cylinder is located below the cooled one, is performed using a two-phase model based on the double-diffusive approach. It is assumed that Brownian diffusion and thermophoresis are the only slip mechanisms by which the solid phase can develop a significant relative velocity with respect to the liquid phase. The system of the governing equations of continuity, momentum and energy for the nanofluid, and continuity for the nanoparticles, is solved through a control-volume formulation of the finite-difference method. Pressure-velocity coupling is handled using the SIMPLE-C algorithm. Convective terms are approximated by the QUICK discretization scheme, whereas a second-order backward scheme is applied for time integration. Full details on the computational code, and its validation, can be found in a recent study conducted by Quintino et al. [7].

Discussion and Results: Numerical simulations are performed using alumina-water nanofluids, for different values of (a) the average volume fraction of the solid phase, ϕ_{av} , in the range between 0 and 0.04, (b) the tilting angle of the enclosure, γ , in the range between 0° and 60° , and (c) the average temperature of the nanofluid, T_{av} , in the range between 300 K and 330 K. The cavity

width, W , is set as 0.04 m, the nanoparticle diameter, d_p , is set as 25 nm, the temperature difference between the cylinders, ΔT , is set as 10 K, the ratio between the cylinders diameters and the cavity width, δ , is set as 0.2, and the ratio between the center-to-center distance and the cavity width, λ , is set as 0.4. Typical local results are reported in Fig. 1, in which steady-state streamline, isotherm and isoconcentration contours relative to different tilting angles in the range 0° – 60° are plotted for $\phi_{av} = 0.02$ and $T_{av} = 315$ K. It is apparent that, for all the tilting angles considered, the flow field consists of a primary circulation occurring between the cylinders, due to the rise of the hot nanofluid adjacent to the heated cylinder and its descent past the opposite cooled cylinder, and of a secondary cell, driven by the same imposed temperature difference, that embraces both cylinders. Moreover, the combined effects of the nanofluid circulation due to the imposed

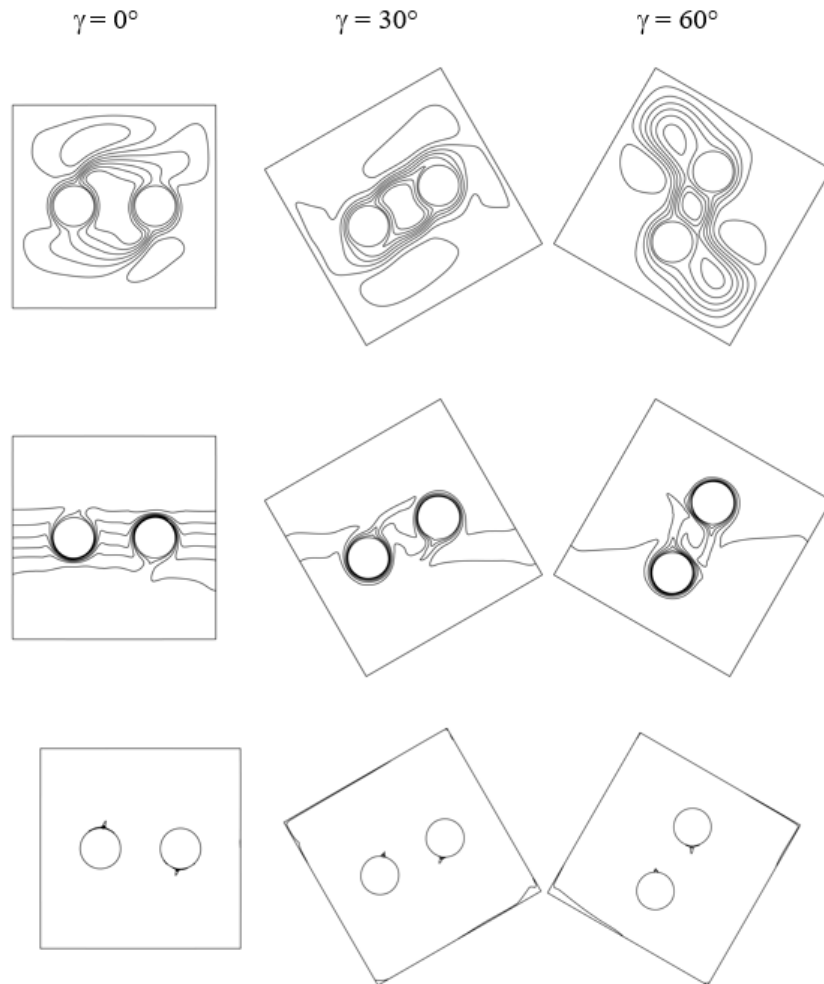


Fig. 1. Streamline, isotherm and isoconcentration contours for $\text{Al}_2\text{O}_3 + \text{H}_2\text{O}$, $\phi_{av} = 0.02$, $T_{av} = 315$ K, at different tilting angles γ in the range 0° – 60° .

differential heating, and the diffusion of the suspended nanoparticles in the direction from hot to cold, give rise to the formation of a low-concentration boundary layer adjacent to the heated cylinder surface, and a high-concentration boundary layer adjacent to the cooled cylinder surface, which means the establishment of a concentration gradient across the enclosure, whose role in determining the heat transfer performance of the nanofluid needs being discussed.

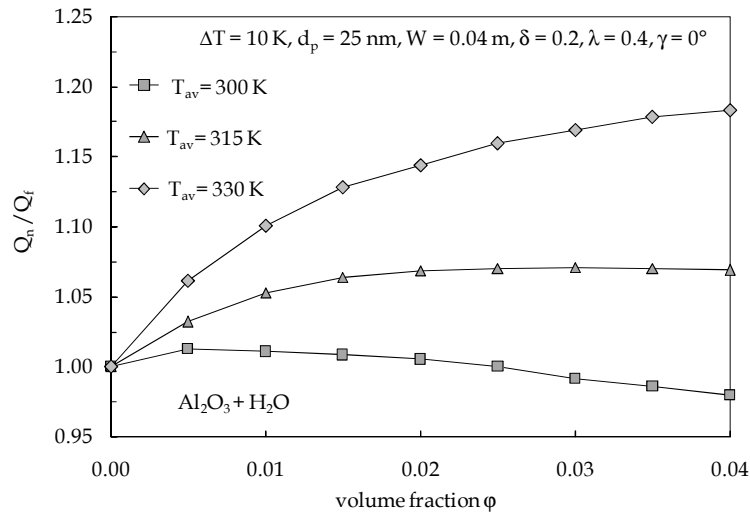


Fig. 2. Distribution of Q_n/Q_f vs. ϕ_{av} for $Al_2O_3 + H_2O$, $W = 40$ mm, $d_p = 25$ nm, $\lambda = 0.4$, $\delta = 0.2$, $\gamma = 0^\circ$, and $\Delta T = 10$ K, using T_{av} as a parameter.

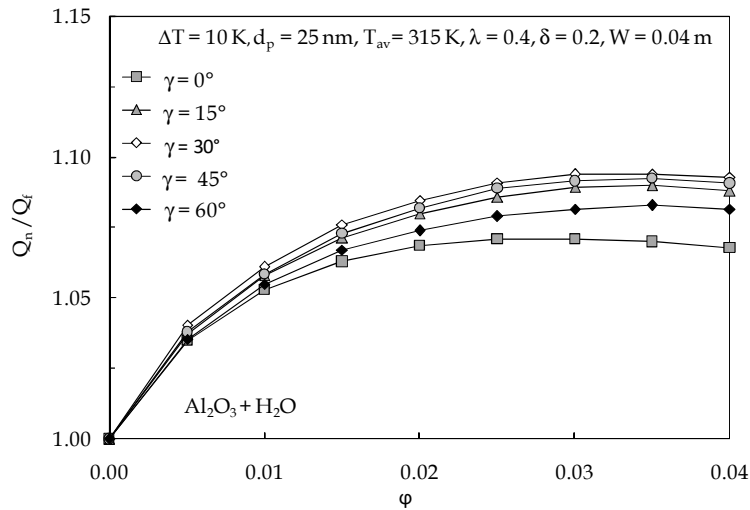


Fig. 3. Distribution of Q_n/Q_f vs. ϕ_{av} for $Al_2O_3 + H_2O$, $W = 40$ mm, $d_p = 25$ nm, $\lambda = 0.4$, $\delta = 0.2$, $T_{av} = 315$ K, and $\Delta T = 10$ K, using γ as a parameter.

In fact, the nanofluid behavior is primarily affected by the two opposite effects arising from the increase of both the thermal conductivity and the dynamic viscosity produced by the dispersion of the nanoparticles into the base liquid: the first effect, which tends to enhance the nanofluid heat transfer performance, prevails at small volume fractions of the suspended solid phase, whereas the second effect, which tends to degrade the nanofluid heat transfer performance, prevails at higher volume fractions. On the other hand, due to the mentioned concentration gradient, a cooperating solutal driving force arises. The situation is such that, as a rule, this extra-buoyancy tends to compensate the increased friction consequent to the viscosity growth, thus implying that the beneficial effect of the increased thermal conductivity plays the major role in determining the heat transfer performance of the nanofluid. Hence, owing to the strong dependence of the effective thermal conductivity on temperature, a pronounced heat transfer enhancement has to be expected at high average temperatures, as shown in Fig. 2, where a number of distributions of the ratio between the heat transfer rates across the nanofluid and the pure base fluid, Q_n / Q_f , are plotted versus ϕ_{av} for the horizontal alignment, i.e. $\gamma = 0^\circ$, using T_{av} as a parameter, in which the existence of an optimal particle loading, ϕ_{opt} , is clearly pointed out. As the tilting angle γ is increased, the increase of the cooperating solutal driving force, as well as the increase of the vertical path available for the acceleration of the nanofluid, result in a growth of the motion intensity, which enhances the heat transfer performance, on the other hand, as γ is further increased, the interactions occurring between the hot and the cold plumes result in a significant decrease of the heat transfer rate. A set of distributions of Q_n/Q_f plotted versus ϕ_{av} using γ as a parameter is reported in Fig. 3, confirming the existence of an optimal tilting angle for maximum heat transfer.

Conclusions: The main results obtained in the present study may be summarized as follows: (a) the inclination of the cavity and the dispersion of the nanoparticles into the base liquid have their maximum effect on the nanofluid heat transfer performance at an optimal tilting angle of the cavity and an optimal particle loading; (b) the impact of the nanoparticle dispersion into the base liquid increases remarkably with increasing the average temperature, which, without any doubt, is the key parameter that determines the heat transfer performance of the nanofluid.

References

1. F. Garoosi, F. Hoseininejad and M.M. Rashidi, Numerical study of natural convection heat transfer in a heat exchanger filled with nanofluids, *Energy* 109 (2016) 664-678.
2. F. Garoosi and F. Hoseininejad, Numerical study of natural and mixed convection heat transfer between differentially heated cylinders in an adiabatic enclosure filled with nanofluid, *Journal of Molecular Liquids* 215 (2016) 1-17.
3. E. Khalili, A. Saboonchi and M. Saghafian, Natural convection of Al₂O₃ nanofluid between two horizontal cylinders inside a circular enclosure, *Heat Transfer Engineering* 38 (2017) 177-189.
4. G.S. McNab and A. Meisen, Thermophoresis in liquids, *Journal of Colloid Interface Science* 44 (1973) 339-346.

5. H. Aminfar and M.R. Haghgoo, Brownian motion and thermophoresis effects on natural convection of alumina-water nanofluid, *Journal of Mechanical Engineering Science* 227 (2012) 100-110.
6. M. Corcione, M. Cianfrini and A. Quintino, Temperature effects on the enhanced or deteriorated buoyancy-driven heat transfer in differentially heated enclosures filled with nanofluids, *Numerical Heat Transfer, Part A* 70 (2016), 223-241.
7. A. Quintino, E. Ricci and M. Corcione, Thermophoresis-induced oscillatory natural convection flows of water-based nanofluids in tilted cavities, *Numerical Heat Transfer, Part A* 71 (2017), 270-289.

NANOENGINEERED WETTABILITY FOR HEAT TRANSFER ENHANCEMENT IN SPRAY COOLING

A.S Moita*, M. Maly and A.L.N. Moreira

IN+, Instituto Superior Técnico, Universidade de Lisboa,

Av. Rovisco Pais 1, Lisboa, Portugal

*Corresponding author: anamoita@tecnico.ulisboa.pt

Keywords: Spray cooling, Nanofluids, Wettability

Introduction: Spray impingement is a popular cooling strategy used in different industrial applications, from metallurgy to electronics cooling [1-2]. In the latter, despite offering high heat transfer coefficients of the order of 10^4 - 10^5 W/m²K or higher [3] the efficient implementation of this strategy must cope with the increasingly demanding heat loads that are dissipated. In this context, several authors addressed surface modification to enhance the heat transfer processes, *e.g.* [2-3]. Alternatively, several authors have explored the use of nanofluids to reach the same goal [4]. However, while many of these researchers dealt with nanofluids as being a single-fluid with novel thermo-physical properties (*e.g.* surface-tension and viscosity), the mechanisms of liquid atomization, droplet-wall interaction and droplet/droplet interactions, which strongly affect the heat transfer mechanisms depend on the intermolecular forces as described by wettability. In this context, a microscopic approach needs to be introduced by considering the external and internal forces on the nanoparticles and the mechanical and thermal interactions between nanoparticles, fluid and surface molecules. Though most applications aim to phase-change heat transfer devices, the mechanisms by which a surface is wetted by a liquid loaded with nanoparticles is not yet completely understood, as studies have yielded contradictory results: while some experiments show inhibition of wetting by nanoparticle addition [5], others show an improvement of wetting with the increase in the nanoparticle concentration [6]. It has been suggested that the spreading of a nanofluid droplet depends on the relation between time-scales associated with wetting and with diffusion of nanoparticles near the confined three-phase contact region, respectively. Moreover, since wettability depends on the micro structure of the nanofluid, it is expected to change with the synthesis process. This is an important issue, since preparation techniques are required to produce uniform and stable suspensions, with negligible agglomeration of particles and no chemical changes of the base fluid. Hence, wettability of a surface by a nanofluid and, therefore, spray-wall interactions, cannot be disregarded from the process of fluid synthesis, particularly in the presence of heat transfer. In line with this, the present study addresses the effect of nanofluid synthesis on the local physical properties of the resulting fluid and their consequent effect on the atomization characteristics (droplet size and velocity distribution and spray angle, among others) and on spray impingement using nanofluids. The nature and the concentration of the nanoparticles of the based fluid are taken as influencing parameters, giving

particular emphasis on their effect on the interfacial mechanisms present in atomization and then in droplet/spray impingement.

Sample Results and Discussion: Different nanofluids, obtained from alumina, zinc, copper and iron oxide and alumina in water, are synthesised using the co-precipitation and solvothermal methods [7]. Different surfactants are used (e.g. citric acid, oleic acid, CTAB - Cetyl trimethylammonium bromide) to infer on their effect in the stability of the nanofluid. The morphology is analysed by scanning and transmission electron microscopies, which also give information about the phase structures and chemical composition, complemented by Fourier transform infrared spectroscopy, X-ray diffraction, Raman and X-ray photoelectron spectroscopy. Surface wetting is then quantified with a goniometer, by the apparent macro-contact angle obtained at the equilibrium between the interfacial tensions acting as a droplet is gently deposited over the surface. In addition, a Laser Scanning Confocal Microscopy – LSCFM - and 3D reconstruction allows to visualize the micro-layer in the very vicinity of the triple contact line and characterize wettability within extreme wetting regimes [8]. High-speed visualization using a Phantom v4.2 and image post-processing is combined with Phase Doppler measurements (a 2 component system from Dantec) to fully describe the atomization characteristics and the spray/droplet wall interactions. The results show that despite surface tension of the bulk fluid does not change with nanoparticles (Table 1), local particle interactions seem to affect the atomization processes, at relatively low particle concentrations, thus affecting the mean size (quantified by the Sauter Mean Diameter) and axial velocity of the spray droplets (Figure 1a and 1b, respectively). These preliminary results suggest that similar interactions may affect droplet/wall interactions at spray impingement.

Table 1. Composition and surface tension of the prepared nanofluids taken at $20\pm 3^\circ\text{C}$.

Fluid	Base fluid	Nanoparticle		Surfactant		Surface tension (mN/m)
		Composition Concentration wt (%)		Composition	Concentration wt (%)	
1	Water	-	-	-	-	73.5
2	Water	-	-	Citric acid	0.15	73.4
2	Water	Al ₂ O ₃	2	Citric acid	0.15	72.8
3	Water	Al ₂ O ₃	0.5	Citric acid	0.15	73.4
4	Water	ZnO	0.5	Citric acid	0.15	74.3
5	Water	ZnO	0.01	Citric acid	0.15	73

6	Water	C_4H_6CuO	0.1	Citric acid	0.15	72
7	Water	$Cl_2Fe_4H_2O$	0.1	Citric acid	0.15	71.6

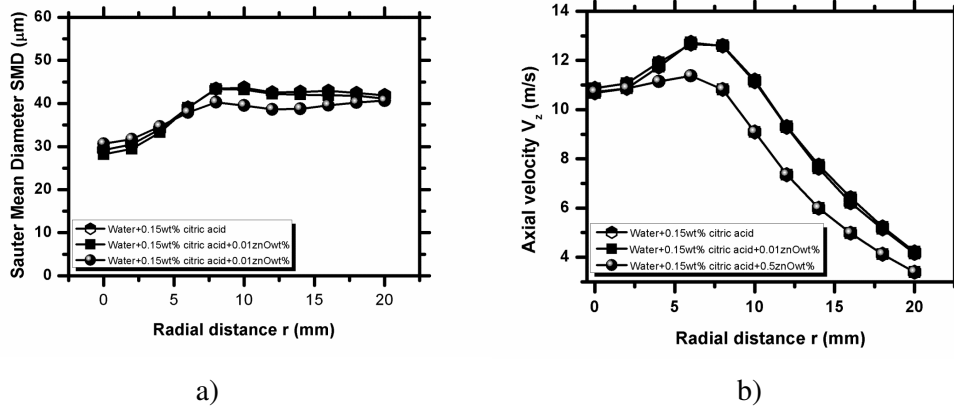


Figure 1. Effect of the nature and concentration of the nanoparticles on: a) the Sauter Mean Diameter and b) the axial velocity of the droplets resulting from the atomization of the nanofluids.

Conclusions: This manuscript addresses the effect of the nature and concentration of nanoparticles on the atomization processes of nanofluid sprays. Emphasis is also given to the potential effect of local wetting modifications caused by the interactions between the nanoparticles and the impinging surfaces on the wettability and consequently on spray/wall interactions. Preliminary results solely performed at ambient temperature show that despite surface tension of the bulk fluid does not change with nanoparticles, local particle interactions seem to affect the atomization processes, at relatively low particle concentrations.

References:

1. Kim, J., Spray cooling heat transfer: The state of the art., *Int. J. Heat Fluid Flow*, 28(4) (2007), 753-767.
2. Moreira, A. L. N., Moita, A. S. and Pañão, M. R., Advances and challenges in explaining fuel spray impingement: how much of single droplet impact research is useful? *Progress Energy and Combustion Sci.* 36 (2010), 554-580.
3. Bostanci, H., Daniel, R., John, K. and Louis, C., Spray cooling with ammonia on microstructured surfaces: performance enhancement and hysteresis effect, *J. Heat Transfer*, 131 (2009).
4. Duursma, G., Sefiane, K. and Kennedy, A., Experimental studies of nanofluid droplets in spray cooling, *Heat Transfer Engineering*, 30(13) (2017), 1108-1120.

5. Vafaei, S., Borca-Tasciuc, T., Podowski, M. Z., Purkayastha, A., Ramanath, G. and Ajayan, P. M., Effect of nanoparticles on sessile droplet contact angle, *Nanotechnology*, 17 (2006) 2523–2527.
6. Wasan, D. T. and Nikolov A D., Spreading of nanofluids on solids, *Nature*, 423 (2003), 156.
7. Pastrana-Martínez, L.M., Pereira, N., Lima, R., Faria, J.L., Gomes, H.T. and Silva, A.M.T., Degradation of diphenhydramine by photo-Fenton using magnetically recoverable iron oxide nanoparticles as catalyst, *Chemical Engineering J.*, 261 (2015), 45-52.
8. Vieira, D., Moita, A. S. M. and Moreira, A. L. N., Non-intrusive wettability characterization on complex surfaces using 3D Laser Scanning Confocal Fluorescence Microscopy, *18th International Symposium on the Application of Laser and Imaging Techniques to Fluid Mechanics*, Lisbon, Portugal, July 4 – 7, 2016.

POSSIBLE APPLICATION OF NANOFLUIDS TO IMPROVE PERFORMANCE OF WET COOLING TOWERS

V. Mijakovski*, T. Geramitcioski and V. Mitrevski

University "St. Kliment Ohridski", Faculty of Technical Sciences, str. Makedonska Falanga
33, 7000 Bitola, Macedonia

*Corresponding author: vladimir.mijakovski@tfb.uklo.edu.mk

Keywords: Nanofluids, Heat transfer, Cooling tower, Power plant, Reduced water usage

Introduction: Nano meter-sized particles suspended in fluids forming colloidal solutions are called nanofluids [1]. Nanofluids are typically made of metals, oxides, carbides or carbon nanotubes in a base fluid like water, oil and ethylene glycol and have an advantage, in terms of heat exchange (heat transfer) over pure cooling fluids. Their great potential in heat removal improvement was first discovered in 2001, [2]. It was discovered that less than 1% volume fraction of copper nanoparticles or carbon nanotubes dispersed in ethylene glycol or oil can increase their thermal conductivity by 40% and 150% respectively. The ongoing research after that extended to a utilization of nanofluids in many processes and industries, especially where intensive heat transfer/exchange occurs.

Thermal power plants are large consumers of water. This especially refers to the so called cold end of the power plant. It is comprised of condenser, cooling tower, circulating pumps, connecting pipelines and air removal system.

Lignite fired thermal power plants have the highest share in electricity production in the Republic of Macedonia. Thermal power plant Bitola is the biggest producer of electricity in the country. It consists of three units having total installed capacity of 699 MW. Since this power plant does not have access to abundant water, it uses wet cooling towers for cooling of the condenser.

Two circulation~~al~~ pump stations are in operation at TPP "Bitola". One is for units 1 and 2, while the other one is for unit 3 with the possibility of enlargement for another unit. Pumps are of axis type, vertical with variable geometry of the working blades, [3, 4]. Unit is comprised of steam generator, turbine, electric generator, condenser and cooling tower. Two pumps, working in parallel, are used on each unit, while the third one is engaged during extreme weather conditions as an auxiliary pump according to needs. Cold water from the cooling tower basin, through open channel that later transforms into two underground pipes (with diameter DN2400 each) is transported into pump station's open basin (chamber). From the open basin water is transported by pumps into main distributive pipeline DN2400. From this pipeline, water flow is divided on two pipes (DN1600) leading to both condenser halves, [5]. Cold end of the Unit-3 is shown on Fig. 1. Nominal flow rate of cooling water through this system is 30000 m³/h per

unit. Nominal cooling range (difference between the cooling tower water inlet and outlet temperature) of the tower is 9,2 K. Evaporation losses are calculated to be approximately 1% of the nominal flow of water through the system, [6].

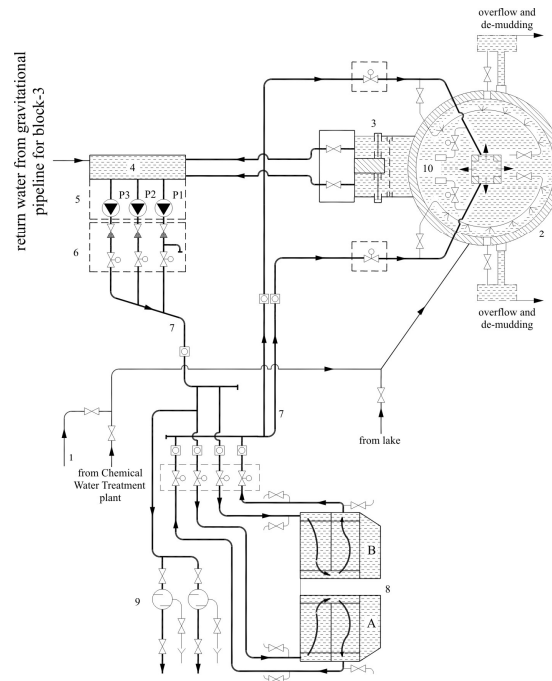


Fig. 1. Schematics of the circulation cooling water system for Unit-3; 1 – water treatment station; 2 – natural draught cooling tower; 3 – valves with colander; 4 – entering water chamber; 5 – pump station; 6 – pit with valves; 7 – circulation pipelines; 8 – condenser; 9 – mechanical water filters; 10 – unit for winter operation of the cooling tower.

Discussion and Results: A review of scientific and technical literature with reference to research conducted in this field has been made in order to determine feasible utilization of nanofluids for enhancing the heat transfer at the cooling tower in the above described power plant.

Improved efficiency of the whole system due to enhanced thermophysical properties (i.e. thermal conductivity) of nanofluids compared to the base fluid (in this case water) is the main motive of its application. Nanoparticle materials include chemically stable metals (i.e. gold, copper), metal oxides (i.e. alumina, silica, zirconia, titania), oxide ceramics (SiC), metal nitrides (diamond, graphite, carbon nanotubes, fullerene) and functionalised nanoparticles, [7]. Typical nanofluid is characterised with uniform dispersion of nanoparticles.

There are few ways to optimize operating parameters of the cooling tower, such as water flow rate, water temperature, thermal characteristics of tower's fill, geometry of the tower etc. While some of these parameters are not controllable or cost-effective to change, some are not applicable for already operational cooling towers.

The use of nanofluids as coolants in intensive heat transfer processes has been extensively studied, mostly for nuclear reactor applications, [8, 9]. The use of nanofluids in cooling tower is an excellent option to improve its performance. Nanofluids can improve the heat performance of the cooling tower by increasing the sensible and evaporating heat transfer leading to significant reduction in water use of the tower and power plant in general. This is very important because around 60% of the total annual water consumption of the above described thermal power plant is attributed to evaporation from the cooling towers, [6].

Recent researches showed that the use of nanofluid improves the performance of both condenser and cooling tower leading to reduction of sizes of both. Application of nanofluids incorporating nanoparticles with phase-change material cores that melt to absorb heat from steam turbine condensate and solidify as cooling proceeds could reduce overall water consumption by as much as 20%. The improved thermal properties offered by these multifunctional nanoparticles also are expected to decrease coolant flow rates by about 15%, helping lower the associated pumping loads and thus own needs' energy losses, [10], Fig. 2. Internal reports regarding own needs' electricity consumption at the TPP Bitola, [11], show that the electricity consumption of pumps used at power plant's cold end amount to 10% of the total annual own needs' electricity consumption.

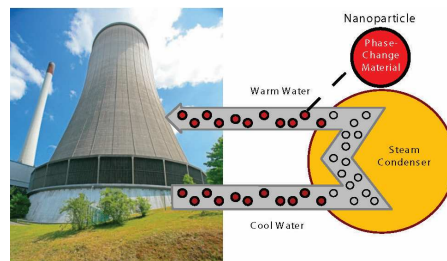


Fig. 2. Heat – absorption nanoparticles are expected to significantly improve the thermophysical performance of steam-condensing coolants, reducing freshwater consumption at power plants with wet cooling towers, Source: [10].

Evaporation rate of cooling water at wet cooling tower with natural draught highly depend on external air conditions (mainly air temperature and humidity). According to [12] and by assuming linear correlation between heat transfer coefficient increase by using nanofluids and decrease in evaporation rate of cooling water, dependence between evaporation rate and external air temperature for nominal cooling range of 9,2 K are shown on Fig. 3. Assumption is made for 4 different rates of heat transfer coefficient increase (5%, 10%, 15% and 20% respectively). Other reference parameters for cooling tower of TPP Bitola: relative air humidity 50%, nominal flow of cooling water 30000 m³/h.

Conclusions: In this paper, a review on potential applications of nanofluids in heat removal from wet cooling tower is addressed. Current level of research in this potentially promising field of thermal engineering is also briefly described. Lignite fired thermal power plant Bitola in Macedonia, as largest electricity producer in the country has been used as a model for comparison of possible benefits from utilization of nanofluids in steam-condensing process.

There are many advantages of using nanofluids in cooling towers, such as: increase in heat transfer performance of the cold end (cooling tower and condenser) leading to overall increase in efficiency; reduction of water loss through evaporation leading to reduction of water consumption in the cooling tower and in the power plant in general; reduction of sizes of cooling tower and condenser and reduction of electricity consumption of pumps used in this system.

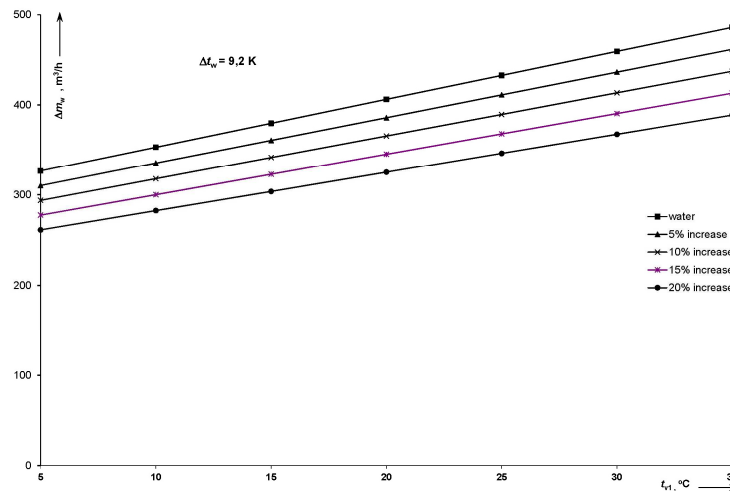


Fig. 3. Dependence of evaporation rate of cooling water vs external air temperature relative to increase in heat transfer coefficient by using nanofluids; Δm_w – evaporation rate of cooling water, t_{v1} – external air temperature.

Applied on the model power plant these improvements can significantly reduce consumption of fresh water in the plant. At the moment, the plant uses around 12 million m^3 of fresh water every year, out of which approximately 7,15 million m^3 are consumed by the cold-end itself. Electricity consumption of pumps is estimated at the level of 35 – 40 GWh/year which is more than 1% of the total electricity produced from the power plant in 2014 (3317 GWh), [13]. Thus, possible improvements applied to the referent power plant have great potential.

Still, despite many possible advantages in utilization of nanofluids in the cooling tower application, there are a lot of challenges that need to be addressed and solved prior to wide-scale usage, [7]. These include: high cost of nanofluids and difficulties in production process, stability of nanoparticles in the base fluid, development of practical methods for adding

nanoparticles to cooling system to replace losses through drift, evaporation and blowdown. Also, full-scale field demonstrations will be required.

References:

1. R. Kumar and V. Kumar Goud, Nanofluids: a promising future, *Journal of Chemical and Pharmaceutical Sciences*, special issue 2014, ISSN: 0974-2115.
2. Eastman JA, Choi SUS, Li S., Yu W., Thompson LJ., Anomalously increased effective thermal conductivities of ethylene glycol based nanofluids containing copper nanoparticles, *Applied Physics Letters*, Volume 78, issue 6, 718 (2001).
3. Mijakovski I., Mijakovski V., Extreme values from the climatic curve and their influence on thermal power plant's Bitola cold-end, *14th international symposium on thermal science and engineering*, Sokobanja, Serbia, October 13-16, 2009.
4. Mijakovski V., Optimal operating regime of the cooling water pump station in TPP "Bitola", *Symposium power plants 2006*, Society of thermal engineers of Serbia and Montenegro, Vrnjačka Banja, Serbia, September 19-22, 2006.
5. Pecakov S., Petreski T., Hristov T., *Local instruction for exploitation of circulation pump stations and technical water systems*, Public Enterprise "Macedonian power plants", Skopje, Macedonia, 1999 (in Macedonian).
6. Mijakovski V., *Influence of the climate conditions on the performance of the cooling tower*, PhD thesis, Faculty of Mechanical Engineering Skopje, Macedonia, 2009 (in Macedonian).
7. Sarkar J., Improving Performance of Cooling Tower, *Cooling India*, (august 2016) 30-32.
8. Buongiorno J., Hu L-W., Nanofluid Heat Transfer Enhancement for Nuclear Reactor Applications, *Proceeding of the ASME 2009 2nd Micro/Nanoscale Heat&Mass Transfer International Conference*, Shanghai, China, December 18-21, 2009.
9. Fahmy A.A., A Comparative Thermal – hydraulic Study on Nano-fluids as a Coolant in Research Nuclear Reactors, *International Journal of Scientific&Engineering Research*, Volume 4, Issue 9, September 2013, ISSN 2229-5518.
10. Heat-absorption nanoparticle additives for reducing cooling tower water consumption, *Report from Electric Power Research Institute (EPRI) published in July 2013*, Palo Alto, California, USA.
11. Internal annual report on the own needs' electricity consumption of the TPP Bitola, JSC "Macedonian Power Plants", Skopje, Macedonia, 2013 (in Macedonian).
12. DIN EN 14705:2005-10, Heat exchanger – Method of measurement and evaluation of thermal performances of wet cooling towers.
13. Annual report on realized results from the operation of JSC "Macedonian power plants" in 2014, Skopje, Macedonia, 2015.

Abstracts

SESSION 4A: HEATING AND OTHERS

THERMOPHYSICAL CHARACTERISTICS OF NANOFUIDS AND TRANSPORT PROCESSES MECHANISMS

V. Rudyak

Novosibirsk State University of Architecture and Civil Engineering
Leningradskays Str., 113, Novosibirsk, 630008, Russian Federation

Email: valery.rudyak@mail.ru

Keywords: Nanofluid, Viscosity, Thermal Conductivity, Heat Transfer

Introduction: Nanofluids are new two-phase system consisting of base liquid (water, ethylene glycol, etc.) and solid nanoparticles, usually metallic or oxide. The interest in nanofluids is associated with two main factors. On the one hand there are numerous existing or future applications of nanofluids (new systems for transportation and production of thermal energy; new coolants; biotechnologies, new medicinal preparations and cosmetic products; drug delivery systems; different contamination detectors, water cleanup systems, and air cleaning units; new lubricants, lacquers, paints, etc.). On the other hand the nanofluids have unusual properties and their thermophysical characteristics are not described by the classical theories. Tens scientific teams around the world study the properties of nanofluids and their flows during last two decades. The obtained results proved extremely contradictory. Nevertheless, today it has been achieved a definite understanding of the physics of transport processes in nanofluids. The present paper is devoted to an analysis of the thermophysical properties (viscosity, thermal conductivity and heat transfer coefficients) of nanofluids. The last experimental and molecular dynamics data obtained by the author and his scientific teams are considered. In conclusion the mechanisms of transport processes in nanofluids are discussed.

Results/Nanofluids Viscosity: Viscosity coefficient of the coarse dispersed fluids is described by the famous Einstein's formula $\eta = \eta_0(1 + 2.5\varphi)$, where η_0 is the viscosity coefficient of the based liquid and φ is the volume concentration of the particles. This formula is applicable only at very small particles concentration. There are many different theories and experimental correlations generalizing this formula. However in all cases the viscosity coefficient of dispersed fluid depends on concentration of the particles only. For a long time researchers of the viscosity of nanofluids also believed that viscosity depends only on the concentration of nanoparticles. Therefore the experimental data were very different and non-universal. It was shown that in all cases the viscosity of nanofluids is much more than that of coarse dispersed liquid. The viscosity coefficient at small particles concentration is again described by the linear relation $\eta = \eta_0(1 + a\varphi)$ but the coefficient a is varied from 4.8 to 22 (in Einstein's fomula $a = 2.5$).

More than ten years ago in our paper [1] it was firstly shown by molecular dynamics method that the effective viscosity coefficient for nanofluids depends not only on the concentration of particles but also on their size. Practically simultaneously this conclusion was confirmed experimentally by several authors. However there were very contradictory points of view about character of this dependence. In order to give an unambiguous answer, we measured the viscosity of more than fifty liquids and showed that the viscosity of the nanofluid increases with decreasing particle size [2-4]. The accuracy of the measurements was about 1–2 percents. This results were confirmed by the molecular dynamics method too.

Dependence of the nanofluid viscosity on material of the particles was established first by the molecular dynamics method [5] and then was confirmed experimentally [6].

Finally, it should be borne in mind that the nanofluid can in general have a non-Newtonian rheology. Today it can be argued that rheology of nanofluid may become non-Newtonian with increasing of the particles concentration and decreasing their size. In many cases the rheology of nanofluid is not bad described by the Power Law fluid model [7].

Results/Nanofluids Thermal Conductivity: Most expectations have long been associated with various thermal applications of nanofluids. As late as the first experiments on measurement of their thermal conductivity showed excellent results: the incorporation of even small, of the order of a percent fraction, concentrations of solid metal nanoparticles enhanced the thermal conductivity of the base fluid by several percent or even tens of percent. This initiated a number of thermal conductivity measurements of the nanofluids, though the obtained data proved to be surprisingly controversial. It was found that the thermal conductivity of nanofluids is not described by the classical theories. In particular, it was found that the thermal conductivity of nanofluids depends not only on particle concentration but also on particle size. An unequivocal answer to the question of what kind this dependence was still missing. The first question that arises in the study of thermal conductivity of any dispersed fluid is formulated quite simply: how thermal conductivity depends on the particle concentration. The systematic measurements of thermal conductivity dependence on different parameters have been carried out in our recent paper [8]. More than fifty various nanofluids based on distilled water, ethylene glycol, and engine oil containing particles of SiO₂, Al₂O₃, TiO₂, ZrO₂, CuO, and diamond were studied. The nanoparticles volume concentration ranged from 0.25 to 8%. The particle size ranged from 5 to 151 nm. Thermal conductivity measurements were performed by non-stationary hot-wire method. The error of fluid thermal conductivity coefficient does not exceed 3%.

Firstly it was shown that the enhancement of nanofluid thermal conductivity over that of based fluid as a rule is greater (by 6–30%) than the values defined by the Maxwell's or other classical theories. A characteristic feature of the nanofluid thermal conductivity is slowdown of its enhancement with increasing of particle concentration. This dependence can be approximated

by the following simple formula $\lambda_f = 1 + b_1\phi - b_2\phi^2$. Similar behavior of the nanofluid thermal conductivity was noted earlier in experiments (see, f. e. [9]), as well as in molecular dynamic simulations [10].

The second important step was to determine the dependence of the thermal conductivity on the particle size. It is established that the thermal conductivity increases with increasing particle size. It was shown that this dependence is good described by the following formula:

$k_r = 1 + (0.0193 + 0.00383\tilde{\rho})\sqrt{\phi\tilde{D}}$ (see also [11]). Here $\tilde{\rho} = \rho_p / \rho_f$, ρ_p , ρ_f are the density of the nanoparticle and carrier liquid material respectively. Thus the nanofluid thermal conductivity is depended on the density of the particles material and it grows with increasing the density. In this regard we have to emphasize that it was not established the correlation between the thermal conductivity of nanofluid and disperse particle material.

The base liquid also significantly influences the effective thermal conductivity of the nanofluid. We have confirmed that the lower the thermal conductivity of the base fluid, the higher the relative thermal conductivity coefficient of the nanofluid. This is quite naturally explained by the fact that in the base fluid with the highest thermal conductivity the enhancement of thermal conductivity is weaker, at other conditions being equal. This, in particular, means that the supplement of the nanoparticles into the fluid will be most effective for the base fluid with low thermal conductivity.

Results/Nanofluid Heat Transfer: The heat transfer coefficient of a nanofluid in a cylindrical channel under constant heat flux density at the walls is measured experimentally. The studied fluid was prepared based on distilled water and CuO, TiO₂, ZrO₂ and Al₂O₃ nanoparticles with an average size from 55 to 105 nm. The volume concentration of nanoparticles was in the range from 0.25 to 2%. The effect of nanofluids is determined by the regime of flow (laminar or turbulent).

In laminar flow the heat transfer coefficient of nanofluids in all cases are much more than that of based fluid. In particular, it is shown that for a fixed value of the Reynolds number, a 2%-nanofluid intensifies the heat exchange more than twice compared to water [7, 12–14].

The effect of using nanofluids in turbulent mode is much more complicated. In this case the heat transfer coefficient depends not only on the thermal conductivity of nanofluid but also on its viscosity. However it was shown that adding nanoparticles to the coolant significantly influences the heat transfer coefficient. It is shown that with increasing nanoparticles concentration, the local and average heat transfer coefficients at a fixed Reynolds number increase. Decrease in heat transfer coefficient with increasing particles concentration may take place at a fixed flow rate. It is shown that, the heat transfer coefficient of the nanofluid in turbulent regime increases with increasing nanoparticles size at a fixed flow rate, while has a certain maximum at a fixed Reynolds number. It is found that the inlet temperature is another factor having a significant effect on turbulent heat transfer performance of nanofluids.

Conclusions: The main conclusion of this presentation is very simple. The nanofluids are new type of the dispersed liquids and their properties are not described by the classical theories. The viscosity and thermal conductivity of nanofluids depend not only on the volume concentration of nanoparticles but also on their sizes and material. This is explained by the fact that the mechanisms of transport processes in nanofluids differ from the corresponding mechanisms for coarse-grained liquids. Their detailed discussion goes beyond the scope of this paper. We would like to note only

that the nanofluid is much more structured (in the sense of having a short-range order) than the base one. The degree of this structuring is the greater, the smaller the particle size. Finally, it should be noted that the thermal conductivity of nanofluids and their heat transfer in the general case is much higher than for carrier fluids. Therefore the using of nanofluids as a working fluid in various thermal devices and systems are very perspective.

Acknowledgement: This paper is supported by the Russian Foundation of Basic Research (Grants No. 17-01-00040, 17-58-45023).

References:

1. V.Ya. Rudyak, A.A. Belkin, E.A. Tomilina and V.V. Egorov, *Molecular dynamic simulation of the transport processes. II. Force acting on the nanoparticle and effective viscosity of nanofluids*, Preprint No. 1(18), Novosibirsk, NSUACE, 2006.
2. V.Ya. Rudyak, S.V. Dimov and V.V. Kuznetsov, On the dependence of the viscosity coefficient of nanofluids on particle size and temperature, *Technical Physics Letters* 39 (2013) 779-782.
3. V.Ya. Rudyak, Viscosity of nanofluids. Why it is not described by the classical theories, *Advances in Nanoparticles* 2 (2013) 266-279.
4. V.Ya. Rudyak and S.L. Krasnolutski, Simulation of the nanofluid viscosity coefficient by the molecular dynamics method, *Technical Physics* 60 (2015) 798-804.
5. V.Ya. Rudyak and S.L. Krasnolutski, Dependence of the viscosity of nanofluids on nanoparticle size and material, *Physics Letters A* 378 (2014) 1845-1849.
6. V.Ya. Rudyak, A.V. Minakov, M.S. Smetanina and M.I. Pryazhnikov, Experimental data on the dependence of the viscosity of water- and ethylene glycol-based nanofluids on the size and material of particles, *Doklady Physics* 61 (2016) 152-154.
7. D.V. Guzei, A.V. Minakov, V.Ya. Rudyak and A.A. Dekterev, Measuring the heat-transfer coefficient of nanofluid based on copper oxide in a cylindrical channel, *Technical Physics Letters* 40 (2014) 203-206.
8. M.I. Pryazhnikov, A.V. Minakov, V.Ya. Rudyak and D.V. Guzei, Thermal conductivity measurements of nanofluids, *Int. J. of Heat and Mass Transfer* 104 (2017) 1275-1282.
9. P. Keblinski, R. Prasher and J. Eapen, Thermal conductance of nanofluids: is the controversy over?, *J. Nanoparticles Research* 10 (2008) 1089-1097.
10. V.Ya. Rudyak and A.A. Belkin, Simulation of the nanofluids transport coefficients, *Nanosystems: Physics, Chemistry, Mathematics* 1 (2010) 156-177.
11. D. Ceotto and V.Ya. Rudyak, Phenomenological formula for the thermal conductivity coefficient of water based nanofluids, *Colloid Journal* 78 (2016) 509-514.
12. A.V. Minakov, A.S. Lobasov, D.V. Guzei, M.I. Pryazhnikov and V.Ya. Rudyak, The experimental and theoretical study of laminar forced convection of nanofluids in the round channel, *Applied Thermal Engineering* 88 (2015) 140-48.
13. A.V. Minakov, D.V. Guzei, M.I. Pryazhnikov, V.A. Zhigarev and V.Ya. Rudyak, Study of turbulent heat transfer of the nanofluids in a cylindrical channel, *Int. J. of Heat and Mass Transfer* 102 (2016) 745-755.
14. D.V. Guzei, A.V. Minakov and V.Ya. Rudyak, Investigation of heat transfer of nanofluids in turbulent flow in a cylindrical channel, *Fluid Dynamics* 51 (2016) 189-199.

EXPERIMENTAL STUDY ON RHEOLOGICAL PROPERTIES, THERMAL CONDUCTIVITY AND DIELECTRIC PROPERTIES OF TiN-EG NANOFUIDS

G. Żyła^{1*}, J. Fal¹ and P. Estellé²

¹Department of Physics and Medical Engineering, Rzeszow University of Technology, Rzeszow, Poland

²Materials and Thermo-Rheology team at LGCGM, Universite Rennes 1, Rennes, France

*Corresponding author: gzyła@prz.edu.pl

Keywords: Nanofluid, Thermal conductivity, Rheology, Dielectric properties, TiN

Introduction: Nanofluids are suspensions of nanometrical particles with high thermal properties dispersed in a common base fluid with many potential applications [1]. These potential applications are mainly due to the significant increase in thermal conductivity of these suspensions, first introduced by Choi in 1995 [2], which strongly depends on nanoparticle loading and nature. Since then, many papers have been published on thermal conductivity of nanofluids [3,4]. In the case of planning the practical use of nanofluids, one must take into account an increase in viscosity of this materials. Actually, it has been reported many times that viscosity of nanofluids increase with increase of the volume fraction of particles in nanosuspensions [5,6]. Because of potential application in heat exchange systems, one of the most popular base fluid used to prepare nanofluids is ethylene glycol (EG) [7-11].

This paper presents results of experimental investigation of thermal conductivity and rheological properties of EG based nanofluids containing two sizes of titanium nitride nanoparticles. A dielectric profile of this material was also presented as a supplement to thermophysical properties. As far as we know this is the first report on thermophysical properties of EG based nanofluids containing TiN nanoparticles. Studies on the influence of particle size on those properties are also limited, and here we present it.

Thermal conductivity was measured with well-known and widely used equipment KD2Pro (Decagon Devices Inc., Pullman, Washington, USA) with 2% relative uncertainty [11]. Rheological properties (viscoelastic structure, thixotropy, dynamic viscosity) were investigated with HAAKE MARS 2 (Thermo Electron Corporation, Karlsruhe, Germany) rheometer. Relative uncertainty of viscosity measurements performed with this rheometer is 5%. Finally dielectric properties were determined with Concept 80 System (NOVOCONTROL Technologies GmbH & Co. KG, Montabaur, Germany) and conductivity meter MultiLine 3630 with conductivity probe LR-925/01 (WTW GmbH, Weilheim, Germany) in which relative measurement uncertainty did not exceed 1% [12-14]. All measurements were performed immediately after sample preparation at constant temperature 298.15K. Details for all experimental procedures, uncertainties and calibration of the devices can be found in our previous papers [11-14].

Discussion and Results: Thermal conductivity of TiN-EG nanofluids increase with the volume fraction of nanoparticles, and is higher for nanofluids containing smaller particles as shown in Fig. 1. This material also exhibit complex rheological properties. It appears that TiN-EG nanofluids are non-Newtonian shear thinning materials, and for higher volume fraction it might be observed viscoelastic structure, yield stress and thixotropy. It was also presented that dielectric properties depends on the size of particles and nanoparticle loading. Experimental data of thermophysical and dielectric properties are modelled and compared to existing theoretical models, new empirical correlations are also proposed. In addition to thermal conductivity (TC), results of electrical conductivity (EC) were presented in Fig.1 considering the effect of nanoparticle content and average size. Both properties were also compared to Maxwell model. A detailed discussion of these results can be found in our recent publication [14].

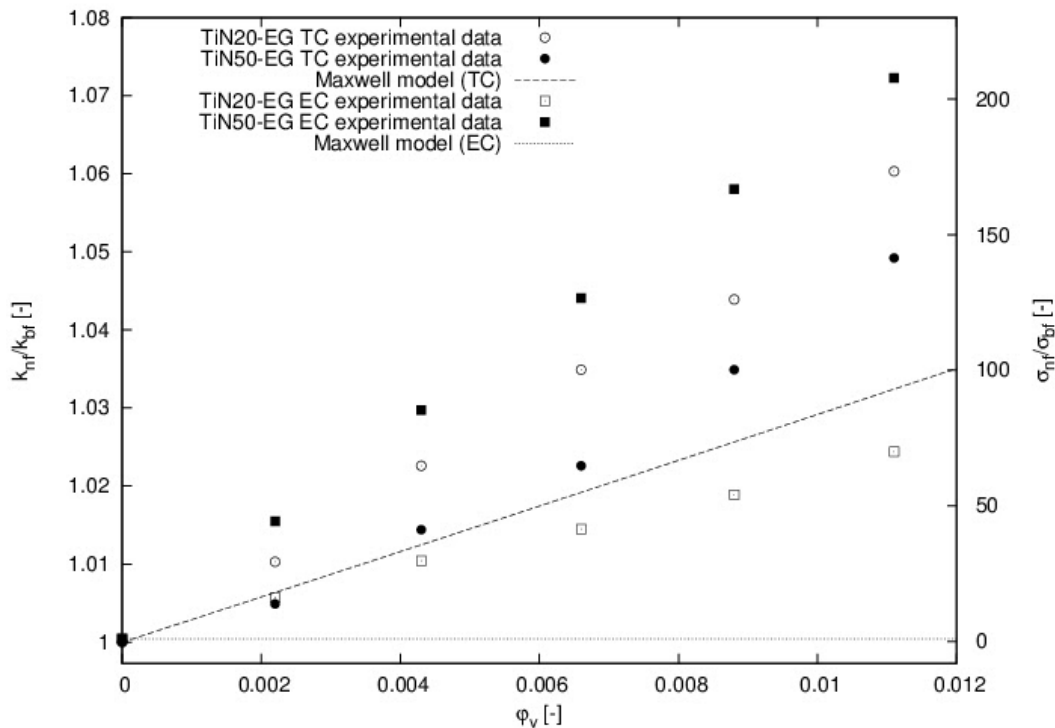


Fig. 1. Thermal conductivity (TC) and electrical conductivity (EC) ratios in TiN-EG nanofluids. Graph was prepared on the base of experimental data reported in Ref. [14].

Conclusions: The paper shows the results of experimental studies on the physical properties of

TiN-EG. It has been shown that the size of the nanoparticles is one of the factor that affects the physical properties of nanofluids, especially rheological and dielectric properties. As this kind of nanofluids were never investigated up to now, this new experimental investigation with consideration of nanoparticle size effect provide complementary data for identifying promising nanofluids for dielectric and thermal applications.

References:

1. Taylor, R. et al., Small particles, big impacts: a review of the diverse applications of nanofluids. *Journal of Applied Physics* 113.1 (2013): 1.
2. Choi, S. U. S., Enhancing thermal conductivity of fluids with nanoparticles. *ASME-Publications-Fed* 231 (1995): 99-106.
3. Thomas, S. and Choondal, B. P. S., A review of experimental investigations on thermal phenomena in nanofluids. *Nanoscale research letters* 6.1 (2011): 377.
4. Aybar, H.Ş. et al., A review of thermal conductivity models for nanofluids. *Heat Transfer Engineering* 36.13 (2015): 1085-1110.
5. Sundar, L. S. et al., Empirical and theoretical correlations on viscosity of nanofluids: a review. *Renewable and sustainable energy reviews* 25 (2013): 670-686.
6. Murshed, SMS and Estellé P., A state of the art review on viscosity of nanofluids." *Renewable and Sustainable Energy Reviews* 76 (2017): 1134-1152.
7. Yu, W. et al., Experimental investigation on the thermal transport properties of ethylene glycol based nanofluids containing low volume concentration diamond nanoparticles. *Colloids and Surfaces A: Physicochemical and Engineering Aspects* 380.1 (2011): 1-5.
8. Pastoriza-Gallego, M.J. et al. Thermophysical profile of ethylene glycol-based ZnO nanofluids. *The Journal of Chemical Thermodynamics* 73 (2014): 23-30.
9. Cabaleiro, D. et al., Rheological and volumetric properties of TiO₂-ethylene glycol nanofluids. *Nanoscale research letters* 8.1 (2013): 286.
10. Li, X. et al., Rheological behavior of ethylene glycol-based SiC nanofluids. *International journal of heat and mass transfer* 84 (2015): 925-930.
11. Żyła, G., Thermophysical properties of ethylene glycol based yttrium aluminum garnet (Y₃Al₅O₁₂-EG) nanofluids. *International Journal of Heat and Mass Transfer* 92 (2016): 751-756.
12. Żyła, G. and Jacek, F., Viscosity, thermal and electrical conductivity of silicon dioxide-ethylene glycol transparent nanofluids: An experimental studies. *Thermochimica Acta* 650 (2017): 106-113.
13. Żyła, G., Jacek, F, and Patrice, E., The influence of ash content on thermophysical properties of ethylene glycol based graphite/diamonds mixture nanofluids. *Diamond and Related Materials* 74 (2017): 81-89.
14. Żyła, G., Jacek, F, and Patrice, E., Thermophysical and dielectric profiles of ethylene glycol based titanium nitride (TiN-EG) nanofluids with various size of particles. *International Journal of Heat and Mass Transfer* 113 (2017): 1189-1199.

TEMPERATURE-COMPENSATED 3ω HOT WIRE FOR QUASI-ISOTHERMAL THERMOPHYSICAL PROPERTIES MEASUREMENT OF INHOMOGENEOUS FLUIDS

M. Chirtoc*, J.-F. Henry and N. Horny

GRESPI Lab., Université de Reims Champagne Ardenne URCA,

Moulin de la Housse, BP 1039, 51687 Reims, France

*Corresponding author: mihai.chirtoc@univ-reims.fr

Keywords: 3ω hot wire, Effective thermal conductivity, Thermal diffusivity, Nanofluids

Introduction: The amplitude and phase of 3ω hot wire (HW) signal can be exploited to simultaneously and independently determine the thermal conductivity k and thermal diffusivity a of fluids. High resolution k and a measurements were performed on nanofluids (silica nanoparticles in water and ferrofluids) [1].

Discussion and Results: By rewriting the expression of the 3ω signal generated by the wire:

$$\frac{\tilde{V}_{3\omega}}{V_{1\omega}^2 I_{1\omega}} \frac{4(2l)}{r_{el}} = \tilde{z}_s \quad (1)$$

one obtains a procedure for data reduction, which allows separating the electrical quantities related to the HW sensor from the thermophysical properties of the fluid sample. In Eq. (1), $\tilde{V}_{3\omega}$ is the complex 3ω signal, $V_{1\omega}$ the amplitude of the voltage signal at 1ω , $I_{1\omega}$ the current amplitude at 1ω imposed by the current generator at the fundamental frequency f , $2l$ the wire length and r_{el} the temperature coefficient of the electrical resistance of the wire, on the left-hand side of Eq. (1). The right-hand side contains only the thermal impedance \tilde{z}_s [m.K/W] of the medium seen by the sensor, which depends in a first approximation on k and a of the sample, on wire radius r and on the thermal modulation frequency $2f$. A patented temperature-compensated dual-probe configuration cancels the large unbalance of the fundamental frequency in temperature-dependent processes [2]. Thus k of vegetable oils for use in concentrated solar power plants was determined in the range from the ambient to 230 °C [3].

Two models for the 3ω HW signal have been developed: an exact model derived from the solution of heat diffusion with axial symmetry and a model based on a series/parallel network of thermal quadrupoles. A comparison is made with the approximate solution for the infinite line heat source [4] which is valid at low frequency when the thermal diffusion length

$\mu=(a/(\pi(2f)))^{1/2}$ in the medium is larger than r . For water the deviation increases to unacceptable levels at high frequency. This is because this model uses the truncation to the first approximation of Bessel functions, which are the correct description of the quadrupole model. The models account to various degree of accuracy for various factors that influence the total thermal impedance of the medium, such as:

- specific heat capacity and thermal conductivity of wire material;
- unwanted convection phenomena (related to high excitation current);
- finite wire length (related to end-effects);
- thermal boundary resistance R_{bd} between the metal and the fluid.

A parametric study allowed drawing the following conclusions, based on numerical results for air and water having two extreme set of thermophysical properties values:

a) The modulated heat stored in the heat capacity of the wire is the main correction to the models which consider only the impedance of the medium. The correction increases with increasing frequency, and is larger for low conductivity fluids (air). In contrast, the wire thermal conductivity plays no role as long as it is much larger than the one of the fluid (which is the case in practice).

b) The effect caused by the finite length of the wire as compared to the simulations for an infinite wire is about 10 % amplitude decrease and +1° phase change at 0.1 Hz in air. It decreases with increasing frequency, and is lower for water. This frequency-dependent error can be corrected for in the models because the frequency is known. This is more difficult to do with the conventional transient HW method, in which the signal at short time and at long time corresponds to different frequencies. In that case a double (short/long) probe differential technique is the experimental solution to cancel end-effects of the probe.

c) The maximum effect caused by a (large) thermal boundary resistance of $R_{bd}=10^{-6}$ m²K/W in water is about +2.4 % in amplitude and +0.5° in phase at a reasonably high frequency of 10 Hz. It would be interesting to simulate the best conditions for increasing this effect, in order to study the heat transfer at solid/liquid interface.

d) The convection phenomena may be relevant in air, at low modulation frequencies and for high excitation current producing tens of °C increase of average wire temperature. Fig. 1 shows the amplitude and phase of the thermal impedance \tilde{z}_s in air, calculated from the measured electrical quantities on the left-hand side of Eq. (1). The fact that the amplitude is practically constant at 1 Hz even for high power indicates that the heat transfer is purely conductive. The measurement can yield correct k and a values of air, despite the fact that the wire resistance is different for different excitation currents. At 0.1 Hz the safe power is below 5 mW, which is enough for accurate measurements. At higher power the convection turns in, as suggested by the difference between the amplitude for horizontal and vertical orientation of the wire. The phase is less affected by the discussed effects. However, in normal operating conditions (average wire temperature increase below 1°C), the convection is negligible.

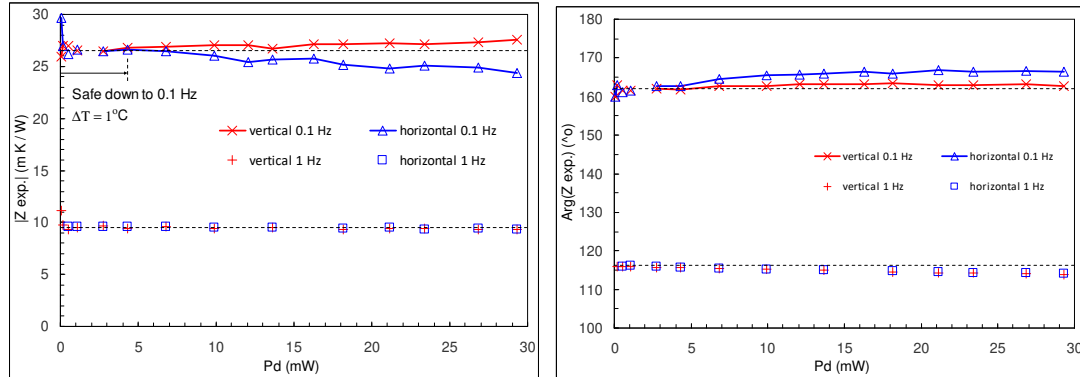


Fig. 1. Amplitude (left) and phase (right) of the thermal impedance seen by the hot wire probe in air, as a function of dissipated power. Deviations from dashed lines are due to convection induced by self-heating of the wire.

Conclusions: Lock-in signal processing in the 3ω HW technique enable quasi-isothermal thermophysical properties measurements. This feature is particularly advantageous with nanofluids, in order to avoid or minimize temperature-driven phenomena such as convection, thermophoresis (Soret effect), Brownian motion, etc. Experimental results will be presented for thermophysical parameters of several types of nanofluids as a function of power dissipated in the wire, in order to assess the safe operating conditions.

Acknowledgements: The instrument development was supported by "Dispotherm" project of SATT Nord Technology Transfer Office, France.

References:

1. A. Turgut, C. Sauter, M. Chirtoc, J.F. Henry, S. Tavman, I. Tavman and J. Pelzl, AC hot wire measurement of thermophysical properties of nanofluids with 3ω method, *The Europ. Phys. J. Special Topics* 153 (2008) 349-352.
2. M. Chirtoc, J. F. Henry, D. Caron and N. Horny, Measurement method of thermophysical properties of a medium, *Patent application* no. FR 16 51774 /02/03/2016.
3. J.F. Hoffmann, J.F. Henry, G. Vaitilingom, R. Olives, M. Chirtoc, D. Caron and X. Py, Temperature dependence of thermal conductivity of vegetable oils for use in concentrated solar power plants, measured by 3ω hot wire method, *Int. J. Thermal Sci.* 107 (2016) 105-110.
4. D.G. Cahill and R.O. Pohl, Thermal conductivity of amorphous solids above the plateau, *Phys. Rev. B*, 35 (1987) 4067–4073.

EXPERIMENTAL CHARACTERIZATION AND THEORETICAL MODELLING OF Cu, Ni AND Ag-NANOFUIDS: A COMPARATIVE STUDY OF THEIR THERMAL PROPERTIES

R. Gómez-Villarejo^{1,*}, E. I. Martín², J. Navas¹, A. Sánchez-Coronilla³, M. Teruel¹, T. Aguilar¹, J. J. Gallardo¹, R. Alcántara¹, D. de los Santos¹ and C. Fernández-Lorenzo¹

¹Departamento de Química Física, Facultad de Ciencias, Universidad de Cádiz, 11510 Puerto Real, Cádiz, España

²Departamento de Ingeniería Química, Facultad de Química, Universidad de Sevilla, 41012 Sevilla, España

³Departamento de Química Física, Facultad de Farmacia, Universidad de Sevilla, 41012 Sevilla, España

*Correspondence author: roberto.gomezvi@uca.es

Keywords: Nanofluid, Thermal properties, Isobaric specific heat, Thermal Conductivity

Introduction: Recently, nanofluids have emerged as an interesting way to improve heat transfer process in Concentrating Solar Power (CSP), due to the enhancement of thermal properties respect to the heat transfer fluid. Suspension of solid nanometric particles in fluids is known to enhance some of their thermal properties. A great number of studies have shown increases in thermal properties using water or ethylene glycol such as base fluid, however, there are few studies about nanofluids using the commonly heat transfer fluid (HTF) used in Concentrating Solar Power (CSP) as a base fluid [1, 2]. Addition, some studies have reported an increase in thermal conductivity in nanofluids based on metal nanoparticles, in some cases, using a low nanoparticles concentration [1-4]. Simultaneously to the experimental characterization, a theoretical study by molecular dynamics simulations was performed in order to better understanding of the nanofluidic system. To interpret the interactions between the metal nanoparticles and the base fluid, structural properties have been studied, determined by analysis of the radial distribution function and spatial distribution function. In this study, three nanofluids were prepared with different metal nanoparticles: copper, nickel and silver; and ever nanofluid were characterized experimentally and theoretically.

Discussion and Results: The nanofluids studied were prepared by means of the two step-method [5]. First step involves the synthesis of metallic nanoparticle, and second step is the dispersion into a base fluid. In this study, commercial copper, nickel and silver nanoparticles were added, in three different mass nanoparticle concentration, into a commercial heat transfer fluid composed of a eutectic mixture of two stable compounds: biphenyl (C₁₂H₁₀, 26.5%) and diphenyl oxide (C₁₂H₁₀O, 73.5%).

Several properties of the nanofluids prepared were characterized to determine their efficiency as heat transfer fluid in applications with heat exchangers. These properties were optical properties and thermal properties.

Optical properties gave us information about chemical and physical stability of nanofluids. To determine whether the addition of nanoparticle could produce chemical modifications in the base fluid, analysis using Vis-NIR spectroscopy reveal that there are no modifications in the base fluid when nanoparticles are added, that suggests no chemical changes in the samples. Measurements of the particle size by dynamic light scattering technique showed a quick increase of particle size until reaching into a value practically stable. These results suggest a tendency of nanoparticles to agglomerate after certain time and then remain stable.

To determine the efficiency of the nanofluids in heat transfer applications under turbulent flow conditions, the ratio of the heat transfer coefficient between nanofluids and base fluid was analysed by Dittus-Boelter correlation [6] (see equation (1)) where values of density, viscosity, isobaric specific heat and thermal conductivity are necessary.

$$FoM = \frac{h_{nf}}{h_{bf}} = \left(\frac{\rho_{nf}}{\rho_{bf}}\right)^{0.8} \left(\frac{k_{nf}}{k_{bf}}\right)^{0.6} \left(\frac{C_{p(nf)}}{C_{p(bf)}}\right)^{0.4} \left(\frac{\mu_{nf}}{\mu_{bf}}\right)^{-0.4} \quad (1)$$

An increase of the density, isobaric specific heat and thermal conductivity values is a beneficial effect for the heat transfer efficiency, while an increase in viscosity is counterproductive. Parameters such as the flow channel diameter and the flow velocity are considered constant and omitted in the equation.

Experimental results showed an increase in values both density and viscosity for all nanofluids, tendency expected due to incorporation of nanoparticles in suspension into a base fluid [7, 8].

The roles of isobaric specific heat and thermal conductivity are essential in the study of heat transfer processes. Thus, a comparison of these values of the nanofluids with those of the base fluid may provide important information regarding the use of nanofluids in heat transfer applications. It is known that the specific heat of liquid is higher than that of solids, so the specific heat of the nanofluids would be expected to be lower than that of the base fluid and decreases when nanoparticle is added [7]. Nevertheless, it is possible the opposite effect due to the formation of an internal structure because of the interaction between the nanoparticles and the base fluid and depending on the nature of both [9]. In the cases of addition of copper and silver nanoparticles, these nanofluids showed an increase in values of isobaric specific heat around 15% for Cu-nanofluids and 7% for Ag-nanofluids, while the incorporation of nickel nanoparticles into the base fluid did not produce a significantly modification in values of isobaric specific heat.

On the other hand, it is well-known that material with high thermal conductivity usually enhances heat transfer performance, and that the suspension of nanoparticles in heat transfer fluid causes more interactions between themselves. This leads to an increment of the thermal conductivity of the fluid [1]. Values obtained for the thermal conductivity showed an increase

about 12% for Cu-nanofluids and 6% for Ag-nanofluids. However, in the case of Ni-nanofluids there was no increase in the thermal conductivity, but rather the opposite.

Dittus-Boelter equation (see equation (1)) gives us information about the enhancement of efficiency of nanofluids. Typically, the efficiency of the system is considered to improve when $h_{nf} / h_{bf} > 1$. Figure 1 shows the heat transfer coefficient ratio estimated according to this equation for the nanofluids prepared at a room temperature.

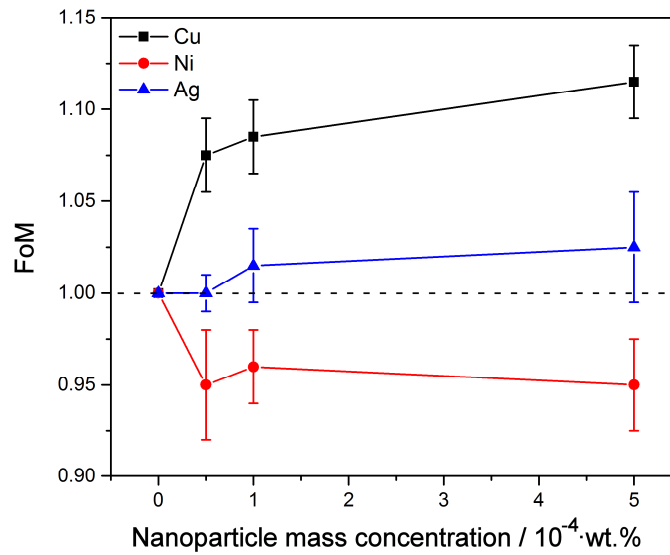


Fig.1. Values of the ratio of the heat transfer coefficient for the nanofluids prepared.

Simultaneously and based on the experimental results of each nanofluids, we have performed theoretical calculations to discover a predictive model of the experimental behaviour of the nanofluids and to obtain a better understanding of the behaviour of the modelled nanofluid system. By dynamic molecular simulations, isobaric specific heat and thermal conductivity values of each nanofluid were determined. To calculate thermal conductivity, diffusion coefficient was also obtained by mean square displacement (MSD) estimation. Although slightly higher, they coincide quite well with the experimental values and show the same experimental tendency: values of both properties for Cu-nanofluids and Ag-nanofluids are higher than base fluid and this is higher than Ni-nanofluids. It would suggest that Cu-nanofluids and Ag-nanofluid are more appropriate than Ni-nanofluids to enhance heat transfer processes.

To gain an accurate molecular-level insight into the sites of the interaction between the metal and the base fluid in the nanofluid system, the radial distribution function (RDF) and spatial distribution function (SDF) were analysed. On the basis of this information, the arrangement of the base fluid around the metal nanoparticle was possible to determine. The number of benzene rings and oxygen atoms from diphenyl oxide around the metal differs depending on the kind of metal incorporated into the base fluid. Due to a stable configuration of orbital d^{10} for copper and silver, it produces a preference for the metal-oxygen interaction. The case of nickel is clearly

different since nickel transfer charge to the benzene rings. Thus, the different arrangement of base fluid around the metal nanoparticle stabilizes the system (in the case of copper and silver nanofluids) and it must be responsible for the improvement of thermal properties [10].

Conclusions: This study shows the preparation of nanofluids based on suspension of copper, silver and nickel nanoparticles into a base fluid composed of the eutectic mixture of diphenyl oxide and biphenyl, commonly used in a Concentrating Solar Power plants. These systems were analysed from an experimental and theoretical perspective. The characterisation revealed no chemical changes were caused in the base fluid when any kind of nanoparticles were added. According to the Dittus-Boelter equation, values of density, viscosity, isobaric specific heat and thermal conductivity were measured, showed an increment of efficiency for copper and silver nanofluids. Theoretical modelling followed the experimental tendency regard to the thermal properties. Addition, the arrangement of the base fluid molecules around the metal nanoparticle was studied as a perspective about how is the internal structure of nanofluid system.

Acknowledgements: We thank the Ministerio de Economía y Competitividad (MINECO) of the Spanish Government for funding under Grant No. ENE2014-58085-R.

References:

1. J. Navas, A. Sanchez-Coronilla, E. I. Martín, M. Teruel, J. J. Gallardo, T. Aguilar, R. Gomez-Villarejo, R. Alcántara, C. Fernandez-Lorenzo, J. C. Pinero and J. Martín-Calleja, On the enhancement of heat transfer fluid for concentrating solar power using Cu and Ni nanofluids: An experimental and molecular dynamics study, *Nano Energy* 27 (2016) 213-224.
2. R. Gómez-Villarejo, E.I. Martín, J.Navas, A. Sánchez-Coronilla, T. Aguilar, J.J. Gallardo, R.Alcántara, D. De los Santos, I. Carrillo-Berdugo, C. Fernández-Lorenzo, Ag-based nanofluidic system to enhance heat transfer fluids for concentrating solar power: Nano-level insights, *Applied Energy* 194 (2017) 19 -29.
3. S.Lee, S.U.S. Choi, S. Li, J.A. Eastman, Measuring thermal conductivity of fluids containing oxide nanoparticles. *J Heat Trans-T Asme* 121 (1999) 280-9.
4. D. Singh, E.V. Timofeeva, M.R. Movarek, S. Cingarapu, W.H. Yu, T. Fischer, S. Mathul, Use of metallic nanoparticles to improve the thermophysical properties of organic heat transfer fluids used in concentrated solar power, *Sol Energy* 105 (2014) 468-78.
5. Y.J. Li, J.E. Zhou, S. Tung, E. Schneider, S.Q. Xi, A review on development of nanofluid preparation and characterization. *Powder Technol* 196 (2009) 89-101.
6. F.W. Dittus and L.M.K. Boelter, *Pioneers in heat transfer – heat transfer in automobile radiators of the tubular type*. University California Publications Eng. 2 (1930) 443-61.
7. M. Chandrasekar, S. Suresh, T. Senthilkumar, Mechanisms proposed through experimental investigations on thermophysical properties and forced convective heat transfer characteristics of various nanofluids – a review. *Renew Sust Energy Rev* 16 (2012) 3917-38.
8. P.K. Namburu, D.P. Kulkarni, A. Dandekar, D.K Das, Experimental investigation of viscosity and specific heat of silicon dioxide nanofluids. *Micro Nano Lett* 2 (2007) 67-71.

9. D. Shin and D.Banerjee, Enhanced specific heat capacity of nanomaterials synthesized by dispersing silica nanoparticles in eutectic mixtures. *J HeatTrans-T Asme* 135 (2013) 032801.
10. J. Philip, P.D. Shima, B. Raj, Enhancement of thermal conductivity in magnetite based nanofluid due to chainlike structures. *Appl Phys Lett* 91 (2007).

PREPARATION OF PERFORMANT COPPER-BASED NANOLUBRICANT FOR AUTOMOTIVE APPLICATION

A. Gondolini^{1*}, E. Mercadelli¹, V. Zin², S. Barison² and A. Sanson¹

¹Institute of Science and Technology for Ceramics (ISTEC) of the National Research Council (CNR), Via Granarolo 64, I-48018 Faenza (RA), Italy

²Institute of Condensed Matter Chemistry and Technologies for Energy (ICMATE) of the National Research Council (CNR), Corso Stati Uniti 4, 35127 Padova (PD), Italy

*Corresponding author: angela.gondolini@istec.cnr.it

Keywords: Nanolubricant, Copper nanoparticles, Non-polar oil, Tribological tests

Introduction: Friction and wear phenomena in various mechanical systems are the principal cause of energy dissipation and damage of materials interface. The improvement of the lubrication properties of fluids operating between sliding surfaces of coupled materials is one of the most effective solution to reduce the friction and lower the excessive heat generation in mechanical couplings. A novel lubricant additive that was recently considered by the industry are nanoparticles [1], which can be dispersed inside conventional lubricating fluids to improve their load-carrying capability and lower the detrimental effects of friction phenomena. However, the main issues for the commercialization of nanolubricants are their long term stability and high production costs [2].

In this work, copper-based nanolubricants containing Cu nanoparticles of different concentration and dimension were produced using a new one-step method, which allows to maintain the nanoparticles suspended in the liquid phase throughout the whole synthesis process. A modified precipitation synthesis method was considered in order to produce stable nano-oils directly in the selected non-polar oil. The tribological behaviors of the synthesized nanolubricants were evaluated as well.

Discussion and Results: Copper nanoparticles were synthesized considering the precipitation method described by Sun et al. [3]. This method was modified as described afterwards in order to transfer the as-produced particles in the lubricant oil without any drying process. The lubricant oil used in this study is PEGASUS 1005 (Mobil, Fairfax, USA). Different nanolubricants were produced with a final concentration of copper equal to 0.005 vol% and 0.01vol%. The synthesis parameters of the 0.01vol% Cu nano-oils were tailored in order to obtain nanolubricants with different Cu particles sizes.

The oil containing the 0.005 vol% of copper was firstly prepared. SEM and DLS analyses confirmed the nanometric nature of the obtained nanoparticles. To produce the final nanolubricants, the as-synthesized nanoparticles were transferred from the aqueous media to heptane solvent using a transferring agent. Once all the particles have been transported in the

heptane, the water-phase was separated and the non-polar-based suspension was introduced directly in the lubricant oil. The obtained suspension was then sonicated for 5 minute, thus letting the heptane to completely evaporate at room temperature. In this way, the as-synthesized particles are maintained in the liquid phase avoiding drying treatment and therefore strong nanoparticles agglomeration. Nanolubricants containing the 0.01vol% of copper nanoparticles of different size were produced in the same way. Table 1 reports the Mean Particle Size (MPS) of the copper particles in lubricants, determined through DLS analysis.

Table 1. Mean Particle Size (MPS) and Polydispersity Index (PI) of the as-prepared Cu particles in lubricants and after 90 days

Sample	[Cu] (%)	MPS _{as-prepared} (nm)	PI _{as-prepared}	MPS _{90days} (nm)	PI _{90days}
<i>Oil+Cu_01</i>	0.005	87±3	0.1	100±8	0.4
<i>Oil+Cu_02</i>	0.01	123±10	0.2	153±8	0.5
<i>Oil+Cu_03</i>	0.01	93±10	0.15	102±5	0.3
<i>Oil+Cu_04</i>	0.01	136±6	0.4	155±5	0.5

These analyses demonstrate the possibility to adapt the Cu particles size transferred into the oil by tuning the synthesis parameters. After 90 days, the nanoparticles maintained a monodispersed distribution with a slightly increased size (Table 1). These results were also confirmed by sedimentation tests (Figure 1).

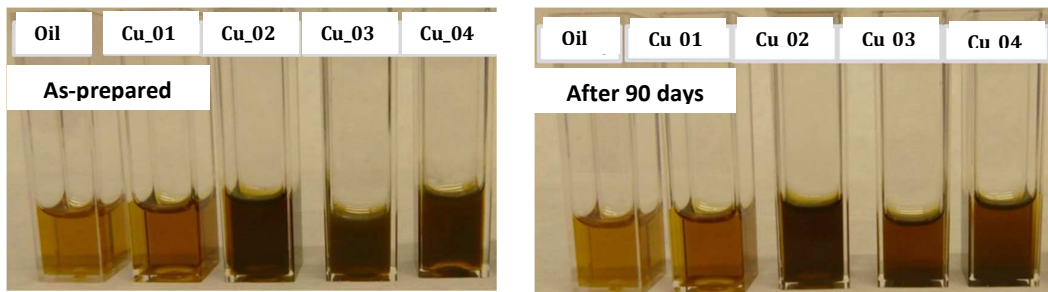


Figure 1. Photo of the as-prepared nanolubricants and of the same after 90 days

The UV-VIS spectra of the produced nanolubricants show an absorbance peak centered at about 450 nm. As reported by Blosi et al [4], this indicates the presence of nanometric Cu₂O particles since the metallic nano-Cu absorbs at about 600 nm.

The viscosity values of the base oil do not change significantly when the copper nanoparticles are additivated between 25 and 80°C.

Tribological characterization has been carried out by means of wear tests at both room temperature and T=80°C (which is the typical working temperature of internal combustion

engines) in a ring-on-flat configuration, (load=30 MPa, sliding speed=10 mm/s, each test lasted for 120 min). The selected geometry allowed better simulating the actual operation conditions of the piston ring-cylinder mechanical coupling. The results of wear tests realized on the prepared oils at room temperature and at $T=80^{\circ}\text{C}$ are reported in Figure 2. All the lubricants additivated with Cu nanoparticles were able to reduce the friction coefficient (COF) at both the temperatures. In particular, the highest COF reduction was obtained using 0.01vol% of Cu having the lowest nanoparticles dimension.

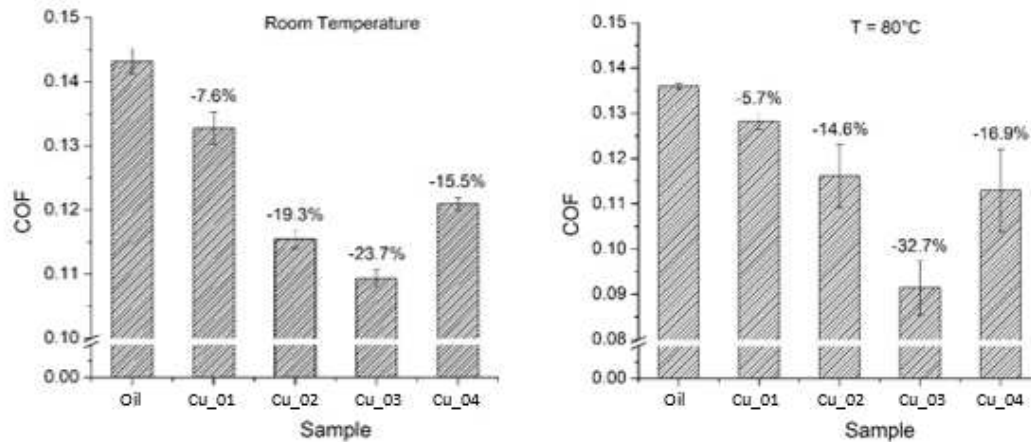


Figure 2. Variation of friction coefficient (COF) for the different as-produced nanolubricants.

Conclusions: Copper based nanolubricants were produced using a modified precipitation method that maintains the nanoparticles in the liquid phase during the entire production process. The produced nanolubricants showed nanometric dimensions of particles and a good stability up to 90 days from their synthesis. The produced nanolubricants are able to reduce the friction coefficients up to the 32.7%.

References:

1. S. Shahnazar, S. Bagheri and S. Bee Abd Hamid, Enhancing lubricant properties by nanoparticle additives, *International Journal of Hydrogen Energy* 41 (2016) 3153-3170.
2. D.K. Devendiran and V.A. Amirtham, A review on preparation, characterization, properties and applications of Nanofluids, *Renewable & Sustainable Energy Reviews* 60 (2016) 21-40.
3. X. Song, S. Sun, W. Zhang and Z. Yin, A method for the synthesis of spherical copper nanoparticles in the organic phase, *Journal of Colloid and Interface Science* 273 (2004) 463-469.
4. M. Blosi, S. Albonetti, M. Dondi, C. Martelli and G. Baldi, Microwave-assisted polyol synthesis of Cu nanoparticles, *Journal of Nanoparticle Research* 13 (2011) 127-138.

FERRONEMATICS- A SPECIAL CLASS OF NANOFUIDS

P. Kopcansky^{1*}, N. Tomasovicova¹, V. Gdovinova¹, J. Majorosova¹, M. Timko¹, N. Eber², T. Toth-Katona² and J. Jadzyn³

¹Institute of Experimental Physics SAS, Kosice, Slovakia

²Institute for Solid State Physics and Optics, Wigner Research Centre for Physics, Hungarian Academy of Sciences, H-1525 Budapest, Hungary

³Institute of Molecular Physics, Polish Academy of Sciences, 60179 Poznan, Poland

*Corresponding author: kopcan@saske.sk

Keywords: liquid crystal, magnetic nanoparticles, ferronematics, Fréedericksz threshold

Introduction: Liquid crystals (LCs) belong to a class of soft condensed matter that are characterized by the combination of fluidity of ordinary liquids with the direction dependent electric and optical properties of crystalline solids. This material is very sensitive to application of an external electric field due to the large value of dielectric anisotropy, whereas they are practically insensitive to application of magnetic field. About 5 decades ago the idea was born to mix nano-sized magnetic particles with nematic LCs, in order to get fluids with a large magnetic susceptibility called ferronematics (FNs) [1]. These materials may serve as sensor of small magnetic fields. This is the way to obtain magnetovision camera similar like thermovision camera. Behaviour of such composite systems near nematic-isotropic transition (T_{I-N}) in the presence of very small magnetic field opens the doors towards application possibilities such as low magnetic field sensors or basic logical elements for information storage technologies. The possible formation of nematic LC phase in solutions containing lysozyme amyloid fibrils (LAFs) and magnetic nanoparticles (MNPs) will be presented. Obtained results may shed light on the effect of MNPs on the liquid crystalline ordering of LAFs which can be helpful in production of biological LCs.

Discussion and Results: The most essential feature of FNs is a strong coupling between the MNPs (their magnetic moment m) and the LC matrix (the director n). The mentioned existing coupling ensures that the effect of magnetic field will be transferred into the nematic host. Based on the experiments, which excluded the presence of parallel orientation of m and n in thermotropic FNs, Burylov and Raikher's theory was constructed [2, 3, 4]. The finite value of the surface density of the anchoring energy W is considered at the nematic- magnetic particle boundary. The finite value of W and the parameter ω is defined as the ratio of anchoring energy to elastic energy of the liquid crystal ($\omega=Wd/K$, where d is the size of the magnetic particles and K represents orientational- elastic Frank modulus). The parameter ω defines the type of anchoring of nematic molecules on magnetic particle surfaces. Rigid anchoring is presented as $\omega \gg 1$, where soft anchoring is characterized by a parameter $\omega \leq 1$ and this type of anchoring permits both types of boundary conditions ($m \perp n$ and $m \parallel n$).

Doping of LCs with small amount of MNPs can lead to the decrease as well as increase of the threshold of the magnetic Fréedericksz transition. It depends on the anisotropy of diamagnetic susceptibility χ_a of the nematic host and also on initial mutual orientation of the nematic director \mathbf{n} and the magnetic moment \mathbf{m} of the MNPs. In work [5] the magnetic Fréedericksz transition was studied in FNs based on the nematic LC 6CHBT that was doped with rod-like MNPs of volume concentration $\phi_1=10^{-4}$ and $\phi_2=10^{-3}$. Fig 1 shows the magnetic Fréedericksz transition of undoped 6CHBT and in FNs doped with the rod-like particles of different volume concentrations. The obtained results show that the reduction of B_c becomes larger if the concentration of the MNPs in FNs is increased.

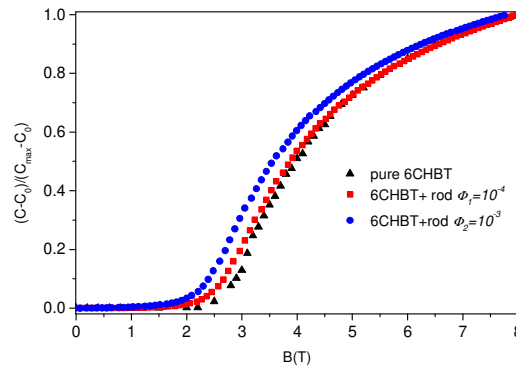


Figure 1: Reduced capacitance versus magnetic field for undoped 6CHBT and 6CHBT doped with rod-like particles of different volume concentrations of magnetic particles.

The magnetic field induced T_{I-N} was also studied in the calamitic LC 6CHBT doped with spherical and rod-like MNPs in volume concentration of $\phi = 2 \cdot 10^{-4}$ [6]. In the undoped 6CHBT as well as in 6CHBT doped with spherical MNPs no measurable field induced shift of the T_{I-N} was observed in magnetic fields up to 10 T. On the contrary, in 6CHBT doped with rod-like MNPs a shift of 0.25 °C was found in the T_{I-N} at 10 T. We have investigated also the influence of doping the mixture (50-50 wt %) of a bent-core (11DCIPBBC) and a calamitic LC (6O08) with spherical MNPs of volume concentration of $\phi = 2 \cdot 10^{-4}$. Results showed a drastically reduction of the critical field of the magnetic Fréedericksz transition after adding MNPs. For instance, a high field of the order of 100 T is required to change the director orientation of undoped LC, while for the case of doped LC with MNPs the critical magnetic field will be only 10 T. Moreover, for the first time was given an experimental evidence of the theoretically predicted magnetically induced negative shift of the T_{I-N} [7].

Our results in study of composite systems based on LC 6CHBT doped with spherical, rod-like MNPs, single-wall carbon nanotubes (SWCNT), and SWCNT functionalized with Fe_3O_4 nanoparticles have shown, that it is possible to increase the sensitivity of LCs on the magnetic field not only in the high magnetic field region (order of several Tesla) but also in the low-magnetic field region [8]. Fig 2 shows the variation of the relative capacitance of the 6CHBT LC and 6CHBT doped with various types of nanoparticles with volume concentration $\phi_1=10^{-4}$

as a function of the magnetic induction B in the low magnetic field range (up to 0.1 T), far below the threshold of the magnetic Fréedericksz transition. The results provide a clear evidence for a linear magnetic field dependence of the capacitance in this low magnetic field region.

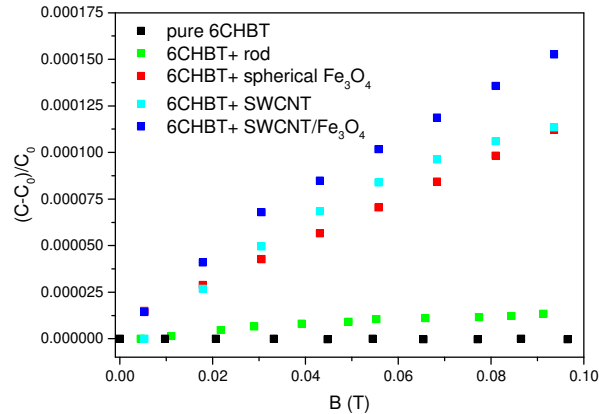


Figure 2: Relative capacitance variation vs. magnetic field for undoped 6CHBT and 6CHBT doped with rod-like nanoparticles, spherical Fe₃O₄ nanoparticles, SWCNT and SWCNT/Fe₃O₄.

The adsorption of MNPs from electrostatically stabilized aqueous ferrofluids on amyloid fibrils of hen egg white lysozyme (HEWL) was studied [9]. It has been observed that extent of adsorption is determined by the MNPs content and the aggregates of the MNPs follow the rod-like structure of fibrils at high concentrations of magnetic nanoparticles. Our results show that there is no adsorption when MNPs are mixed with the solution of lysozyme monomers. The presented results also show a possibility for fibrils ordering into the LC phase by applying external magnetic fields. Thus, the observed formation of specific aggregates from nanoparticles in the studied solutions allows us to consider LAFs as a basis for fabrication of various nanomaterials from MNPs which are sensitive to the external magnetic field.

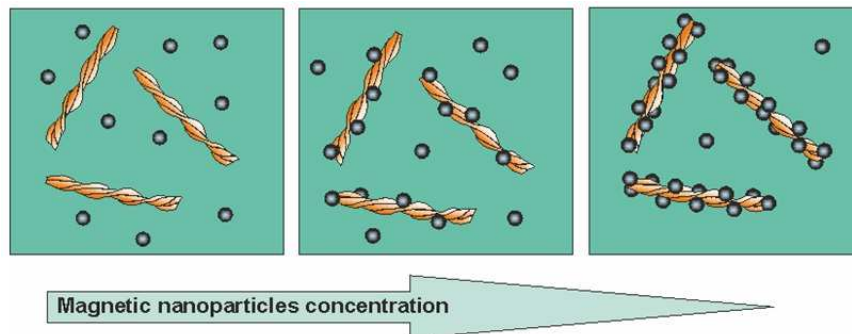


Figure 3: Schematic illustration of the adsorption of magnetic nanoparticles on amyloid fibrils with increasing of magnetic nanoparticles concentration.

Conclusions: We reviewed our experimental work on FNs, namely on the LC 6CHBT doped with various MNPs. It was demonstrated that addition of the nanoparticles has a substantial influence on the sensitivity of FNs to external magnetic fields. Due to bonding between magnetic particles and molecules of the LC, the MNPs help to turn the molecules toward the direction of magnetic field. We have shown that the shape and the size of the MNPs play a significant role in structural transitions. The MNPs as well as SWCNTs can influence the response of LCs also in the low magnetic field range, far below the Fréedericksz transition. Moreover, an increase of the T_{I-N} by 0.25 °C was observed in FNs based on a calamitic LC 6CHBT doped with rod-like MNPs at magnetic field of 10 T. We have shown that the critical field of the magnetic Fréedericksz transition in a LC mixture can be reduced by doping with spherical MNPs. Doping results in a considerable reduction of the T_{I-N} in the absence of a magnetic field. Furthermore, the measured magnetic field induced negative shift of the T_{I-N} is proportional. The impact of various concentrations of MNPs on interaction of LAF was also investigated. Analysis of measurements indicates existence of some “critical” concentration of MNPs at which nanoparticles start to adsorb to the amyloids surface and form cylinder like objects themselves. The adsorption has been studied with the aim to order the fibrils in LC phase by applying external magnetic field. Obtained results may shed light on the effect of MNPs on the liquid crystalline ordering of LAFs which can be helpful in production of biological LCs.

Acknowledgements: This work was supported by project VEGA 2/0016/17, Ministry of Education Agency for Structural Funds of EU in frame of project 26220120033, the Slovak Research and Development Agency under the contact No. APVV-015-0453 and COST Nanouptake.

References:

1. F. Brochard and P. G. de Gennes, Theory of magnetic suspensions in liquid crystals, *Journal de Physique* 31 (1970) 691.
2. S. V. Burylov and Y. L. Raikher, On the orientation of an anisometric particle suspended in a bulk uniform nematic, *Phys. Lett. A* 149 (1990) 279.
3. S. V. Burylov and Y. L. Raikher, Magnetic Fredericksz transition in a ferronematic, *J. Magn. Magn. Mater* 122 (1993) 62.
4. S. V. Burylov and Y. L. Raikher, Macroscopic properties of ferronematics caused by orientational interactions on the particle surfaces. I. Extended continuum model, *Mol. Cryst. Liq. Cryst.* 258 (1995) 107.
5. N. Tomasovicova, M. Timko, V. Zavisova, A. Hashim, J. Jadzyn, X. Chaud, E. Beaugnon and P. Kopcansky, How to change the sensitivity of liquid crystal in external magnetic field, *Magnetohydrodynamics* 48 (2012) 407.
6. P. Kopcansky, N. Tomasovicova, M. Koneracka, V. Zavisova, M. Timko, M. Hnatic, N. Eber, T. Toth-Katona, J. Jadzyn, J. Honkonen, E. Beaugnon and X. Chaud, Magnetic-Field Induced Isotropic to Nematic Phase Transition in Ferronematics, *IEEE Trans. Magn.* 47 (2011) 4409.
7. N. Tomasovicova, M. Timko, N. Eber, T. Toth-Katona, K. Fodor-Csorba, A. Vajda, V. Gdovinova, X. Chaud and P. Kopcansky, Magnetically induced shift of the isotropic-

- nematic phase transition temperature in a mixture of bent-core and calamitic liquid crystals doped with magnetic particles, *Liquid Crystals* 42 (2015) 959.
8. N. Tomasovicova, M. Timko, Z. Mitroova, M. Koneracka, M. Rajnak, N. Eber, T. Toth-Katona, X. Chaud, J. Jadzyn and P. Kopcansky, Capacitance changes in ferronematics liquid crystals induced by low magnetic field, *Phys. Rev. E* 87 (2013) 014501.
 9. J. Majorosova, V. I. Petrenko, K. Siposova, M. Timko, N. Tomasovicova, V. M. Garamus, M. Koralewski, M. V. Avdeev, B. Leszczynski, S. Jurga, Z. Gazova, S. Hayryan, CH. Hu, and P. Kopcansky, On the adsorption of magnetite nanoparticles on lysozyme amyloid fibrils, *Colloids and Surfaces B* 146 (2016) 794-800.

Abstracts

SESSION 4B: COOLING AND OTHERS

THERMOPHYSICAL PROFILE AND HEAT TRANSFER PERFORMANCE OF DISPERSIONS OF FUNCTIONALIZED GRAPHENE NANOPATELETS IN AN INDUSTRIAL COOLANT

J. P. Vallejo^{1,2}, E. Álvarez-Regueiro^{1,2}, D. Cabaleiro¹, J. Fernández-Seara², J. Fernández³ and L. Lugo^{1*}

¹Departamento de Física Aplicada, Facultade de Ciencias, Universidade de Vigo, 36310, Vigo, Spain

²Área de Máquinas e Motores Térmicos, Escola de Enxeñería Industrial, Universidade de Vigo, 36310, Vigo, Spain

³Laboratorio de Propiedades Termofísicas, Grupo NaFoMat, Departamento de Física Aplicada, Universidade de Santiago de Compostela, 15782, Santiago de Compostela, Spain

*Corresponding author: luis.lugo@uvigo.es

Keywords: Functionalized graphene nanoplatelets; Ethylene glycol; Heat transfer; Thermophysical properties

Introduction: The moderate thermal conductivity of current working fluids is a continuous restriction in the process of enhancing heat transfer performance. Hence, during the last decades the attention has been focused on its improving. Nanofluids have been suggested as a promising solution because of the high thermal conductivity of the potential dispersed solids. Thus, numerous studies have been carried out determining their heat transfer performance using metals [1], nitrides [2], oxides [3] and carbon allotropes [4] as nanoadditives. Since the graphene isolation discovery, graphene nanoplatelets have proved their efficiency in this field due to their enhancement of thermal conductivity in base fluids like water [5], ethylene glycol [6] and different oils [7]. Nevertheless, scarce studies have been carried out using commercial coolants as base fluids.

Thermophysical characterization based on the determination of density, heat capacity, thermal conductivity and viscosity, is essential to assess a fluid heat transfer performance. In this study, the thermophysical profile of functionalized graphene nanoplatelet dispersions in an industrial heat transfer fluid ensuring a good stability have been determined. In addition, heat transfer coefficients were experimentally determined together with the associated pressure drops at different flow conditions by using a sensorized experimental facility.

Discussion and Results: Following a two-step method, four different mass concentrations (0.25, 0.50, 0.75 and 1.0) % of polycarboxylate chemically modified graphene nanoplatelets, fGnP, commercially available as graphenit-HYDRO (NanoInnova Technologies S.L., Madrid, Spain), were dispersed in Havoline XCL Premixed 50/50 (Chevron, London, United Kingdom). This commercial working fluid is a long-life coolant based on an ethylene glycol–water mixture and used in many applications providing corrosion protection at high temperatures for the majority of

engine metals and frost protection down to 233.15 K. Furthermore, as part of the base fluid it was added an optimized mass fraction of sodium dodecyl benzene sulphonate dispersant, SDBS (Sigma-Aldrich, Louis, Missouri, USA). The corresponding amounts of each component were weighted in a CPA225 electronic balance (Sartorius AG, Goettingen, Germany) and the dispersions were sonicated by an ultrasonic bath (Ultrasounds, JP Selecta S.A., Barcelona, Spain) at 200 W sonication power and 20 kHz frequency for 240 min.

The thermophysical characterization of the commercial coolant, without and with SBDS, and the different nanofluids was performed in the temperature range from (293.15 to 323.15) K. Densities were experimentally measured using a borosilicate glass Gay-Lussac pycnometer for liquids of 25 ml (Hermanos Alamo, Spain). Specific heat capacities were experimentally determined for the nanopowder and base fluid through a heat-flux differential scanning calorimeter, DSC Q2000 (TA Instruments, New Castel, USA) and then determined for the nanofluids [8]. Effective thermal conductivities, k , were experimentally measured by a KD2 Pro thermal analyzer (Decagon Devices, Inc., Pullman, USA) with a KS-1 probe [9]. Dynamic viscosities, η , under different flow conditions were experimentally determined by a rotational rheometer Physica MCR 101 (Anton Paar, Graz, Austria) with a cone-plate geometry of 25 mm diameter and 1° cone angle [10], observing Newtonian behaviour for all the analysed samples.

Experimental properties of Havoline XCL Premixed 50/50, defined by the supplier as a mixture of 50 vol.% Havoline (93 wt.% ethylene glycol) and 50 vol.% water, were compared to thus published by Melinder [11] for a mixture of 50 vol.% ethylene glycol and 50 vol.% water. Absolute average deviations (AADs) of 0.29 %, 0.45 %, 0.35 % and 2.1 % were found for density, heat capacity, thermal conductivity and viscosity, respectively.

Measured properties of Havoline XCL Premixed 50/50 do not undergo significant changes with the addition of SBDS. The maximum AAD is reached for the viscosity, with a 0.83 %.

Regarding to the nanofluids, densities increase with the nanoadditive loading up to 0.44 % and decrease with the temperature rise up to 1.5 %. With respect specific heat capacities, the dispersion of fGnP leads to decreases of 7.1-7.4 % for the 1 wt.% nanofluid and the increasing temperature causes rises of up to 5.4 % in the analysed temperature range. Figure 1 plots the enhancement in the thermal conductivity and dynamic viscosity increases for the four designed nanofluids in relation to the base fluid at the analysed temperatures.

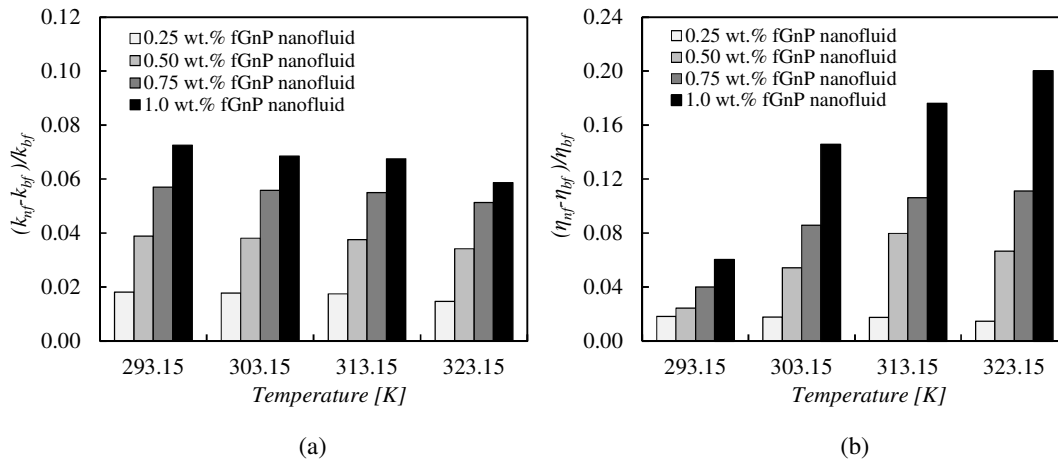


Figure 1: Thermal conductivity (a) and dynamic viscosity (b) increases of fGnP nanofluids regarding the base fluid at different temperatures.

Thermal conductivity enhancements with the fGnP addition achieve 7.3 % for the 1 wt.% nanofluid at 293.15 K, as it can be seen in Figure 1 (a). The observed enhancements are quite similar for each nanofluid concentration overall temperature range whereas the effective thermal conductivity increases with the increasing temperature reach up to 8.9 %, for 1 wt.% nanofluid.

Dynamic viscosity shows an increasing trend with the nanoadditive mass fraction rises, as expected. Percentage increase values range between 1.1 % and 20% as it can be seen in Figure 1 (b). There were also found viscosity decreases with the rising temperature of up to 38 % for the 0.25 wt.% nanofluid.

The experimental facility used to determine the heat transfer coefficients and pressure drops consists of three different circuits: the tested fluid circuit, the heating circuit and the cooling circuit. The main part of this setup is a tube-in-tube heat exchanger of stainless steel. The tested fluid is pumped through the inner tube of the heat exchanger and is heated by the hot water from the heating circuit. The cooling circuit allows the tested fluid to return to its initial conditions and three electric resistances heat the water of the heating circuit again. Various temperature sensors and a differential pressure sensor allow collecting all the test information [5].

Different tests were performed to obtain the convection coefficients and the pressure drops at varied conditions. The tests were defined by the tested fluid flow rate and the average temperatures of tested fluid and hot water. The hot water flow rate was kept constant at 700 L·h⁻¹ in all tests. The well-known Gnielinski correlations for concentric annular ducts in turbulent flow conditions were used to obtain the hot water convection coefficients [12].

In Figure 2, we can see the convection coefficients, h , for those tests in which average temperature pairs of tested fluid/hot water were 308.15/323.15 K and 318.15/333.15 K.

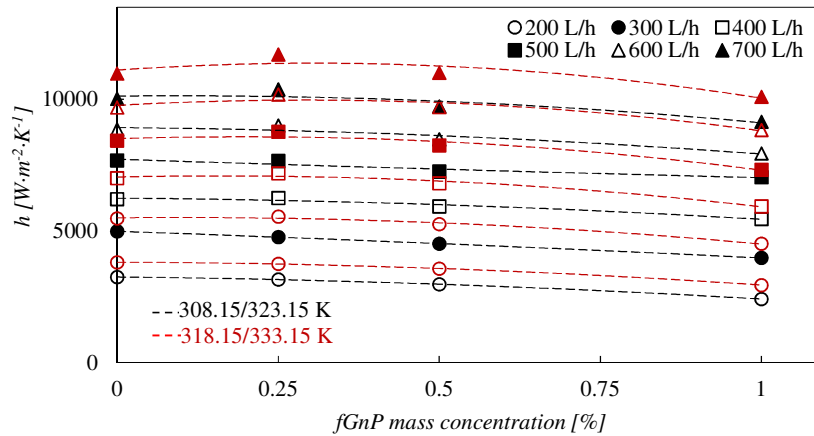


Figure 2: Convection coefficients against functionalized graphene nanoplatelet mass concentration for the 308.15/323.15 K and 318.15/333.15 K tests at different flow rates.

Despite the increases observed in thermal conductivity for all the analysed fGnP mass concentrations, in Figure 2 it can be seen as the only concentration that enhances the convection coefficients of the base fluid at the majority of the flow rates, especially at the highest ones, is 0.25 wt.%. A maximum enhancement of 6.5 % was reached. Furthermore, it can be seen as the increasing flow rate leads to higher convection coefficients and as the increasing tested fluid temperature produces the same effect. With respect to the pressure drop tests, it was detected a slight increasing trend with the increasing fGnP concentration, which does not exceed 1.5 % for the 0.25 % nanofluid for the tested conditions.

Conclusions:

In this work, it was determined the thermophysical profile of four nanofluids consisting of different functionalized graphene nanoplatelet dispersions in a commercial coolant with SDBS for ensure stability, in the temperature range between (293.15 and 323.15) K. Thermal conductivity enhancements up to 7.3 % were reached with the fGnP dispersion, with dynamic viscosity increases between 1.1 % and 20 %.

Furthermore, the heat transfer performance of these new fluids was tested in an experimental facility, determining the heat transfer coefficients and the pressure drops at different flow conditions. Despite the increases observed in thermal conductivity for all the analysed mass concentrations, it was detected that only the 0.25 wt.% nanofluid gets better convection coefficients that the base fluid for most of the tested conditions, achieving enhancements up to 6.5 % for high flow rates. The pressure drop increase with respect base fluid for this concentration is lower than 1.5 % for the analysed test conditions.

Acknowledgements: This work was supported by the “Ministerio de Economía y Competitividad” (Spain) and the FEDER program through the ENE2014-55489-C2-2-R and ENE2014-55489-C2-1-R Projects. Authors also acknowledge the functionalized graphene nanoplatelets powder provided by Nanoinnova Technologies S.L. (www.nanoinnova.com) and the industrial working fluid provided by

Enel Green Power (EGP). Javier P. Vallejo acknowledges the FPI Program of the “Ministerio de Economía y Competitividad”.

References:

1. J.A. Eastman, S. Choi, S. Li, W. Yu, L. Thompson, Anomalously increased effective thermal conductivities of ethylene glycol-based nanofluids containing copper nanoparticles, *Applied physics letters* 78 (2001) 718-720.
2. C. Zhi, Y. Xu, Y. Bando, D. Golberg, Highly thermo-conductive fluid with boron nitride nanofillers, *ACS nano* 5 (2011) 6571-6577.
3. D. Cabaleiro, M. Pastoriza-Gallego, M. Piñeiro, L. Lugo, Characterization and measurements of thermal conductivity, density and rheological properties of zinc oxide nanoparticles dispersed in (ethane-1, 2-diol+ water) mixture, *The Journal of Chemical Thermodynamics* 58 (2013) 405-415.
4. J. Wang, H. Xie, Z. Xin, Y. Li, Increasing the thermal conductivity of palmitic acid by the addition of carbon nanotubes, *Carbon* 48 (2010) 3979-3986.
5. R. Agromayor, D. Cabaleiro, A.A. Pardinás, J.P. Vallejo, J. Fernández-Seara, L. Lugo, Heat Transfer Performance of Functionalized Graphene Nanoplatelet Aqueous Nanofluids, *Materials* 9 (2016) 455.
6. W. Yu, H. Xie, D. Bao, Enhanced thermal conductivities of nanofluids containing graphene oxide nanosheets, *Nanotechnology*, 21 (2009) 055705.
7. S.S.N. Azman, N.W.M. Zulkifli, H. Masjuki, M. Gulzar, R. Zahid, Study of tribological properties of lubricating oil blend added with graphene nanoplatelets, *Journal of Materials Research* 31 (2016) 1932-1938.
8. D. Cabaleiro, C. Gracia-Fernández, J. Legido, L. Lugo, Specific heat of metal oxide nanofluids at high concentrations for heat transfer, *International Journal of Heat and Mass Transfer* 88 (2015) 872-879.
9. D. Cabaleiro, J. Nimo, M. Pastoriza-Gallego, M. Piñeiro, J. Legido, L. Lugo, Thermal conductivity of dry anatase and rutile nano-powders and ethylene and propylene glycol-based TiO₂ nanofluids, *The Journal of Chemical Thermodynamics* 83 (2015) 67-76.
10. D. Cabaleiro, M.J. Pastoriza-Gallego, C. Gracia-Fernández, M.M. Piñeiro, L. Lugo, Rheological and volumetric properties of TiO₂-ethylene glycol nanofluids, *Nanoscale Research Letters* 8 (2013).
11. Å. Melinder, Properties of Secondary Work Fluids for Indirect Systems: Secondary Refrigerants Or Coolants, Heat Transfer Fluids, International institute of refrigeration, 2010.
12. V. Gnielinski, G2 Heat Transfer in Concentric Annular and Parallel Plate Ducts, in *VDI Heat Atlas*, Ed. VDI-Gesellschaft Verfahrenstechnik und Chemieingenieurwesen, Chapter G2, pp. 701-708, Düsseldorf, Springer, 2010.

PERFORMANCE INVESTIGATION OF A MINIATURE PLATE HEAT EXCHANGER WITH GRAPHENE NANOPATELET BASED EG/WATER NANOFLUIDS

Z. Wang, Z. Wu and B. Sundén*

Department of Energy Sciences, Faculty of Engineering, Lund University

Lund SE 22100, Sweden

*Corresponding author: bengt.sunden@energy.lth.se

Keywords: Graphene nanoplatelet nanofluids, Miniature plate heat exchanger, Ethylene glycol, Performance

Introduction:

With the advancement in miniaturization, more efficient miniature heat transfer equipments are needed. As a lot of research [1-2], especially in the design of heat transfer enhancement, focused on extending the heat transfer area, creating turbulence to destroy the boundary layer and adding vortex generators, etc. However, these measures often bring unnecessary pump work to increase flow resistance. For constant surface temperature, the Nusselt number is constant in the laminar flow fully-developed region, which indicates that the smaller the hydraulic diameter, the larger the convective heat-transfer coefficient [3]. The conventional direct technology such as those mentioned above cannot be applied to the miniature equipment with higher heat flux. Another approach to improve the heat transfer is using a fluid medium with better thermophysical properties [4-5]. Because water, ethylene glycol (EG) and engine oil have relatively poor thermophysical properties, some nanoparticles (metal, oxides, carbides, or carbon nanotubes) were added to the above base fluids, forming a colloidal suspension of nanoparticles [6]. These nanofluids usually have higher heat transfer performance than the base fluids and tend to cause little friction penalty. This potential makes them widely usable in microelectronics, fuel cells, heat exchangers, vehicle thermal management, domestic refrigerators, etc. Pantzali et al. [7], Huminic et al. [8] and Solangi et al. [9] presented reviews of nanofluids for heat transfer applications. These reviews implied that nanofluids could have greater potential for usage in different types of heat exchangers. Previous experimental work mainly focused on simple flow geometries, such as a horizontal tube, square heated pipe, and circular tube, etc. The investigations on nanofluids in complex geometries of the heat exchangers are limited. Recent investigations [10] show that the graphene nanoplatelet nanofluids (GNP) could provide higher thermal conductivity enhancement (up to 5000W/m·K) in comparison to that of other examined nanofluids. Because of the special 2D structure with a thickness from 5 to 10 nm, GNP has a high specific surface area (up to 750 m²/g), also has characteristics such as high crystal quality and ballistic electronic transport at room temperature. Some studies found that using the GNP improved heat transfer performance [11]. However, the literature described above focused on the constant heat flux/wall temperature

boundary condition [12]. The heat transfer and flow characteristics of GNP in a miniature plate heat exchanger (MPHE) have not been studied deeply.

The present work investigates the performance of a miniature plate heat exchanger with graphene nanoplatelet-based EG/water nanofluids. The main reasons for choosing this are: no previous research has been performed regarding effect of GNP nanofluids on MPHEs, and the significant improvement in convective heat-transfer coefficient may be obtained in MPHE based on the high thermal conductivity of GNP. For this reason, some relevant experiments and analyses on heat transfer performance and pressure drop are required to apply GNP in the MPHE system.

Results and Discussion:

In this study, commercial nanofluids of EG/water (50:50) graphene nanoplatelet (GNP R-7, 5 wt.%) that present satisfying stability was provided by XG Sciences, Inc., Lansing, MI, USA. The primary thickness of the GNP is about 2 nm, their diameter is about 2 μm , and the average specific surface area is 750 m^2/g . The tested weight concentrations (0.01 to 2 wt.%) were obtained by diluting the 5 wt.% nanofluid. The diluted GNP nanofluid was mechanically mixed for 1 hour, followed by using a high-power ultrasonication to oscillate four hours. The effective thermal conductivity under different concentrations were measured by a thermal constants analyzer (Hot Disk TPS 2500S, Sweden). The uncertainty deviations of thermal conductivity were verified by several standard specimens, which is lower than 3.0%. A DV2TLV viscometer with UL adapter accessory (Brookfield AMETEK, US) was used to measure viscosity of different concentrations. The range of accuracy with test data is $\pm 1.0\%$ and the repeatability is $\pm 0.2\%$.

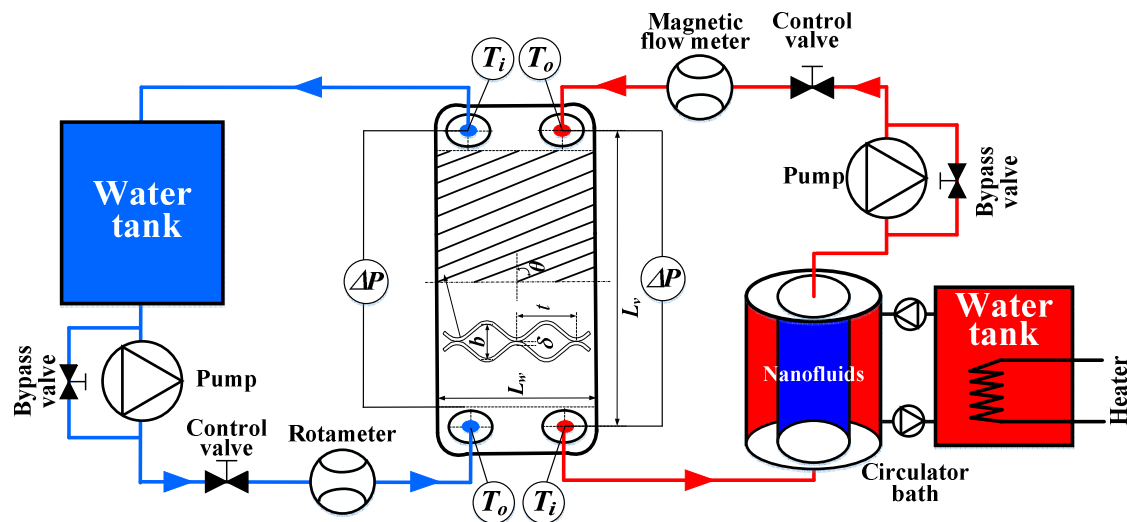


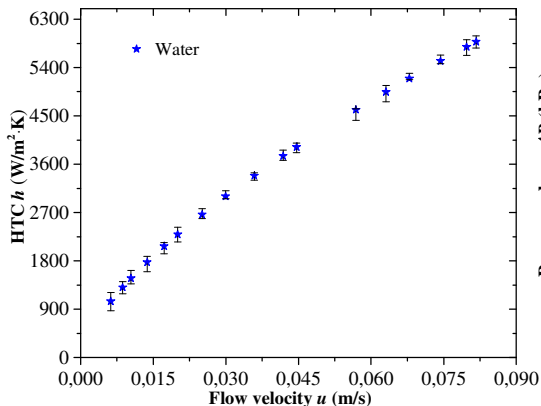
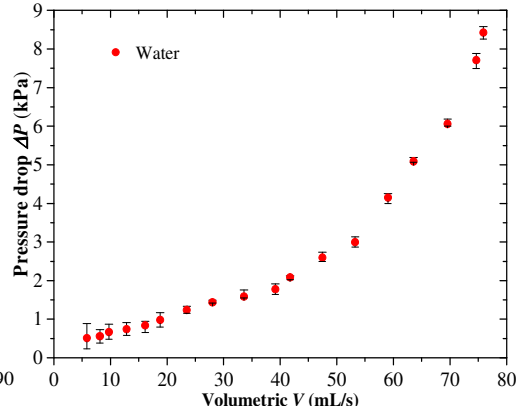
Figure 1. Schematic diagram of the experimental setup and MPHE

Table 1. Error analysis of relevant parameters

Measurement items	Unit	Value
Temperature	K	± 0.1
Pressure drop	kPa	$\pm 1.5\%$
Thermal conductivity	W/m·K	$\pm 3.0\%$
Viscosity	cp	$\pm 1.0\%$
Flow rate	L/h	$\pm 2.0\%$
Heat flux	W/m ²	$\pm 3.7\%$
LMTD	K	$\pm 1.5\%$
Heat transfer coefficient	W/m ² ·K	$\pm 4.1\%$

The MPHE, provided by Alfa Laval, comprises several stainless steel chevron-type plates that form two spaced fluid passages for the hot and cold fluids. The experimental setup for heat transfer in MPHE is shown in Figure 1. It mainly consists of a hot fluid closed loop, a cold fluid open loop and the corresponding temperature, mass flow rate and pressure measuring instruments. The GNP nanofluid was the hot fluid and heated to the required inlet fluid temperature in a heating tank. Then it was fed into the MPHE by a pump, passing through a rotameter, and returned to the heating tank. The water was stored in a cold tank and circulated by a pump. It passed a control valve, a rotameter and then entered the PHE in a counter flow. After absorbed the heat from the nanofluid, the cold water was drained. The measurement parameters of test bed consist of rotameters, K-type thermocouples and a differential pressure transducer, etc. The error of relevant parameters of this experiment system was shown in Table 1.

Experiments using water-to-water were carried out first to obtain heat transfer and pressure drop correlations for pure fluids flowing in the MPHE. The experimental measurements were temperature at inlet and outlet of the MPHE, pressure and flow rates for hot and cold water. These data were used to calculate the related heat transfer and pressure drop parameters. The comparisons of the heat transfer performance between the GNP nanofluids and water are shown based on a constant flow velocity, which avoids the effect of nanofluid physical properties on a constant Reynolds number basis. Figure 2 shows the heat transfer coefficient (HTC) versus flow velocity. The flow velocity is defined as $u=V/L_w b_c N$, where V is the volumetric flow rate, and N is the number of flow channels. With increasing flow velocity, the heat transfer coefficient increases in the MPHE. The relationship between the pressure drop ΔP and the volumetric flow rate V for water is displayed in Figure 3. The fluid properties, flow velocity and geometry of heat exchanger determine the pressure drop.

Figure 2. HTC versus u Figure 3. ΔP versus V

Next, the effect of concentrations (0.01-2 wt.%) and temperature (20-55°C) of GNP nanofluids on convective heat transfer coefficient and pressure drop in the MPHE will be investigated and compared with water.

Summary: As a general conclusion, it is evident in most cases that nanofluids provide a plausible solution to high heat flux and small size limit situation. Motivated by these challenges, the thermal conductivity and viscosity along with convective heat transfer and pressure drop of graphene nanoplatelet-based EG/water nanofluids at various concentrations and temperatures in MPHE have been studied experimentally. The preliminary results show that the heat transfer performance improves with an increase in flow velocity and with a decrease in nanofluid concentration. The GNP nanofluid has brought an acceptable pressure drop penalty but has a higher heat transfer performance compared with water in the MPHE. The enhancement of pumping power is moderate under this experimental condition which favors GNP nanofluid to be used in the MPHE for thermal systems. The results from the latest experiment of GNP nanofluid are now being analyzed, and further improvement work is ongoing.

References:

1. Wang Z, Li Y, Layer pattern thermal design and optimization for multistream plate-fin heat exchangers-A review, *Renewable and Sustainable Energy Reviews* 53 (2016) 500-514.
2. Wang Z, Li Y, A combined method for surface selection and layer pattern optimization of a multistream plate-fin heat exchanger, *Applied Energy* 165 (2016) 815-827.
3. Mohammed, H. A., Bhaskaran, G., Shuaib, N. H., & Saidur, R., Heat transfer and fluid flow characteristics in microchannels heat exchanger using nanofluids: a review, *Renewable and Sustainable Energy Reviews* 15 (2011) 1502-1512.
4. Murshed S M S, de Castro C A N. Conduction and convection heat transfer characteristics of ethylene glycol based nanofluids-A review, *Applied Energy* 184 (2016) 681-695.
5. Solangi, K. H., Kazi, S. N., Luhur, M. R., Badarudin, A., Amiri, A., Sadri, R., Teng, K. H., A comprehensive review of thermo-physical properties and convective heat transfer to nanofluids, *Energy* 89 (2015) 1065-1086.

6. Hussien A A, Abdullah M Z, Moh'd A A N, Single-phase heat transfer enhancement in micro/minichannels using nanofluids: Theory and applications, *Applied Energy* 164 (2016) 733-755.
7. Pantzali M N, Mouza A A, Paras S V, Investigating the efficacy of nanofluids as coolants in plate heat exchangers (PHE), *Chemical Engineering Science* 64 (2009) 3290-3300.
8. Humnic G, Humnic A, Application of nanofluids in heat exchangers: a review, *Renewable and Sustainable Energy Reviews* 16 (2012) 5625-5638.
9. Sajedi R, Taheri M, Taghilou M., On the multi-objective optimization of finned air-cooling heat exchanger: Nano-fluid effects. *Journal of the Taiwan Institute of Chemical Engineers* 68 (2016) 360-371.
10. Sadeghinezhad, E., Mehrali, M., Saidur, R., Mehrali, M., Latibari, S. T., Akhiani, A. R., Metselaar, H. S. C., A comprehensive review on graphene nanofluids: recent research, development and applications. *Energy Conversion and Management* 111 (2016) 466-487.
11. Amiri, A., Arzani, H. K., Kazi, S. N., Chew, B. T., Badarudin, A., Backward-facing step heat transfer of the turbulent regime for functionalized graphene nanoplatelets based water–ethylene glycol nanofluids, *International Journal of Heat and Mass Transfer* 97 (2016) 538-546.
12. Akhavan-Zanjani, H., Saffar-Avval, M., Mansourkiaei, M., Sharif, F., Ahadi, M., Experimental investigation of laminar forced convective heat transfer of Graphene–water nanofluid inside a circular tube, *International Journal of Thermal Sciences* 100 (2016) 316-323.

LAMINAR FORCED CONVECTION IN FLAT TUBES WITH Al_2O_3 -WATER MIXTURE FOR AUTOMOTIVE APPLICATIONS

B. Buonomo¹, D. Ercole¹, O. Manca^{1*}, A. Minea² and S. Nardini¹

¹Dipartimento di Ingegneria Industriale e dell'Informazione, Università degli Studi della Campania, Via Roma 29, Aversa (CE), 81031, Italy

²Faculty of Materials Science and Engineering, Technical University "Gh. Asachi" from Iasi Bd. D. Mangeron 60, Iasi, 700050, Romania

*Corresponding author: oronzio.manca@unicampania.it

Keywords: Nanofluids, Numerical models, Mixture, Flat tubes, Automotive

Introduction: In recent years, the fast development of vehicle engine performance has determined a strong request of high cooling efficiency of a vehicle radiator and it is a vital equipment to remove the engine waste heat for keeping normal operating of automotive system as underlined in [1]. Convective heat transfer can be enhanced passively by changing flow geometry, boundary conditions or by enhancing the thermal conductivity of the working fluid [2]. For an assigned heat exchanger system, conventional fluids, such as pure water and ethylene glycol, present low thermal conductivity and, consequently, a low heat transfer performance. Therefore, it is highly desired to have innovative and effective heat transfer fluids to enhance vehicle radiator cooling rate [3]. Engine cooling system using nanofluids provides a new foundation for technological integration and innovation. Nowadays, an increased attention is focused on the using nanofluids for vehicle radiator in order to improve the heat transfer performance of engine cooling systems, as reviewed in [1, 4-11]. Moreover, a technique which is employed for heat transfer augmentation is the use of flattened tubes and a recent study which combines both nanofluids and flattened tubes was proposed in [10-12].

The use of nanofluids instead of the conventional fluids in car radiators was studied for the first time in [13]. In this study was reported a project to target fuel savings for the automotive industries through the development of energy efficient nanofluids and smaller and lighter radiators. Later, several numerical and experimental investigations have been accomplished on the use of nanofluids in automotive car radiators.

A short review on numerical studies is accomplished, mainly on laminar flow. Laminar flow in the flat tubes of an automobile radiator with two mixtures of Al_2O_3 and CuO nanoparticles in an ethylene glycol and water was presented in [14]. The cooling performances of an automotive radiator using ethylene glycol based CuO nanofluids as coolants was studied in [15]. A three-dimensional analysis was used to study the heat transfer performance of nanofluid flows through a flattened tube in a laminar flow regime and constant heat flux boundary condition.

More recent numerical studies in laminar flow are reported in [10,11,16-18]. Steady state laminar convection in a flat tube with nanofluids, Al₂O₃ in water or in water-ethylene glycol mixture, was numerically investigated in [16]. The friction factor and forced convection heat transfer of SiO₂ nanoparticle dispersed in water as a base fluid were evaluated in a car radiator experimentally and numerically in [17]. A numerical investigation on laminar forced convection flow of Al₂O₃ nanoparticles in water or water and glycol in a flat tube was accomplished in [18]. A three-dimensional numerical study to evaluate the laminar heat transfer and flow behaviors of Al₂O₃-water nanofluids through a flat tube at constant heat flux boundary condition is reported in [10]. A flat tube of an engine radiator was numerically studied in [11] to enhance the cooling process or heat recovery of the engine using nanofluids.

Some issues in laminar convective flow in flat tubes geometry with nanofluids presents a lack of information such as the effect of tube/duct thickness on heat transfer inside the duct and the effective convenience to employ the nanofluids in practical applications such as car cooling systems and radiators. Moreover, the comparison between single phase and mixture models allows to evaluate the possible errors related to the use of a simpler model. In the present study both single phase model and mixture model are employed to simulate laminar convective flow in Al₂O₃-water nanofluid mixtures in a flat duct with assigned wall heat flux on the external surface of a duct with an assigned thickness.

Discussion and Results: The geometrical configuration under consideration consists in a duct with two parallel flat plates and the lateral sides with a circular shape as shown in Fig. 1. The length of the duct, the edge one and the channel height is 0.5 m, 0.0081 m and 0.00254 m, respectively. In this way, the hydraulic diameter is set equal to 4.58×10^{-3} m. The thickness of the duct is 0.23×10^{-3} m. A steady laminar flow and different nanoparticle volume fractions have been considered. The analysis has been performed for nanofluids with water as base fluid and spherical nanoparticles of alumina (Al₂O₃) with a diameter equal to 38 nm. Thermophysical properties are considered constant with temperature. The CFD commercial code Ansys-Fluent [19] was employed in order to solve the 3-D numerical model. A grid independence analysis has been accomplished to evaluate the optimal node number in terms of computational time and accuracy. Moreover, a validation procedure was performed in the case of pure water and fully developed laminar flow, with data reported in [20].

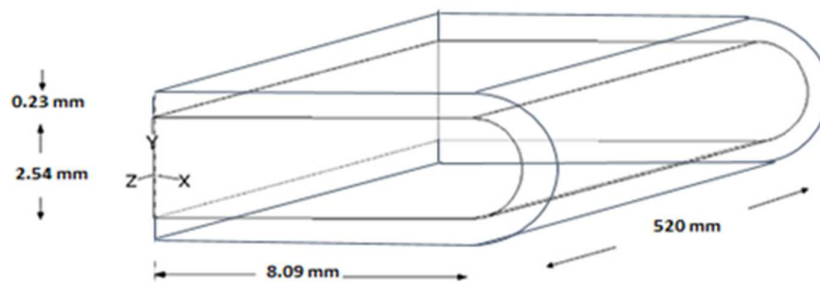


Figure 1. Sketch of the geometrical model.

Results are presented in terms of internal wall and bulk temperatures, local and average convective heat transfer coefficient, pressure drops, required pumping power profiles and two energy performance ratios, as a function of Re, ranging from 100 to 1000, and particle concentrations, in the range 0%-5% in pure water mixture. A constant and uniform heat flux of 2 kW/m² is applied on all the channel walls.

In Fig. 2, the internal wall and bulk temperatures, Fig. 2a, and the heat transfer coefficient, Fig. 2b, are given, along the axis, for a volumetric concentration equal to 5%. The temperature profiles are evaluated for three Re values and it is noted, as expected, that the greater the Re the temperature values. In Fig. 2b, the h profiles are evaluated for the single phase and mixture models. At the entrance the h values evaluated with mixture model are higher than that the ones evaluated with the single phase model. The differences decreases with the increase of z coordinate and are smaller in fully developed conditions. It is interesting to observe that the h values along z, for different volumetric concentrations and not reported, are greater as greater the volumetric concentration with the higher differences at the entrance zone. In Fig. 3, pressure losses and C_f coefficient are reported for single phase and mixture models for different volumetric concentrations. It is noted, in Fig. 3a, that the pressure losses are slightly higher in the mixture model whereas the friction factor, C_f values, does not depend on the model and volumetric concentrations. In order to evaluate the performance of the heat transfer by means of nanofluids and its advantage the evaluation performance ratio, EPR, is considered. In Fig. 4, two different EPRs are reported:

$$EPR = \frac{Q_{nf} - Q_{bf}}{W_{nf} - W_{bf}} \quad \text{and} \quad EPR' = \frac{Nu_{nf} / Nu_{bf}}{(C_{f,nf} / C_{f,bf})^{1/3}} \quad (1)$$

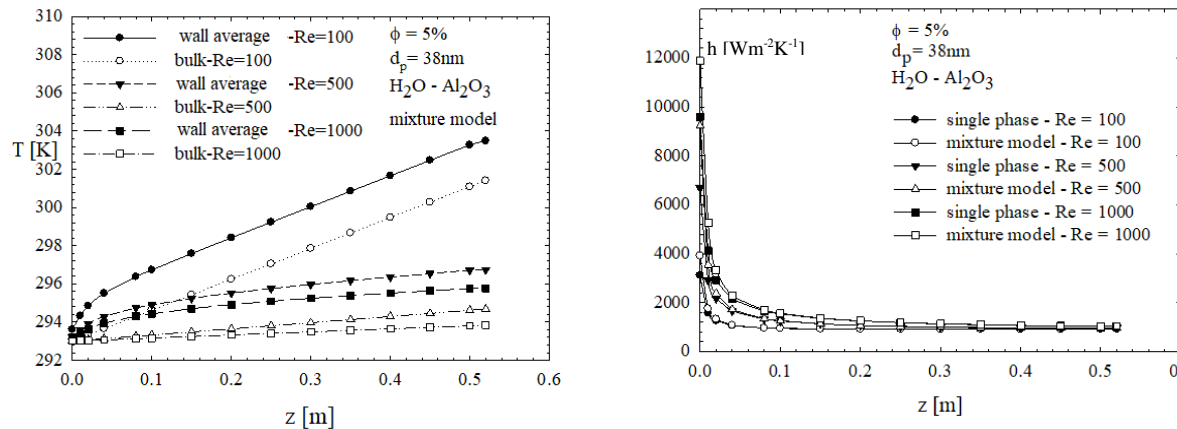


Figure 2. Profiles of local variables along the tube axis: a) wall and bulk temperatures
b) convective heat transfer coefficient.

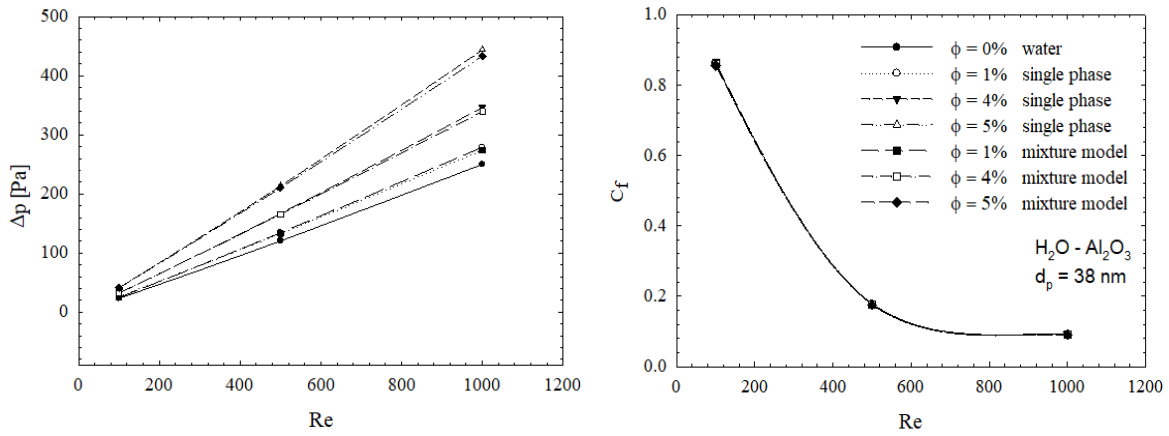


Figure 3. Fluid dynamics variables as a function of Reynolds number: a) pressure losses
b) friction factor.

with Q and W the heat transfer rate moved to the fluid and the mechanical power given to move the fluid, nf and bf are related to the nanofluid and base fluid, respectively. The first ratio indicates that the pure fluid has the best performances but the differences decrease as the Reynolds number increases whereas the second ratio, EPR' , provides an opposite information, i.e., the use of nanofluids determines a better performance of the heat transfer.

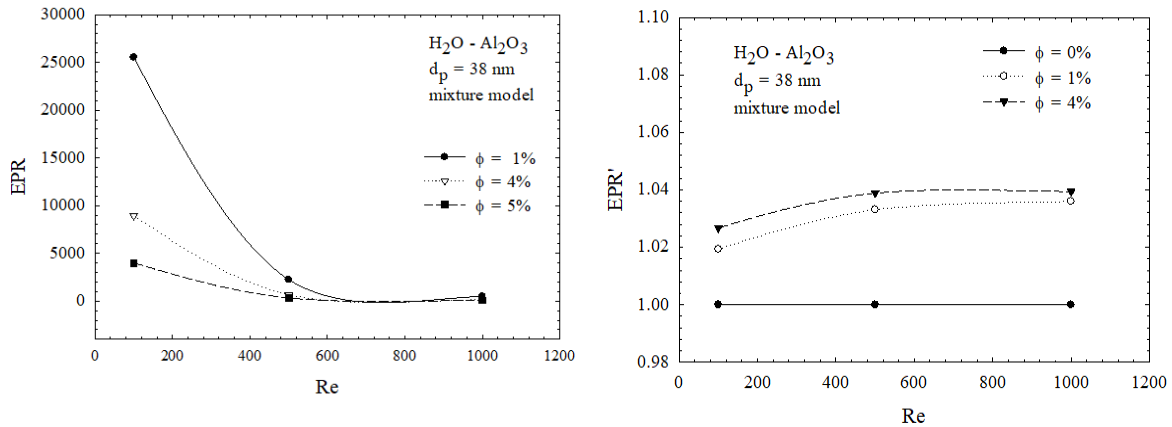


Figure 4. Evaluation performance ratio as in eq. (1).

Conclusions: A numerical investigation on laminar convective heat transfer in flattened ducts with nanofluids was performed to compare single phase and mixture models and evaluate the performance of the system by means of two different ratios. Some differences in terms of heat transfer coefficients and pressure drops were detected between the two models. As expected, the heat transfer coefficients increase as the volumetric concentration increases and for local heat

transfer coefficients the most significant increases were detected in the entrance zone. It was showed that the definition of evaluation performance ratio determined if the nanofluid presents a better performance with respect to the base fluid. In fact, in terms of energy ratio the base fluid is more convenient whereas in terms of Nusselt ratio related to the friction factor ratio the nanofluid provides a better performance.

References:

1. N.A. Che Sidik, M.N.A. Witri Mohd Yazid and R. Mamat, Recent advancement of nanofluids in engine cooling system, *Renewable and Sustainable Energy Reviews* 75 (2017) 137-144.
2. R.L. Webb and N.H. Kim, *Principles of Enhanced Heat Transfer*, 2nd ed., Taylor&Francis Group, New York, 2005.
3. P. Kulkarni Devdatta, S. Vajjha Ravikanth, K. Das Debendra and D. Oliva, Application of aluminum oxide nanofluids in diesel electric generator as jacket water coolant, *Applied Thermal Engineering* 28 (2008) 1774-1781.
4. N.A.C. Sidik, M.N.A.W.M. Yazid and R. Mamat, A review on the application of nanofluids in vehicle engine cooling system, *International Communications in Heat and Mass Transfer* 68 (2015) 85-90.
5. N. Zhao, S. Li and J. Yang, A review on nanofluids, Data-driven modeling of thermalphysical properties and the application in automotive radiator, *Renewable and Sustainable Energy Reviews* 66 (2016) 596-616.
6. S.S. Murshed, K. Leong and C. Yang, A combined model for the effective thermal conductivity of nanofluids, *Applied Thermal Engineering* 29 (2009) 2477-2483.
7. S.S. Murshed and C.N. de Castro, Conduction and convection heat transfer characteristics of ethylene glycol based nanofluids—a review, *Applied Energy* 184 (2016) 681-695.
8. S.S. Murshed and P. Estellé, A state of the art review on viscosity of nanofluids, *Renewable and Sustainable Energy Reviews* 76 (2017) 1134-1152.
9. G. Zyla, J. Fal and P. Estellé, Thermophysical and dielectric profiles of ethylene glycol based titanium nitride (TiN-EG) nanofluids with various size of particles, *International Journal of Heat and Mass Transfer* 113 (2017) 1189-1199.
10. N. Zhao, J. Yang, H. Li, Z. Zhang and S. Li, Numerical investigations of laminar heat transfer and flow performance of Al₂O₃-water nanofluids in a flat tube, *International Journal of Heat and Mass Transfer* 92 (2016) 268-282.
11. M. Hatami, M. Jafaryar, J. Zhou and D. Jing, Investigation of engines radiator heat recovery using different shapes of nanoparticles in H₂O/(CH₂OH)₂ based nanofluids, *International Journal of Hydrogen Energy* 42 (2017) 10891-10900.
12. A.M. Hussein, H.K. Dawood, R.A. Bakara and K. Kadirgamaa, Numerical study on turbulent forced convective heat transfer using nanofluids TiO₂ in an automotive cooling system, *Case Studies in Thermal Engineering*, 9 (2017) 72-78
13. S. Choi, Nanofluids for improved efficiency in cooling systems, *Heavy Vehicle Systems Review*, Argonne National Laboratory, April 18-20, 2006.

14. R.S. Vajjha, D.K. Das and P.K. Namburu, Numerical study of fluid dynamic and heat transfer performance of Al₂O₃ and CuO nanofluids in the flat tubes of a radiator, *International Journal of Heat and Fluid Flow* 31 (2010) 613–621.
15. G. Huminic and A. Huminic, Numerical analysis of laminar flow heat transfer of nanofluids in a flattened tube, *International Communication in Heat and Mass Transfer* 44 (2013) 52–57.
16. B. Buonomo, O. Manca, L. Marinelli, S. Nardini, Laminar Forced Convection in Flat Tubes with Nanofluids for Automotive Applications, *Proceedings of Third International Conference on Computational Methods for Thermal Problems THERMACOMP2014*, pp. 125-128, Lake Bled, Slovenia, June 2-4, 2014.
17. Hussein AM, Bakar RA, Kadirgama K. Study of forced convection nanofluid heat transfer in the automotive cooling system. *Case Stud Therm Eng* 2014; 2:50–61.
18. B. Buonomo, D. Ercole, O. Manca and A.A. Minea, A numerical investigation on laminar forced convection with nanofluid in heated flat tubes, paper n. 88, *Proceedings of 26th International Symposium on Transport Phenomena (ISTP-26)*, Leoben, Austria, 27 September - 01 October, 2015.
19. Ansys Incorporated, *Fluent 16.0 User Manual*, 2016.
20. R.K. Shah and A.L. London, *Laminar Flow Forced Convection in Ducts*, Academic Press, New York, 1978.

THERMAL PERFORMANCE OF SUSPENSIONS OF GRAPHANE NANOPATELETS IN PLATE HEAT EXCHANGER

F.E.B. Bioucas, M.L. Matos Lopes*, S.M.S. Murshed and C.A. Nieto de Castro

Centro de Química Estrutural, Faculdade de Ciências, Universidade de Lisboa,
1749-016 Lisboa, Portugal

*Corresponding author: matoslopes@ciencias.ulisboa.pt

Keywords: Nanofluids, Convective heat transfer, Overall heat transfer coefficient, Pressure drop, Graphene

Introduction:

Many experimental studies have been reported in the literature, which suggest that the addition of nanoparticles enhance the heat transfer coefficient (HTC) in the laminar and turbulent flow regime as well as during pool and flow boiling. However, the effect on heat transfer is not clear as many of these studies have also shown that nanoparticles have no effect or deteriorate HTC [1].

In the present work, the effect of the use of a nanofluid consisting of a mixture of nanoplatelets of graphene (with a concentration between 0.027 to 0.10 w/w %) in a miniature plate heat exchanger (PHE) with corrugated surface has been experimentally studied. The PHE performance was compared to that of a conventional thermal fluid, water and ethylene-glycol mixture.

Experimental:

The heat exchanging experiments were performed with the setup shown in Figure 1. A miniature plate heat exchanger (PHE) was used, using a relative small quantity of cooling liquid (~0.3L) for its operation. This PHE is part of a Technical Teaching Equipment (EDIBON), and is connected to a tubing base unit comprising flow pump, valves and, flowmeters. The ensemble is operated through a computer controlled system that also measures the inlet and outlet temperatures and fluxes of both hot and cold fluids. The cold fluid is demineralized tap water and the hot fluid under study, is heated/refrigerated thermostatic bath, kept in closed circuit with approximately 4L total volume. For each experiment different inlet temperatures of the hot fluid are obtained by setting the thermostatic bath temperatures and the flow rates of the two streams. After steady state is established the data is recorded, allowing to obtain the heat flux in both hot and cold streams and the average heat transfer rate \bar{Q} in the PHE.

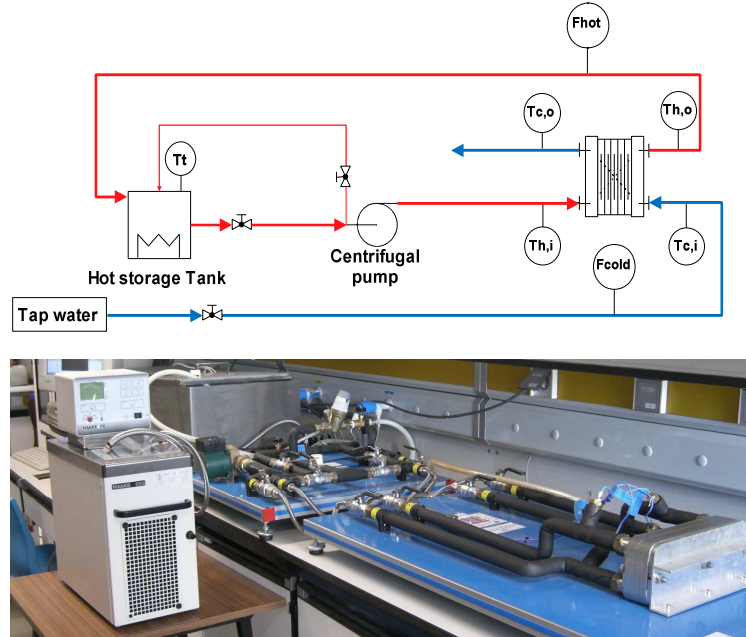


Figure 1. Schematic diagram (top) and picture (bottom) of the heat exchanger experimental setup

Correlation Development Methodology:

The correlation was developed based on the experimental results for water in both hot and cold streams following the algorithm schematically presented in Figure 2.

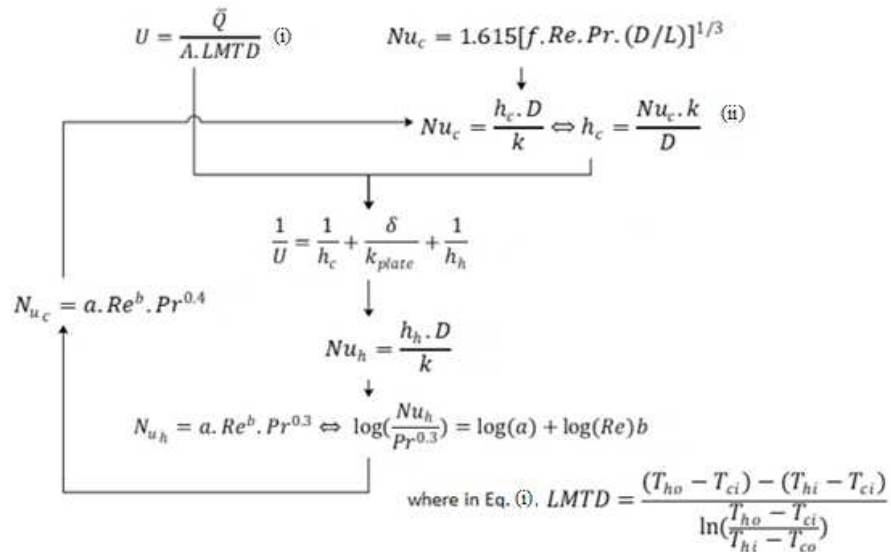


Figure 2. Schematic of the concept of development of correlations for hot and cold fluids.

This uses well known equations and definitions for, (i) the overall heat transfer coefficient, U , related to the hot and cold heat transfer coefficients, h_h, h_c , and the wall resistance, δ/k_{plate} , and calculated from the heat transfer rate, \bar{Q} , the heat transfer area, A and the logarithmic mean temperature difference, $LMTD$ and (ii) for the Nusselt number related to the heat transfer coefficient, h , the thermal conductivity, k , of each stream and the equivalent diameter, D of the PHE ducts. General correlations of the Nusselt number with the Reynolds and Prandtl numbers were used in the form $Nu = a.Re^b.Pr^c$, where the parameter c is taken as 0.3 and 0.4 for cold and hot streams, respectively and parameters a and b , are adjusted in the iteration process until no change is obtained for their values. For the starting value of h_c , any common correlation based on a L ev eque type equation with a suitable form for the friction factor, f , can be used [2]. This same procedure has been used by other authors [3-6] and allows to take into account, with the parameters a and b , the geometry and flow patterns of different types of heat exchangers. From different operating conditions (temperature and flow rates) we obtained for our PHE the values shown Table 1, where they are also compared with values reported by other authors for similar plate heat exchangers. The differences observed correspond in reality to different observed heat transfer coefficients because each of these correlations is applied to slightly different geometries for the same kind of chevron-type corrugation pattern plate heat exchangers.

Table 1. Parameters in the correlation obtained for similar PHE.

a	b	Ref.
0.456	0.548	This work
0.247	0.66	Pantzali et al. (2009)
0.455	0.66	Mar�e et al. (2011)
0.2302	0.745	Huang et al. (2015)
0.3762	0.6681	Huang et al. (2016)

This results in different flux patterns that of course influence the value of the heat transfer coefficient.

Results and Discussion:

The correlation was used for water as cold stream and hot streams of water and water, ethylene glycol mixtures. The expected effect was observed (Figure 3). That is, the ethylene glycol as known decreases the HTC. Nevertheless, its use mixed with water in heat exchangers is quite spread since it works as anti-freezing agent.

From the measurements performed no apparent effect is observed when adding graphene nanoplatelets of characteristic dimensions length 15 μm width 6-8 nm. In the representation we use a simple linear fit to the experimental data which is very dispersed. There seems to be a tendency for lower HTC relating to the base fluids but, within the experimental uncertainty there is no effect.

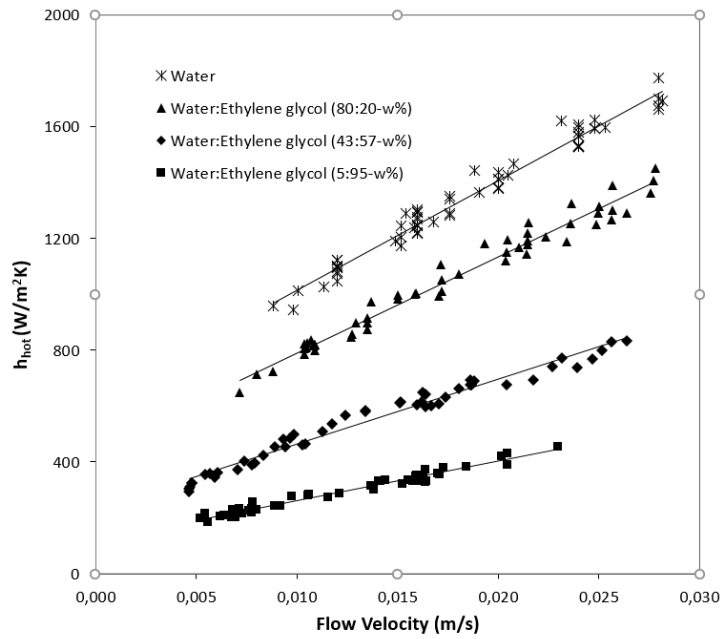


Figure 3. Heat transfer coefficients for water and water, ethylene glycol mixtures with different weight fractions

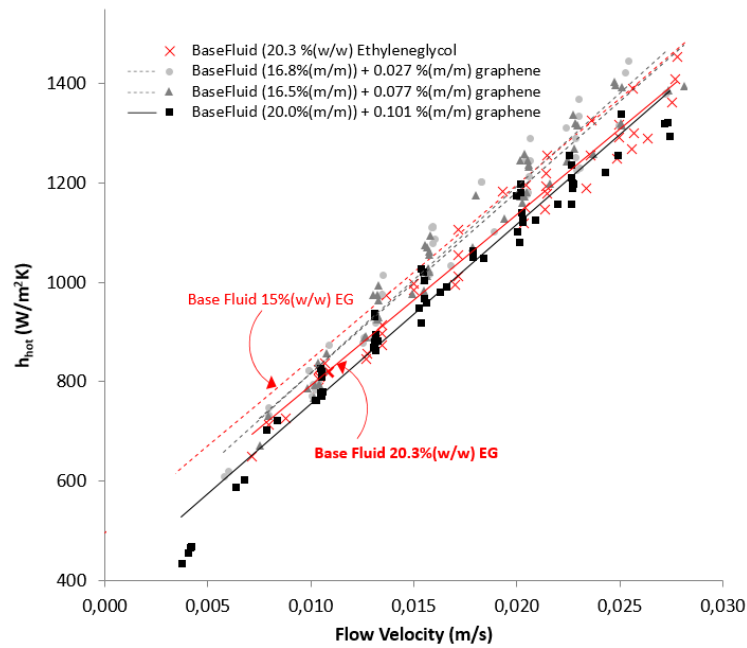


Figure 4. Heat transfer coefficients for graphene nanoplatelets nanofluids with different concentrations, in relation with the base fluids.

However, we have reasons to believe that there is deposition of the nanoparticles on the surfaces of the heat exchanger plates that would alter the geometry and flow patterns of the PHE making the correlation determined not valid to obtain reliable results for the heat transfer coefficients. We are currently investigating this possibility and a thorough study of the suspension stability, particle size control, occurring agglomeration and sedimentation, will follow before being able to take any conclusions regarding the existence of any enhancement of the HTC related to the presence of the graphene nanoplatelets.

Summary/Conclusions:

At its present stage, the study shows inconclusive results for the use of this kind of nanofluids as a solution towards designing efficient heat exchanging systems and points out the concern to the well-known instability of the nanoparticle suspensions. In cases like this where flow is involved, suspension stability, particle size control and sedimentation and agglomeration of nanoparticles is critical in the development and application of these heat transfer fluids.

References:

1. S.M.S. Murshed and C.A. Nieto de Castro, *Nanofluids: Synthesis, Properties and Applications*, Nova Science Publishers Inc., New York, 2014.
2. H. Martin, A theoretical approach to predict the performance of chevron-type plate heat exchangers. *Chemical Engineering and Processing* 35 (1996) 301-310.
3. M.N. Pantzali, A.G. Kanaris, K.D. Antoniadis, A.A. Mouza, S.V. Paras, Effect of nanofluids on the performance of a miniature plate heat exchanger with modulated surface. *International Journal of Heat and Fluid Flow* 30 (2009) 691–699.
4. T. Maré, S. Halelfadl, O. Sow, P. Estellé, S. Duret, F. Bazantay, Comparison of the thermal performances of two nanofluids at low temperature in a plate heat exchanger. *Experimental Thermal and Fluid Science* 35 (2011) 1535–1543
5. D. Huang, Z. Wub, B Sunden, Pressure drop and convective heat transfer of Al₂O₃/water and MWCNT/water nanofluids in a chevron plate heat exchanger. *International Journal of Heat and Mass Transfer* 89 (2015) 620–626.
6. D. Huang, Z. Wub, B Sunden, Effects of hybrid nanofluid mixture in plate heat exchangers. *Experimental Thermal and Fluid Science* 72 (2016) 190–196.
7. V. Kumar, A. K. Tiwari, S. K. Ghosh, Application of nanofluids in plate heat exchanger: A review. *Energy Conversion and Management* 105 (2015) 1017–1036.

ASPECT RATIO EFFECT ON THE EFFECTIVENESS OF A SINGLE PHASE NATURAL CIRCULATION MINI LOOP

S. Doğanay¹, M. Alaboud², Z.H. Karadeniz^{3*} and A. Turgut⁴

¹Department of Mechatronics Engineering, The Graduate School of Natural and Applied Sciences, Dokuz Eylül University, Buca, İzmir, Turkey

²Department of Mechanical Engineering, The Graduate School of Natural and Applied Sciences, İzmir Kâtip Çelebi University, Çiğli, İzmir, Turkey

³Department of Mechanical Engineering, İzmir Kâtip Çelebi University, Çiğli, İzmir, Turkey

⁴Department of Mechanical Engineering, Dokuz Eylül University, Buca, İzmir, Turkey

*Corresponding author: zhaktan.karadeniz@ikc.edu.tr

Keywords: Aspect ratio, nanofluid, natural circulation loop, numerical study

Introduction: Technological developments have led to miniaturization of electronic devices which cause high heat flux rates from considerably small areas for past few decades. Liquid cooling systems satisfy higher heat flux rates than air cooled heat sinks [1]. Natural circulation loops (NCLs) are known as passive, reliable and safe systems, owing to its simple working principle without any moving or rotating mechanical components. The first attempts on single-phase NCL (SPNCL) appeared in the literature five decades ago [2]. Wang et al. [3] made a transient numerical study by considering the experimental setup of Misale et al. [4] and the results were compared with the experimental results. Their predicted results show a good agreement with the experimental results. The fluid type is the one of the most essential parameter for a mini SPNCL (SPNCmL). For a decade, a new generation heat transfer fluid called as nanofluid has drawn researchers' attention. Turgut et al. [5] made an experimental effort with a SPNCmL at a constant heat sink temperature (20°C) and input power between 10-50 W. Doganay et al. [6] conducted their experiments by varying input power, heat sink temperature and inclination angle. Turgut et al. [5] and Doganay et al. [6] concluded that the thermal performance of the SPNCmL enhanced with the increase of the particle concentration of nanofluid, input power and inclination angle. Koca et al. [7] performed an experimental study similar to Turgut et al. [5] by using Ag-water nanofluid. They observed that effectiveness of the SPNCmL enhanced by using nanofluid rather than DIW. Although nanofluid based SPNCmL studies are available in the literature, the number of numerical studies still under the expectations. Karadeniz et al. [8] investigate the effect of using nanofluid on the thermal performance of a SPNCmL in inclined conditions by using a three dimensional steady numerical model. They use the experimental setup of Turgut et al. [5] as base for the numerical study. Their results indicated a good agreement with the experimental results. Among geometrical parameters, aspect ratio is the one of the most essential geometrical parameter to be

taken into account while designing a miniaturized loop. Chen [9] carried out a pioneering analytical and numerical study for different aspect ratios. It is found that flow is least stable when the aspect ratio of the water based rectangular loop approaches unity.

In perusing the available literature, it seems that there is a gap in numerical nanofluid based SPNCmL studies focused on the aspect ratio. This three dimensional steady numerical study aims to investigate the influence of aspect ratio on Al_2O_3 -DIW nanofluid based SPNCmL. During the study, the loop length kept constant and the aspect ratio altered between 0.4 and 1.38. The analyses were conducted with DIW and Al_2O_3 -DIW nanofluids with 1, 2, 3 % volumetric particle concentrations. The input power was varied among 10-50 W.

Discussion and Results: 3D numerical model was adopted from the experimental study of Turgut et al. [5] (Figure 1). An aspect ratio (A) has been defined as the ratio of loop height to the loop width. The aspect ratio of the experimental setup calculated as 1.38.

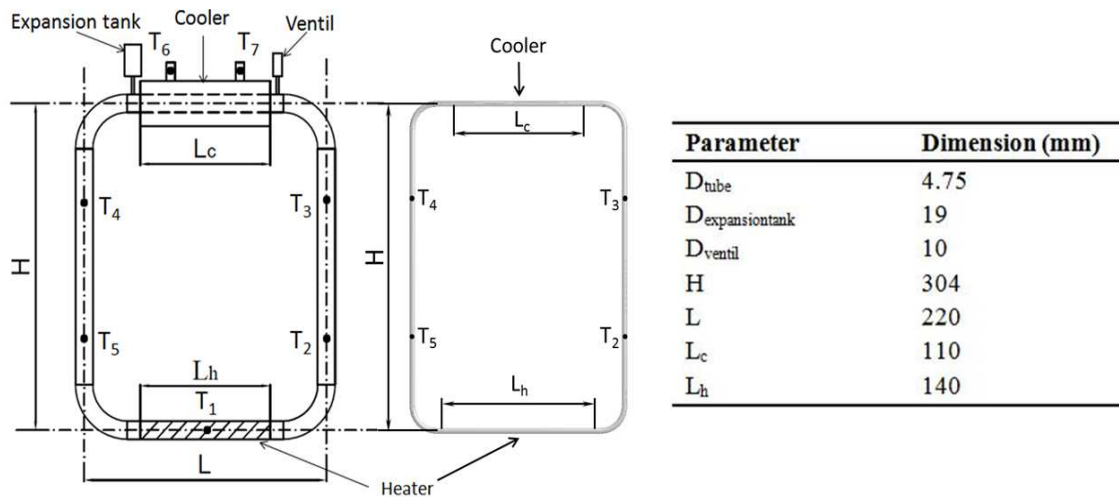


Figure 1 Schematic view of experimental setup [5], corresponding numerical model and dimensions.

In order to keep comparable numerical results with the results of Turgut et al. [5], the dimensions of elbows have been taken as constant. Hence, the minimum possible aspect ratio was observed as 0.18. As a result, the aspect ratio range was determined as 0.4 and 1.38 by keeping the total loop length constant (Figure 2).

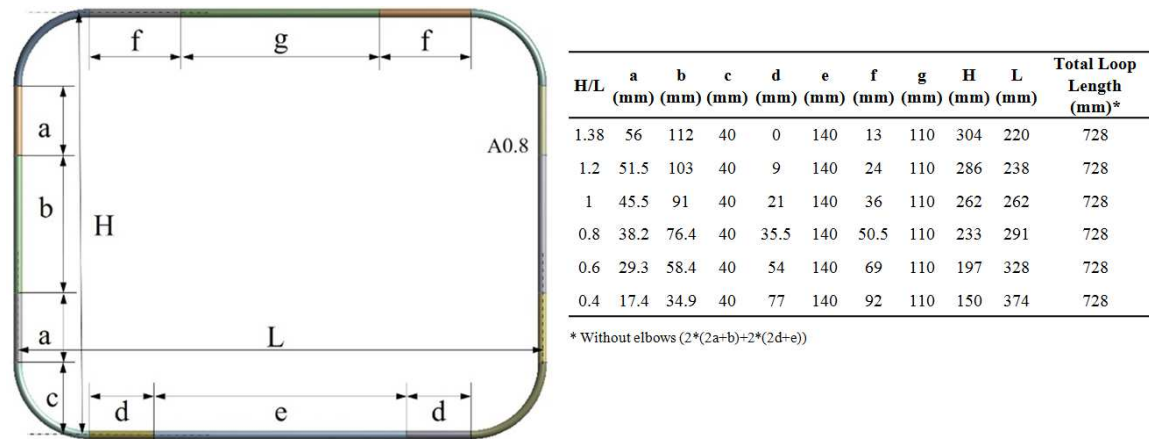


Figure 2 Geometrical parameters of the numerical study.

In order to build the model and solve the model with the corresponding boundary conditions, a commercial software (ANSYS CFX) was used. Heater and cooler parts were modelled as boundary conditions. Cooler part was assumed to be at constant temperature (20°C) which is the cooling fluid temperature for the experimental study. Constant wall heat flux (10, 30, 50 W) was applied to the heater part. All other boundaries of the numerical model were defined as adiabatic walls. A full buoyancy model was used for modelling the laminar natural convection flow. Viscosity, thermal expansivity and thermal conductivity were taken as functions of temperature in the numerical calculations. The effective specific heat (C_e) values have been calculated by Eq. (1) and taken as constant at the average loop temperature for each sample. Table values were used to define the dependency of properties on temperature when water is the working fluid. However, for Al_2O_3 -DIW nanofluid, models adopted from the literature for determining the effective density (ρ_e) and effective thermal expansivity (β_e) for different volumetric concentrations as given in Eq. (2) and Eq. (3), respectively.

$$C_e = \frac{\phi_p(\rho C)_p + (1 - \phi_p)(\rho C)_f}{\phi_p \rho_p + (1 - \phi_p) \rho_f}, \quad (1)$$

$$\rho_e = (1 - \phi_p) \rho_f + \phi_p \rho_p, \quad (2)$$

$$(\rho \beta)_e = (1 - \phi_p)(\rho \beta)_f + \phi_p(\rho \beta)_p, \quad (3)$$

Further information on the numerical study details, mesh dependency, validation study and some other results were presented by Karadeniz et al. [8].

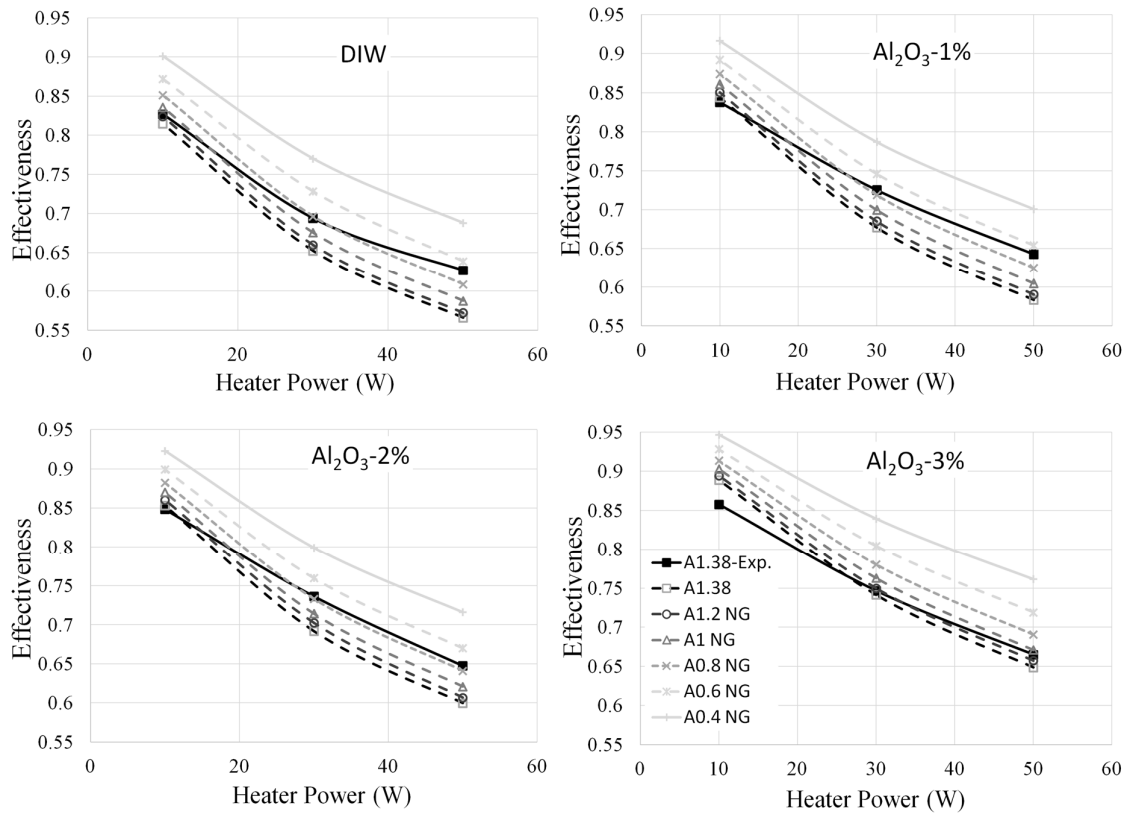


Figure 3 Effectiveness factor with respect to heater power for all aspect ratios and samples.

$$\varepsilon = \frac{T_2 - T_5}{T_2 - T_6} \quad (4)$$

As the thermal performance criteria effectiveness factor (ε) were employed (Eq. 4). It represents the ratio of the actual heat transfer to the maximum possible heat transfer [5]. Figure 3 depicts the variation of effectiveness factor with respect to applied power and aspect ratio for all nanofluid samples. It seems that numerical results in a good agreement with experimental results for 10 W applied power for all cases. When heater power increases, a difference occurs between numerical and experimental results. This is probably caused by not modelled heat losses from the numerical model. Moreover, the highest difference between numerical and experimental study happens for 3% vol. concentration and this can be related to the measured thermophysical properties in the experimental study. Figure 3 indicates that the system has higher effectiveness values when nanofluid samples are used rather than using DIW. Besides, the effectiveness factor increases with the increment of volumetric concentration and decrement of applied power. In terms of aspect ratio, it is clearly seen from Figure 3 that effectiveness factor increases with decreasing aspect ratio. Although, the loop length is constant for all aspect ratio values which mean the amount of

nanofluid in the system is same, the aspect ratio influences the effectiveness of the SPNCmL. This reveals the importance of the geometry when the SPNCmL are designed.

Conclusions: In this study the thermal performance of a SPNCmL has been investigated numerically. The conclusions can be drawn have been presented as follows:

- The effectiveness factor of nanofluid based SPNCmL increases with the increasing vol. concentration and decreasing aspect ratio and applied power.
- Decreasing the aspect ratio provides an enhancement up to 20% in effectiveness.
- Numerical model is powerful to estimate the loop performance with small errors.
- The designed numerical model can be useful to save time, where comparative results are necessary for different geometries and different nanofluid types and concentrations.

References:

1. X.C. Tong, *Advanced materials for thermal management of electronic packaging*, Springer Science & Business Media, New York, 2011.
2. J.B. Keller, Periodic oscillations in a model of thermal convection, *Journal of Fluid Mechanics* 26 (1966) 599-606.
3. J.Y. Wang, T.J. Chuang and Y.M. Ferng, CFD investigating flow and heat transfer characteristics in a natural circulation loop, *Annals of Nuclear Energy* 58 (2013) 65-71.
4. M. Misale, P. Garibaldi, J.C. Passos and G. G. Bitencourt, Experiments in a single-phase natural circulation mini-loop, *Experimental Thermal Fluid Science* 31 (2007) 1111–1120.
5. A. Turgut and S. Doganay, Thermal performance of a single phase natural circulation mini loop working with nanofluid, *High Temperatures-High Pressures* 46 (2014) 311-320.
6. S. Doganay and A. Turgut, Enhanced effectiveness of nanofluid based natural circulation mini loop, *Applied Thermal Engineering* 75 (2015) 669-676.
7. H.D. Koca, S. Doganay and A. Turgut, Thermal characteristics and performance of Ag-water nanofluid: Application to natural circulation loops, *Energy Conversion and Management* 135 (2017) 9-20.
8. Z.H. Karadeniz, S. Doganay and A. Turgut, Numerical study on nanofluid based single phase natural circulation mini loops: A steady 3D approach, *High Temperatures--High Pressures*, 45 (2016) 321-335.
9. K. Chen, On the oscillatory instability of closed-loop thermosyphons, *Journal of Heat Transfer*, 107 (1985) 826-832.

THERMAL ENHANCEMENT USING NANOFLUIDS ON HIGH HEAT DISSIPATION ELECTRONIC COMPONENTS

R.R. Riehl

National Institute for Space Research, INPE – DMC
Av dos Astronautas 1758, São José dos Campos, 12227-010 SP Brazil

Email: roger.riehl@inpe.br

Keywords: thermal enhancement, electronics cooling, thermal control, pressure drop, nanofluids

Abstract: Following today's needs for improvement on heat transfer, new technologies and innovative solutions must be found in order to meet current requirements for both active and passive thermal control. There has been substantial growth on the heat fluxes that need to be dissipated, which require different approaches from designers, especially those designed for defense purposes. With the increase of heat dissipation needs, conventional designs are not suitable due to several factors such as operation in hostile environments, high thermal density of electronics that need their temperature to be controlled, which require innovative designs. In such cases, the application of nanofluids can greatly contribute to give designers more degrees of freedom to face the project's requirements. The subject of this article is related to a surveillance system designed for defense purposes, which needs to dissipate high levels of heat loads. For this present investigation, a single-phase forced circulation loop has been designed to promote the thermal management of up to 50 kW of heat, being dissipated to the environment by a fan cooling system. Results show that with an addition of 20% by mass of copper oxide nanoparticles to the base fluid (water), enhancements of 12% on the heat transfer coefficients were achieved but the increase on the pressure drop was around 32%.

Introduction

The need for thermal management has increased dramatically over the last decade and the prediction is that a steeper increase is yet to come for the next years. Such an increase is directly related to more powerful electronics used for data processing in high-tech equipments used for satellites and defense/military purposes. Several investigations related to nanofluids applications have been conducted with important contributions to many areas (Ebrahimnia-Bajestan et al., 2011; Ghadimi et al., 2011). Considering previous experiences, current and future thermal management needs, the use of nanofluids is becoming inevitable. The use of nanofluids present to be an important approach to enhance the heat transfer capability of heat pipes and loop heat pipes systems, which has already been proven (Riehl and Santos, 2012). Similar investigation has also been performed by Alizad et al (2012) where it showed that smaller sizes heat pipes can be used when operating with nanofluids. Other applications are related to the use of nanofluids in regular heat exchanger devices already installed in industries

in order to enhance their performance in face of the increase of heat dissipation needs (Leong et al., 2012). Evaluation of nanofluids have been performed by many researchers in order to better understand the effects of the nanoparticles on transport properties, which are important for the prediction of the pumping requirements (Murshed et al., 2011; Murshed and Estellé, 2017). Applications related to PCB thermal management using nanofluids have also been reported (Colla et al. 2016). However, important issues still require attention, especially when considering the verification of a nanofluid regarding its own design, since many authors have reported different results for the same combination of base fluid and nanoparticles (Marcelino and Riehl, 2016). An important application for today's needs for heat dissipation is related to surveillance systems designed for defense/military purposes. As more compact and powerful defense equipments are necessary, higher heat fluxes need to be properly addressed. Considering the need for designing a reliable and effective thermal management system that need to operate in hostile environments, with potential use of nanofluid, this article presents an investigation on this subject.

Nanofluid's Properties Consideration

The base fluid's transport properties is influenced by the addition of the solid nanoparticles, which in one hand enhances the fluid's thermal conductivity but also directly contribute to enhance its liquid density and viscosity. Proper consideration must be made regarding the addition of the solid nanoparticles as those properties might directly influence the overall thermal management and pumping analysis. Some models have been developed to better describe the influence of the addition of nanoparticles in pure substances and the gain on the liquid thermal conductivity that might represent (Koo and Kleinstreuer, 2004) as usually the Maxwell model is applied on this case as

$$k_n = \frac{k_p + 2 k_l + 2(k_p - k_l) f}{k_p + 2 k_l - (k_p - k_l) f} k_l \cdot \quad \text{W/m}^\circ\text{C} \quad [1]$$

Equation [1] represents the effective thermal conductivity of a homogeneous nanofluid (k_n), while k_p , k_l and f are the particle and base fluid thermal conductivities and f is the nanoparticle mass fraction, respectively. Since the liquid thermal conductivity is affected by the addition of a nanoparticle in the substance, proper consideration and evaluation of the solid particles in a liquid must be taken according to the two-phase theory (Carey, 2008). Thus, the nanofluid density (ρ_n) is then calculated as

$$\frac{1}{\rho_n} = \left(\frac{f}{\rho_p} + \frac{1-f}{\rho_l} \right), \quad \text{kg/m}^3 \quad [2]$$

where ρ_p and ρ_l are the nanoparticle and the base fluid densities, respectively. The nanofluid dynamic viscosity (μ_n) can then be calculated as (Xuan and Roetzel, 2000)

$$\mu_n = \mu_l \frac{1}{(1-f)^{2.5}}, \quad \text{Pa.s} \quad [3]$$

where μ_l is the base fluid dynamic viscosity. The modification of the transport properties indicated in Eqs. [1] to [3] should be included in any analysis to correctly address their influence on the system's thermal performance. In the present analysis, Eqs. (1)-(3) were implemented in a design model to predict the nanofluid influence on the overall thermal and hydraulic performance of the surveillance thermal management system.

Equipment Design and Operation

A specific design for a surveillance system has been conceived to operate in hostile environments where the ambient temperatures can range from +5 to +50 °C and humidity levels up to 95%. In this case, a single-phase thermal control loop has been designed to use a nanofluid, presenting a forced circulation using a pump to move the working fluid throughout the circuit to remove heat from the electronic components, rejecting this heat to the environment by a fan cooling system. For this thermal management system, a hybrid design has been applied where the heat generated by all PCBs are removed by open loop pulsating heat pipes, delivering the heat to the heat sinks allocated throughout the surveillance equipment (cold plates). The heat sinks are then connected to the single-phase thermal control loop that collects all the heat and dissipate it to the environment. The schematics of such arrangement is presented by Fig. 1a and the surveillance equipment where it is installed is shown by Fig. 1b, whilst Fig. 1c presents the hybrid setup where the pulsating heat pipe and the heat sink are connected.

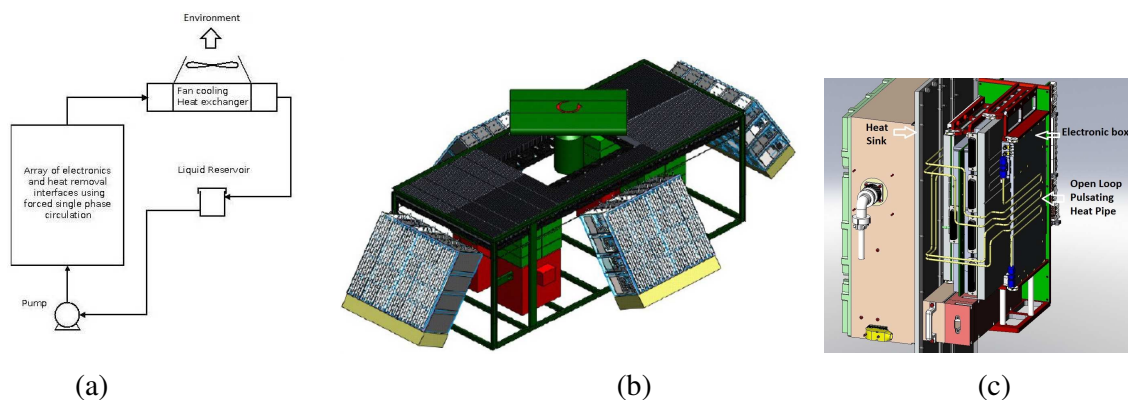


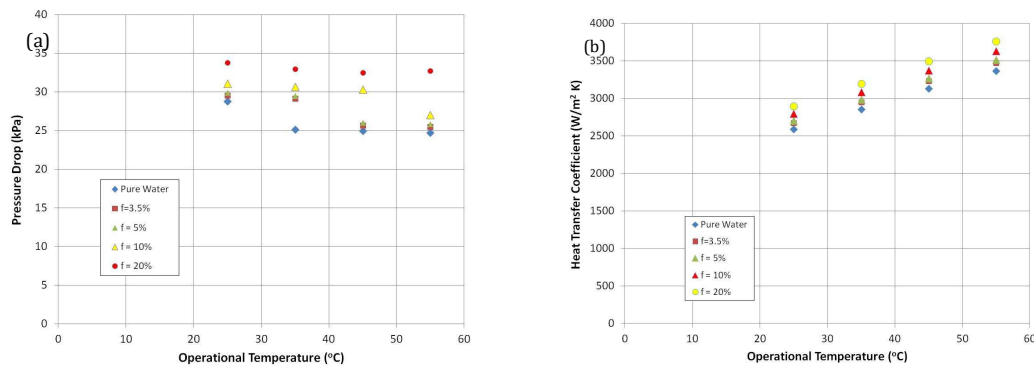
Figure 1: Schematics of the thermal control system arrangement.

As the base fluid, water has been selected for this approach. The CuO nanoparticles present an average diameter of 29 nm and purity of 99.8%. The nanoparticles concentration (f) shall vary from 3.5% to 20% (by mass of the base fluid) to verify their effect on the overall thermal performance of the system.

Results and Discussion

The presented results were well correlated to the thermal tests applied to this equipment, and further analysis will be disclosed in future reports. For the sake of presenting the most important results obtained so far, the following data were selected among several hours of operation and follow the NDA (non-disclosure agreement) set between all parts.

Figures 2a and 2b present some results for the pressure drop and heat transfer coefficients, respectively, on a comparison between the use of pure water and the addition of copper nanoparticles at different concentrations (f), by mass percentage of the working fluid in the system. The results are related to each individual electronics module (composed of 3 PCBs), which dissipate a maximum of 50 W of heat, thus, based on the module's footprint and heat dissipation, the calculation for the heat transfer coefficient was performed. As shown by Fig. 2c, less volumetric flow rate is necessary to promote the heat dissipation when using the nanofluid, as the heat transfer coefficient increases. It is clear that as the nanoparticle concentration increases, the pressure drop also increases up to 32% for $f=20\%$ as more solid nanoparticles are present in the system (Fig. 2d). The pump needs to overcome the extra resistance as the transport properties are changed with the addition of the nanoparticles. However, the increase on the heat transfer coefficients is also clear and can represent a gain around 12% for the same $f=20\%$ which cannot be neglected.



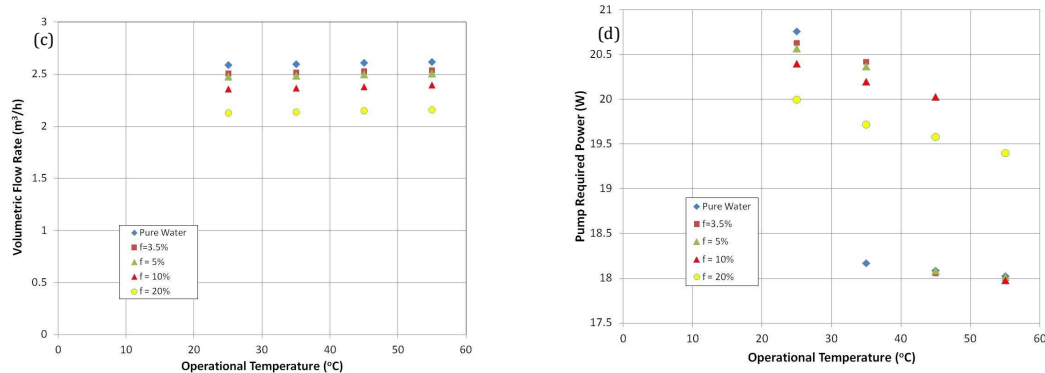


Figure 2: Results for (a) pressure drop and (b) heat transfer coefficient (c) volumetric flow rate and (d) pump required power.

Conclusions

In general, the main conclusions that can be derived from this investigation are:

1. Higher heat transfer coefficients can be reached with the increase of the solid nanoparticles concentration, representing an enhancement of up to 12% for $f=20\%$ at 55 °C when compared with the operation with water;
2. The pressure drop also increases as the concentration of nanoparticles increases, which could compromise the pump operation;
3. Lower volumetric flow rates are observed for higher concentration of nanoparticles, as this factor contributes to increase the working fluid's viscosity and density;
4. Even with the use of solid nanoparticles, the required pumping power does not represent to be the major issue on this specific project, as this requirement can be easily addressed as the calculated values are rather low;
5. The overall analysis indicates that the application of the nanofluid with higher concentrations can be used, as the major parameter for this analysis is the heat transfer coefficient, which is reducing the size of the thermal management system applied to control the temperature of the electronics components.

When considering that the thermal management system is operating at higher capacities, while keeping the working fluid's temperature differences between the fan cooling inlet and outlet within certain required parameters, the use of a nanofluid presents to be an important innovative approach for this project. This is directly resulting in more gains than losses for the overall thermal system analysis and should remain as the most indicated solution for this application.

References

1. Alizad, K., Vafai, K., Shafahi, M., "Thermal performance and operational attributes of the startup characteristics of flat-shaped heat pipes using nanofluids", *International Journal of Heat and Mass Transfer* 55 (2012) 140-155.
2. Leong, K. Y., Saidur, R., Mahlia, T. M. I., Yau, Y. H., "Modeling of shell and tube heat recovery exchanger operated with nanofluid based coolants", *International Journal of Heat and Mass Transfer* 55 (2012) 808-816.
3. Murshed, S. M. S., Estellé, P., "A state of the art review on viscosity of nanofluids", *Renewable and Sustainable Energy Reviews* 76 (2017) 1134-1152.
4. Murshed, S. M. S., Nietro de Castro, C. A., Lourenço, M. J. V., Lopes, M. L. M., Santos, F. J. V., "A review of boiling and convective heat transfer with nanofluids", *Renewable and Sustainable Energy Reviews* 15 (2011) 2342-2354.
5. Colla, L., Fedele, L., Mancin, S., Bobbo, S., Ercole, D., Manca, O., "Nano-PCMs for electronics cooling applications", *Proceedings of the 5th International Conference on Micro/Nanoscale Heat and Mass transfer, Jan 4-6, 2016, Biopolis, Singapore*.
6. Marcelino, E., Riehl, R. R., "A review on thermal performance of CuO-water nanofluids applied to heat pipes and their characteristics", *Proceedings of the 15th IEEE Intersociety Conference on Thermal and Thermomechanical Phenomena in Electronic Systems (ITherm)*, May 31 - June 3, 2016, Las Vegas NV, USA.
7. Ebrahimi-Bajestan, E., Niazmand, H., Dungthonsuk, W., Wongwises, S., "Numerical investigation of effective parameters in convective heat transfer of nanofluids flowing under a laminar flow regime", *International Journal of Heat and Mass Transfer* 54 (2011) 4376-4388.
8. Ghadimi, A., Saidur, R., Metselaar, H. S. C., "A review of nanofluid stability properties and characterization in stationary conditions", *International Journal of Heat and Mass Transfer* 54 (2011) 4051-4068.
9. Riehl, R. R., Santos, N., "Water-copper nanofluid application in an open loop pulsating heat pipe", *Applied Thermal Engineering* 42 (2012) 6-10.

Abstracts

SESSION 5A: STORAGE

ON THE USE OF NANO-ENCAPSULATED PHASE CHANGE MATERIALS FOR THERMAL-OIL AND MOLTEN SALT-BASED NANOFLUIDS

N. Navarrete¹, A. Gimeno-Furio¹, R. Mondragon¹, L. Hernandez¹, L. Cabedo², E. Cordoncillo³ and J.E. Julia^{1*}

¹Departamento de Ingeniería Mecánica y Construcción. Universitat Jaume I.
12071-Castellón de la Plana, Spain

²Polymers and Advanced Materials Group (PIMA). Universitat Jaume I.
12071-Castellón de la Plana, Spain

³Departamento de Química Inorgánica y Orgánica. Universitat Jaume I.
12071-Castellón de la Plana, Spain

*Corresponding author: enrique.julia@uji.es

Keywords: Thermal oil, Molten salt, Heat capacity, Thermal conductivity, Nanoencapsulated Phase Change Materials

Introduction: The thermal properties of Heat Transfer Fluids (HTF) play an important role in the efficiency of Concentrated Solar Power (CSP) plants. Thermal oils and molten salts are used as HTF in medium and high temperature applications since they present high stability at high temperature conditions. However, the thermal properties of these HTFs are quite poor, with thermal conductivity (k) and specific heat capacity (cp) values lower than 0.4 W/m K and 2.5 J/g K, respectively. Nanofluids are defined as engineered colloidal suspensions of nanoparticles in a base fluid. They allow to introduce a solid inside a liquid, transferring, to some extent, the solid properties to the liquid and keeping, also to some extent, its liquid transport properties. Therefore, nanofluids present an effective route to improve the thermal properties of HTFs.

Earliest nanofluid works were related to the thermal conductivity enhancement using water as base fluid [1, 2]. After that, nanofluid related research topics were expanded and nanofluid viscosity and specific heat were involved. From 2010, new nanofluid approaches using additional solid particle properties have been researched. One of them is the use of nano-encapsulated Phase Change Materials (nePCM) as solid phase. In this approach, the nanoparticles have a PCM core and a high melting temperature shell that keeps the PCM confined when it is in liquid phase. The use of nePCM allows to increment the thermal conductivity as well as the thermal capacity of the base fluid by the latent heat contribution of the cores of the nePCM. Metal and metal alloy nanoparticles can be used as cores of nePCMs suitable for mid and high temperature applications. In most cases, the encapsulation is obtained growing a silica shell [3-8] or trioctyl phosphine oxide TOPO [9] around them. Different metal cores have been investigated. Lower crystallization temperature values, defined as

supercooling, are always found due to the absence of nucleation spots inside the nuclei. The nePCM supercooling depends on the nucleus material and size. One important parameter in shell-type nePCMs is the encapsulation ratio defined as the ratio between the phase change enthalpy per unit of mass of the nePCM and the PCM bulk material. Encapsulation ratios below 1 are found due to the mass contribution of the nePCM shell (which is not melted in the temperature working range of the nePCM) and the enthalpy decrement due to size effects (only for nePCM with nuclei smaller than 50 nm). In order to maximize the nePCM latent heat contribution, the encapsulation ratio should be as high as possible, assuring the shell mechanical integrity.

Silica or TOPO-shell type nePCMs can be dispersed into fluids to develop nePCM-based nanofluids. In this regard, a wide range of base fluids, such as methanol [3], molten salt [6, 9], poly-alpha-olefin (PAO) [4], and commercial thermal oil (Therminol 66) [7], have been used.

NePCM present important advantages over conventional nanoparticles such as heat capacity increment. However, complex chemical synthesis process are needed to obtain shell-type nePCMs, involving, at least, four chemical processes: the first one to produce the metal nanoparticles, a second one to grow a polymeric template around them, the third one to grow the silica or TOPO shell on the template and the last one to eliminate the polymeric template.

In this work, a new approach to simplify the nePCMs production is proposed and experimentally checked. This way, it is proved that the metal oxide shell that is produced during the metal nanoparticle fabrication process using standard commercial methods can be used as self-encapsulation in static and dynamic conditions. However, potential chemical reactions between the metal oxide shell and the solar salt components should be taken into account.

Discussion and Results: Two types of nePCMs nanofluids have been tested. The first one consists of commercial Sn nanoparticles of nominal size <80 nm purchased from US Research Nanomaterials, Inc. added to a synthetic thermal oil used frequently as a HTF, Therminol 66 (Solutia, Inc.) in a weight concentration of 30% and sonicating the mixture.

The second nanofluid was prepared adding commercial Zn nanoparticles of nominal size 35-45nm (US Research Nanomaterials, Inc.) in a weight concentration of 30% to solar salt (60% wt. NaNO₃, 40% wt. KNO₃, Sigma-Aldrich), following the preparation procedure described in [4].

Both commercial metal NPs have a metal oxide shell that can be used as self-encapsulation (Figure 1a). NePCM morphology, shell thickness and diameters have been measured using a Transmission Electronic Microscope (TEM, JEOL 2100).

NFs heat capacity and NePCM strength inside the base fluid have been measured using a Differential Scanning Calorimeter (DSC, DSC2 Mettler Toledo) using different thermal heating and cooling rates as well as several thermal cycles.

Figure 1 shows some example of the results. Figure 1a) shows a TEM image of a NePCM (SnO_x shell/Sn core) after thermal cycling (200 cycles between 70°C and 250°C). It is possible to observe the shell integrity after thermal cycling. Figure 1b) shows the phase change enthalpy of the SnO_x shell/Sn core NePCMs inside the thermal oil after thermal cycling in the DSC. Thermal cycles have been performed at 40K/min and the enthalpy measurement at 5K/min. It is

possible to observe that both enthalpies, melting and crystallization, are almost constant after 200 thermal cycles.

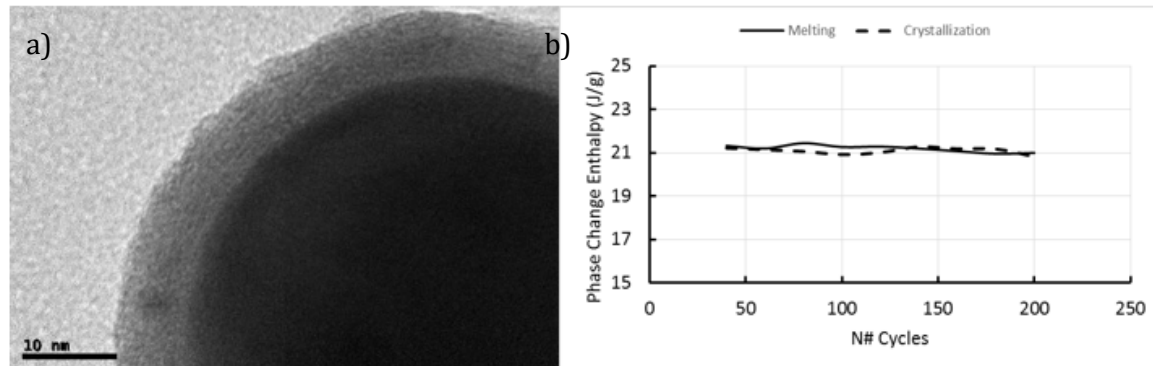


Figure 1. a) TEM image of a Sn/SnOx nePCM after thermal cycling, and b) Evolution of the enthalpies of nePCM/Thermal oil nanofluid with thermal cycling.

Figure 1 shows some example of the results. Figure 1a) shows a TEM image of a NePCM (SnOx shell/Sn core) after thermal cycling (200 cycles between 70°C and 250°C). It is possible to observe the shell integrity after thermal cycling. Figure 1b) shows the phase change enthalpy of the SnOx shell/Sn core NePCMs inside the thermal oil after thermal cycling in the DSC. Thermal cycles have been performed at 40K/min and the enthalpy measurement at 5K/min. It is possible to observe that both enthalpies, melting and crystallization, are almost constant after 200 thermal cycles.

Conclusions: In this work it has been proven that the metal oxide shell that is present in Sn and Zn nanoparticles can be used as encapsulation for thermal engineering applications. This shell is present in several metal nanoparticles produced by different methods and it is formed during the nanoparticle fabrication process. This new encapsulation proposal simplifies the production of nePCMs, showing that commercial metal nanoparticles are self-encapsulated by its own metal oxide shell. However, potential interactions between the metal oxide shell and the base fluid components should be taken into account in order to select the nePCM.

References:

1. S. Choi, Enhancing thermal conductivity of fluids with nanoparticles, *ASME Fluids Engineering Division* 231 (1995) 99.
2. H. Masuda, A. Ebata, K. Teramae and N. Hishinuma, Alteration of thermal conductivity and viscosity of liquid by dispersing ultrafine particles (dispersion of gamma-al₂o₃, sio₂ and tio₂ ultrafine particles) *Netsu Bussei* 4 (1993) 227–233.
3. M. Zhang, Y. Hong, S. Ding, J. Hu, Y. Fan, A.A. Voevodin, M. Su, Encapsulated nano-heat-sinks for thermal management of heterogeneous chemical reactions, *Nanoscale* 2 (2010) 2790–2797.

4. Y. Hong, S. Ding, W. Wu, J. Hu, A.A. Voevodin, L. Gschwender, E. Snyder, L. Chow, M. Su, Enhancing heat capacity of colloidal suspension using nanoscale encapsulated phase-change materials for heat transfer, *ACS Applied Materials & Interfaces*. 2 (2010) 1685–1691.
5. Y. Hong, W. Wu, J. Hu, M. Zhang, A.A. Voevodin, L. Chow, M. Su, Controlling supercooling of encapsulated phase change nanoparticles for enhanced heat transfer *Chemical Physics Letters* 504 (2011) 180–184.
6. C.-C. Lai, W.-C. Chang, W.-L. Hu, Z.M. Wang, M.-C. Lu, Y.-L. Chueh, A solar-thermal energy harvesting scheme: enhanced heat capacity of molten HITEC salt mixed with Sn/SiO(x) core-shell nanoparticles *Nanoscale* 6 (2014) 4555–9.
7. M. Wang, B. Duong, H. Fenniri, M. Su, Nanomaterial-based barcodes *Nanoscale* (2015) 11240–11247.
8. S. Cingarapu, D. Singh, E.V. Timofeeva and M.R. Moravek, Nanofluids with encapsulated tin nanoparticles for advanced heat transfer and thermal energy storage *International Journal of Energy Research* 38 (2014) 51–59.
9. S. Cingarapu, D. Singh, E. V. Timofeeva, M.R. Moravek, Use of encapsulated zinc particles in a eutectic chloride salt to enhance thermal energy storage capacity for concentrated solar power *Renewable Energy* 80 (2015) 508–516.

THE INFLUENCE OF Al_2O_3 NANOPARTICLES ON THE HEAT CAPACITY OF ISOPROPANOL

I. Motovoy*, V. Zhelezny and T. Lozovsky

Department of Thermal Physics and Applied Ecology, Odessa National Academy of Food Technologies, Kanatna str., 112, Odessa, Ukraine

*Corresponding author: motovoj@gmail.com

Keywords: Nanofluid, Isopropanol, Al_2O_3 nanoparticles, Heat capacity

Introduction: Nanofluids are colloidal solutions that are formed by means of dispersing solid nanoparticles in base fluids. Despite a large number of publications dedicated to investigation of the thermophysical properties of nanofluids, the amount of experimental data describing the nanofluid thermal capacity in a wide range of temperatures is negligible. This aspect hinders the potential for developing the model to predict the nanofluids' heat capacity.

Nanofluid solutions of the nanofluid isopropyl alcohol (IPA) / nanoparticles Al_2O_3 (702129 Aldrich 20 wt.% of Al_2O_3 nanoparticles) with isopropyl alcohol (CAS # 67-63-0) were chosen as study subjects.

Discussion and Results: The two-phase heat capacity was measured on a variable-temperature adiabatic calorimeter by means of monotonic heating within the temperature range of 190-330 K, at mass concentrations of nanoparticles of 2.01%, 5.11% and 9.96% (1.2, 3.1 and 6.1 mole%, respectively). The results of the study of the heat capacity of nanofluids are shown in Fig. 1. Experimental uncertainty for the heat capacity values does not exceed 0.7%.

The obtained data show that nanoparticle additives provide for the decrease of the heat capacity in the liquid phase.

The performed analysis shows that the correlations for predicting isobaric heat capacity published by Pak and Cho [1], and Xuan and Roetzel [2] do not reflect the structural transformations in the nanofluid.

Nanofluid heat capacity values calculated using Pak and Cho, Xuan and Roetzel correlations are always higher than the values obtained in the experiment (see Fig. 2).

It is our opinion that that these results were to be expected, since the published correlations [1, 2] do not take into considerations that any time-stable nanofluid is a colloidal system. When considering a colloid solution, some of the molecules of the base liquid (i.e. isopropyl alcohol) are absorbed on the surface of the nanoparticles. This effect will provide the excess heat capacity that should be taken into consideration when predicting nanofluid heat capacity.

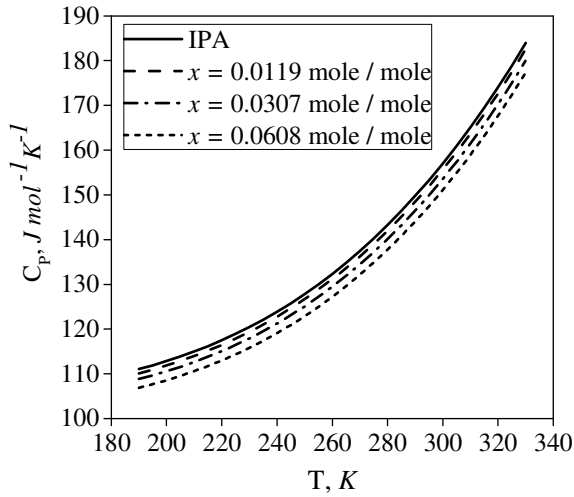


Fig. 1. Heat capacity dependence of temperature.

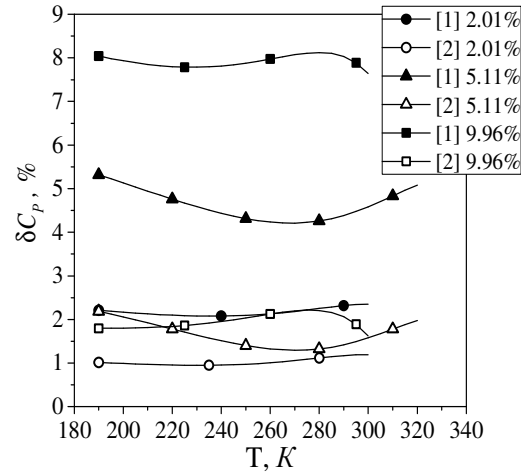


Fig. 2. The relative deviations of the values of the isopropyl alcohol / Al_2O_3 nanoparticles heat capacity calculated using the models [1] and [2] from the experimental data acquired

Therefore, prediction model for the nanofluid heat capacity can be represented as:

$$C_P^{nf} = C_P^{np} x_{np} + C_P^{bf} (1 - x_{np}) + \Delta C_P^{ex}, \quad (1)$$

where C_P^{nf} is nanofluid heat capacity, $J \text{ mole}^{-1} K^{-1}$; C_P^{np} is the heat capacity of nanoparticles material (Al_2O_3), $J \text{ mole}^{-1} K^{-1}$; x_{np} is the mole fraction of the nanoparticle material in the nanofluid, mole/mole; C_P^{bf} is the heat capacity of the dispersion medium (base fluid - isopropyl alcohol) in the nanofluid, $J \text{ mole}^{-1} K^{-1}$; ΔC_P^{ex} is the excess heat capacity of the nanofluid, $J \text{ mole}^{-1} K^{-1}$.

Hence, we suggest to consider the nanofluid as a thermodynamic system that includes: 1 - nanoparticles, 2 - surface adsorption phase, 3 - diffuse layer, 4 - base liquid. Figure 4 shows the effective values of diameters, thicknesses, and volumes of the phases formed with certain effective thermophysical properties.

The proposed model assumes that nanoparticles are spherical. This assumption is justified in condition of the multilayer adsorption of the base material molecules on the surface of the nanoparticle, as well as the presence of nanoparticles of different sizes and temporal cluster-type [3].

To predict the excess heat capacity, we suggest to consider the excess heat capacity as follows:

$$\Delta C_P^{ex} = C_P^{al} x_{al} + C_P^{dl} x_{dl} - C_P^{dl} (x_{al} + x_{dl}), \quad (2)$$

where C_p^{al} is the heat capacity of the dispersion medium within the absorption layer, $J\ mole^{-1}K^{-1}$; x_{al} is the mole fraction of the dispersion medium within the absorption layer, $mole/mole$; C_p^{dl} is the heat capacity of the dispersion medium within the diffuse layer, $J\ mole^{-1}K^{-1}$; x_{dl} is the mole fraction of the dispersion medium within the diffuse layer, $mole/mole$.

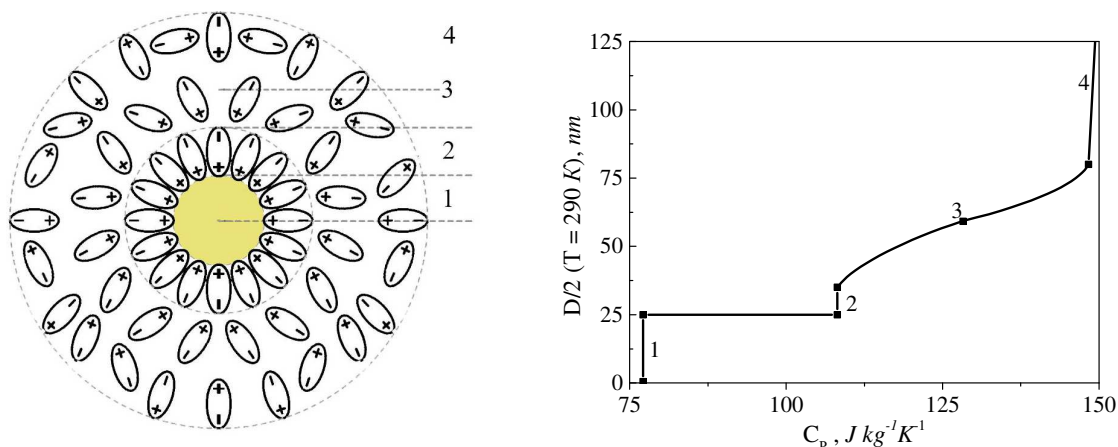


Fig. 3. "Four-phase" prediction model for nanofluid heat capacity

Figure 5 demonstrates comparison of the experimental data on the heat capacity of the nanofluids (at 3 concentrations) and calculating values of the heat capacity by (Eqs. (1) and (2)) at 293 K.

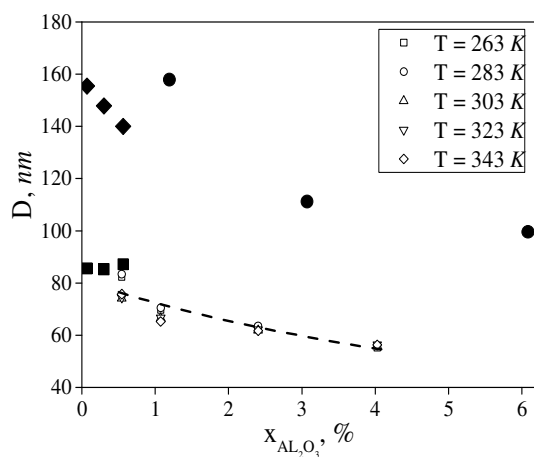


Fig. 4. Concentration dependence of diameters of the adsorbed D_{al} layer and diffuse layer D_{dl} of isopropyl alcohol molecules on the surface of Al_2O_3 nanoparticles

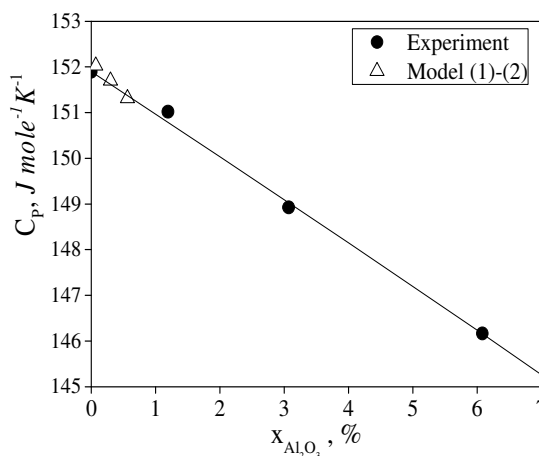


Fig. 5. Concentration dependence of nanofluid heat capacity at 293 K

Figure 5 shows: \blacklozenge – spectroturbidimetry method at 293 K; \blacksquare – dynamic light scattering at 293 K; --- – the diameter of the adsorption phase obtained from the data on the density of nanofluids [3]; \bullet – data on the diameter of the diffuse layer obtained from data on the heat capacity at 293 K.

The performed study shows that the diameter values of adsorption phase, and the diffuse layer of micelles can be determined from the nanofluids density data [3]; these values could also be obtained by using the dynamic light scattering [3], and spectrophotometric methods. The results of calculating the adsorption layer D_{ab} and diffuse layer D_{dl} for the molecules of isopropyl alcohol on the surface of Al_2O_3 nanoparticles are shown in Fig. 4.

The information in Fig. 5 shows that the values of the isobaric molar heat capacity calculated using the typical sizes of nanoparticles in the base fluid are consistent with the experimental data on the heat capacity of the isopropyl alcohol / Al_2O_3 nanoparticle at a temperature of 293 K.

To predict the heat capacity of nanofluids over a wide temperature range, we suggest to use the extended scaling model, which was proposed in [4]:

$$C_p = C_{p0} t^{(-\gamma\Psi)} \quad (3)$$

where C_{p0} is an amplitude depended on the properties of the substance; γ is a critical index, which has a universal value of $\gamma = 1.24$ [5] for various substances; $\Psi(t)$ is the crossover function which is universal for the studied nanofluids and depended from $t = 1 - \frac{T}{T_c}$; T_c is the critical temperature of isopropyl alcohol.

This correlation contains only one unknown amplitude C_{p0} . The value of C_{p0} can be calculated using model (1), and (2) at the temperature used to perform optical measurements of diameters D_{dl} and D_{ab} . The deviations of the heat capacity values calculated by Eqs. (1) - (3) from experimental data in the temperature range of 190-330 K do not exceed 0.75%.

Conclusions: The experiments show that Al_2O_3 nanoparticle additives lead to a decrease of the isopropyl alcohol heat capacity in the liquid phase throughout the whole temperature range of the experimental study.

It was also found that calculating the heat capacity using Pak and Cho, Xuan and Roetzel models leads to obtaining slightly higher values of the heat capacity for nanofluids.

In our paper, we introduce a new “four-phase” model to predict the nanofluid heat capacity that includes the excess molar heat capacity of nanofluid. This value is determined by the heat capacity of structurally oriented layers of base fluid molecules near the surface of nanoparticles. The deviations of nanofluid heat capacity values for isopropyl alcohol / Al_2O_3 nanoparticles calculated using the proposed model are commensurate with the experimental uncertainty.

References:

1. B.C. Pak and Y.I. Cho, *Hydrodynamic and heat transfer study of dispersed fluids with*

- submicron metallic oxide particles*, Exp. Heat Transf., 1998.
2. Y. Xuan and W. Roetzel, *Conceptions for heat transfer correlation of nanofluids*, Int. J. Heat Mass Transf., 2000.
 3. V.P. Zhelezny, T.L. Lozovsky, V. Gotsulskiy, N. Lukianov, I.V. Motovoy, *Research into the influence of Al₂O₃ nanoparticle admixtures on the magnitude of isopropanol molar volume*, Eastern-European J. Enterp. Technol. pp.33–38, 2017.
 4. S.N. Ancherbak, YU.V. Semenyuk, T.L. Lozovsky and D.A. Ivchenko, *Methods for predicting the caloric properties of substances on characteristic curves (in Russian)*, Holodilnaya tehnika i tehnologiya, № 4,- p.32-40, 2009.
 5. M.A. Anisimov, *Critical phenomena in liquids and liquid crystals*, CRC Press, p.272, 1991.

AN INFLUENCE OF Al_2O_3 NANOPARTICLES ON THE HEAT CAPACITY OF ISOPROPYL ALCOHOL IN METASTABLE AND SOLID PHASE

I. Motovoy*, V. Zhelezny and T. Lozovsky

Department of Thermal Physics and Applied Ecology, Odessa National Academy of Food Technologies, Kanatna str., 112, Odessa, Ukraine

*Corresponding author: motovoj@gmail.com

Keywords: Heat capacity, Metastable state, Solid phase, Nanoparticles

Introduction: Effects of the influence of nanoparticles on the caloric properties and parameters of basic substances' phase transitions in condensed state remain understudied. When exposed to low temperatures (below the melting point of the base liquid), the nanofluid sample can be in various aggregate states, such as metastable liquid, crystalline phase or glassy state. Crystalline solids have a high degree of orderliness, i.e. have a long-range order of the molecules of the base material and nanoparticles. Molecules of the base material and nanoparticles in amorphous solid state are more chaotic, and can be distinguished by short-range order. Therefore, the properties of nanofluids in condensed state are determined by their structure and the interaction between molecules and nanoparticles. The mechanism of this interaction remains understudied so far. Available publications currently provide no data regarding the effect of nanoparticles on the caloric properties of thermodynamic systems or the solid phase of the basic substance / nanoparticle. There is also no reliable observed data regarding the influence of nanoparticles on the parameters of phase transitions for the investigated samples in condensed state.

Nanofluid solutions of the isopropyl alcohol (IPA) / Al_2O_3 nanoparticles (702129 Aldrich 20 wt.% of Al_2O_3 nanoparticles) with isopropyl alcohol (CAS67-63-0) were chosen for experimental investigation.

Discussion and Results: The two-phase heat capacity was measured on a variable-temperature adiabatic calorimeter by means of monotonic heating within the temperature range of 85-180 K, at mass concentrations of nanoparticles of 2.01%, 5.11% and 9.96% (1.2, 3.1 and 6.1 mole%, respectively). Experimental uncertainty of the heat capacity measurements does not exceed 0.7%.

The obtained results show that nanoparticle additives caused the decrease of the heat capacity in the solid phase. The conducted experiments show that the cooling rate of the test sample is of great importance. At a cooling rate of 0.1 to $4.8 \cdot 10^{-2}$ K/s, the test sample turned into a solid amorphous state, showing no apparent crystal lattice (glassy state of the substance). The validity of this statement is confirmed by the information given in the thermogram (see Fig.1). As is seen from Fig. 1, the several phase transitions take place at the heating of the samples of isopropanol / Al_2O_3 that cooled down (thermogram section 1-2) till 85 K at a rate ranging from 0.1 to $4.8 \cdot 10^{-2}$ K/s.

The characteristics of the reference points on the thermogram refer to the sample that has a composition of isopropanol 94.89 wt.% / nanoparticle 5.11 wt.%. Section 2-3 of the thermogram describes heating of the glassy sample (the rate of temperature change from 0.009 to 0.007 K/s). At point 3, the samples begin to turn into the state of the supercooled liquid. Section 3-4 of the thermogram describes continuous transition from glassy state to supercooled liquid. This process is followed by a partial destruction of intermolecular bonds. Therefore, the temperature variation rate for the samples in the temperature range of $112 \leq T \leq 135$ is decreased from 0.007 K/s to 0.005 K/s. The effective heat capacity of the supercooled liquid is increased from about $1027.5 \text{ J kg}^{-1} \text{ K}^{-1}$ to about $1640 \text{ J kg}^{-1} \text{ K}^{-1}$ (see Fig.2).

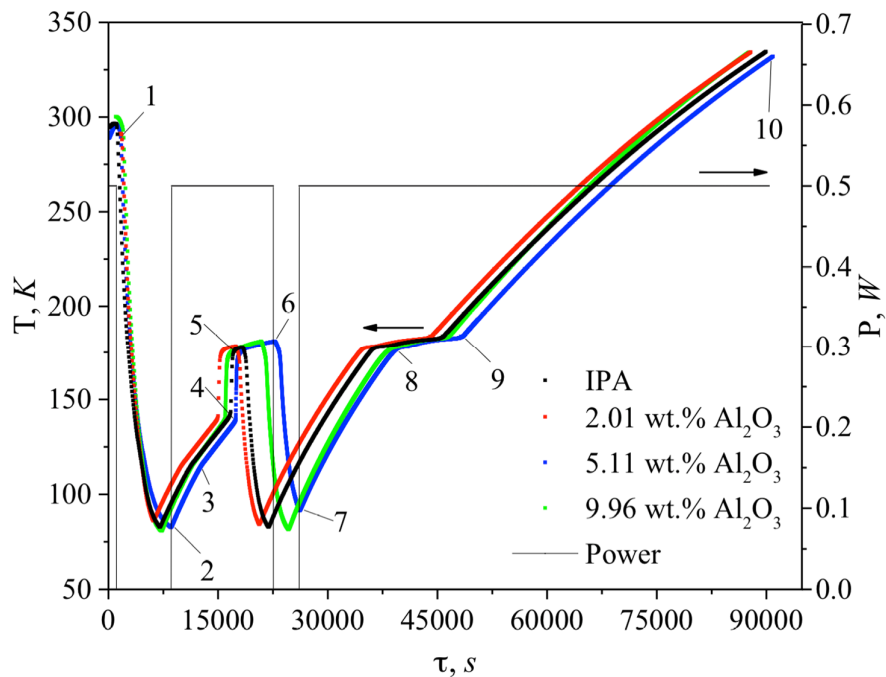


Figure 1. Thermogram of heating nanofluid samples.

It should be noted that increase of the concentration of Al_2O_3 nanoparticles in the sample, leads to decrease the effective heat capacity. This result is quite expected, since the heat capacity of Al_2O_3 nanoparticles is less than the heat capacity of the base liquid. Thermogram section 4-5 (Fig. 1) describes the phase transition from the supercooled liquid to solid phase. This phase transition is followed by a large release of heat, since the temperature of the sample increases from 136 K to the temperature of the solid state - liquid phase transition. Performed experiments show that in order to turn the investigated samples to the crystalline phase, it is necessary to re-cool the sample (thermogram section 6-7). These thermogram sections describe the following: process of increasing temperature of the sample in the crystalline phase (7-8),

melting (8-9), and increase the temperature of the sample in the liquid phase (9-10). At the reheating of the sample (7-8), which was in the crystalline phase, the structural phase transitions up to the melting point were not observed.

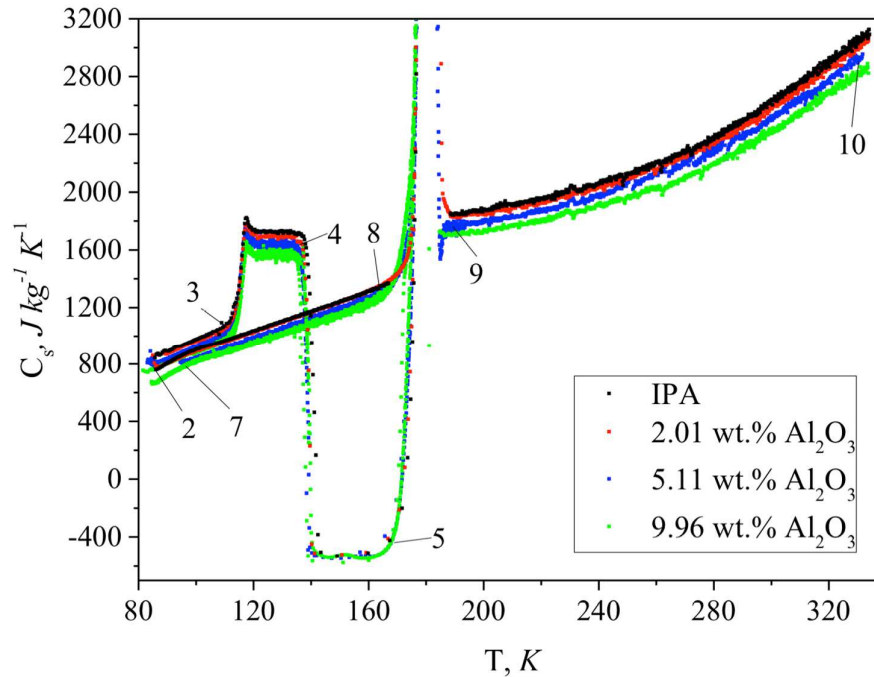


Figure 2. Temperature dependence of the effective heat capacity for heating nanofluid samples.

The presented above model of structural transformations can be confirmed by temperature dependence of the effective heat capacity (Fig.2). The effective heat capacity describes the amount of heat necessary to raise the temperature of the investigated by a degree under the conditions of experiment (including the thermal effects of phase transitions during crystallization and melting).

As follows from the information given in the figures, the presence of nanoparticles in isopropyl alcohol contributes to reducing the heat capacity in both the solid and liquid phases.

The performed study shows that the decrease of the heat capacity is not proportional to the concentration of the nanoparticle. The heat capacity of the samples in the glassy state is higher than the heat capacity of the samples of the same concentration in the crystalline phase. The heat capacity of a substance in a metastable state is higher than its heat capacity in a glassy state. Figs. 3-5 demonstrate more detailed information on the specific heat capacity values of the samples in various aggregate states.

The conducted calorimetric experiments made it possible to determine the quantitative effects of the nanoparticle influence on the characteristics of phase transitions (see Table 1). It was demonstrated that the nanoparticle additives in isopropyl alcohol cause an insignificant change in the temperature of the phase transitions - T_{pt} . The effect of the nanoparticle influence on the heat of phase transitions λ depends on the concentration of nanoparticles, and is very significant.

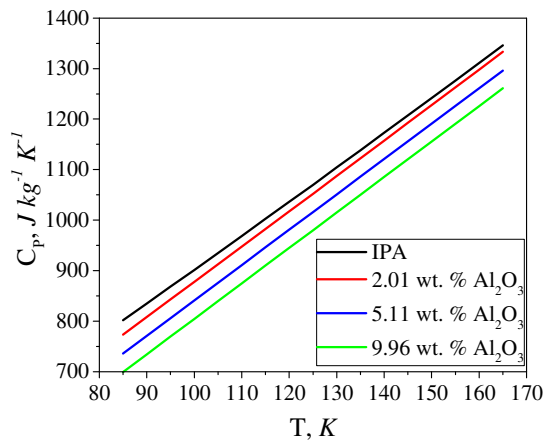


Figure 3 Temperature dependence of heat capacity of nanofluid in the solid phase

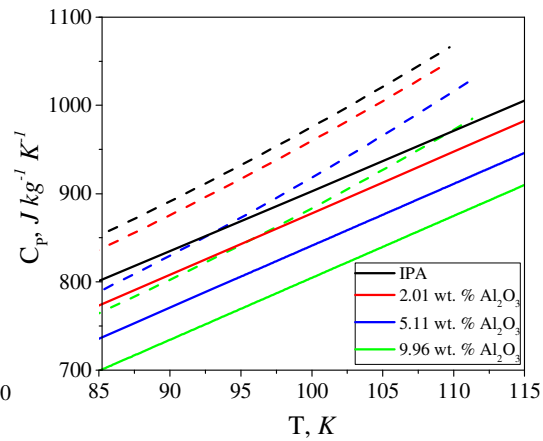


Figure 4 Temperature dependence of the heat capacity of nanofluid in the crystalline phase (solid lines) and the glassy state (dashed lines)

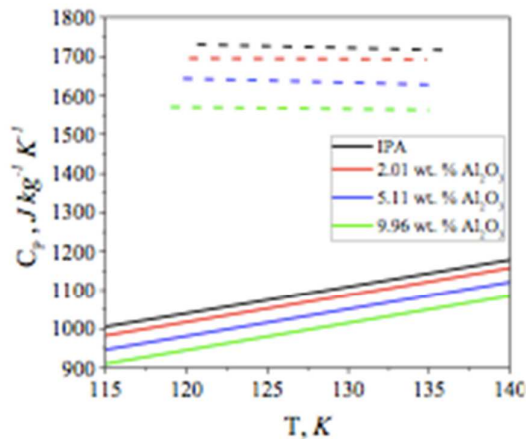


Figure 5 Temperature dependence of heat capacity of nanofluid in the solid phase (solid lines) and metastable state (dashed lines)

Table 1 Parameters of phase transitions in nanofluids

ω_{np} wt. %	T_{tr} K	Δc_p $J\ kg^{-1}\ K^{-1}$	λ $J\ kg^{-1}$
<i>Crystalline - liquid</i>			
0	184.7	271.8	88647.2
2.01	184.9	290.0	86473.0
5.11	185.1	313.5	83855.6
9.96	185.1	253.5	78427.0
<i>Glassy state- metastable state</i>			
0	117.1	602	1202.4
2.01	117.1	576.3	1150.4
5.11	117.0	570.9	1131.8
9.96	117.2	531.6	1109.9

Summary: The conducted calorimetric experiments prove that nanoparticle additives decrease the heat capacity and values of the heat of phase transitions for the isopropyl alcohol in the solid phase. This effect is caused by the complex structure of the nanofluids in the liquid phase. The dispersion phase (base liquid) in the vicinity of nanoparticle has an absorption phase structure that is similar to the glassy state. Therefore, a smaller amount of the dispersion phase changes its aggregate state during phase transitions. The thickness of the absorbed layer of isopropyl alcohol molecules near the nanoparticles depends on their concentration, size and temperature.

References:

1. V.P. Zhelezny, T.L. Lozovsky, M.A. Shimchuk, An experimental investigation and modelling of the heat capacity for nanofluids isopropanol/ Al_2O_3 on the saturation line, *7th International Conference Physics of liquid matter: modern problems (PLMMP7)*, May 27-30, pp.5-9, 2016.

SOLAR SALT WITH SiO₂ NANOPARTICLES FOR THERMAL ENERGY STORAGE HIGH TEMPERATURE APPLICATIONS: SCALE UP OF THE SYNTHESIS PROCEDURE

A. Solé¹, M. Liu², F. Bruno², J.E. Julià¹ and L.F. Cabeza^{3,*}

¹Department of Mechanical Engineering and Construction, Universitat Jaume I, Campus del Riu Sec s/n, 12071 Castelló de la Plana, Spain

²Barbara Hardy Institute, School of Engineering, University of South Australia, Mawson Lakes Boulevard, Mawson Lakes, SA5095 Australia

³GREA Innovació concurrent, INSPIRES Research Centre, University of Lleida, Pere de Cabrera s/n, 25001, Lleida, Spain

*Corresponding author: lcabeza@diei.udl.cat

Keywords: Nanoparticles, Solar salt, Concentrated solar power (CSP) plants, Thermal energy storage

Introduction: The solar salt (60 wt.% NaNO₃ and 40 wt.% KNO₃) is being used for thermal energy storage in high temperature applications (i.e. concentrated solar power (CSP) plants). Since 2013, in different laboratories around the world, nanofluids based on the solar salt have been synthesized doped with alumina (Al₂O₃), silica (SiO₂) and titanium dioxide (TiO₂) nanoparticles to enhance its specific heat capacity (Cp). Figure 1 shows that depending on the concentration of the nanoparticle in the salt, the enhancement differs. This leads to think that there is an optimum concentration of the nanoparticle in the salt, which is 1 % in the case of solar salt (blue bars in Figure 1).

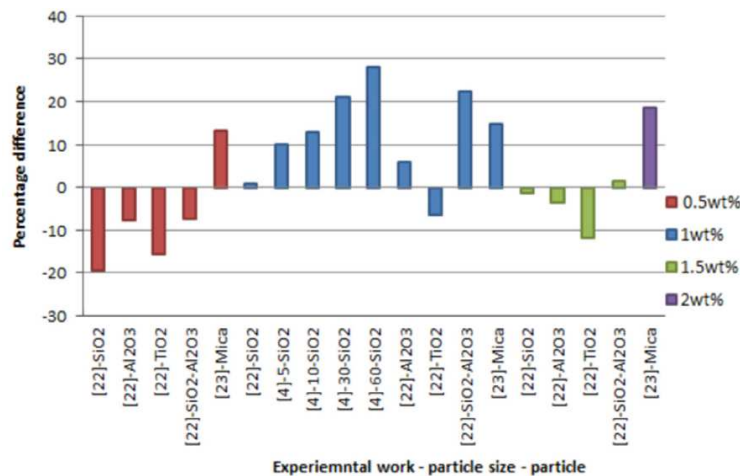


Figure 1. Specific heat enhancement of the solar salt with different nanoparticles and concentrations [1].

The three published studies concerning solar salt and nanoparticles addition agreed that there is around a 25 % of Cp enhancement in liquid state for 1 wt.% of nanoparticles concentration [2-4]. Furthermore, in spite of presenting some differences in ultrasonic bath time and evaporation temperature, the methodology that is being followed to produce molten salt nanofluids is widespread and all the studies [2-4] refer to Shin and Banerjee's methodology [5]. Until now, all the manufacturing process of the nanofluid at the different labs is being done up to 200 mg samples scale.

Therefore, to ensure to the industry that this process is scalable and reproducible maintaining the expected properties (mainly Cp and degradation temperature), the objective of the present study is to synthesize the nanofluid in larger scale, specifically 250 times larger than ever done.

Materials and methodology: Two types of silica (SiO₂) nanoparticles were used: own synthesized and commercial ones. The followed procedure to synthesize the nanoparticles is detailed in [6], where different SiO₂ particle sizes can be derived depending on the reactants concentration. As a starting point, 80 nm was chosen. There is only one study comparing how the nanoparticle size affects the Cp and the best results are given by 60 nm of SiO₂ particle size (being the higher particle size that the authors tested) [3]. Commercial SiO₂ nanoparticles, 250 nm particle size, used for this study were manufactured by Fiber Optic center in New Bedford, Massachusetts. NaNO₃ and KNO₃ are technical grade purchased from the company ACE Chemical from Australia.

Two batches of the nanofluid, each one of 50 g, with both types of nanoparticle, own synthesized and commercial, were done to ensure repeatability of the results. After the synthesis procedure of the nanofluid, based on Shin and Banerjee methodology [5], the samples were placed in an oven for a certain period of time (200 and 400 h) at 450 °C to simulate the behavior in a CSP plant. The nanofluid starts to decompose at 750 °C under nitrogen atmosphere [4]. Under oxygen atmosphere, degradation is expected somewhere around 500 °C.

The developed nanofluid at medium scale (50 g each batch) has been characterized, before and after the oven test, seeking for the Cp enhancement, morphology and composition, degradation temperature, and particle size distribution. The used techniques along with the obtained information are:

Differential scanning calorimeter (DSC) allows measuring the specific heat of the nanofluid in solid and liquid state. From each nanofluid batch 3 samples and 3 runs of each sample will be analyzed to obtain the Cp. The solar salt is also analyzed to have a reference. The DSC is a Mettler-Toledo 822e.

Scanning electron microscopy (SEM) shows how the morphology of the nanofluid is and it allows knowing how the nanoparticles are dispersed in the salt, if they are clustering or not and have a rough number of the nanoparticles size. The samples were mounted on SEM stub with double-sided carbon adhesive. The SEM is Merlin with the GEMINI II column and made by Carl Zeiss Microscopy.

Energy dispersive spectrometry (EDS) gives the composition and the percentage of each chemical element of a given sample. This technique is coupled to SEM. This information will

support SEM one, by showing if SiO_2 is found in the nanofluid (mainly for the own synthesized samples). The EDS is Silicon Drift Detector (SDD) – X-MaxN (20 mm^2) and made by Oxford Instruments.

TEM shows the morphology and gives a rough value of particle size. This technique is used only for the own synthesized silica nanoparticles. The TEM is a JEM-2100F-HR by JEOL.

With thermogravimetric analysis (TGA) TG-STDA Mettler Toledo model TGA/SDTA851e/LF/1600, the maximum working/operating temperature will be known. This technique will allow knowing whether the addition of the nanoparticles can positively or negatively change the maximum operating temperature.

Dynamic light scattering (DLS) technique, Zetasizer nano ZS (Malvern Instruments Ltd., UK), provides useful information about the particle size distribution.

Discussion and results: The experimental testing is on-going, but the first results which show the material synthesis and morphology are promising.

In Figure 2 left, a sample of the own synthesized silica nanoparticles can be observed. Figure 2 left shows that the nanoparticles were successfully synthesized and, although they were expected to be 80 nm of particle size, they seem to be around 200 nm. The morphology of the commercial nanoparticles can be seen in Figure 2 right, from where it can be deduced that nanoparticles are pretty similar in diameter size, uniformity and they seem to be around 200 nm.

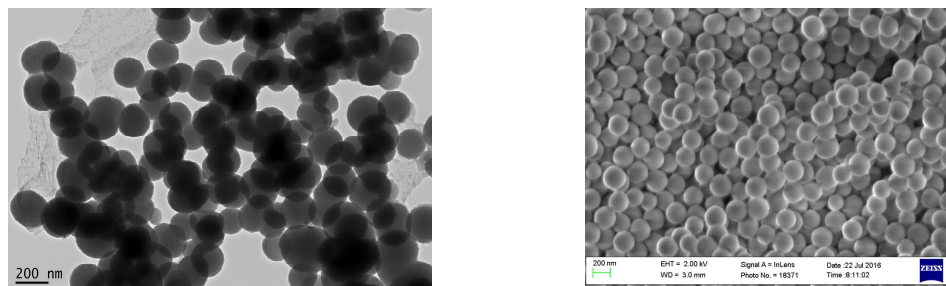


Figure 2. Left: TEM image of own synthesized SiO_2 , right: SEM image of commercial SiO_2 .

SEM images of the solar salt with of own synthesized nanoparticles clearly show that the nanoparticles have been successfully dispersed in the solar salt and show some clusters formation (Figure 3).

EDS spectrum confirms that Si and O are present, coming from the SiO_2 nanoparticles, also oxygen is present in the solar salt and Na, K, and N account for the salt. In addition, C, Cl and even S are found which the last two could be due to impurities in the salts.

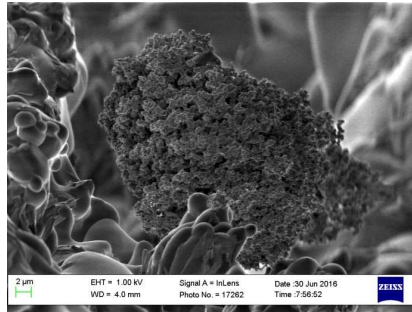


Figure 3. SEM image of batch 1 of the solar salt with own synthesized SiO₂.

Conclusions: Two nanofluids based on the solar salt and silica nanoparticles, with own synthesized nanoparticles and with the commercial nanoparticles, were produced at medium scale in the lab. The feasibility that molten salt based nanofluid with promising Cp can be manufactured at larger scale will be proven depending on the experimental results. The results of the present study provide a step forward for the industrial processing of this potential material for real high temperature applications.

Acknowledgements: The research leading to these results has received funding from the European Union's Seventh Framework Programme (FP7/2007-2013) under grant agreement n° PIRSES-GA-2013-610692 (INNOSTORAGE) and from the European Union's Horizon 2020 research and innovation programme under grant agreement No 657466 (INPATH-TES). The work is partially funded by the Spanish government (ENE2015-64117-C5-1-R (MINECO/FEDER)). The authors would like to thank the Catalan Government for the quality accreditation given to their research group GREA (2014 SGR 123). GREA is certified agent TECNIO in the category of technology developers from the Government of Catalonia. Aran Solé would like to thank Ministerio de Economía y Competitividad de España for Grant Juan de la Cierva, FJCI-2015-25741. The authors also acknowledge the South Australian Department of State Development who have funded this research through the Premier's Research Industry Fund - International Research Grant Program (IRGP 33).

References:

1. O. Arthur and M.A. Karim. An investigation into the thermophysical and rheological properties of nanofluids for solar thermal applications, *Renewable and Sustainable Energy Reviews* 55 (2016) 739-755.
2. M. Chieruzzi, G. F. Cerritelli, A. Miliozzi and J. M. Kenny. Effect of nanoparticles on heat capacity of nanofluids based on molten salts as PCM for thermal energy storage, *Nanoscale research letters* (2013) 8:448.
3. B. Dudda and D. Shin. Effect of nanoparticle dispersion on specific heat capacity of a binary nitrate salt eutectic for concentrated solar power applications, *International journal of thermal sciences* 69 (2013) 37-42.

4. P. Andreu-Cabedo, R. Mondragon, L. Hernandez, R. Martinez-Cuenca, L. Cabedo and J. E. Julia. Increment of specific heat capacity of solar salt with SiO₂ nanoparticles, *Nanoscale Research Letters* (2014) 9:582.
5. D. Shin and D. Banerjee. Enhancement of specific heat capacity of high-temperature silica-nanofluids synthesized in alkali chloride salt eutectics for solar thermal-energy storage applications, *International Journal of Heat and Mass Transfer* 54 (2011) 1064-1070.
6. K.S. Rao, K. El-Hami, T. Kodaki, K. Matsushige and K. Makino. A novel method for synthesis of silica nanoparticles, *Journal of colloid and interface science* 289 (2005) 125-131.

Abstracts

SESSION 5B: BOILING

AN EXPERIMENTAL STUDY OF HEAT TRANSFER COEFFICIENT AND INTERNAL CHARACTERISTICS OF NUCLEATE POOL BOILING OF NANOFLUID R141B/TiO₂

O. Khlijeva^{1*}, A. Nikulin², T. Gordeychuk¹, N. Lukianov¹ and Y. Semenyuk¹

¹Odessa National Academy of Food Technologies, Odessa, Kanatnaya str. 112, Ukraine

²Instituto Superior Técnico, Universidade de Lisboa, IN+, Lisbon, Portugal

*Corresponding author: khlijev@ukr.net

Keywords: Nanofluids, Pool boiling, Heat transfer coefficient, Internal characteristics of boiling process

Introduction: The main purpose of this study was to evaluate the effect of surfactant and TiO₂ nanoparticles additives into the refrigerant R141b on the heat transfer coefficient (HTC) and internal characteristics of the nucleate pool boiling process.

The experiments were carried out with the following substances: refrigerant R141b; solution R141b / surfactant Span-80 (0.1 % mass.) (CAS No. 1338-43-8, Sigma-Aldrich); nanofluid R141b / surfactant Span-80 (0.1 % mass.) / TiO₂ nanoparticles (0.1 % mass.). The size of TiO₂ nanoparticles (nanopowder) did not exceed 25 nm (CAS No. 1317-70-0, Sigma-Aldrich).

Discussion and Results: The two-step method was used to prepare the nanofluid. The nanofluid R141b / TiO₂ without surfactant was unstable and nanoparticles aggregation was observed. Although, as reported in paper [1] the stable nanofluid R141b / TiO₂ can be prepared without surfactants. The measurements of the mean size of nanoparticles (by spectroturbidimetry method) in the R141b / surfactant / TiO₂ were carried out both during the experimental study of HTC and during storage within three months. It was found that nanofluid has a good aggregative stability with mean nanoparticle radius of 125 ± 7 nm.

The study of HTC during nucleate pool boiling was carried out using the original experimental setup [2] under the pressure of 0.2, 0.3 and 0.4 MPa and in the range of heat fluxes from 5 to 70 kW·m⁻². A stainless steel (AISI 321) capillary with 2 mm in diameter was used as a heating surface. The experimental results of HTC depending on heat flux are shown in the Fig. 1.a – 1.c.

The internal boiling characteristics (bubble departure diameter, bubble departure frequency and mean velocity of bubble growth) were studied experimentally under atmospheric pressure and in the range of heat fluxes from 29 to 57 kW·m⁻². The snapshots of boiling process were taken using the camera and the stroboscope. The exposure time was 50 μs and the intervals between flashes were 3 ms. During the obtained images processing (see Fig. 2) the number of bubbles was 80-140 to determine the mean bubble departure diameter \bar{d}_0 and 50-110 to determine the mean bubble departure frequency \bar{f} . The mean velocity of bubble growth $\bar{w}'' = \bar{d}_0 \cdot \bar{f}$ defined

by mean values of \bar{d}_0 and \bar{f} is shown in the Fig. 3.

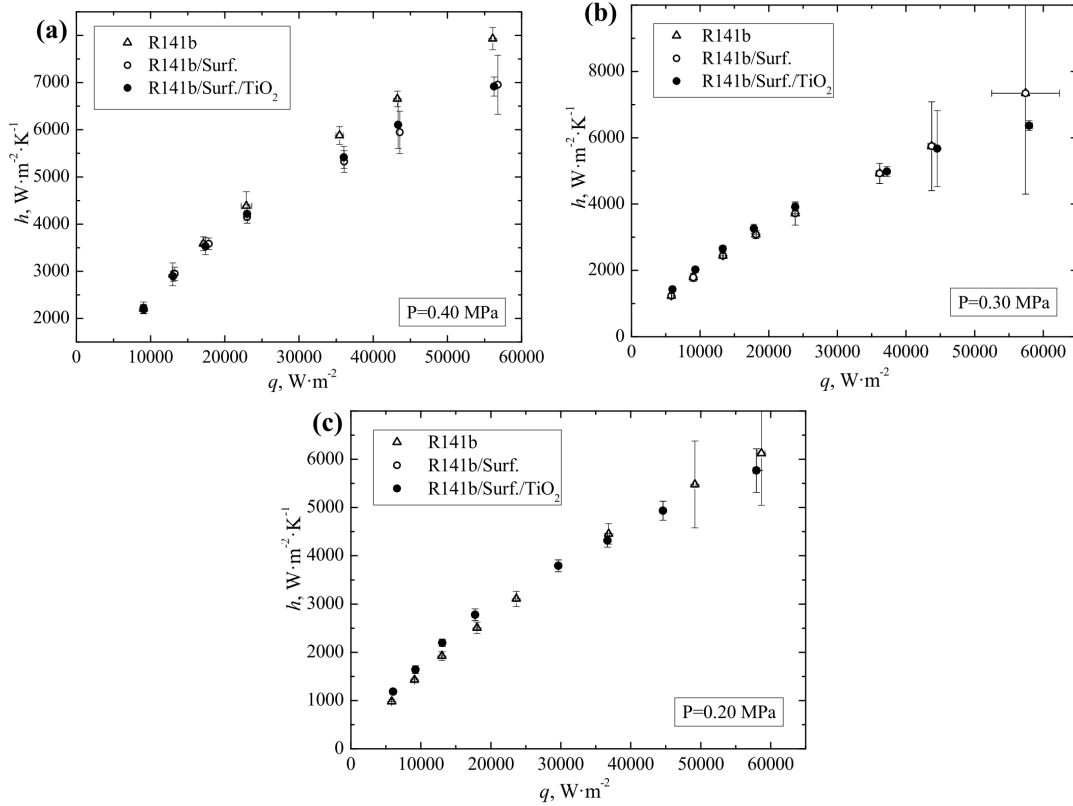


Figure 1. HTC and expanded uncertainty of experimental data for R141b / surfactant and R141b / surfactant / TiO₂ solutions in contrast with pure R141b: (a) 0.4·MPa, (b) 0.3·MPa, (c) 0.2·MPa

A comparison of the experimental values of HTC with calculated ones using the proposed by V.I. Tolubinsky [3] equation (1) has been carried out.

$$\frac{h}{k} = \sqrt{\frac{\sigma}{g(\rho' - \rho'')}} = 75 \left(\frac{q}{h_{vap} \rho'' \bar{w}''} \right)^{0.7} \left(\frac{\alpha}{\nu} \right)^{0.2} \quad (1)$$

where h is the heat transfer coefficient, $\text{W}\cdot\text{m}^{-2}\cdot\text{K}^{-1}$; k is the thermal conductivity, $\text{W}\cdot\text{m}^{-1}\cdot\text{K}^{-1}$; σ is the surface tension, $\text{N}\cdot\text{m}^{-1}$; ρ' and ρ'' are the density of liquid and vapor respectively, $\text{kg}\cdot\text{m}^{-3}$; q is the heat flux, $\text{W}\cdot\text{m}^{-2}$; h_{vap} is the latent heat of vaporization, $\text{J}\cdot\text{kg}^{-1}$; α is the thermal diffusivity, $\text{m}^2\cdot\text{s}^{-1}$; ν is the kinematic viscosity, $\text{m}^2\cdot\text{s}^{-1}$.

The experimental data on mean velocity of bubble growth \bar{w}'' were used in order to predict HTC by equation (1). To estimate the mean velocity of bubble growth at the pressures under which the experiments were performed the empirical equation (2) [3] was used.

$$\bar{w}''/\bar{w}_{0.1}'' = (\rho_{0.1}''/\rho'')^{2.3+0.5lg\pi} \quad (2)$$

where $\bar{w}_{0.1}''$ and $\rho_{0.1}''$ are the mean velocity of bubble growth and vapor density at $P=0.1013 \cdot \text{MPa}$ respectively; $\pi = P/P_C$ is the reduced pressure.

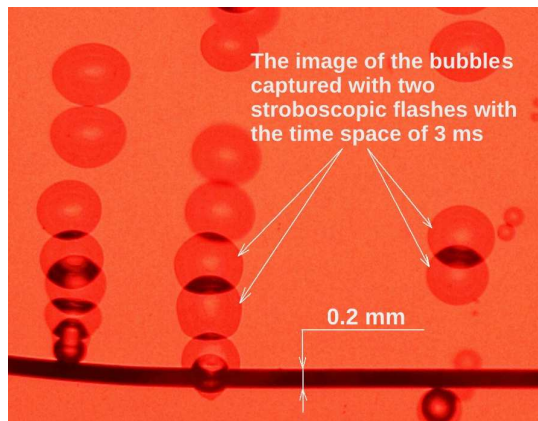


Figure 2. The snapshots of boiling process for R141b / surfactant at heat flux $29.6 \text{ kW}\cdot\text{m}^{-2}$ (150 pixel per 1 mm)

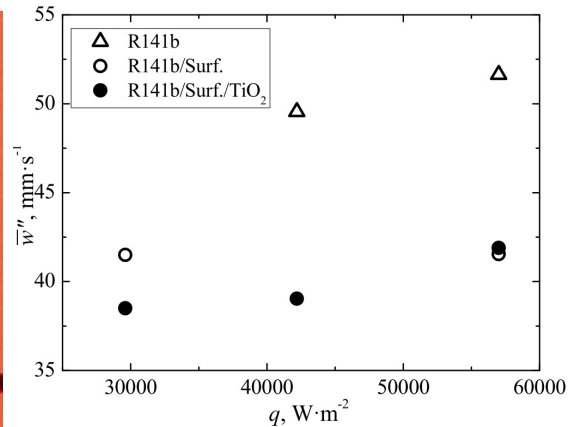


Figure 3. Mean velocity of bubble growth \bar{w}'' for R141b / surfactant and R141b / surfactant / TiO₂ solutions in contrast with pure R141b

The properties of pure R141b were used for HTC calculation using the eq. (1). However, it is known that the nanoparticles additives lead to increase in thermal conductivity and viscosity of base fluids. The information on nanofluids surface tension is rather scant in the published works. Nevertheless, it was shown in the paper [4] that the additives of 0.5 % mass. TiO₂ nanoparticles with oleic acid (as surfactant) into the solution of R600a / compressor oil leads to a slight decrease in surface tension.

Experimental and calculated HTC values depending on heat flux at $P = 0.3 \text{ MPa}$ are shown in Fig. 4.

Conclusions: As follow from the obtained data, the pool boiling heat transfer coefficient of R141b / surfactant / TiO₂ nanofluid is higher in contrast with R141b at low heat fluxes and lower at high heat fluxes. The most significant effect of nanoparticles additives on heat transfer coefficient enhancement was observed at low heat fluxes and pressure. The results of pool boiling HTC calculation by Eq.1 using the experimental values of mean velocity of bubble growth had shown a good agreement with the experimental HTC data for pure refrigerant.

At the same time, the calculated HTC data for the R141b / surfactant solution and R141b / surfactant / TiO₂ nanofluid is higher than experimental HTC. There are several explanations of such results. Firstly, the effect of nanoparticles and surfactant additives on the thermophysical properties was not taken into account. Secondly, the alteration in nucleation sites density during boiling caused by nanoparticles and surfactant additives to R141b also can effect HTC. Thus, the further studies of thermophysical properties and the nucleation sites density change on nanofluids pool boiling HTC are of high interest.

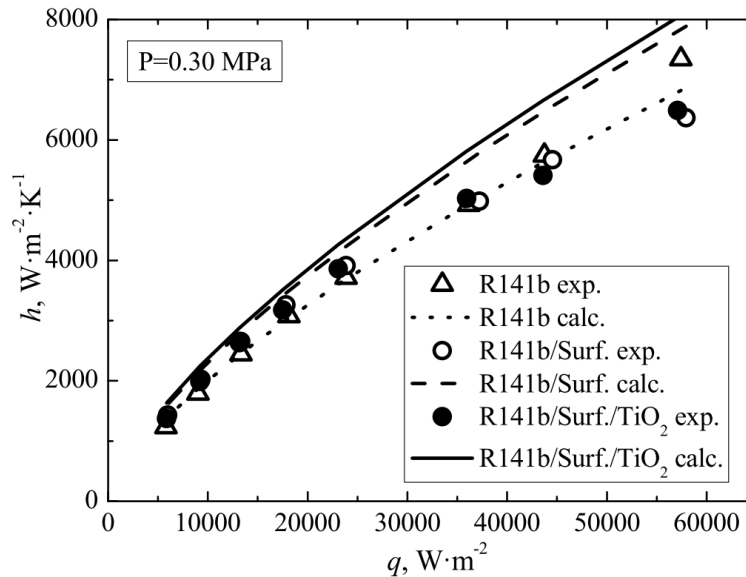


Figure 4. Experimental and calculated HTC for R141b / surfactant and R141b / surfactant / TiO₂ solutions in contrast with R141b.

References:

1. V. Trisaksri, S. Wongwises Nucleate pool boiling heat transfer of TiO₂-R141b nanofluids, *International Journal of Heat and Mass Transfer*, 52/5 (2009) 1582-1588.
2. A. Nikulin, A. Melnyk, Y Semenyuk, M. Lukianov, V. Zhelezny, Effect Of Nanoparticles On Pool Boiling Characteristics, *International Symposium on Convective Heat and Mass Transfer (CONV-14 ICHMT)*, Kusadasi, Turkey, 2014.
3. V.I. Tolubinskiy, Heat Transfer under Boiling (in Russian), Naukova Dumka, Kiev, 1980 (Chapters 4 and 5).
4. V. P. Zhelezny, N. N. Lukianov, O. Y. Khliyeva, A. S. Nikulina, A. V. Melnyk A complex investigation of the nanofluids R600a-mineral oil - AL₂O₃ and R600a-mineral oil - TiO₂. Thermophysical properties, *International Journal of Refrigeration* 74 (2017) 486-502.

EXPERIMENTAL STUDY OF POOL BOILING HEAT TRANSFER ON NANOPARTICLE-DEPOSITED SURFACES

Z. Cao, Z. Wu, S. Abood and B. Sunden*

¹Department of Energy Sciences, Lund University, Lund Sweden

*Corresponding author: bengt.sunden@energy.lth.se

Keywords: Pool boiling, Nanofluid, Al₂O₃, Graphene

Introduction: Heat transfer dissipation has been a major issue in many industries, such as power plants, electronic chip cooling, refrigeration systems and heat-exchanger systems [1]. Usually, the single-phase heat transfer cannot satisfy the requirements of heat removal in the aforementioned cases. Therefore, phase-change heat transfer, like pool boiling, is highly requested to facilitate transport of high heat flux at low superheat. Many factors can affect the performance of pool boiling heat transfer, like subcooling, the surface materials and morphology, properties of the liquid and nucleation sites density. Nanofluid, first reported by Choi [2] in 1995, is a new type of fluid by dispersing nanoparticles (1-100 nm) in the base fluids and has more preferable thermal properties. Compared with other technologies to enhance pool boiling heat transfer, nanofluid technology is an easier way to implement. Nanofluid boiling studies began to increase from 2003 and has become an important research branch until now [3].

Up to now, different type of nanoparticles, e.g., Al₂O₃, CuO, TiO₂ with different base liquids, e.g., water, ethylene glycol, have been tested. However, here only water-based nanofluids are reviewed. Neto et al. [4] studied the pool boiling heat transfer of Al₂O₃, Fe₂O₃ and CNTs nanofluids. The results showed that CHF_s were increased by 26-37%, but heat transfer coefficients were the same or lower compared with distilled water. They explained that the increase in wettability and the thickness of the deposition layer resulted in the outcomes. A reduction in the static contact angle required more power to activate boiling. Karimzadehkhoei et al. [5] compared the performance of TiO₂ and CuO nanofluids. It was found that heat transfer was enhanced and deteriorated by the nanofluid with low (0.001 wt.%) and high mass fraction (0.2 wt.%) of TiO₂, respectively, while CuO nanofluids with different concentrations always enhanced the heat transfer. It was conceived that the deposition of nanoparticles on the surface might cause deterioration or enhancement of heat transfer coefficient, depending on the type of nanoparticles and other factors. Similarly, very high fraction of TiO₂ (12 wt.% and 15 wt.%) were tested by Ali et al. [6] and enhanced heat transfer was achieved. Cheedarala et al. [7] prepared a type of nano composites with CuO and Chitoan, namely CuO-chitosan nanofluid. The new type of nanofluid gave higher CHF than CuO nanofluid. This is probably because that

the nanoparticle is hydrophilic which provides better liquid supply. Shoghl and Bahrami [8] carried out experiments to study pool boiling heat transfer of ZnO and CuO nanofluid. Deterioration of heat transfer was observed in both types of nanofluid with mass fractions of 0.01% and 0.02%, which resulted from the roughness changes by the nanofluid, as stated by the authors. Quan et al. [9] investigated the wettability effect of Si nanoparticles in pool boiling of a nanofluid. It was concluded that nanofluids containing moderately hydrophilic nanoparticles are most effective in enhancing boiling heat transfer, because moderately hydrophilic nanoparticles could decrease the size of departing bubbles and the deposited moderately hydrophilic nanoparticles promote roughness of the heater surface, providing more active nucleation cavities. Though several kinds of water-based nanofluids were described as aforementioned, Al₂O₃ nanofluid is still the most commonly studied [9]. Therefore, attentions are concentrated on Al₂O₃/ water nanofluid next. Table 1 provides a brief review on Al₂O₃/ water nanofluid. It shows conflicting results on HTC and CHF in different studies. However, some conclusion could be extracted. In most cases, heat transfer of nanofluid is deteriorated or unchanged, but CHF is increased compared to water. The concentration of nanofluid has a significant effect on HTC and CHF. It is expected that the low concentration benefits boiling heat transfer performance in comparison to high concentration. In addition, the roughness of heating surfaces is strongly coupled with the performance. Usually, a nanofluid performs better on the smooth surface. Several possible mechanisms were also proposed to explain the results of nanofluid in pool boiling. Normally the explanations derived from the coating on the surface due to nanoparticle deposition which could change the wettability, the number of active nucleation sites, the roughness, thermal resistance and even bubble behaviors.

In summary, Al₂O₃/ water nanofluid has been investigated a lot on pool boiling heat transfer, but hybrid nanofluid has not been tested to the best knowledge of the authors. In the present study, the pool boiling of Al₂O₃/ water nanofluid with low concentrations will be tested and grapheme nanoplatelets will be added to the nanofluid to study the pool boiling of mixed nanofluids.

Discussion and Results: The pool boiling experiments were first conducted on a bare copper plate. The results regarding superheat and heat flux were compared with the commonly used Rohsenow correlation to validate the accuracy and reliability of the setup. Fig. 1 compares the present experimental results and the correlation with $n = 1$ for water and $C_{sf} = 0.009$. It is indicated that the results of experiments agree well with those of the correlation. In addition, the critical heat flux (CHF) on the bare copper surface was also tested. At present, CHF was measured to 101.7 W/cm² which is smaller than the prediction of the well-known CHF model proposed by Zuber ~110 W/cm². The deviation is about 8% which might be acceptable. The experiments on nanofluids are still ongoing. No results are shown at the moment, but will be available soon.

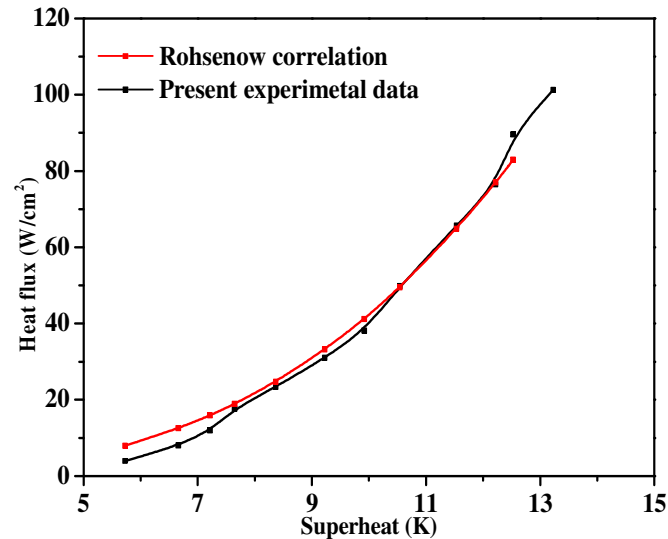


Fig. 1 The comparison between the present results and Rohsenow correlation on bare copper surface.

Table 1 Literature review of Al₂O₃/ water nanofluid on pool boiling

Ref.	Concentration	Surface	Results, explanations and remarks
9	0.0007 vol.% 0.007 vol.%	Copper	HTC increases and max. 75% and 15% are achieved at low concentration and below 400 W/cm ² on smooth surface $Ra=0.05 \mu\text{m}$ and on rough surface $Ra=0.23 \mu\text{m}$, respectively; The behaviour is caused by the deposition of nanoparticles, which increase active nucleation sites, but increase the thermal resistance of nanolayer from a certain heat flux threshold
10	0.001, 0.005, 0.01, 0.025, 0.05 g/L	Copper 3 kPa	HTCs are almost not affected. Maximum CHF 300% is achieved at 0.025g/L beyond which CHF almost does not change. The average size of departing bubbles increases and the bubble frequency decreases significantly in nanofluids compared to those in the pure water.
11	0.026, 0.05, 0.1, 0.25, 0.525, 1.02 g/L	Copper	CHF degrades or is unchanged at the concentration under 0.1 g/L, and increases from 0.25 g/L and maximum CHF is achieved at a concentration of 0.525

			g/L HTC degrades or is unchanged. The CHF improvement is contributed to the wetting improvement
12	0.001, 0.005, 0.01, 0.025, 0.1, 0.5, 1 g/L	Copper	HTC of nanofluid is almost the same as for pure water and CHF increases with increasing concentration and becomes stable at the concentration of 0.025 g/L (80% enhancement, optimal) HTC on the coating surfaces is almost the same as that of nanofluid The coating due to microlayer evaporation changes the surface wettability
13	0.01, 0.1, 0.5 vol.%	Copper	HTC is enhanced, almost the same and deteriorated at concentration of 0.01, 0.1 and 0.5 vol.%, respectively HTC on the coating surfaces is deteriorated The enhancement is due to the dominant effect of thermal conductivity of nanofluid but less due to nanoparticle deposition The deterioration is due to the deposition which decreases the number of active nucleation sites and increases thermal resistance.
14	0.001, 0.01, 0.05, 0.1 vol.%	Copper 3 kPa	On the surface $Ra=177.5$ nm, HTC is almost the same as for pure water. On the surface $Ra=292.8$ nm, HTC deteriorates. On both surfaces, CHF is increased and highest at 0.05 vol.% The results are due to the contribution by the nanoparticle deposition and wettability changes

Table 2 The tests in the present study

Runs	Concentration of Al ₂ O ₃	Concentration of graphene
1	0.0001 vol.%	0
2	0.001 vol.%	0
3	0.01 vol.%	0
4	0.0001 vol.%	0.001 vol.%
5	0.001 vol.%	0.0001 vol.%

References:

1. D. Ciloglu, A. Bolukbasi, A comprehensive review on pool boiling of nanofluids, *Applied Thermal Engineering*.84 (2015) 45–63.
2. Please correct and write as for other refs. , Enhanceing thermal conductivity of fluids with nanoparticles, *Fluids Engineering Division, FED 231. ASME Publication*. (1995) 99-105
3. X.D. Fang, Y.F. Chen, H.L. Zhang, W.W. Chen, A.Q. Dong, R. Wang, Heat transfer and critical heat flux of nanofluid boiling: A comprehensive review, *Renewable and Sustainable Energy Reviews*. 62 (2016) 924-940.
4. Neto, A. R., Oliveira, J. L. G., & Passos, J. C., Heat transfer coefficient and critical heat flux during nucleate pool boiling of water in the presence of nanoparticles of alumina, maghemite and CNTs. *Applied Thermal Engineering*, 111 (2017)1493-1506.
5. Karimzadehkhoei, M., Shojaeian, M., Şendur, K., Mengüç, M. P., & Koşar, A., The effect of nanoparticle type and nanoparticle mass fraction on heat transfer enhancement in pool boiling. *International Journal of Heat and Mass Transfer*, 109 (2017) 157-166.
6. Ali, H. M., Generous, M. M., Ahmad, F., & Irfan, M., Experimental investigation of nucleate pool boiling heat transfer enhancement of TiO₂-water based nanofluids. *Applied Thermal Engineering*, 113 (2017) 1146-1151.
7. Cheedarala, R. K., Park, E., Kong, K., Park, Y. B., & Park, H. W., Experimental study on critical heat flux of highly efficient soft hydrophilic CuO–chitosan nanofluid templates. *International Journal of Heat and Mass Transfer*, 100 (2016) 396-406.
8. Shoghl, S. N., Experimental investigation on pool boiling heat transfer of ZnO, and CuO water-based nanofluids and effect of surfactant on heat transfer coefficient. *International Communications in Heat and Mass Transfer*, 45 (2013) 122-129.
9. Manetti, L. L., Stephen, M. T., Beck, P. A., & Cardoso, E. M., Evaluation of the heat transfer enhancement during pool boiling using low concentrations of Al₂O₃-water based nanofluid. *Experimental Thermal and Fluid Science*. (2017)
10. You, S. M., Kim, J. H., & Kim, K. H., Effect of nanoparticles on critical heat flux of water in pool boiling heat transfer. *Applied Physics Letters*, 83 (2003) 3374-3376.

11. Coursey, J. S., & Kim, J., Nanofluid boiling: the effect of surface wettability. *International Journal of Heat and Fluid Flow*, 29 (2008) 1577-1585.
12. Kwark, S. M., Kumar, R., Moreno, G., Yoo, J., & You, S. M., Pool boiling characteristics of low concentration nanofluids. *International Journal of Heat and Mass Transfer*, 53 (2010) 972-981.
13. Ahmed, O., & Hamed, M. S., Experimental investigation of the effect of particle deposition on pool boiling of nanofluids. *International Journal of Heat and Mass Transfer*, 55 (2012) 3423-3436.
14. Ham, J., Kim, H., Shin, Y., & Cho, H., Experimental investigation of pool boiling characteristics in Al₂O₃ nanofluid according to surface roughness and concentration. *International Journal of Thermal Sciences*, 114(2017) 86-97.

NANOFLUIDS AS WORKING FLUID IN THERMOSYPHON

A. Wlazlak¹, B. Zajaczkowski¹, S. Barison², F. Agresti², L.M. Wilde³, M.H. Buschmann^{3*}

¹Wrocław University of Science and Technology,
St. Wyspiańskiego 27, 50-370 Wrocław, Poland

²CNR-ICMATE Institute of Condensed Matter Chemistry and Technologies for Energy,
Corso Stati Uniti, 4, 35127 Padova, Italy

³Institut für Luft- und Kältetechnik GmbH
Bertolt-Brecht-Allee 20, 01309 Dresden, Germany

*Corresponding author: Matthias.Buschmann@ilkdresden.de

Keywords: Thermosyphon, Nanofluids, Gold, Nanohorns, Silica

Introduction: Nanofluids are suspensions of particles with an average size of about 10-100 nm in various base fluids. The most common nanoparticles are metals or metal oxides dispersed in water. The addition of nanoparticles improves heat transfer processes which results in enhanced efficiency and miniaturization of energy transfer and storage systems. The motivation for studying on this topic comes from increasing global energy demands combined with the need for efficient and environmentally friendly solutions. Upward trends in excess heat that should be removed from electronic devices intensify research on such solutions. The usage of nanoparticles allows to omit clogging, sedimentation and abrasion - common problems occurring with larger particles [1, 2].

Aim of the study presented here is to investigate and compare thermal performance of thermosyphon (TS) employing different nanofluids. For that purpose, series of experiments in a test rig are conducted. Measurements employing water (baseline), gold nanoparticles, single-walled carbon nanohorns stabilized with sodium dodecyl sulfate (SDS) and silica (SiO₂) stabilized with potassium hydroxide (KOH) are conducted. The differences between working fluids in terms of thermal performance are described and compared.

Test rig and employed nanofluids: The experiments are carried out employing the big ILK-thermosyphon, shown in Fig. 1. The device is made of a copper pipe with an inner diameter of 20 mm and a length of 1800 mm covered by an ARMAFLEX insulation (20 mm). Evaporator is heated and condenser cooled by coil heat exchangers (di = 4 mm, l = 500 mm) made of copper. Temperature of working fluid in evaporator is measured employing a special-designed probe consisting of six Pt 100 (Fig. 1 right). Temperature of inlet and outlet of cooling and heating water is determined employing Pt100 sensors. Volume fluxes of cooling and heating water are measured employing Krohne Optiflux 5000 flowmeters.

Internal pressure of TS is measured along the adiabatic section and in the condenser with the frequency of 1 kHz. Three transmitters each with a measurement range of 0...400 Pa are placed along the adiabatic section. In the condenser, data are taken by piezoresistive pressure transmitters with a measurement ranges of 0...104 Pa and 0...105 Pa.

Each measurement starts by adjusting inlet temperatures and volume fluxes of cooling and heating cycle. Inlet temperature of the heating medium is varied between 30°C and 85°C with an increment of 5 K. Inlet temperatures of condenser is 15°C. Volume fluxes in evaporator and condenser are kept constant at a value of 12 l/h. Testing time is one hour for each parameter combination.

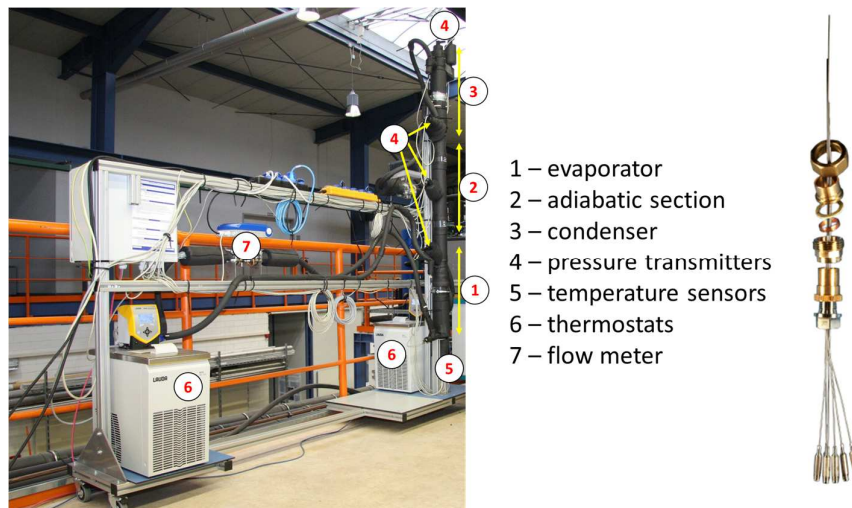


Fig.1. Test rig: thermosyphon with measurements system (left) and special-designed temperature probe (right).

Three kinds of nanofluids were tested and compared with water as reference data. Gold nanofluids were prepared by Particular GmbH (Germany). Nanoparticles with sizes varying between 50 and 70 nm were suspended in water with a concentration of 100 mg/L. Stabilization was carried out with KOH.

Single wall carbon nanohorns, commonly called nanohorns, are aggregates of graphene sheets. Thousands of them tend to associate with each other to form structures like dahlias or buds with high surface to volume ratio and large surface area [3]. A water based suspension of 0.1 g/L nanohorns (Carbonium Srl) stabilized with 0.01 g/L of SDS was prepared by high-pressure homogenization and is investigated in this study. The average hydrodynamic size of aggregates measured by dynamic light scattering (DLS) is between 100 and 150 nm.

The silica nanofluid is made of SIPERNAT©22S with a concentration of 2.0 vol. %. Stabilization is done with KOH so that a pH-value of 10.5 is achieved.

Discussion and Results: Results are exemplarily presented in Fig.2 to 4 for water, gold, nanohorn and silica nanofluids. Thermal resistance of the thermosyphon R_{th} (Fig. 2) is defined as the ratio of mean temperature difference between evaporator and condenser to transferred amount of heat. This parameter decreases with the increase of heat received at the condenser and reaches an almost constant value of about 0.078 W/mK for higher heat fluxes (approx. above 220 W). A significant difference in thermal resistance depending on the working fluid is found at low heat fluxes. The most noteworthy decrease in thermal resistance is caused by the silica nanofluid. Reductions up to 60 % compared to the baseline (water) are found. The presumed mechanism responsible for this effect is the nanoporous layer in the evaporation region formed by the silica nanoparticles. Boiling curves - heat taken out at the condenser versus overheating at evaporator wall - are presented with Fig.3. Once again for high heat fluxes (inlet temperature of heating medium above 65°C) no big differences are seen between different working fluids. However, nanofluids change boiling regime significantly at low overheating. This finding points toward a change of bubble release behaviour due to a changed wall quality in the evaporator.

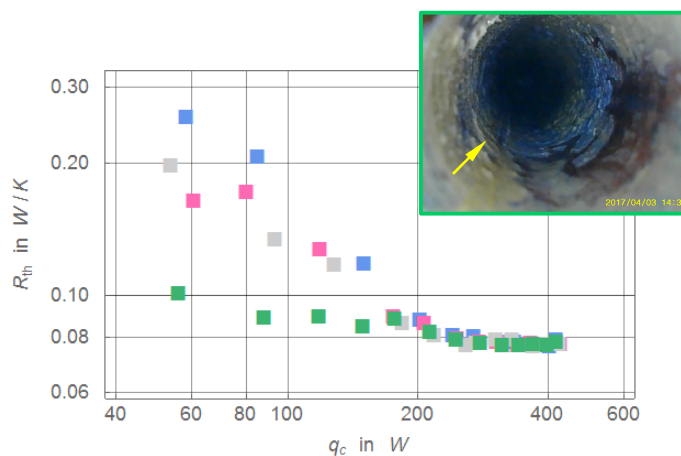


Fig. 2. Thermal resistance of different working fluids. Condenser inlet temperature was in all cases 15°C. Evaporator inlet temperature varied between 30°C and 85°C. Colours indicate water (blue), nanohorns nanofluid (grey), gold nanofluid (pink) and silica nanofluid (green). Insert shows interior of TS seen from the evaporator end after use of silica nanofluid. Yellow arrow indicates nanoporous layer formed by silica nanoparticles.

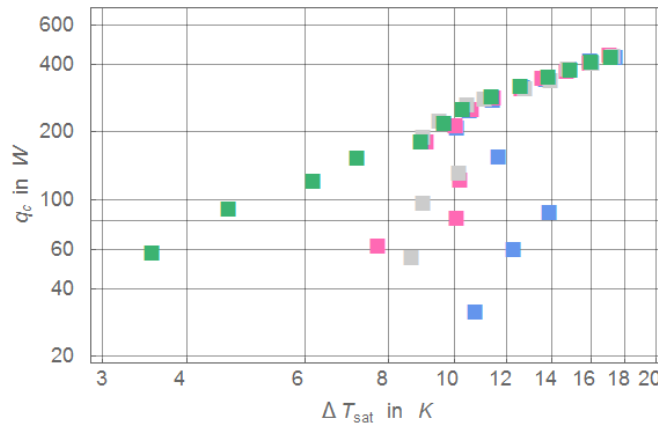


Fig. 3. Boiling curves for different working fluids. Conditions and symbols as in

Non-dimensional representation of data is shown in Fig.4. Here Nu denotes the Nusselt number according to eq. (1) and D is the non-dimensional averaged temperature of the TS.

$$Nu = \frac{q_c}{\bar{t}_e \cdot k \cdot d_i}; \quad D = \frac{c_p}{\Delta h_p} \frac{t_{ei} + t_{eo} + t_{ci} + t_{co}}{4} \quad (1)$$

Where \bar{t}_e is the mean value between inlet and outlet of water in the evaporator, k is thermal conductivity of working fluid, d_i inner diameter of thermosyphon, c_p heat capacity of working fluid, Δh_p latent heat of working fluid and t_{ei} , t_{eo} , t_{ci} , t_{co} denote inlet and outlet temperatures of cooling and heating medium.

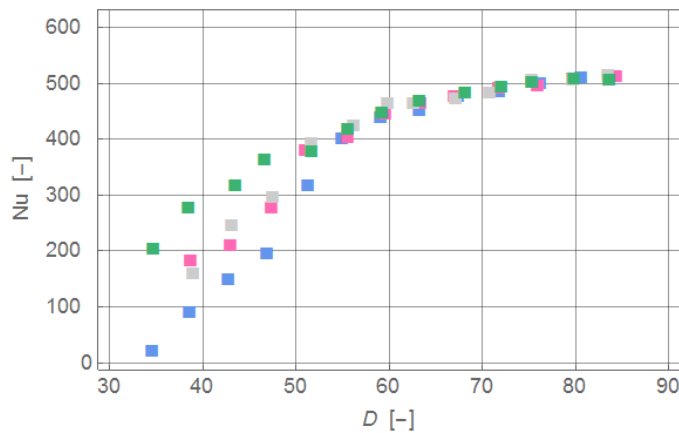


Fig.4. Normalised amount of transferred heat (Nusselt number correlation) in dependency of normalised mean temperature difference of thermosyphon. Conditions and symbols as in

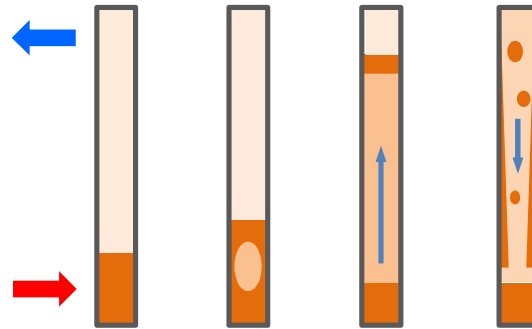


Fig. 5: Simplified sketch of geysir effect in thermosyphon. The sketches indicate from left to right: overheating of evaporator zone, forming of large bubble, expelling working fluid toward condenser and back falling working fluid.

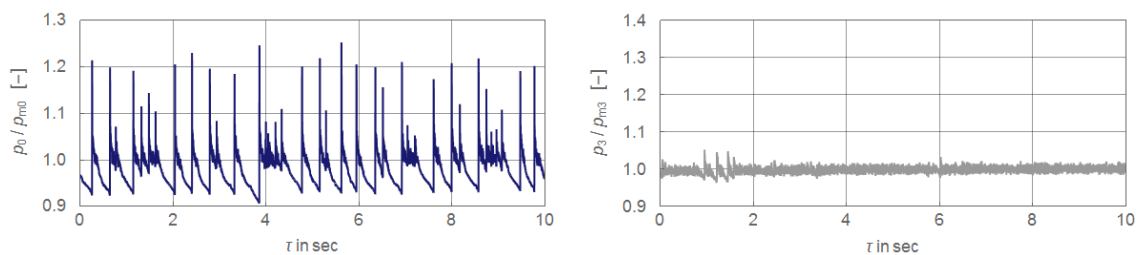


Fig. 6: Typical instantaneous pressure distribution for water (left) and nanohorn nanofluid under geysiring conditions. Inlet conditions at evaporator and condenser are identical in both cases ($t_{ei} = 85$ °C, $t_{ci} = 25$ °C)

Nusselt number increases monotonic with increasing normalized averaged temperature of TS. For low values of D , Nusselt number is significantly higher for nanofluid than for water. However, the increases depend strongly on the nanofluid. While the gold and the nanohorn nanofluid show nearly the same improvement the silica nanofluid gives significantly higher values. It is assumed, that the nanoporous layers are differently efficient formed. While for silica a massive layer is found (Fig.2) the coating found for the gold and the nanohorn nanofluid are mere loose nanoparticle deposits.

Besides the thermal performance the dynamical behaviour of the thermosyphon might be significantly affected by adding nanoparticles to the working fluid. This effect was especially seen with the nanohorn nanofluid.

Dynamical instabilities of a thermosyphon result from thermal instability mainly geysiring. Under geysiring the overheating of the working fluid followed by an eruption expelling larger parts of the working fluid into the condenser (Fig. 5). Such a behaviour is seen when the working fluid of our thermosyphon is pure water. A typical pressure distribution over time is

shown in Fig. 6 left plot. Changing the working fluid to the nanohorn nanofluid stabilized with SDS leads to a suppression of the instabilities observed with pure water.

Conclusions:

From the experiments carried out so far the following conclusions are drawn.

- Nanofluids affect the thermal resistance of thermosyphons, in particular for low values of transported heat. The intensity of the effect depends on the nanofluid employed. Best results are obtained with a silica nanofluid with a concentration of 2 vol. %.
- Boiling behaviour is significantly influenced by nanoparticles forming nanoporous layers on the wall of the evaporator. For a given overheating of the evaporator wall a higher amount of heat can be transferred.
- As a side effect a substantial reduction of thermal instabilities – geysiring – is obtained when nanohorn nanofluid is employed as working fluid.

To summarize nanofluids offer a chance to improve the thermal performance of thermosyphons considerably. However, care has to be taken with respect to the nanofluid employed and the operation range of the device.

Acknowledgement: This work is a contribution to the Grant MF140079 and the COST Action (European Cooperation in Science and Technology) CA15119: Overcoming Barriers to Nanofluids Market Uptake (NanoUptake).

References:

1. M.H. Buschmann, Nanofluids in thermosyphons and heat pipes: Overview of recent experiments and modelling approaches, *Int. J. Therm. Sci.*, 72 (2014), 1–17.
2. V. Bianco, O. Manca, S. Nardini, and K. Vafai, *Heat Transfer Enhancement with Nanofluids*, CRC Press, 2015.
3. C. Pagura, S. Barison, C. Mortalo, N. Comisso, and M. Schiavon, Large scale and low cost production of pristine and oxidized single wall carbon nanohorns as material for hydrogen storage, *Nanosci. Nanotechnol. Letter*, vol. 4, 2(2012), 160–164.

NANOPARTICULATE DEPOSITION DURING CU-WATER NANOFLUID POOL BOILING ON ROUGHENED COPPER SURFACES

S. Mancin^{1*}, L. Doretto², T. P. Allred³ and J. A. Weibel³

¹Dept. of Management and Engineering, University of Padova, Str.lla S. Nicola 3, 36100, Vicenza, Italy

²Dept. of Civil, Architectural and Environmental Engineering, University of Padova, Via Venezia 1, 35131, Padova, Italy

³School of Mechanical Engineering, Purdue University, 585 Purdue Mall, 47907-2088, West Lafayette, IN, USA

*Corresponding author: simone.mancin@unipd.it

Keywords: Pool Boiling, Nanoparticulate Deposition, Wettability, Heat Transfer

Introduction: Boiling is widely relied upon in many different engineering systems: *e.g.*, chemical and nuclear reactors, refrigerating and air conditioning equipment, and thermal management of electronic devices. These applications have a shared constraint on the maximum heat flux that can be rejected by the cooling systems to ensure safe, reliable, and efficient operation.

The characterization of pool boiling has been a topic of worldwide research since Nukiyama [1] conducted experiments to measure a ‘boiling curve’ of the heat rejected from a surface submerged in stagnant liquid as a function of its temperature. It is well known that various surface treatment approaches can effectively enhance boiling heat transfer. In particular, microparticle coatings have been experimentally demonstrated to have promising capabilities for the enhancement of nucleate boiling heat transfer coefficients and critical heat flux (CHF) [2-3].

Recent work has led to new concepts for surface modification at the nanoscale. Nanostructured materials (*e.g.*, nanowire coatings, nanoporous layers, carbon nanotube arrays, etc.) have been also shown to enhance nucleate boiling (NB) and critical heat flux (CHF) [4-6]. A comprehensive review can be found in Ref. [7].

An alternative strategy to enhance boiling heat transfer is by seeding the fluid with a small concentration of nanoscale particles to produce a nanofluid. The boiling heat transfer behaviour of nanofluids has been extensively studied by many researchers who have observed some significant, though scattered, enhancements of the pool boiling CHF between 10% and 400% [8-12]. There are also contrasting reports of significant deterioration in boiling performance [13-16]. Results in the literature are inconsistent even for the same nanoparticle size/type under similar experimental conditions.

There are a few parameters that have been postulated to affect boiling heat transfer with nanofluids, which include morphological and thermophysical properties of nanoparticles and nanofluids, the long-term stability of the nanofluid suspension, the presence of surfactants and

ions, and the deposition and interaction of nanoparticles with the heating surface. As boiling heat transfer is very sensitive to surface topology and wettability, any change in the surface could alter the boiling behaviour. There is some general agreement on the fact that the enhancement or the deterioration observed during nanofluid boiling can be attributed to modification of the surface via nanoparticle deposition [17].

The present research activity aims to investigate nanofluid pool boiling to produce nanoparticulate-coated surfaces that can enhance the nucleated boiling heat transfer and critical heat flux. This paper presents preliminary nanoparticulate deposition results obtained during Cu-water (1.5 wt%) nanofluid pool boiling on a roughened copper surface.

The Cu-water nanofluid was obtained by seeding 25 nm copper nanoparticles into distilled pure water. Specifically, 25 g of copper nanoparticles were dispersed in 1.5 liters of distilled water, obtaining a 1.6 wt% Cu-water nanofluid, which was then stirred for 24 hr and sonicated for 6 hr to ensure uniform dispersion.

Discussion and Results: Tests are performed in experimental setups designed and built to study pool boiling of both pure water and nanofluids on smooth or enhanced surfaces. In order to avoid any contamination of the components by the nanoparticles contained in the nanofluid, two identical setups are used, one for the pure fluid tests and one for the nanofluid tests.

The test sample block is designed to have a characteristic heater size equal to the Rayleigh-Taylor wavelength, being 27.2 mm in the case of water at saturation condition at ambient pressure. Prior to each test, the test block is sealed into a polyether ether ketone (PEEK) (thermal conductivity, $\lambda=0.28 \text{ W m}^{-1} \text{ K}^{-1}$) base that exposes its top surface (smooth or enhanced) to the working fluid (water or nanofluid). The sample is then affixed into a pool boiling test apparatus that heats the surface in a controlled manner until CHF is reached.

In order to rigorously study the nanoparticulate deposition during nanofluid boiling, two copper samples were identically laser-etched to obtain a similar surface topography with uniform roughness. A microscope image and scanning electron microscope (SEM) image of one sample are reported in Figure 1; a profilometer analysis revealed that the values of the roughness, R_a were $359 \pm 42 \text{ nm}$ and $389 \pm 41 \text{ nm}$ for Sample A and Sample B, respectively. Furthermore, the static contact angle was measured on both samples and it was found to be $63.2^\circ \pm 3.3^\circ$ and $73.4^\circ \pm 3.7^\circ$ for Sample A and Sample B, respectively.

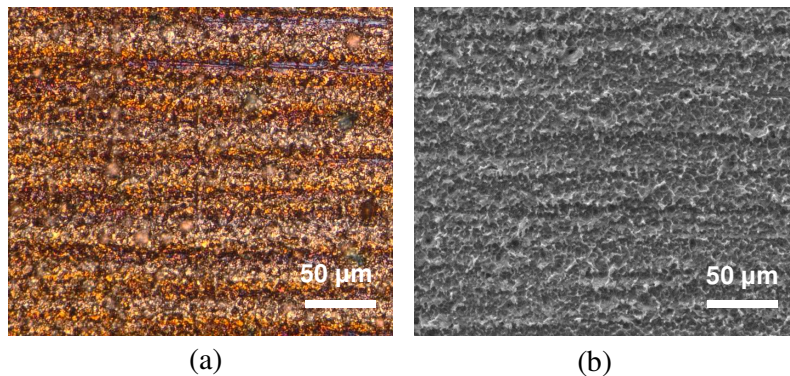


Figure 1: (a) Microscope image and (b) SEM image of the sample after laser-roughening.

A benchmark reference boiling curve up to CHF was obtained for Sample A using pure water as the working fluid. Sample B was boiled in the Cu-water (1.6 %wt) nanofluid; the heat flux was increased continuously up to the CHF measured for Sample A, and then the sample was cooled down.

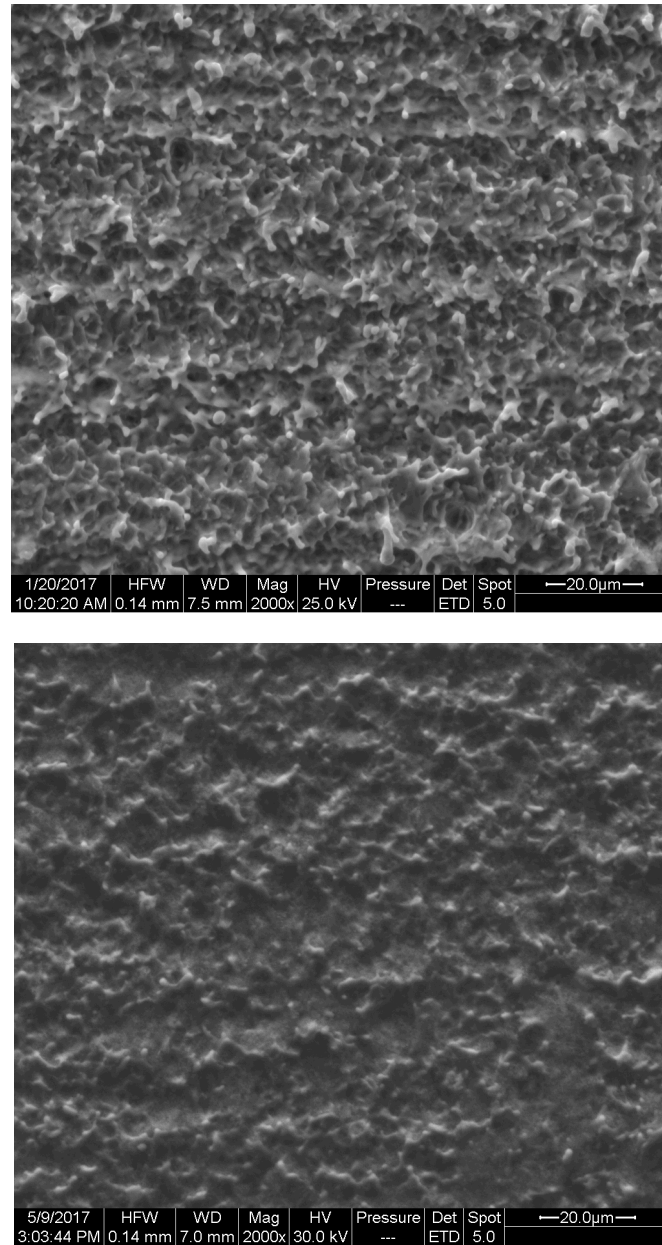


Figure 2: Uncoated (TOP) and coated (BOTTOM) surface of Sample B.

Figure 2 compares two SEM images taken before and after the nanofluid boiling on Sample B; a clear thin layer of nanoparticulate can be observed on the surface due to the deposition process occurred during the boiling process. The wettability of the surface remarkably changed; in fact, the contact angle varied from $73.4^\circ \pm 3.7^\circ$ to $134.0^\circ \pm 3.4^\circ$.

As future work, the particulate deposition on the surface of Sample B, post nanofluid boiling, will be interrogated and evaluated as a permanent coating for nucleate boiling heat transfer and critical heat flux enhancement.

Conclusions: This work represents one of the first to investigate nanoparticulate deposition on a rough surface during nanofluid pool boiling. The preliminary results show that a thin layer of nanoparticles was deposited during the Cu-Water nanofluid pool boiling, which drastically modified the surface wettability and the pool boiling characteristics of the surface.

References:

1. S. Nukiyama, *J. of the Japan Society of Mech. Eng.*, 37 (206) (1934) 367-374
2. G.S. Hwang and M. Kaviany, *Int. J. Heat Mass Transf.* 49 (2006) 844-849
3. J.H. Kim, K.N. Rainey, S.M. You and J.Y. Pak, *J. Heat Transf.* 124 (2002) 500-506
4. Y.W. Lu and S. Kandlikar, *Heat Transf. Eng.* 32 (10) (2011) 827-842
5. S. Ujereh, T. Fisher and I. Mudawar, *Int. J. Heat Mass Transf.* 50 (2007) 4023-4038
6. S. Li, R. Furberg, M.S. Toprak, B. Palm and M. Muhammed, *Adv. Funct. Mater.* 18 (2008) 2215-2220
7. M.S. El-Genk and A.F. Ali, *Int. J. Multiphase Flow* 36 (2010) 780-792
8. M. Kedzierski, *J. Heat Transf.* 131 (2009) 043205
9. K-J. Park and D. Jung, *Int. J. Heat Mass Transf.* 50 (2007) 4499-4502
10. Z. Liu, J. Xiong and R. Bao, *Int. J. Multiphase Flow* 33 (2007) 1284-1295
11. K-J. Park, D. Jung and S.E. Shim, *Int. J. Multiphase Flow* 35 (2009) 525-534
12. R. Kathiravan, R. Kumar, A. Gupta, and R. Chandra, *J. Heat Transf.* 131 (2009) 081902
13. V. Trisaksri and S. Wongwises, *Int. J. Heat Mass Transf.* 52 (2009) 1582-1588
14. H.D. Kim and M.H. Kim, *App. Phys. Lett.* 91 (2007) 014104
15. I.C. Bang and S.H. Chan, *Int. J. Heat Mass Transf.* 48 (2005) 2407-2419
16. S.K. Das, N. Putra, W. Roetzel, *Int. J. Heat Mass Transf.* 46 (2003) 851-862
17. D. Wen, *Applied Therm. Eng.* 41 (2012) 2-9

Abstracts

SESSION 6A: OPTICAL PROPERTIES AND OTHERS

PARAFFIN-BASED NANO-ENCAPSULATED PCM PREPARED FROM SOLVENT-ASSISTED EMULSIONS IN WATER

F. Agresti¹, S. Barison^{1*}, L. Fedele², S. Rossi², S. Mancin³

¹CNR – Institute of Condensed Matter Chemistry and Technologies for Energy, Corso Stati Uniti 4, 35127 Padova, Italy

²CNR – Institute of Construction Technologies, Corso Stati Uniti 4, 35127 Padova, Italy

³University of Padova, Department of Management and Engineering, Str.lla S. Nicola 3, Vicenza I-36100, Italy

*Corresponding author:: simona.barison@cnr.it

Keywords: Nano-encapsulated PCM, Emulsion, Paraffin

Introduction: Phase Change Materials (PCM) like paraffin waxes have attracted much attention due to the possibility of exploiting their latent heat of fusion or solidification for the purpose of heat storage during heating or cooling, in addition to their chemical stability and tuneable melting at moderate temperatures [1]. Anyway, due to some drawbacks as the low thermal conductivity and thermal hysteresis of PCM, the scientific community has been pushed to study more complex systems based on paraffin emulsions in water. Emulsions or nano-encapsulated PCM offer the advantage of higher heat transfer due to the presence of water phase and higher surface area of PCM phases. Applications include solar thermal storage [2], waste heat recovery, intelligent building, thermal regulating fabric, etc. [3]. The main problems related to these systems are the colloidal instability of emulsions that can lead to particles settling, creaming or flocculation, and the effect of supercooling that often arises for nano-sized PCM.

In this work, nano-emulsions of paraffin waxes in water have been produced by a solvent-assisted route. Concentrations as high as 10 wt% have been obtained starting from two commercial paraffin waxes, with nominal melting temperatures of 55 °C and 70 °C respectively.

Discussion and Results:

In the synthesis of a 2 wt% emulsion of paraffin melting at 55 °C (RT55, provided by Rubitherm Technologies GmbH, phase change temperature: 55 °C, latent heat 170 J/g), 1 g of a 10 wt% solution in hexane of paraffin wax RT55 and 5 g of a 0.25 wt% solution of sodium dodecyl sulphate (SDS) in water were prepared. The two solutions were placed into the same sonication bath at 50 °C for 30 min in order to achieve stable solutions. The solutions were joined and sonicated for further 30 min to obtain a stable emulsion. The emulsion were then heated at 100 °C for 2 h to remove the hexane and to obtain bare nano-encapsulated paraffin. The evaporated water was replenished continuously during the heating and the proper amount was added finally to obtain the right concentration. A 4 wt% emulsion was produced with the same procedure, using a 20 wt%

solution of paraffin in hexane and a 0.5 wt% solution of sodium dodecyl sulphate (SDS) in water. A 10 wt% emulsion was produced as for the 4 wt% emulsion, letting water evaporate during heating until the right concentration was achieved. Analogous suspensions based on a paraffin melting at 70 °C (RT70HC, provided by Rubitherm Technologies GmbH, phase change temperature: 70 °C, latent heat 260 J/g) were produced accordingly.

The hydrodynamic size of paraffin nanocapsules and the stability of suspensions were evaluated by Dynamic Light Scattering (DLS) and ζ -potential measurements.

Table 1. Average hydrodynamic size and ζ -potential of suspensions

Sample	average size (nm)	ζ -potential (mV)
RT55 2 wt%	91	--
RT55 4 wt%	83	-74
RT55 10 wt%	177	-68
RT70HC 2 wt%	65	-67
RT70HC 4 wt%	110	-57
RT70HC 10 wt%	223	-46

From table 1 it is possible to note that very stable nano-suspensions have been obtained, especially with the lowest concentrations. Anyway, even though with both the paraffin the size is almost double with respect to the 2 wt% and the 4 wt% samples, quite high ζ -potential value are retained, making the suspensions very stable even at 10 wt%.

Thermal properties as the thermal diffusivity of suspensions, temperature and latent heat of melting and solidification of nano-PCM are under investigation. Figure 1 shows preliminary data on calorimetric measurements of specific heat for the RT55 2 wt% sample.

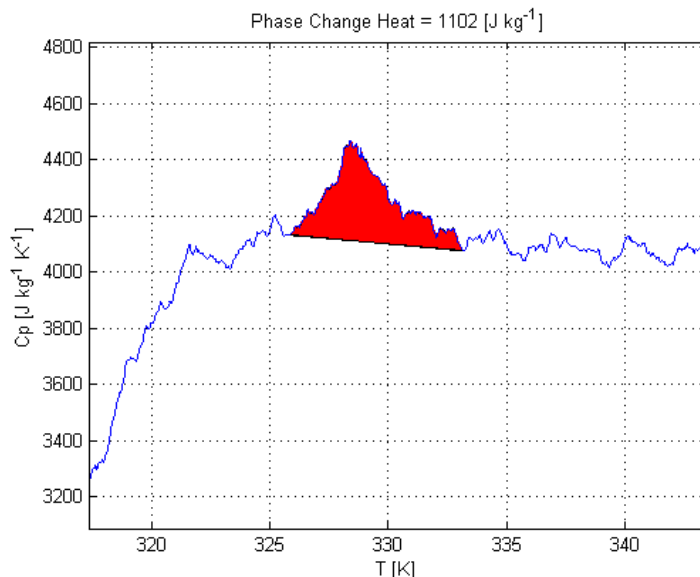


Figure 1. Specific heat and phase change heat measurement for sample RT55 2wt%

The peak corresponding to the fusion latent heat has a maximum at 55 °C, which is the same fusion temperature of the bulk paraffin sample. The estimate latent heat of fusion is 1.1 J/g, considerably lower with respect the theoretical expected value of 3.4 J/g. Further experiments are under way to complete the thermal characterizations of all samples and to verify the exactness of this value.

Conclusions: Surfactant nano-encapsulated PCMs based on commercial paraffins have been produced by using a solvent assisted emulsification. The nanofluids have been produced at concentrations as high as 10 wt% in water, showing excellent colloidal stability. Thermo-physical properties are under investigation to provide a complete characterization of samples and discuss potential applications.

References

1. M.M. Farid, A.M. Khudhair, S.A.K. Razack, S. Al-Hallaj, A review on phase change energy storage: materials and applications, *Energy Convers Manag* 45 (2014) 1597–1615.
2. X. Zhang, Wu J, J. Niu, PCM-in-water emulsion for solar thermal applications: The effects of emulsifiers and emulsification conditions on thermal performance, stability and rheology characteristics, *Sol Energy Mater Sol Cells* 147 (2016) 211–224.
3. C. Liu, Z. Rao, J. Zhao, et al, Review on nanoencapsulated phase change materials: Preparation, characterization and heat transfer enhancement, *Nano Energy* 13 (2015) 814–826.

NONLINEAR OPTICAL PROPERTIES OF CARBON NANOHORN-BASED AQUEOUS NANOFUIDS

E. Sani^{1*}, N. Papi¹, L. Mercatelli¹, S. Barison², F. Agresti², C. Pagura³, S. Bobbo⁴ and S. Rossi⁴

¹CNR-INO National Institute of Optics, Largo E. Fermi, 6, I-50125 Firenze, Italy

²CNR-ICMATE Institute of Condensed Matter Chemistry and Technologies for Energy, Corso Stati Uniti, 4, I-35127 Padova, Italy

³CNR-IFN Istituto di Fotonica e Nanotecnologie, Via Trasea, 7, I-35131 Padova, Italy

⁴CNR-ITC Istituto di Tecnologie della Costruzione, Corso Stati Uniti, 4, I-35127 Padova, Italy

Corresponding author: elisa.sani@ino.it

Keywords: Nanofluids, Carbon nanohorns, optical limiting, nonlinear optical properties

Introduction: The efficient manipulation of optical beams is required for different application fields (e.g. optical communications, optical computing, security etc). The light intensity is one of the most important parameters that needs to be predictably controlled. The many available techniques for manipulating light intensity can be basically divided in two families: dynamic and passive methods. Dynamic control needs an active feedback system and can be roughly schematized by three modules: a sensor, a processor and an actuator. These three modules must communicate each other, arising in higher complexity and slower speeds of the entire system. On the other hand, a passive control is considerably simpler, as it can be obtained using a single component with proper characteristics and able to work, at the same time, as sensor, processor and actuator. An example of materials able to do that are nonlinear optical materials, that, for this reason, can be referred as *intelligent* or *smart materials*. Since the optical control function is part of the physical characteristics of the material, the speed is not limited by communication between individual modules and the device can potentially be very simple and fast. An important kind of passive device to control the amplitude of an optical signal are optical limiters. They are characterized by a linear transmittance at weak input intensities and a low transmittance at high intensities. Such devices are important for eye and optical sensors protection, with application in different fields e.g. in military and security. Generally, an ideal optical limiting material should possess three main features: a low fluence threshold for the limiting effect, an instantaneous response to any laser pulse duration and an effective operation over a wide wavelength range. Different kinds of carbon-based nanomaterials, such as carbon nanotubes fullerenes and carbon-black nanoparticles in different base fluids [1-4] have been shown to possess favourable optical limiting characteristics. Single-wall carbon nanohorns (SWCNHs) [5] consist of single layers of a graphene sheet wrapped into an irregular tubule with a variable diameter of 2-5 nm and a length of 30-50 nm. The tips of the nanohorns are

cone-shaped with an average angle of about 20° [5-8], corresponding to five pentagonal carbon rings at the tip of the tubule. The SWCNHs typically assemble to form roughly spherical aggregates with diameters of about 100-120 nm [8]. They exhibit both large surface area and large number of cavities [9] and therefore appear promising for a variety of applications, such as electrode material in fuel cells [10], gas storage material [11] and carrier vehicles for delivering therapeutic drugs, genes or proteins [12].

When the differences between SWCNHs and the better known carbon nanotubes are concerned, the minimum van der Waals interactions between the superstructures of SWCNH aggregates gives rise to a better dispersion of SWCNHs in liquid media [13] and a much longer time stability of their suspensions. Moreover, a very important property in view of their practical use with respect to carbon nanotubes arises from the metal-free structure of nanohorns that makes their cytotoxicity negligible, as it has been widely confirmed by experiments on mice and rats [14]. This makes SWCNHs very appealing for applications requiring nanoparticle handling and in all cases where even accidental leakages into the environment are possible. Their linear optical properties have been extensively studied in last years [15-18] and SWCNH suspensions in liquids have been found promising for solar energy and biomedical applications [15-18]. Very recently, optical limiting at 1064 and 532 nm has been demonstrated on SWCNH suspension in acetone [19]. However, acetone is a highly flammable liquid and a pollutant. With the aim to promote the use of environmental-friendly materials, the present work is focused on the investigation of optical limiting in SWCNH suspensions in water at 355, 532 and 1064 nm.

Discussion and Results: To prepare sample SC8, 250 ml of a solution containing 0.005 g L^{-1} of Sodium Dodecyl Sulfate (SDS) (99%, provided by Sigma-Aldrich) in water was prepared and 0.05 g L^{-1} of SWCNHs (provided by Carbonium S.r.l.) were pre-dispersed in the solution by sonication with a VCX 130, Sonics & Materials ultrasonic processor operated at 20 kHz and 65 W for 10 min. The final optimized dispersion was obtained by high-pressure homogenization using a Panda, GEA Niro Soavi, operated at 1000 bar for 45 min. The obtained sample was further diluted with distilled water to obtain lower concentrations. Particle size and zeta potential were measured using a Zetasizer Nano ZS (Malvern) based on dynamic light scattering. The light source for the optical limiting experiment is a pulsed nanosecond Nd:YAG laser (Quantel Q-smart 850) emitting 6 ns pulses on the fundamental, second and third harmonic (1064, 532 and 355 nm wavelength). The three laser emission wavelengths are spatially separated by proper optical elements and focused on the sample by a lens of 300 mm focal length. The sample is held in a quartz cuvette with 10 mm optical path, put in a defocused position to avoid cuvette damage. The beam exiting the sample is collected by a couple of lenses of focal lengths 40 and 100 mm and focused on a pyroelectric detector (Ophir PE25C). The energy incident on the cuvette is varied by means of proper polarizer beam splitters and measured using a pyroelectric detector (Ophir PE50BE). For diagnostic purposes, linear spectral transmittance has been measured as well, by means of a double-beam UV-VIS-NIR spectrophotometer (PerkinElmer Lambda900). Due to the spectral characteristics of SWCNH extinction spectra, the linear extinction coefficient decreases for increasing laser wavelengths. At the three investigated laser wavelengths, we typically observed that the output energy was

linearly depending on the input energy until this reaches a threshold value. For input energies exceeding this threshold and within a range depending wavelength, the output energy is reduced with respect to that expected on the basis of the linear dependence. If the energy is further increased above this range, sample damage occurs, with nanoparticle clustering and sedimentation. Figure 1 shows the curves of normalized transmittance (E_{out}/E_{in}) as a function of the input energy. The choice of showing two plots for each figure (linear/linear the upper ones and semilogarithmic the lower ones) is for better visualizing slope and threshold values, respectively, of optical limiting. All the curves are characterized by three regimes: the linear region at lower incident energies ($E_{out}/E_{in} \approx 1$), the optical limiting region at intermediate energies (E_{out}/E_{in} decreasing with increasing E_{in} values) and the optical damage region (E_{out}/E_{in} increasing again with increasing E_{in}). From Fig. 1a we can see that the sample shows optical limiting at all the three investigated wavelengths. This is a very important result, as it demonstrates that SWCNH aqueous suspensions are broadband optical limiters at least from ultraviolet (355 nm) to near infrared (1064 nm). The threshold energy value increases with the wavelength, because of the decreasing value of extinction coefficient from UV to IR. For the same reason, the slope of optical limiting curve decreases with increasing wavelength. For fixed input energy, sample damage occurs more easily if the incident wavelength is 1064 nm. Finally, if the dependence of optical limiting on the nanoparticle concentration is concerned (Figure 1-b), we can observe that increasing the nanoparticle concentration increases the threshold and decreases the slope of optical limiting.

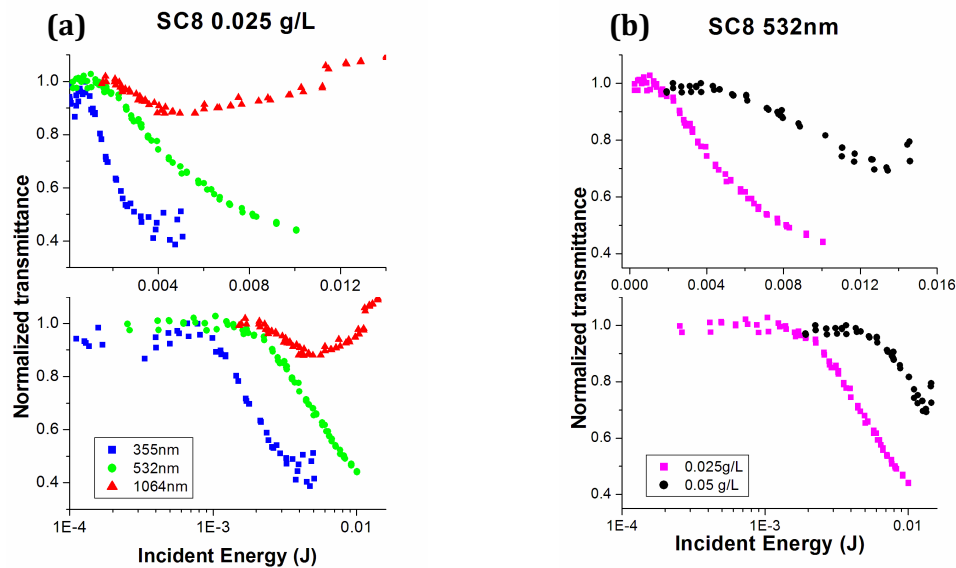


Figure 1: Normalized transmittance for a fixed SWCNH concentration as a function of the laser wavelength (a) and for fixed laser wavelength as a function of the SWCNH concentration (b).

Conclusions: Stable water suspensions of single-wall carbon nanohorns have been prepared and characterized with focus on nonlinear transmittance. Optical limiting has been demonstrated at 355, 532 and 1064 nm in the nanosecond regime.

References:

1. X. Sun, R.Q. Yu, G.Q. Xu, T.S.A. Hor, and W. Ji, Broadband optical limiting with multiwalled carbon nanotubes. *Appl. Phys. Lett.* 73, 3632 (1998).
2. J.E. Riggs, D.B. Walker, D.L. Carroll, and Y.P. Sun, Optical limiting properties of suspended and solubilized carbon nanotubes. *J. Phys. Chem. B* 104, 7071 (2000).
3. K.M. Nashold and D.P. Walter, Investigations of optical limiting mechanisms in carbon particles suspensions and fullerene solutions, *J. Opt. Soc. Am. B* 12, 1228 (1995).
4. D. Vincent, S. Petit, and S.L. Chin: Optical limiting studies in a carbon-black suspension for subnanosecond and subpicosecond laser. *Appl. Opt.* 41, 2944 (2002).
5. Iijima S, Yudasaka M, Yamada R, Bandow S, Suenaga K, Kokai F et al. Nano-aggregates of single-walled graphitic carbon nano-horns. *Chem. Phys. Letters* 1999; 309 (3-4): 165-170.
6. Krungleviciute V, Migone AD, Pepka M. Characterization of single-walled carbon nanohorns using neon adsorption isotherms. *Carbon* 2009; 47 (3): 769-774.
7. Murata K, Kaneko K, Kokai F, Takahashi K, Yudasaka M, Iijima S. Pore structure of single-wall carbon nanohorn aggregates. *Chem. Phys. Letters* 2000; 331 (1): 14-20.
8. Yudasaka M, Iijima S, Crespi VH. Single-wall carbon nanohorns and nanocones. In: Jorio A, Dresselhaus G, Dresselhaus MS editors. *Carbon nanotubes, Topics in Applied Physics* vol. 111, Berlin/Heidelberg; Springer; 2008; p. 605-629.
9. Fan X, Tan J, Zhang G, Zhang F. Isolation of carbon nanohorn assemblies and their potential for intracellular delivery. *Nanotechnology* 2007; 18 (19): 195103.
10. Yoshitake YT, Shimakawa Y, Kuroshima S, Kimura H, Ichihashi T, Kubo Y et al. Preparation of fine platinum catalyst supported on single-wall carbon nanohorns for fuel cell application. *Physica B* 2002; 323 (1-4): 124-126.
11. Bekyarova E, Murata K, Yudasaka M, Kasuya D, Iijima S, Tanaka H et al. Single-wall nanostructured carbon for methane storage. *J. Phys. Chem. B* 2003; 107 (20): 4682-4684.
12. Ajima K, Yudasaka M, Murakami T, Maigne A, Shiba K, Iijima S. Carbon nanohorns as anticancer drug carriers. *Mol. Pharm.* 2005; 2 (6): 475-480.
13. Pagona G, Sandanayaka ASD, Araki Y, Fan J, Tagmatarchis N, Yudasaka M et al. Electronic Interplay on Illuminated Aqueous Carbon Nanohorn-Porphyrin Ensembles. *J. Phys. Chem. B* 2006; 110 (42): 20729-20732.
14. Lynch RM, Voy BH, Glass DF, Mahurin SM, Zhao B, Hu H et al. Assessing the pulmonary toxicity of single-walled carbon nanohorns. *Nanotoxicology* 2007; 1 (2): 157-166.

15. E. Sani, S. Barison, C. Pagura, L. Mercatelli, P. Sansoni, D. Fontani, D. Jafrancesco and F. Francini, “Carbon nanohorns-based nanofluids as direct sunlight absorbers”, *Optics Express*, vol. 18, No. 5, pp. 5179-5187 (2010)
16. L. Mercatelli, E. Sani, G. Zaccanti, F. Martelli, P. Di Ninni, S. Barison, C. Pagura, F. Agresti, D. Jafrancesco “Absorption and scattering properties of carbon nanohorn-based nanofluids for direct sunlight absorbers”, *Nanoscale Research Letters*, vol. 6, p. 282 (9pages), (2011)
17. E. Sani, L. Mercatelli, S. Barison, C. Pagura, F. Agresti, L. Colla, P. Sansoni “Potential of carbon nanohorn-based suspensions for solar thermal collectors”, *Solar Energy Materials and Solar Cells*, vol. 95, pp. 2994-3000 (2011)
18. L. Mercatelli, E. Sani, A. Giannini, P. Di Ninni, F. Martelli, G. Zaccanti “Carbon nanohorn-based nanofluids: characterization of the spectral scattering albedo”, *Nanoscale Research Letters*, vol. 7, 96 (2012)
19. S. Dengler, et al, Nonlinear optical effects in colloidal carbon nanohorns—a new optical limiting material, *J. Physics D: Applied Physics* 49 (2016) 365501.

EFFECT OF NANOPARTICLES ON FLUID TRANSPORT IN ULTRACONFINED CAPILLARY

X. Wang, S. Xiao, Z. Zhang and J. He*

NTNU Nanomechanical Lab, Department of Structural Engineering, Norwegian University of Science and Technology (NTNU), 7491, Trondheim, Norway

*Corresponding author: jianying.he@ntnu.no

Keywords: Nanoparticles, Imbibition, Transport, Capillary, Molecular dynamic simulation

Introduction: Nanotechnology plays an important role in many industries and across the healthcare sector. The capabilities in nanotechnology are rapidly expanding as new synthesis techniques and new characterization methods evolve for nanoscale structures, and as new numerical simulations are developed to describe their transport in complex systems. One of the emerging interests is the new generation fluids based on nanofluids and nanoparticles (NPs) transport in confined channel [1]. Nanofluids are a class of fluids engineered by dispersing NPs in base fluids, which are first known because of its thermal properties [2]. Recently, a renewed interest arises in the application of nanofluids for enhanced oil recovery, such as changing the properties of the fluid, wettability alternation of rocks, advanced drag reduction, strengthening sand consolidation, reducing the interfacial tension and increasing the mobility of the capillary-trapped oil [3,4]. In this study, we focus on the fundamental understanding of the role of NPs on the spontaneous water imbibition into an ultraconfined capillary by molecular dynamic (MD) simulation using LAMMPS code.

Results and Discussion: The simulation system is shown in Figure 1, containing a water-based fluid with dispersed spherical NPs and a capillary. The solid capillary used in the system is face-centered cubic (fcc) crystal lattice structure of silicon. The fluid consists of 10000 water molecules and 16 nanoparticles with a diameter of 7.0 Å, so the volume fraction of NPs is about 5%. The standard pairwise 12-6 Lennard-Jones (L-J) potential is used to describe the van der Waals interaction between water and NPs, water and capillary, and NPs and capillary. In order to ensure the spontaneous imbibition, the characteristic energy between capillary and water is chose to be 0.35, which means a hydrophilic capillary. By tuning characteristic energy between NPs and water, different wettability of NPs can be obtained. Hydrophobic, mixed-wet, and hydrophilic NPs are applied in the water imbibition process to explore the migration mechanism of nanofluids into porous media.

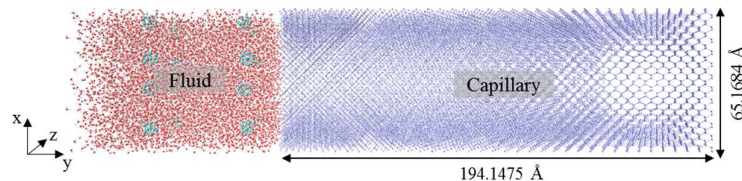


Figure 1. The simulation system contains a water-based nanofluid (red) laden with well-distributed sphere NPs (light green) and a capillary (blue).

The snapshots of imbibition process of nanofluids into reservoir are summarized in Figure 2, which reveal the influence of wetting properties of NPs on imbibition behaviour. It can be seen that water molecules can spontaneously diffuse into the vacancy of the capillary in the referenced NP-free system. Once NPs are added into fluids, the transportation of fluids into capillary is hindered. The displacement of nanofluids into capillary increases with NPs characteristic energy increasing from 0.1 (hydrophobic) to 0.5 (hydrophilic) kcal/mol. The results indicate that the addition of NPs will retard the transportation of fluids into capillary.

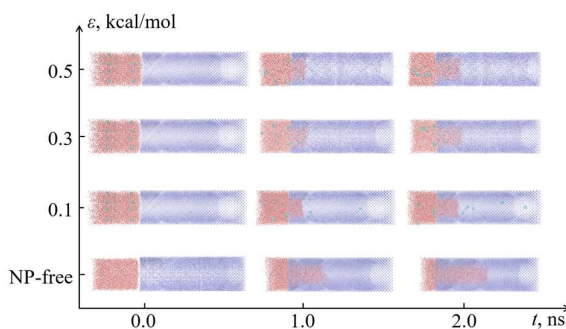


Figure 2. The snapshots of nanofluids with different type of NPs as time evolutions. Here x -axis shows the simulation time and y -axis the wettability of NPs changing via characteristic energy.

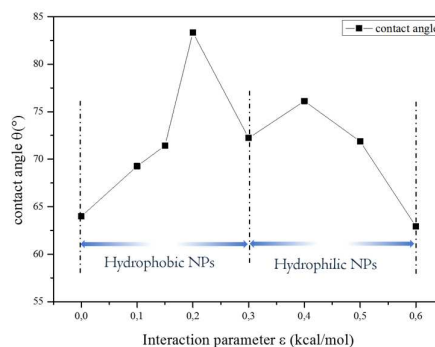


Figure 3. The contact angle varying with characteristic energy of NPs.

The obtained contact angle as a function of characteristic energy of NPs is shown in Figure 3. The equilibrium contact angle for NP-free is about 64.60° , showing the water-wet property of the capillary. When NPs are added into fluid, all the equilibrium contact angles are found to be larger than that of NP-free system, which indicates that the addition of NPs alters the wettability of fluids in the solid capillary, and thus affects the imbibition of nanofluids. It is interesting to see that the contact angle θ increases rapidly when the NP changes from hydrophobic to mixed-wet, and then decreases when NP increases hydrophilicity.

Conclusions: Molecular dynamics simulation has been carried out to investigate spontaneous imbibition process of nanofluids into capillary influenced by the surface wettability of NPs. Ideal material model is adopted to tune the interactions between NPs, water and capillary. It is clear that adding NPs will influence the contact angle and hence alternate the wettability of nanofluids in the solid capillary. The displacement of the nanofluid is hindered compared with NP-free case, due to the confinement of nanochannels.

Acknowledgment: This work is financially supported by the Research Council of Norway via WINPA project No. 234626. The computational resources are provided by Norwegian Metacenter for Computational Science (NOTUR NN9110k and NN9391k).

References:

1. J.Y. Wu, J.Y. He, O. Torsæter and Z.L. Zhang, Effect of nanoparticles on oil-water flow in a confined nanochannels: a molecular dynamics study. SPE 156995, 2012.
2. S.U.S. Choi, and J.A. Eastman, Enhancing Thermal Conductivity of Fluids with Nanoparticles, in *The Proceedings of the 1995 ASME International Mechanical Engineering Congress and Exposition*. San Francisco, 1995, pp. 99–105.
3. Z. Hu , S.M. Azmi, G. Raza, P.W.J. Glover and D. Wen, Nanoparticle-Assisted Water-Flooding in Berea Sandstones, *Energy & Fuels* 30 (2016) 2791-2804.
4. X. Wang, S.B. Xiao, Z.L. Zhang and J.Y. He, Effect of Nanoparticles on Spontaneous Imbibition of Water into Ultraconfined Reservoir Capillary by Molecular Dynamics Simulation. *Energies*, 10 (2017) 506.

DIELECTRIC PROPERTIES OF GRAPHITE/DIAMONDS MIXTURE NANOPARTICLES SUSPENDED IN ETHYLENE GLYCOL

J. Fal* and G. Żyła

Department of Physics and Medical Engineering, Rzeszow University of Technology,
Rzeszow, Poland

*Corresponding author: jacekfal@prz.edu.pl

Keywords: Nanofluid, Ethylene glycol, Dielectric properties, Nanoparticles, Graphite/diamond

Introduction: Since S. Choi [1] introduced nanofluids as suspension of solid particles with at least one nanometric dimension in base fluid and their unusual thermal properties, the popularity of nanofluids still growth. Nanofluids exhibit many potential applications as presented in Ref. [2]. The huge interest of this type of fluids is due to their unique thermophysical properties, which result from a large ratio of specific surface area to nanoparticle volume. The most often studied properties of nanofluids are thermal conductivity and rheological properties [3]. Less often investigated are optical [4] or electrical properties [5].

Among various types of nanofluids a quite popular are suspensions with carbon nanoparticles in various forms, such like nanodiamonds, graphite or carbon tubes. Sundar et al. [6] studied thermophysical properties of nanodiamonds particles suspended in water and they observed higher thermal conductivity than theoretical models predict for this type of fluid. Nanodiamonds suspended in deionized water was also studied by Yeganeh et al. [7]. They tested fluids with volume fractions from 0.8% to 3% and observed that maximum enhancement was achieved for a 3% volume fraction at 50°C and it was 9.8%. Branson et al. [8] carried out investigation on two types of nanofluids with nanodiamonds inclusion in poly(glycidol) polymer brush:EG and oleic acid:mineral oil and they revealed that thermal conductivity enhancement for this type of fluids is linear and it is much higher than Maxwell model predict. Sundar et al. [9] conducted studies on electrical conductivity for nanodiamond-nickel nanocomposite suspended in water and ethylene glycol with 0.02%, 0.05% and 0.1% volume concentration. Based on experimental results, they concluded that nanosuspensions based on water have higher electrical conductivity enhancement than ethylene glycol based. The complex investigation of influence of ash content on thermophysical properties of ethylene glycol based graphite/diamonds mixture nanofluids was presented in Ref. [10]. It was observed that ash content effect in rheological properties and electrical conductivity but for the thermal conductivity ash load was not so relevant.

Dielectric properties of nanofluids are even less often investigated by researchers than electrical conductivity. Tagmouti et al. [11] investigated dielectric properties of nanofluids containing multiwalled carbon nanotubes suspended in transformer oil at constant temperature (300K) and frequency range 100Hz – 1MHz for various fractions. They concluded that changes in volume

fraction of nanotubes cause change in relaxation time. They also observed increase in conductivity with increasing volume fraction on nanotubes. Subramaniyan et al. [12] studied dielectric constant for TiO₂ nanoparticles dispersed in three different base fluids at various temperatures. Also few other researchers studied dielectric properties of various nanofluids [13,14].

This paper is a continuation of our research presented in Ref. [10], and contain results of experimental studies of complex permittivity and ac conductivity of suspensions of two types of graphite/diamonds mixture with various ash content and volume fraction in ethylene glycol. Measurements were performed using broadband dielectric spectroscopy device Concept 80 System (NOVOCONTROL Technologies GmbH & Co. KG, Montabaur, Germany). Each sample was tested in controlled temperature range from 293.15K to 330.15K with 5K step. The accuracy of temperature stabilization was 0.5K, and frequency was changed from 10MHz to 0.02Hz in 49 steps.

Discussion and Results: Dielectric properties of ethylene glycol with suspended two types of graphite/diamonds nanoparticles with different ash content and specific surface area for five volume fraction (0.004, 0.009, 0.013, 0.018, 0.023) were studied. Findings indicate that increase in volume concentration of nanoparticles in ethylene glycol cause an increase in both complex permittivity and ac conductivity of nanosuspensions. Effect of volume fraction on real part of permittivity for both types of nanofluids was presented in Fig. 1. Also temperature effect was observed, but with much less impact on dielectric properties. Combined effect of volume fraction and temperature was also observed for SC-TiO₂-EG [15] and BN-EG [16] nanofluids. The increase in values of dielectric properties was observed for both types of graphite/diamonds mixtures, with the difference that samples with higher purity of mixture and higher specific surface area have higher enhancement in permittivity and conductivity. Additionally it was observed that experimental results are in agreement with universal power law.

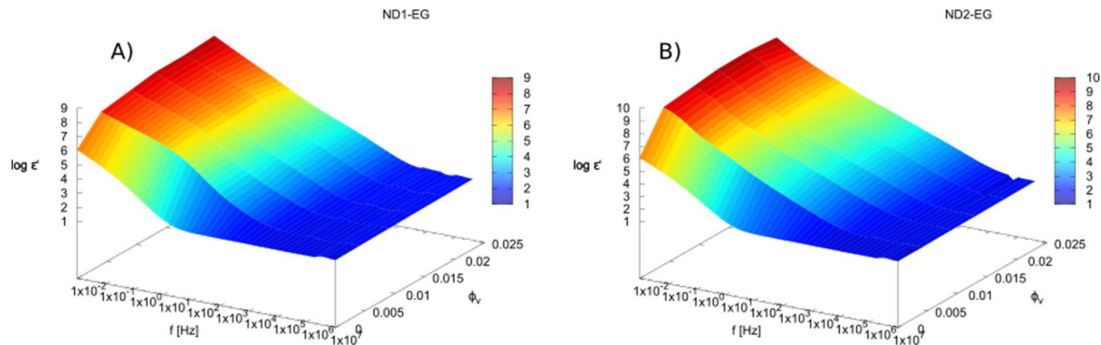


Figure 1. Real part of permittivity as function of frequency and volume fraction at 398.15K: A) ND1-EG, B) ND2-EG.

Conclusions: The paper presents experimental results of investigation of dielectric properties of nanofluids containing two different types graphite/diamond mixtures with various ash content. The findings indicate that load of nanoparticles in ethylene glycol has a strong effect for both complex permittivity and ac conductivity, also purity of graphite/diamonds mixture is relevant.

References:

1. S.U.S. Choi, *Enhancing thermal conductivity of fluids with nanoparticles*, Developments Applications of Non-Newtonian Flows, ASME, New York, 1995.
2. D.K. Devendiran, V.A. Amirtham, A review on preparation, characterization, properties and applications of nanofluids, *Renewable and Sustainable Energy Review* 60 (2016) 21-40.
3. A. Amiri, M. Shanbedi, H. Dashti, Thermophysical and rheological properties of water-based graphene quantum dots nanofluids, *Journal of the Taiwan Institute of Chemical Engineers* 76 (2017) 132-140.
4. E. Sani, P. Di Ninni, L. Colla, S. Barison, F. Agresti, Optical properties of mixed nanofluids containing carbon nanohorns and silver nanoparticles for solar energy applications, *Journal of nanoscience and nanotechnology* 78 (2017) 452-465.
5. G. Żyła, J. Fal, Viscosity, thermal and electrical conductivity of silicon dioxide – ethylene glycol transparent nanofluids: an experimental studies, *Thermochimica Acta*, 650 (2017) 106–113.
6. L.S. Sundar, M.J. Hortiguela, M.K. Singh, A.C. Sousa Thermal conductivity and viscosity of water based nanodiamond (ND) nanofluids: An experimental study, *International Communications in Heat and Mass Transfer*, 76 (2016) 245–255.
7. M. Yeganeh, N. Shahtahmasebi, A. Kompany, E. Goharshadi, A. Youssefi, L. Šiller Volume fraction and temperature variations of the effective thermal conductivity of nanodiamond fluids in deionized water, *International Journal of Heat and Mass Transfer*, 53 (15) (2010) 3186–3192.
8. B.T. Branson, P.S. Beauchamp, J.C. Beam, C.M. Lukehart, J.L. Davidson Nanodiamond nanofluids for enhanced thermal conductivity, *Acs Nano*, 7 (4) (2013) 3183–3189.
9. L.S. Sundar, K. Shusmitha, M.K. Singh, A.C. Sousa Electrical conductivity enhancement of nanodiamond-nickel (ND-NI) nanocomposite based magnetic nanofluids, *International Communications in Heat and Mass Transfer*, 57 (2014), 1–7.
10. G. Żyła, J. Fal, P. Estellé, The influence of ash content on thermophysical properties of ethylene glycol based graphite/diamonds mixture nanofluids, *Diamond and Related Materials* 74 (2017) 81–89.
11. S. Tagmouti, S.E. Bouzit, L.C. Costa, M.P.F. Graca, A. Outzourhit Impedance spectroscopy of nanofluids based on Multiwall Carbon Nanotubes, *Spectroscopy Letters: An International Journal for Rapid Communication*, 48(10) (2015) 761-766.
12. A. Subramaniyana, L.P. Sukumarana, R. Ilangoanb Investigation of the dielectric properties of TiO₂ nanofluids, *Journal of Taibah University of Science*, 10(3) (2016) 403–406.
13. M. T. Imani, J. F. Miethe, P. Werle, N. C. Bigall, H. Borsi Engineering of Multifunctional Nanofluids for Insulation Systems of High Voltage Apparatus, *Conference on Electrical Insulation and Dielectric Phenomena (CEIDP)*, Toronto, Canada, October 16-19, 2016.

14. M. M. Emara, D-E. A. Monsour, A. M. Azmy Dielectric properties of aged mineral oil filled with TiO₂ nanoparticles, *4th International Conference on Electric Power and Energy Conversation System (EPECS)*, Sharjah, United Arab Emirates, November 24-26, 2015.
15. J. Fal, A. Barylyak, K. Besaha, Y. V. Bobitski, M. Cholewa, I. Zawlik, K. Szmuc, J. Cebulski, G. Żyła, Experimental Investigation of Electrical Conductivity and Permittivity of SC-TiO₂-EG Nanofluids, *Nanoscale Research Letters*, 11, 375 (2016).
16. J. Fal, M. Cholewa, M. Gizowska, A. Witek , G. Żyła, Dielectric properties of boron nitride-ethylene glycol (BN-EG) nanofluids, *Journal of Electronic Materials*, 46(2) (2017) 856–865.

LINEAR AND NONLINEAR OPTICAL PROPERTIES OF GRAPHITE/DIAMOND NANOSUSPENSIONS

E. Sani^{1*}, N. Papi¹, L. Mercatelli¹ and G. Żyła²

¹CNR-INO National Institute of Optics, Largo E. Fermi, 6, I-50125 Firenze, Italy

²Department of Physics and Medical Engineering, Rzeszow University of Technology, 35-905 Rzeszow, Poland

*Corresponding author: elisa.sani@ino.it

Keywords: Carbon, graphite, nanodiamond, nanofluids, optical properties, solar energy, optical limiting

Introduction: We prepared nanofluids composed by a mixture of graphite and nanodiamonds (ND) in ethylene glycol and we investigated the linear and nonlinear optical properties of the obtained suspensions, in the perspective to assess the potential of this new nanofluid for thermal solar energy and optical limiting, respectively. As for solar energy exploitation, it should be noticed that black fluids working both as volumetric light absorber and heat exchanger in low- and mid-temperature solar collectors can potentially simplify the system architecture and improve the performances. In 1975 was launched the first idea of a direct-absorption solar collector (DASC) using a black liquid [1]. However, the India ink-based fluid investigated in that work, being subject to thermal and light-induced degradation was not suitable and the idea was substantially abandoned for many years, until that the development of nanotechnology has allowed the production of new nanoparticle-loaded dark fluids with superior stability properties [2-8].

As for application of nonlinear optical properties, an efficient manipulation of optical beams is required in different fields like for instance optical communications, optical computing, security etc. Passive control systems, in which a single component works, at the same time, as sensor, processor and actuator, are usually preferred because they are simpler and faster. An optical limiter is a device to passively control light intensity. It is characterized by a linear response on radiation transmittance at weak input intensities, but by a low or very low transmittance under high input light intensities. Such devices are important for eye and optical sensors protection, with application in different fields e.g. in military and security.

Discussion and Results: Nanofluids has been prepared by dispersing commercially available (produced by PlasmaChem GmbH (Berlin, Germany)) nanopowders in ethylene glycol. Nanopowder was a mixture of graphite and nanodiamonds with ND phase over 26% as declared by manufacturer. Detailed informations on physical properties of used nanoparticles might be found in Ref. [9] and it is labeled there as NP1. Mentioned paper presents also SEM pictures, EDS spectra analysis and XRD diffractogram of nanoparticles.

First step of nanofluids preparation was measure the mass of nanoparticles on analytic balance WAS 220/X (Radwag, Radom, Poland). Then EG was added and sample was mixing for 30 minutes in Genius 3 Vortex (IKA, Staufen, Germany). After that ultrasound was used for 200 minutes in Emmi 60 HC (EMAG, Moerfelden-Walldorf, Germany), and it breaks agglomerates of nanoparticles.

Spectral optical transmittance in the linearity regime has been measured using a double-beam UV-VIS spectrophotometer (PerkinElmer Lambda900). The obtained extinction coefficient of nanofluids has allowed to assess good sunlight absorption characteristics even with very low nanoparticle concentrations 0.005% and 0.01% wt, with promising potential in DASC application. Figure 1 compares the transmittance spectra of nanodiamond suspensions and pure base fluid for 2 mm path length. Superimposed in Fig.1 we can also see the sunlight spectral irradiance. We can appreciate how nanodiamond addition considerably decrease the transmittance of the fluid with respect to the pure glycol, with a major effect on the spectral region where sunlight emission is higher. This result opens interesting perspectives for the use of these nanofluids as volumetric solar absorbers.

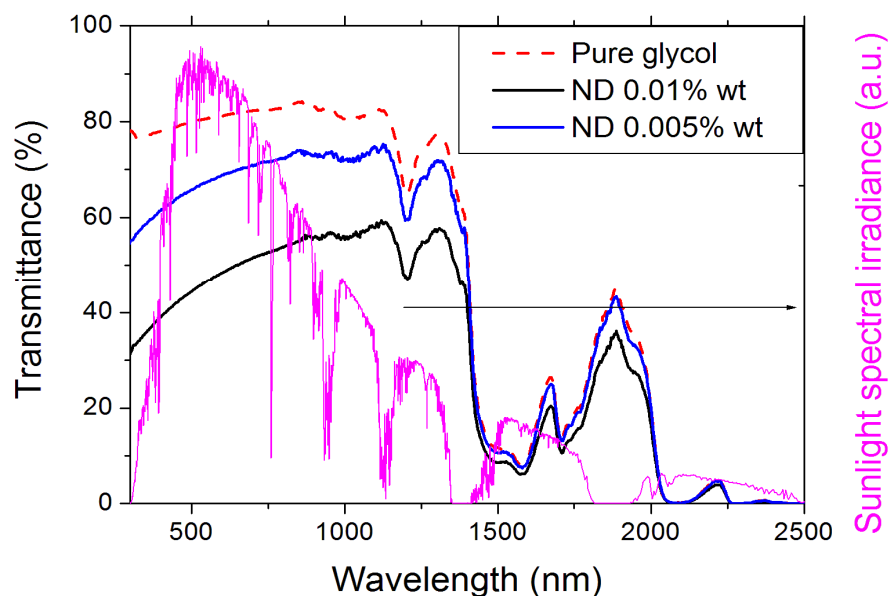


Figure 1: Transmittance spectra of nanodiamond-nanofluids and comparison with the transmittance of the pure glycol. Sunlight spectral irradiance is also superimposed for reference.

Optical limiting experiments have been carried out using a pulsed nanosecond Nd:YAG laser (Quantel Q-smart 850) as light source (6 ns pulses at 1064, 532 and 355 nm wavelength). The three laser emission wavelengths are spatially separated by proper optical elements and focused on the sample by a lens of 300 mm focal length. The sample is held in a quartz cuvette with 10

mm path length, put in a defocused position to avoid cuvette damage. The beam exiting the sample is collected by a couple of lenses of focal lengths 40 and 100 mm and focused on a pyroelectric detector (Ophir PE25C). The energy incident on the cuvette can be varied by means of proper polarizer beam splitters and measured using a pyroelectric detector (Ophir PE50BE). A dramatic nonlinear behaviour has been demonstrated for our nanofluids, with a low optical limiting threshold at all the three investigated wavelengths (Figure 2).

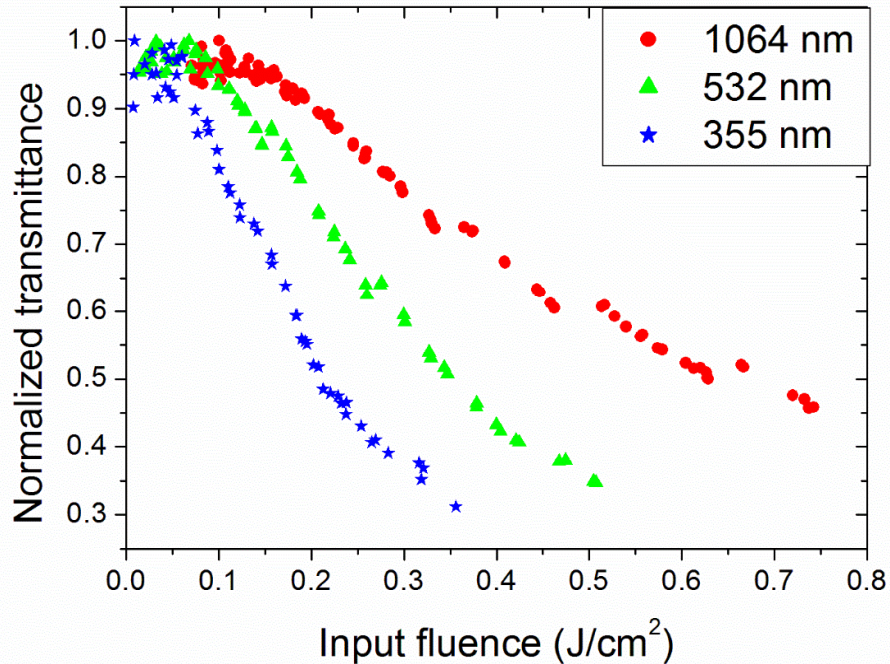


Figure 2: Optical limiting performances of the sample with 0.005%wt concentration.

Conclusions: In this work, we have prepared and characterized suspensions of graphite/nanodiamond nanoparticles in ethylene glycol. Spectrally-resolved linear optical properties have shown a significantly lower transmittance than pure base fluid, arising in a high sunlight absorption of these nanofluids with promising potential in direct-absorption solar collectors. Optical limiting in the nanosecond regime with low nonlinear threshold, high efficiency and almost no sample damage has been demonstrated at 355, 532 and 1064 nm.

References:

1. J. E. Minardi and H. N. Chuang, Performance of black liquid flat-plate solar collector, *Solar Energy* 17 (1975) 179.
2. T. P. Otanicar, P. E. Phelan, R. S. Prasher, G. Rosengarten and R. A. Taylor, Nanofluid-

- based direct absorption solar collector, *J. Renew. Sust. Energy* 2 (2010) 033102.
3. A. Moradi, E. Sani, M. Simonetti, F. Francini, E. Chiavazzo and P. Asinari, Carbon-Nanohorn Based Nanofluids for a Direct Absorption Solar Collector for Civil Application, *J. Nanoscience and Nanotechnology* 15 (2015) 3488.
 4. A. Lenert and E. N. Wang, Optimization of nanofluid volumetric receivers for solar Thermal energy conversion, *Solar Energy* 86 (2012) 253–265.
 5. Z. Luo, C. Wang, W. Wei, G. Xiao and M. Ni, Performance improvement of a nanofluid solar collector based on direct absorption collection (DAC) concepts, *Int. J. Heat and Mass Transf.* 75 (2014) 262–271.
 6. E. Sani, et al, Carbon nanohorns-based nanofluids as direct sunlight absorbers, *Optics Express* 18 (2010) 5180-5187.
 7. E. Sani, L. Mercatelli, S. Barison, C. Pagura, F. Agresti, L. Colla and P. Sansoni, Potential of carbon nanohorn- based suspensions for solar thermal collectors, *Solar Energy Materials and Solar Cells* 95 (2011) 2994–3000.
 8. R. A. Taylor, P. E. Phelan, T. P. Otanicar, R. Adrian and R. Prasher, Nanofluid optical property characterization: towards efficient direct absorption solar collectors, *Nanoscale Research Letters* 6 (2011) 225.
 9. G. Żyła, J. Fal, and P. Estellé, The influence of ash content on thermophysical properties of ethylene glycol based graphite/diamonds mixture nanofluids, *Diamond and Related Materials* 74 (2017) 81-89.

OPTICAL PROPERTIES OF FUNCTIONALIZED GRAPHENE NANOPATELET-NANOFLUIDS

E. Sani^{1*}, N. Papi¹, J. P. Vallejo², D. Cabaleiro² and L. Lugo²

¹CNR-INO National Institute of Optics, Largo E. Fermi, 6, I-50125 Firenze, Italy

²Departamento de Física Aplicada, Facultade de Ciencias, Universidade de Vigo, E-36310 Vigo, Spain

*Corresponding authors: elisa.sani@ino.it

Keywords: Functionalized graphene nanoplatelets, Optical properties, Rheological behaviour, Solar energy

Introduction: Conventional solar collectors operating at low-mid temperatures consist of a sunlight absorbing coating deposited on a solid surface exchanging heat with a working fluid. To reduce energy losses due to thermal re-radiation by the heated absorber, a vacuum insulation of the absorbing surface is typically required. This scheme can be significantly simplified by the use of a dark fluid working both as volumetric light absorber and heat exchanger. The first idea of a direct-absorption solar collector (DASC) dated back to 1975 and employed India ink [1]. However, organic dyes rapidly degrade when exposed to solar radiation. Thus in this field, the development of nanotechnology, allowing both the creation of new nanoparticles and their stable suspension in fluids (nanofluids), has a high potential. In fact, nanofluids have given a new pulse to DASC concept, as shown by the impressive growth of studies on this topic [2-8].

Graphene nanoplatelets or nanosheets consist of small flakes of several-layer stacked graphene that partially inherit the good properties of graphene with much lower production costs. Nevertheless, to achieve a better dispersion process in most aqueous or organic solvents it is necessary to chemically modify graphene surface.

In this work, we present new heat transfer fluids with thermophysical properties nano-enhanced by the dispersion of commercial functionalized graphene nanoplatelets in a base fluid. Initially, we focus the attention on their stability determining zeta potential and pH values to propose nanofluids with enhanced capabilities. Optical properties were determined in the perspective to evaluate force and weakness points of this nanofluid for solar energy application. Furthermore, it was performed a rheological analysis of the dispersions, key to understanding the flow behaviour of these new fluids in this application.

Discussion and Results: The base fluid used in our study, Havoline XLC Premixed 50/50 is a commercial mixture at 50:50% vol of Havoline XLC and water and it is widely used as coolant in the engine industry. Sodium dodecyl benzene sulphonate, SDBS has been added to the fluid at the optimized mass fraction of 0.125% to improve the long-term stability of produced nanofluids. Dispersions of polycarboxylate chemically modified graphene nanoplatelets (fGnP)

have been prepared with nanoparticle concentrations 0.005% wt and 0.05% wt. pH values of suspensions have been checked and found to be practically equal to that of the base fluid.

According to the literature, absolute zeta potential values higher than 30 mV in aqueous solutions denote good dispersion stabilities due to the stronger electrostatic repulsions among particles [9]. The zeta potential of the studied nanofluids was analysed through a dynamic light scattering technique by using a Zetasizer Nano ZS (Malvern Instruments Ltd, Malvern, United Kingdom). Figure 1 shows the zeta potentials of the analysed fGnP mass fractions in the temperature range from (293.15 to 323.15) K. As it can be observed, zeta potential values are lower than -30 mV, except for 0.005% wt concentration at 293.15 K for which this property exhibits a value close to that limit. The absolute zeta potential rises with the increasing temperature up to -51 mV. Therefore, the mentioned optimized concentration of SDBS was selected for the purpose of this study.

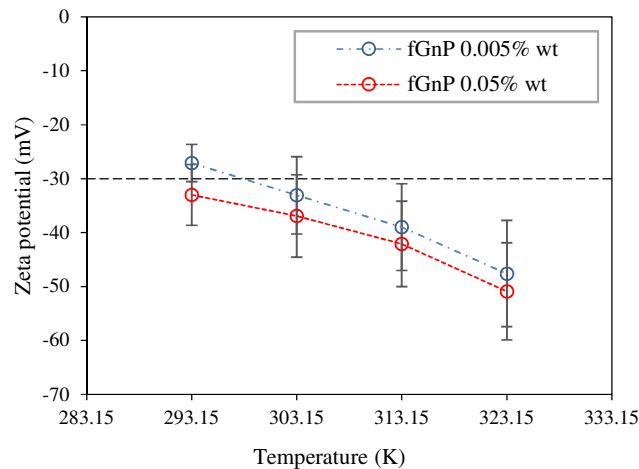


Figure 1: Zeta potential of fGnP suspensions at different temperatures.

Optical transmittance spectra at room temperature have been measured using a double-beam UV-VIS spectrophotometer (PerkinElmer Lambda900). In Figure 2 we show the extinction coefficient of fGnP suspensions and that of the base fluid in the spectral range 300-2700 nm. In the spectral region of high transparency of the base fluid an addition of fGnPs as low as 0.005% wt increases the extinction coefficient by more than four times in the interval 590 nm-950 nm and by about ten times in the range 600-870 nm. Increasing the nanoparticle loading only up to 0.05% wt dramatically affects the light extinction properties of nanofluid in the whole spectral range (Figure 2).

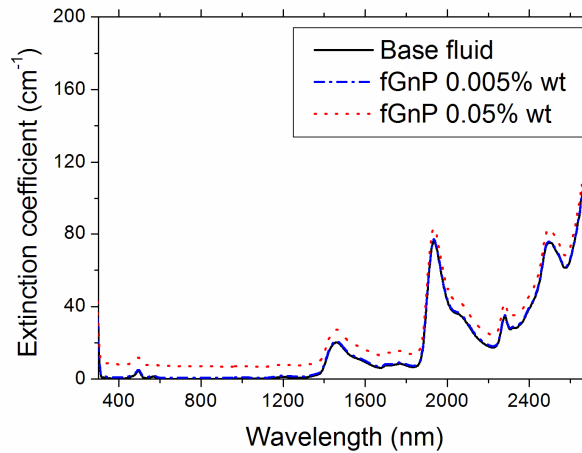


Figure 2: Extinction coefficient of fGnP suspensions and base fluid.

If we calculate the fraction F of the incident sunlight $I(\lambda)$ [10] which is extinct in the fluid after a propagation path of length x [6,7]:

$$F(x) = 1 - \frac{\int_{\lambda_{\min}}^{\lambda_{\max}} I(\lambda) \cdot e^{-\mu(\lambda)x} d\lambda}{\int_{\lambda_{\min}}^{\lambda_{\max}} I(\lambda) d\lambda} \quad (1)$$

where $\mu(\lambda)$ is the experimental extinction coefficient, $\lambda_{\min}=300$ nm and $\lambda_{\max}=2700$ nm, we obtain that for the lowest fGnP concentration, an almost full sunlight extinction is reached within 50 mm, while for the base fluid without nanoparticles, at the same path length the extinction is about 70%. For the sample with 0.05% wt fGnPs, the full sunlight extinction is reached after a path length as short as 7 mm. Even if this estimation has been carried out using the extinction coefficient (which includes also the light scattering contribution), the effect on sunlight absorption of even small fGnP loadings, like those investigated in this work, is clear.

The rheological behaviour was analysed in the temperature range from (293.15 to 323.15) K by means of a rotational Physica MCR 101 rheometer (Anton Paar, Graz, Austria) equipped with a cone-plate geometry with 50 mm diameter, 1° cone angle and 100 μm cone truncation. Rotational tests maintaining for at least 500 s various constant shear rates ranging from (10 to 1000) s^{-1} were performed. No viscosity-time dependence for the samples was observed and it can be pointed out that analysed fluids are Newtonian in the studied range.

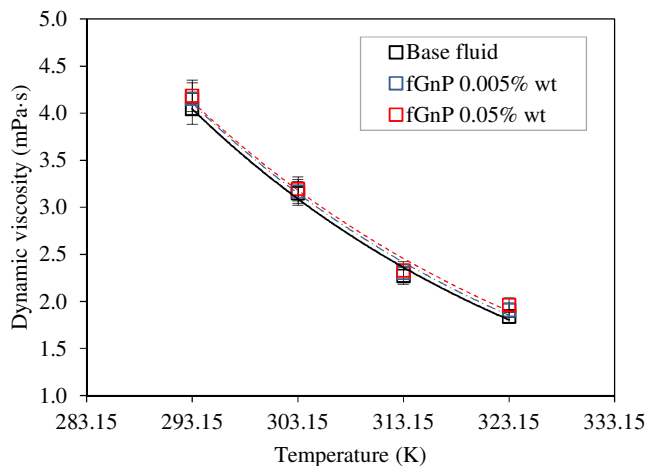


Figure 3: Dynamic viscosities for fGnP suspensions and base fluid against temperature.

As it can be observed in Figure 3, dynamic viscosity values do not show noticeable differences between them, with a trend to slight increase with the fGnP mass fraction that reach a maximum increase of 6.6% for the highest temperature.

Conclusions: We developed polycarboxylate chemically modified graphene nanoplatelet dispersions in Havoline XLC Premixed 50/50 using SDBS as surfactant. The SDBS additive concentration was optimized from zeta potential and pH analyses to achieve durable stabilities, critical issue of nanofluids. We found that fGnPs, even at very low concentrations like 0.005% and 0.05% wt, consistently change the optical characteristics of the fluid, producing a high sunlight absorption in short (tens of mm) or very short (mm) layers. This opens interesting perspectives for different architectures of solar collectors, allowing a tailored sunlight absorption level even in compact designs. Rheology tests show a Newtonian behaviour in the shear rate range between (10 and 1000) s^{-1} for base fluid and fGnP suspensions. No significant viscosity increases with the fGnP addition was found what allows concluding that the pumping powers necessary to make these new fluids flow will not noticeably rise.

References:

1. J. E. Minardi and H. N. Chuang, Performance of black liquid flat-plate solar collector, *Solar Energy* 17 (1975) 179.
2. T. P. Otanicar, P. E. Phelan, R. S. Prasher, G. Rosengarten and R. A. Taylor, Nanofluid-based direct absorption solar collector, *J. Renew. Sust. Energy* 2 (2010) 033102.
3. A. Moradi, E. Sani, M. Simonetti, F. Francini, E. Chiavazzo and P. Asinari, Carbon-Nanohorn Based Nanofluids for a Direct Absorption Solar Collector for Civil Application, *J. Nanoscience and Nanotechnology* 15 (2015) 3488.

4. A. Lenert and E. N. Wang, Optimization of nanofluid volumetric receivers for solar Thermal energy conversion, *Solar Energy* 86 (2012) 253–265.
5. Z. Luo, C. Wang, W. Wei, G. Xiao and M. Ni, Performance improvement of a nanofluid solar collector based on direct absorption collection (DAC) concepts, *Int. J. Heat and Mass Transf.* 75 (2014) 262–271.
6. E. Sani, et al, Carbon nanohorns-based nanofluids as direct sunlight absorbers, *Optics Express* 18 (2010) 5180-5187.
7. E. Sani, L. Mercatelli, S. Barison, C. Pagura, F. Agresti, L. Colla and P. Sansoni, Potential of carbon nanohorn- based suspensions for solar thermal collectors, *Solar Energy Materials and Solar Cells* 95 (2011) 2994–3000.
8. R. A. Taylor, P. E. Phelan, T. P. Otanicar, R. Adrian and R. Prasher, Nanofluid optical property characterization: towards efficient direct absorption solar collectors, *Nanoscale Research Letters* 6 (2011) 225.
9. A. Ghadimi, R. Saidur, H. Metselaar, A review of nanofluid stability properties and characterization in stationary conditions, *Int. J. Heat and Mass Transf.* 54 (2011) 4051-4068.
10. Standard Tables for Reference Solar Spectral Irradiances: Direct Normal and Hemispherical on 37° Tilted Surface, Active Standard ASTM G173. ASTM G173 - 03(2012).

Abstracts

SESSION 6B: SOLAR

MOLTEN SALT-BASED NANOFLUIDS WITH CERAMIC NANOPARTICLES FOR CONCENTRATED SOLAR POWER APPLICATION

A. Palacios¹, Z. Jiang¹, E. Mura², M.E Navarro¹, G.Qiao² and Y. Ding¹

¹BCES Birmingham Centre for Energy Storage, University of Birmingham, United Kingdom

²Global Energy Interconnection Research Institute Europe GmbH, Berlin, 10117, Germany

*Corresponding author: y.ding@bham.ac.uk

Keywords: Molten salts, Ceramic nanoparticle, Thermal energy storage, Heat transfer fluid

Introduction: For decades, nanofluids have been studied as heat transfer fluids (HTFs) in concentrated solar power (CSP) systems. Nanofluids present higher specific heat capacity and thermal conductivity than the pure fluid. The addition of a small concentration of nanoparticles can dramatically enhance the thermophysical properties of the base fluid (molten salt) [1]. The heat transfer capacity is a key attribute in terms of storing the heat received from the sun and then transferring it when it is needed in a later use. Besides a high specific heat capacity to store energy, a high thermal conductivity is required. The thermal conductivity is a key parameter that can affect energy storage and cooling rate of the CSP system. The most reported nanoparticles used to enhance the thermal conductivity of molten salts are silicon dioxide, carbon nanotubes, carbon spheres, graphite flakes and titanium dioxide [2], [3]. In the present work, the effect of adding silicon dioxide to a ternary and quaternary molten salt is studied. The authors are intended to evaluate the effect of adding high thermal conductivity nanoparticles into HTFs to provide evidence of a heat transfer enhancement. Also the rheological behaviour of the heat transfer fluid during the charging/discharging process was studied.

Materials and methodology: The molten salts listed in Table 1 were selected as the base fluid for this study. Silicon dioxide nanoparticles with 15-20nm diameter was used as ceramic high thermal conductivity nanoparticles. Nanofluids with different nanoparticles concentration (0.1, 0.5 and 1 wt%) were formulated. The procedure, see Figure 1, was conducted following Jo and Banerjee [4] three step method.

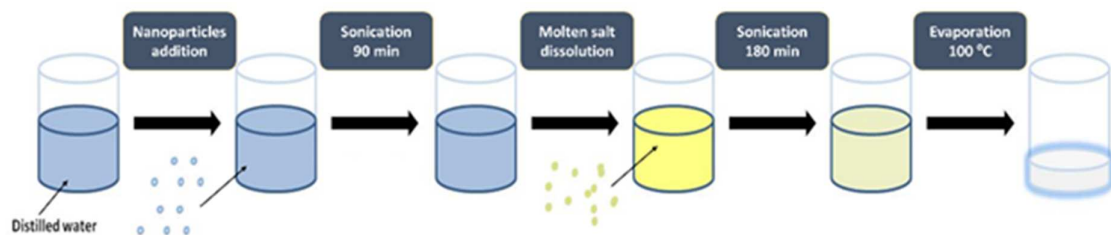


Figure 2: Three-step method nanofluid formulation

Table 1. Molten salts used as a base fluid in the present study.

Molten salt	Composition	Melting temperature (°C)
Ternary	LiNO ₃ -NaNO ₃ -KNO ₃	120
Quaternary	CaNO ₃ -LiNO ₃ -NaNO ₃ -KNO ₃	105

As it was mentioned before, the study is aimed to evidence the improvement of the heat transfer during the charging/discharging on LHTES technologies. A laser flash analyser (LFA427, Netzsch) and the three layer method were used with that purpose. The measurements were conducted under nitrogen atmosphere and a temperature range from 50 to 400°C.

MCR 502 rheometer commercialised by Anton Paar was used to measure the viscosity of the nanofluid. The working temperature was varied from 250°C to 400°C with an interval of 50°C, the measurements were conducted with a shear rate from 0.1 to 250 s⁻¹ under air atmosphere.

Discussion and Results: The thermal diffusivity results for the ternary nanofluids are shown in Table 2. The thermal diffusivity of the nanofluids with 0.5% and 1% of silicon dioxide are higher than the pure ternary salt in the temperature range from 200 to 450°C. At 450°C, the samples with 0.5 and 1% SiO₂ nanoparticles present a thermal diffusivity enhancement of 25% and 36%, respectively. The addition of SiO₂ nanoparticles (0.1%) does not lead to an enhancement of the thermal diffusivity.

The SiO₂ nanoparticles induce to a thermal diffusivity enhancement (10%) of the quaternary salt by means of adding a 1% in weight to the pure salt in the temperature range of 250 to 450°C (see Table 2). The thermal diffusivity increases with the silicon dioxide content, 0.5% and 1%, reaching an enhancement of 5% and 12%, respectively. Although the thermal diffusivity is increasing with the nanoparticle content, with 0.1 SiO₂ it presents lower values than the pure salt in the whole temperature range under study.

The viscosity of the ternary and quaternary molten salt formulations was also measured. The addition of silicon dioxide nanoparticles result on a substantially increase of the viscosity in both cases. In Figure 3 it can be seen the results for the ternary salt measurements with different amounts of nanoparticles. The viscosity is increasing with a higher nanoparticles content, when 0.5% and 1% of the nanoparticles were added, the overall viscosity was increased by about 47% and 60%, respectively. As expected, the viscosity of the formulations decrease with temperature.

Table 2. Thermal diffusivity of ternary and quaternary molten salt nanofluids.

Sample	Thermal diffusivity (mm ² /s)						
	200°C	250°C	300°C	350°C	400°C	450°C	Mean (200- 450°C)
Ternary	0.118	0.123	0.125	0.128	0.130	0.108	0.122
Ternary + 0.1% SiO ₂	0.108	0.113	0.117	0.108	0.081	0.107	0.106
Ternary + 0.5% SiO ₂	0.111	0.115	0.118	0.122	0.126	0.143	0.123
Ternary + 1% SiO ₂	0.112	0.120	0.128	0.135	0.144	0.170	0.135
Quaternary	0.126	0.135	0.146	0.152	0.163	0.184	0.151
Quaternary + 0.1% SiO ₂	0.097	0.104	0.109	0.119	0.128	0.150	0.118
Quaternary + 0.5% SiO ₂	0.118	0.122	0.126	0.131	0.139	0.194	0.138
Quaternary + 1% SiO ₂	0.128	0.142	0.159	0.175	0.183	0.209	0.166

Regarding the quaternary based nanofluids, it can be seen (Figure 3) that the addition of silicon dioxide nanoparticles result on an increase of the viscosity up to 214% with a value close to 22 mPa·s at 250°C with 1% of SiO₂ nanoparticles. At higher temperatures (up to 400°C) the viscosity of the fluid decreases reaching values close to the quaternary pure salt, even lower in the case of 0.1 and 0.5% in wt. which the viscosity is reduced by 6%.

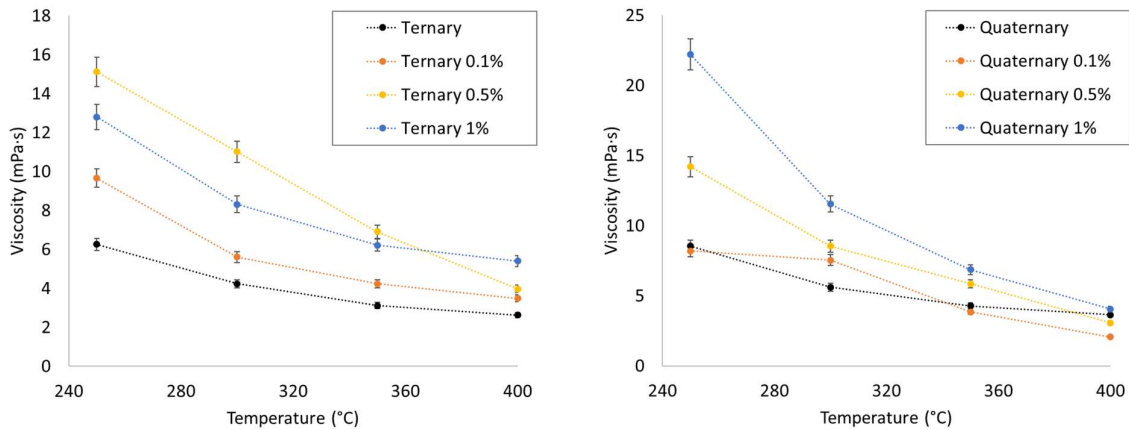


Figure 3. Viscosity of ternary (left) and quaternary (right) molten salt nanofluids with silicon dioxide.

Conclusions: In the present study, the experimental data of ternary and quaternary with different content of silicon dioxide nanoparticles are reported. The main outcomes from the experimental data analysed are shown as follows:

- (1) The ternary molten salt presents a thermal diffusivity enhanced up to 25% and 36% by the addition of silicon oxide 0.5% and 1% in weight, respectively. At high temperatures (up to 400°C), the salt presents viscosity values close to 6% higher than the pure salt ones.
- (2) The quaternary molten salt with 1% SiO₂ presents a thermal diffusivity 12% higher than the pure salt at 450°C. The addition of lower percentages of silicon dioxide does not lead to an enhancement. The rheological behavior of the nanofluid at 400°C shows a viscosity value close to the pure salt, within the tolerance of the equipment ($\pm 3\%$).

References:

- [1] P. Kumar and D. Dey, A Recent Review on Thermo-Physical Properties of Nanofluid, *International Conference on Electrical, Electronics, and Optimization Techniques (ICEEOT)*, Chennai, India, Mar 03- 05, 2016.
- [2] B. Jo and D. Banerjee, Enhanced Specific Heat Capacity of Molten Salt-Based Carbon Nanotubes Nanomaterials, *Journal of Heat Transfer* 137 (2015) 91013.
- [3] T. Bauer, N. Breidenbach, and M. Eck, Overview of Molten Salt Storage Systems and Material Development for Solar Thermal Power Plants, *The 2012 National Solar Conference for (SOLAR 2012)*, Denver, Colorado, May 13-17, 2012.
- [4] B. Jo and D. Banerjee, "Enhanced specific heat capacity of molten salt-based nanomaterials: Effects of nanoparticle dispersion and solvent material," *Acta Materialia* 75 (2014) 80–91.

MOUROMTSEFF NUMBER ANALYSIS ON NANOFUID BASED SYSTEMS: FLAT PLATE SOLAR COLLECTORS

A. M. Genc¹, M. A. Ezan² and A. Turgut^{2*}

¹Dokuz Eylul University, The Graduate School of Natural and Applied Sciences, Mechanical Engineering Department, Tinaztepe Campus, Buca 35397, Izmir-Turkey

²Dokuz Eylul University, Engineering Faculty, Mechanical Engineering Department, Tinaztepe Campus, Buca 35397, Izmir-Turkey

* Corresponding author: alpaslan.turgut@deu.edu.tr

Keywords: Mouromtseff number, Al₂O₃-water nanofluids, flat plate solar collector

Introduction: In general, Nusselt number or heat transfer coefficient are used to determine the heat transfer capability of fluids. Alternatively, the Mouromtseff number, known as the figure of merit in the literature, is being used for comparison of the heat transfer capability for laminar or turbulent flows. It was presented by Mouromtseff (1942) [1] depending on the thermal properties of the fluid, such as density, heat capacity, dynamic viscosity and thermal conductivity [2]. For the fully developed flow inside a circular pipe [3], the Mouromtseff number (Mo) is defined as follows:

$$\text{Mo} = \frac{\rho^a k^b c_p^d}{\mu^e} \quad (1)$$

where the subscripts, a , b , d , and e , are determined by using an appropriate Nusselt number for the selected heat transfer application. Since the Mo number is an integrated non-dimensional parameter, it was commonly used to evaluate the thermal performance of a traditional heat transfer fluid, such as water or ethylene glycol, for either laminar or turbulent flow conditions. Recently, it has also been used to compare for nanofluids to compare the overall effectiveness of a candidate nanofluid with the traditional base fluid. It is well known that, in the case of the flow in a straight pipeline, either with constant wall temperature or heat flux, the Nusselt number converges to a constant value in the fully developed conditions. That is, for the fully developed conditions, the relative Mo number [4], which designates the ratio of the Mo numbers for nanofluid and base fluid, can be obtained as follows:

$$\text{FOM}_{\text{lam}} = \frac{\text{Mo}_{nf}}{\text{Mo}_{bf}} = \frac{h_{nf}}{h_{bf}} = \frac{k_{nf}}{k_{bf}} \quad (2)$$

FOM_{lam} is valid for only laminar and fully developed flow conditions inside pipes. For the fully developed turbulent flow conditions, on the other hand, the following figure of merit equation (FOM_{turb}) can be obtained by using the expression proposed by Vajjha and Das (2012) [5]:

$$\text{FOM}_{\text{turb}} = \frac{\text{Mo}_{nf}}{\text{Mo}_{bf}} = \frac{h_{nf}}{h_{bf}} = \left(\frac{\rho_{nf}}{\rho_{bf}} \right)^{0.8} \left(\frac{k_{nf}}{k_{bf}} \right)^{0.5} \left(\frac{c_{pnf}}{c_{pbf}} \right)^{0.5} \left(\frac{\mu_{bf}}{\mu_{nf}} \right)^{0.4} \quad (3)$$

Alternatively, FOM_{turb} can be obtained by using Dittus-Boelter correlation as follows:

$$Nu = 0.023 \text{Re}^{0.8} \text{Pr}^{0.4} \quad (4)$$

$$\text{FOM}_{\text{turb}} = \frac{\text{Mo}_{nf}}{\text{Mo}_{bf}} = \frac{h_{nf}}{h_{bf}} = \left(\frac{\rho_{nf}}{\rho_{bf}} \right)^{0.8} \left(\frac{k_{nf}}{k_{bf}} \right)^{0.6} \left(\frac{c_{pnf}}{c_{pbf}} \right)^{0.4} \left(\frac{\mu_{bf}}{\mu_{nf}} \right)^{0.4} \quad (5)$$

In the current study, we have used Eq. (2) and Eq. (5) for the laminar and turbulent flow conditions, respectively. One can notice that the nanofluids are considered as more efficient than the base fluid if the FOM's are greater than unity. Recently, Minea and Moldovenau (2017) [6] investigated the effectiveness of TiO₂, Al₂O₃, and CuO nanofluids under laminar and turbulent flow conditions. They mentioned that the relative Mo number is an effective and straightforward way to find the effectiveness of nanofluids. In this study, the effectiveness of Al₂O₃-water nanofluids was investigated with using Mo number in laminar and turbulent flow conditions. The obtained results are compared with our previous numerical study [7] in which the effects of Al₂O₃-water nanofluids on the flat plate solar collectors (FPSCs) were investigated. Al₂O₃-water nanofluid is selected due to well-known thermophysical properties [8] and thermal performance [9, 10] based on our previous experimentations.

Discussion and Results: FOM's are calculated for fully developed laminar and turbulent flow conditions and the results are given in Figure 1. According to Eq. (2), FOM_{lam} depends on only the thermal conductivity of sample. Therefore, increasing the particle concentration improves the FOM_{lam} and it is greater than unity for all concentrations due to the higher thermal conductivity of nanofluids. Regarding the current non-dimensional performance metric nanofluids with higher concentrations have better performance in a thermal system.

However, in the case of turbulent flow the trend is in contrast with the laminar one. Although the thermal conductivity of the nanofluid samples increases with the concentration, Mo number in turbulent flow decreases due to the higher viscosity and lower specific heat capacity of nanofluids. So, the FOM_{turb} values are less than unity because the Mo number of water is higher

than the selected nanofluids. In this regards, it seems that investigated nanofluids are not favorable for the heat transfer applications under turbulent flow conditions. Moreover, the effectiveness of nanofluids decreases with increasing nanoparticle concentration. The current results are in contradiction with the previous works in the literature [5, 6] in which the turbulent flow conditions were investigated.

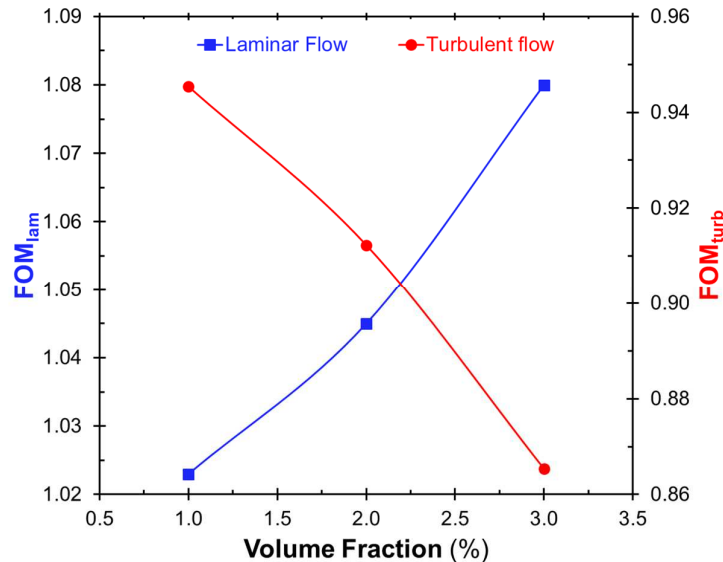


Figure 1 The FOM_{lam} for laminar conditions and the FOM_{turb} for turbulent conditions

In a recent work of the authors [7], a numerical model was developed to simulate the transient heat transfer of FPSCs. The influences of type of working fluids (either water or nanofluids), mass flow rate of the HTF and the climatic conditions were compared regarding the energetic and exergetic aspects. The mass flow rate of the heat transfer fluids is varied in a wide range, 0.004 to 0.06 kg/s, to introduce the effect of nanoparticle dispersion within water under laminar and turbulent flow conditions. Figure 2(a) shows the variations of the thermal efficiencies of the FPSC under various flow rates and particle concentrations in October. Here one can see that for the mass flow rates lower than 0.016 kg/s, the efficiency of the FPSC enhances as the particle concentration increases and the nanofluids are efficient than water. On the contrary, beyond 0.016 kg/s increasing the particle concentration has an adverse effect on the heat transfer and reduces the thermal efficiency of FPSC. It is also interesting to note that the thermal efficiencies of FPSCs with nanofluids are slightly lower than the ones with water at higher mass flow rates. In the current model, 0.016 kg/s is the critical mass flow rate for the transition to the turbulent flow condition. While at 0.016 kg/s only water shows turbulent behavior, beyond this value each of fluids is fully turbulent. One can realize that the inversion of the thermal efficiencies of FPSC at the verge of the turbulent is compatible with the relative Mo number variations for laminar and turbulent flow conditions that are given in Figure 1. Below 0.016 kg/s, in laminar flow zone, nanofluids are efficient since FOM_{lam} is higher at higher particle concentrations.

However, beyond 0.016 kg/s, in the turbulent flow zone, water becomes the efficient working fluid, and the particle concentration reduces the efficiency of the FPSC since the FOM_{turb} reduces with increasing concentration. Consequently, the FOMs are compatible with findings of the numerical model.

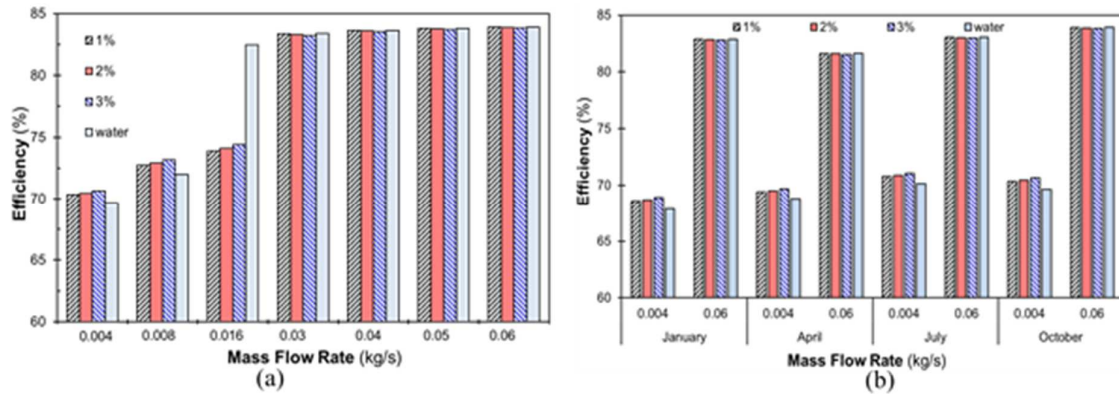


Figure 2 (a) Thermal efficiency of the FPSC for various mass flow rates in October (b) Thermal efficiency of the FPSC for various HTFs under different climatic conditions

In Figure 2(b), on the other hand, the thermal efficiencies are given at lower and higher mass flow rates for four different months. In each month, the efficiency of FPSC increases dramatically as the flow rate is increased from 0.004 g/s to 0.06 kg/s. Similar to the variations in Figure 2(a), there is an inversion point for the thermal efficiency of FPSC depending on the particle concentration. At lower flow rates (for *laminar flow*) the nanofluids are better than the water whereas at the higher flow rates (for *turbulent flow*) FPSCs with water as a working fluid have slightly higher efficiencies. That is, under both laminar and turbulent flow conditions, efficiency values are compatible with non-dimensional FOM_{lam} and FOM_{turb} values.

Conclusions: In this study, the effectiveness of Al₂O₃/water nanofluids are investigated with using relative Mo numbers for laminar and turbulent flow conditions. The results were compared with the numerical findings of the authors. Following conclusions can be listed:

- The effectiveness of selected nanofluids is higher than the base fluid under laminar flow conditions, and this effectiveness increases with increasing nanoparticle concentrations.
- For turbulent flow conditions, the Mo number of nanofluids are less than water, and the effectiveness of nanofluids decreases with increasing nanoparticle concentrations. For turbulent flow, nanofluids are not convenient for heat transfer applications.
- Non-dimensional FOM_{lam} and FOM_{turb} values are consistent with our previous numerical study for FPSC.

References:

1. Mouromtseff, I. E. (1942). Water and forced-air cooling of vacuum tubes nonelectronic problems in electronic tubes. *Proceedings of the IRE*, 30(4), 190-205.
2. Yu, W., France, D. M., Timofeeva, E. V., Singh, D., & Routbort, J. L. (2012). Comparative review of turbulent heat transfer of nanofluids. *International journal of heat and mass transfer*, 55(21), 5380-5396.
3. Simons, R. E., Comparing Heat Transfer Rates of Liquid Coolants Using the Mouromtseff Number, *Electronic Cooling*, vol. 12,
http://electronicscooling.com/articles/2006/2006_may_cc.php, 2006.
4. Minea, A. A. (2013). Effect of microtube length on heat transfer enhancement of an water/Al₂O₃ nanofluid at high Reynolds numbers. *International Journal of Heat and Mass Transfer*, 62, 22-30.
5. Vajjha, R. S., & Das, D. K. (2012). A review and analysis on influence of temperature and concentration of nanofluids on thermophysical properties, heat transfer and pumping power. *International journal of heat and mass transfer*, 55(15), 4063-4078.
6. Minea, A. A., & Moldoveanu, M. G. (2017). Studies on Al₂O₃, CuO, and TiO₂ water-based nanofluids: A comparative approach in laminar and turbulent flow. *Journal of Engineering Thermophysics*, 26(2), 291-301.
7. Genc, A. M., Ezan, M. A., & Turgut, A. Thermal performance of a nanofluid based flat plate solar collector: A transient numerical study. (Under Revision).
8. Turgut, A., Saglanmak, S., & Doganay, S. (2016). Experimental Investigation on Thermal Conductivity and Viscosity of Nanofluids: Particle Size Effect. *Journal of The Faculty of Engineering and Architecture of Gazi University*, 31(1), 95-103.
9. Turgut, A., & Doganay, S. (2014). Thermal performance of a single phase natural circulation mini loop working with nanofluid. *High Temperatures--High Pressures*, 43(4).
10. Doganay, S., & Turgut, A. (2015). Enhanced effectiveness of nanofluid based natural circulation mini loop. *Applied Thermal Engineering*, 75, 669-676.

NANOFLUIDS AS DIRECT SOLAR ENERGY ABSORBERS

A. Gimeno Furió^{1*}, J.E. Juliá¹, S Barison², F. Agresti², M.H. Buschmann³ and C. Friebe³

¹Mechanical Engineering and Construction Department

Universitat Jaume I, 12071 Castellón de la Plana, Spain

²CNR-ICMATE Institute of Condensed Matter Chemistry and Technologies for Energy,
Corso Stati Uniti, 4, 35127 Padova, Italy

³Institut für Luft- und Kältetechnik GmbH

Bertolt-Brecht-Allee 20, 01309 Dresden, Germany

*Corresponding author: afurio@uji.es

Keywords: Solar nanofluid, Nanohorns, Silica, Absorption

Introduction:

Nanofluids are fluids (usually liquids) that contains nanoparticles between 1 and 100 nm suspended on it and they have been used to improve thermal conductivity and heat transfer of base fluid. The most common nanoparticles are metals or metal oxides dispersed in water. Nanoparticles are added because they improve heat transfer and absorption processes. It has been studied in different researches that thermal properties of nanofluids present differences regard to the conventional heat transfer fluids. On the other hand, solar nanofluids are defined as liquids that contain nanoparticles suspended that absorb solar radiation. These type of particles used to be metal (Au, Ag, Cu...) due to their resonance plasmon. These solar nanofluids were proposed as volumetric solar radiation receivers. Based water nanofluids may have advantages over water because the nanoparticles can directly absorb the solar radiation. Thus, it is possible to reach a high efficiency from solar radiation to thermal energy conversion process. Because of that, some research focuses on solar nanofluids as probable material used in future renewable energy technologies [1-3].

This work is based on the study of the energy absorbed for different water-based nanofluids.

Discussion and Results:

The experiments were carried out using an artificial sun which consists of ten lamps with a power of 2000 W each, shown in Fig. 1.



Figure 1 Lamps structure imitating an artificial sun lighting the samples

The inclination of the structure containing these ten lamps is $64\pm 0.3^\circ$ degrees in order to achieve the highest intensity in the experiment site.

It was also used a black plate (1 m x 1 m) with 5 glass tubes held on it. Tubes have an inner diameter of 25 mm and a length of 400 mm except for one which is a vacuum tube with an inner diameter of 20 mm and a length of 300 mm. All of them were closed with a rubber tap. In order to measure the working fluid temperature, five thermocouples Pt100 were introduced in each tube. Moreover, three more thermocouples were used to measure ambient temperatures. One of them was located behind the plate, another one at the front of the plate and last one, under the lamps. Before starting any test, thermocouples must be calibrated. A moisture meter was placed under the lamps and a light meter was placed at the top of the plate. There are also fans used to avoid reaching very high temperatures, one is located under the lamps to cold the light system; and the other fan is located in room's wall to maintain an acceptable temperature in the chamber. It has to be mentioned, that all the experiments were carried out under controlled conditions.

Once the thermocouples were calibrated, the test starts by switching on the lamps and the fans. After that, the samples were heated during 4 hours and every second temperature value is registered. When this value remains constant, the artificial sun and the fans were switched off.

Four kinds of fluids were tested and compared with water as reference data. Silica nanofluid which is made of SIPERNAT©22S with a concentration of 0.01g/L and stabilized with KOH

reaching a pH value of 10.5. Two single wall carbon nanohorns suspensions (NH), were used. In one of them, 0.02 g/L nanohorns (Carbonium Srl) were stabilized with 0,005 g/L of sodiumdodecylsulphate (SDS), and the other one was stabilised adding 0,05 g/L of polyvinylpyrrolidone (PVP) and 0,005 g/L of SDS. Carbon nanohorns have been used because it has already test before that they play an important role improving solar radiation absorption [4-5]. Finally, a water solution of Chinese ink with a concentration of 0,2 g/L was used.

The whole set-up with the five different samples used is shown in Figure 2. In each plate, from left to right, tubes are named as A, B, S, C, D. A and S contains the highest concentration of the study fluid. Then, the working fluids were diluted to 1/10, 1/100 and 1/1000 which are in B, C and D tubes, respectively.



Figure 2 From left to right, from top to bottom: water, silica nanofluid, Chinese ink, carbon nanohorns + SDS and carbon nanohorns + SDS + PVP

This work is only focused on the study of temperature evolution for different fluids with respect to water, and then concentration comparisons do not fall within the scope of this paper.

The results obtained in heating-up the different fluids are presented in Figure 3. In order to study the solar energy absorbed by the fluids, temperature against time has been plotted for the samples studied.

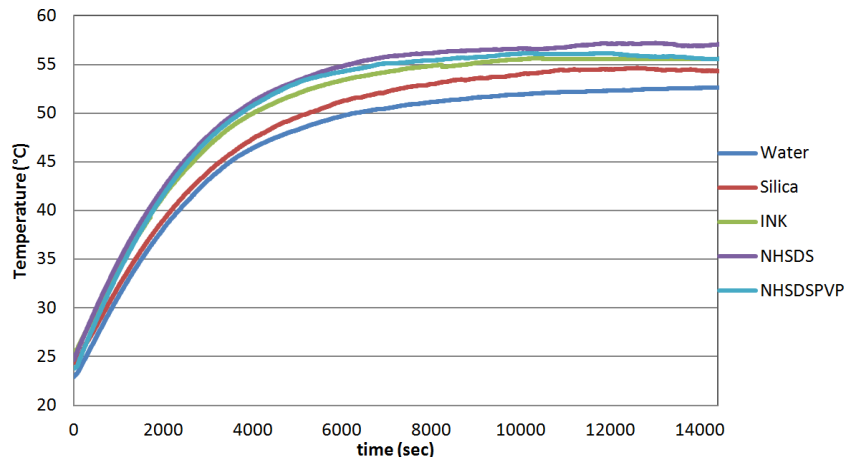


Figure 3 Temperature evolutions against time for different nanofluids in tube A

Representing these values, it is possible to observe that for darker fluids the temperature rises up faster than for white fluid or water. Moreover, black nanofluids reach a higher temperature than black ink solution, as expected, since nanofluids are suspensions with a fine dispersion of nanohorns that has a higher efficiency in absorption with respect to inks that typically contain micrometric particles.

Conclusions:

Silica nanofluid would not be effective for solar harvesting applications because there is not considerable improvement of energy absorption compared to water. In contrast, black fluids improve the absorption solar energy process. Water-based nanofluids present higher solar energy absorption than black Chinese ink due to the presence of nanoparticles whose specific surface area is large. Therefore, they would offer a chance to improve the efficiency of volumetric solar radiation receivers as direct absorbers.

Acknowledgement:

This work is a contribution of the COST Action (European Cooperation in Science and Technology) CA15119: Overcoming Barriers to Nanofluids Market Uptake (NanoUptake), the Institut für Luft- und Kältetechnik GmbH where the experiments were developed thanks to the facilities provided and the CNR-ICMATE Institute of Condensed Matter Chemistry and Technologies for Energy for its contribution of solar nanofluids.

References:

1. B.A.J. Rose, H. Singh, N. Verma, S. Tassou, S. Suresh, N. Anantharaman, D. Mariotti, P. Maguire, *Investigations into nanofluids as direct solar radiation collectors*, Solar Energy, Volume 147, 2017, Pages 426-431, ISSN 0038-092X
2. S.H.A. Ahmad, R. Saidur, I.M. Mahbubul, F.A. Al-Sulaiman, *Optical properties of various nanofluids used in solar collector: A review*, Renewable and Sustainable Energy Reviews, Volume 73, 2017, Pages 1014-1030, ISSN 1364-0321
3. R.A. Taylor, P.E. Phelan, T.P. Otanicar, C.A. Walker, M. Nguyen, S. Trimble, R.S. Prasher *Applicability of nanofluids in high flux solar collectors*. J. Renewable Sustainable Energy 3, 2011, 023104.
4. E. Sani, L. Mercatelli, S. Barison, C. Pagura, F. Agresto, L. Colla, P. Sansoni *Potential of carbon nanohorns-based suspensions for solar thermal collectors*. Solar Energy Materials and Solar Cells, Volume 95, Issue 11, November 2011, 2994-3000
5. S. Barison, L. Fedele, F. Agresti, S. Rossi, S. Bobbo, C. Pagura *Carbon nanohorn-based nanofluids for solar thermal harvesting applications*. Journal of Nanoscience and Nanotechnology, Volume 15, Number 5, May 2015, 3488-3495

NANOFLUIDS WITH ENHANCED THERMAL PROPERTIES BASED ON METALLIC NANOPARTICLES FOR CONCENTRATING SOLAR POWER: A THEORETICAL AND EXPERIMENTAL PERSPECTIVE

J. Navas^{1*}, A. Sánchez-Coronilla^{2*}, R. Gómez-Villarejo¹, E. I. Martín³, P. Martínez-Merino¹, T. Aguilar¹, J. J. Gallardo¹, R. Alcántara¹ and C. Fernández-Lorenzo¹

¹Departamento de Química Física, Universidad de Cádiz. Facultad de Ciencias, E-11510 Puerto Real (Cádiz), Spain

²Departamento de Química Física, Universidad de Sevilla. Facultad de Farmacia, E-41012 Sevilla, Spain

³Departamento de Ingeniería Química, Universidad de Sevilla. Facultad de Química, E-41012 Sevilla, Spain

*Corresponding author: javier.navas@uca.es; antsancor@us.es

Keywords: Nanofluid, Concentrating Solar Power, Thermal Conductivity, Molecular Dynamics, Au and Pt nanoparticles

Introduction: One of the challenges facing society today is the need to meet the growing demand for energy while minimizing the environmental impact on the planet [1]. Solar energy is a renewable source of energy that can be used to a large extent to this end. In this regard, the conversion of solar energy into electricity is of interest, and Concentrating Solar Power (CSP) systems play an important role as thermal energy converters to be used in electric power generation [2]. One line of research aimed at improving the efficiency of CSP plants involves improving the thermal properties of the Heat Transfer Fluid (HTF) used in these plants, which will lead to improvements in the heat transfer processes taking place. In this sense, the use of nanofluids seems to be an interesting alternative for improving the thermal properties of the base fluids [3,4], considering nanofluids as colloidal suspensions of nanometric systems in a base fluid. Suspending nanoparticles in an HTF has been shown to improve such properties as its thermal conductivity, heat transfer coefficient or isobaric specific heat [3-7].

Thus, the review of the literature reveals that CSP is one of the most interesting alternatives to conventional energy sources nowadays, and that there are advantages to be gained from the use of nanofluids in CSP for high temperature applications. In this sense, the study of new nanofluids prepared with heat transfer fluids other than water or ethylene glycol is of great interest, particularly if these fluids are to have a future commercial use. The use of nanofluids within the heat transfer energy market is forecast to increase by over 2 billion dollars in the future, making it a promising field of study [8,9]. Thus, effective nanofluids that can optimise the use of a resource such as solar energy are candidates for consideration as value-added materials that produced a decreased impact on the environment [10,11].

Thus, taking into consideration that CSP could be a promising alternative to traditional sources of energy and that the thermal properties of nanofluids present clear advantages, the analysis from experimental and theoretical perspectives of nanofluids based on the base fluids that are used as HTFs in CSP plants is of interest. Therefore, this study involved the preparation of nanofluids based on the HTF used in CSP plants, which is the eutectic mixture of biphenyl ($C_{12}H_{10}$) and diphenyl oxide ($C_{12}H_{10}O$), and metallic nanoparticles.

Discussion and Results: The nanofluids are based on a commercial heat transfer fluid (HTF) used as a base fluid, being a eutectic mixture of biphenyl ($C_{12}H_{10}$, 26.5%) and diphenyl oxide ($C_{12}H_{10}O$, 73.5%). Also, we have prepared two kind on nanofluids based on nanoparticles of Au and Pt in order to analyse the thermal properties in function of the nature of the nanoparticles. The nanofluids were prepared using the one-step method, where the precursor of the metallic nanoparticles are transferred from aqueous phase to the base fluid, and after the reduction of the precursor is performed.

The nanofluids prepared were characterised in their basic properties, such as chemical and physical stability, density, viscosity, isobaric specific heat and thermal conductivity. The measurement of these properties leads to evaluate the improvement in the heat transfer coefficient of the nanofluids with respect to the base fluid. On the other hand, from Molecular Dynamics calculations, we have analysed the behaviour of the nanofluids. The isobaric specific heat and the thermal conductivity were estimated for the both systems analysed, based on Au and Pt nanoparticles. The arrangement of the base fluid and the phase transferring agent was analysed from the radial distribution function (RDF) and the spatial distribution function (SDF).

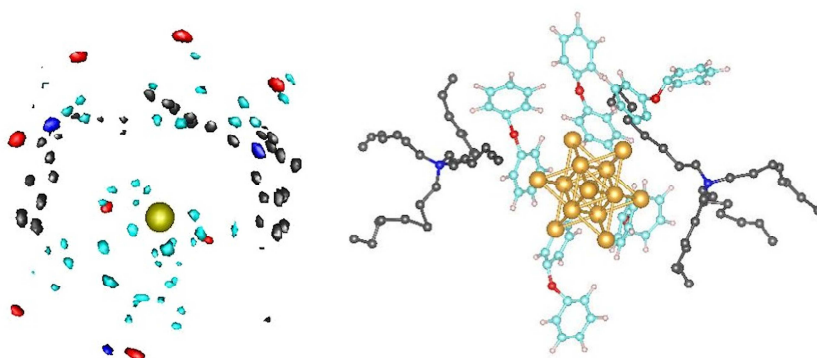


Figure 1. SDF for Au-nanofluid.

As results, particle size measurements, UV-vis spectroscopy ζ potential show a good stability for the nanofluids prepared. Also, an improvement of both isobaric specific heat (up to 10%) and thermal conductivity (up to 70%) is found for all the nanofluids prepared. These improvements lead to an enhancement in the efficiency of the nanofluids prepared with respect to the base fluid, analysed as the ratio between the heat transfer coefficient of the nanofluid and the base fluid. An increase up to 36% was observed in the heat transfer coefficient. From a

theoretical perspective, the isobaric specific heat and thermal conductivity values followed the same experimental trend. The analysis of the radial distribution functions (RDFs) and spatial distribution functions (SDFs) showed that the surfactant participates as an active component within the nanofluids, contributing to efficient heat transfer processes.

Conclusions: This work shows the preparation of the nanofluid based on a heat transfer fluid used typically in Concentrating Solar Power plants and Au and Pt nanoparticles synthesized in the base fluid used. An improvement of the thermal properties, such as isobaric specific heat, thermal conductivity and heat transfer coefficient has been found. Also, the effect of the interactions of the base fluid/surfactants/nanoparticles has been analysed in order to understand the behaviour of the nanofluids studied.

References:

1. J. Khan and M. H. Arsalan, Solar power technologies for sustainable electricity generation – A review, *Renewable and Sustainable Energy Review* 55 (2016) 414-425.
2. J. P. Bijarniya, K. Sudhakar and P. Baredar, Concentrated solar power technology in India: A review, *Renewable and Sustainable Energy Review* 63 (2016) 593-603.
3. J. Navas, A. Sánchez-Coronilla, E. I. Martín, M. Teruel, J. J. Gallardo, T. Aguilar, R. Gómez-Villarejo, R. Alcántara, C. Fernández-Lorenzo, J. C. Piñero, J. Martín-Calleja, On the enhancement of heat transfer fluid for concentrating solar power using Cu and Ni nanofluids: An experimental and molecular dynamics study, *Nano Energy* 27, (2016) 213-224.
4. R. Gómez-Villarejo, E. I. Martín, J. Navas, A. Sánchez-Coronilla, T. Aguilar, J. J. Gallardo, R. Alcántara, D. De los Santos, I. Carrillo-Berdugo, C. Fernández-Lorenzo, Ag-based nanofluidic system to enhance heat transfer fluids for concentrating solar power: Nano-level insights, *Applied Energy* 194 (2017) 19-29.
5. D. Singh, E. V. Timofeeva, M. R. Moravek, S. Cingarapu, W. H. Yu, T. Fischer, S. Mathur, Use of metallic nanoparticles to improve the thermophysical properties of organic heat transfer fluids used in concentrated solar power, *Solar Energy* 105 (2014) 468-478.
6. S. U. S. Choi, Nanofluids: from vision to reality through research, *Journal of Heat Transfer – ASME* 131 (2009) 033106.
7. D. H. Yoo, K. S. Hong, H. S. Yang, Study of thermal conductivity of nanofluids for the application of heat transfer fluids, *Thermochimica Acta* 455 (2007) 66-69.
8. D. S. Wen, G. P. Lin, S. Vafaei, and K. Zhang, Review of nanofluids for heat transfer applications, *Particuology* 7 (2009) 141-150.
9. CEA. Nanofluids for heat transfer applications. France: Marketing Study Unit, CEA; 2007.
10. S. K. Verma, and A. K. Tiwari, Progress of nanofluid application in solar collectors: a review, *Energy Conversion and Management* 100 (2015) 324-346.
11. H. A. Mohammed, A. A. Al-Aswadi, N. H. Shuaib, and R. Saidur, Convective heat transfer and fluid flow study over a step using nanofluids: a review, *Renewable and Sustainable Energy Review* 15 (2011) 2921-2939.

INFLUENCE OF HIGH TEMPERATURE EXPOSURE IN THERMAL AND OPTICAL PROPERTIES OF THERMAL OIL-BASED SOLAR NANOFLUID

A. Gimeno-Furio, N. Navarrete, R. Martínez-Cuenca, J.E. Julia* and L. Hernandez

Departamento de Ingeniería Mecánica y Construcción

Universitat Jaume I

12071 Castellón de la Plana, Spain

*Corresponding author: Enrique.julia@uji.es

Keywords: solar nanofluid, thermal oil, thermal cycling

Introduction: Solar nanofluids are transparent fluids in the visible and near infrared range with low loads of dispersed nanoparticles with high absorption for the solar radiation. These solar nanofluids were proposed as volumetric solar radiation receivers [1-2]. Additionally, if a thermal oil is used as the base fluid of the nanofluid, the nanoparticles directly absorb the solar radiation, transferring the heat to the heat transfer fluid. In this way, high efficiency from solar radiation to thermal energy can be obtained, which makes these thermal oil-based solar nanofluid a promising material for future renewable energy technologies. However, industrial implementation of the solar nanofluids depend on several factors, including nanofluid stability, good thermal and optical response at temperatures as close as possible to that found in the applications and good response to high temperature exposure.

Discussion and Results: In this work, a solar nanofluid of Therminol 66 and tin (Sn) nanoparticles (80nm) is developed and characterized. The selection of Sn is based on their absorption spectrum in the visible range of solar radiation. In order to assure the solar nanofluid stability, different dispersants were evaluated and Diphenyl Sulphone (DS) was selected due to their good response under thermal cycling.

The solar nanofluid was kept up to 3 hours in an oven with a temperature up to 200°C. Thermal and optical characterization of the solar nanofluid were performed before and after the high temperature exposure. These measurements include absorption spectrum, thermal conductivity, specific heat and particle size distribution of the sample. The measurements have been performed at room temperature and also at temperatures closer to those found in the industry.

The results obtained for the thermal oil- solar based nanofluid absorption spectrum at room temperature before the thermal cycling are shown in the next figure:

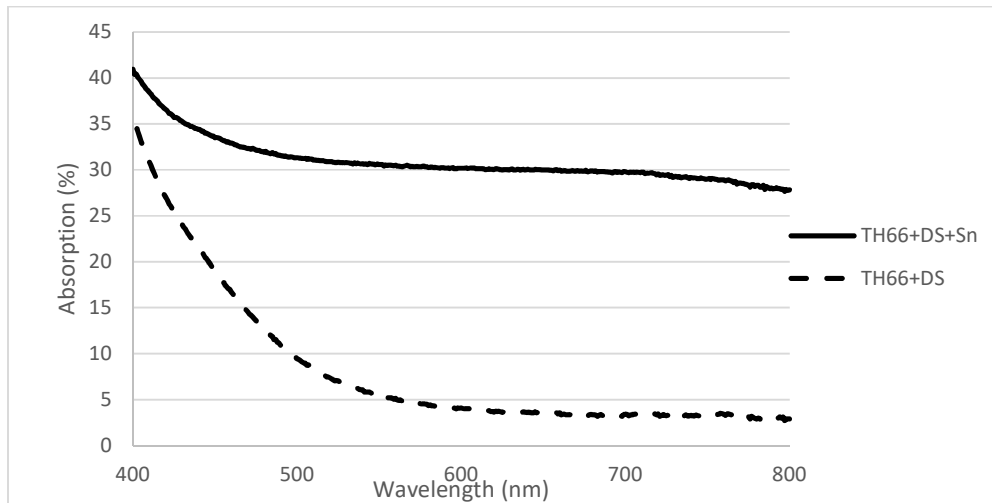


Fig 1. Absorption spectrum at room temperature of thermal oil-based nanofluid

Conclusions: Sn thermal oil-based nanofluids have been synthesized and thermal and optically characterized. This type of nanofluid can be used for solar harvesting applications since it has a constant absorption spectrum in the entire solar radiation wavelength. Thermal properties of Sn thermal oil-based nanofluids have been characterized at high temperature conditions showing expected results. The modification of the properties of the solar nanofluid after the high temperature exposure has been also evaluated.

References:

1. R.A. Taylor, P.E. Phelan, R.S. Prasher. *Experimental results for light-induced boiling in water-based graphite nanoparticle suspensions*, Proceedings of the ASME 2009 Summer Heat Transfer Conference 2009, pp. 1–9.
2. R.A. Taylor, P.E. Phelan, T.P. Otanicar, C.A. Walker, M. Nguyen, S. Trimble, R.S. Prasher *Applicability of nanofluids in high flux solar collectors*. *J. Renewable Sustainable Energy* 3, 2011, 023104. <http://dx.doi.org/10.1063/1.3571565>

SYNTHESIS OF TIN/ETHYLENE GLYCOL SOLAR NANOFLUID BY A FEMTOSECOND LASER-ASSISTED TECHNIQUE

R. Torres Mendieta¹, R. Mondragón², V. Puerto Belda^{1*}, O. Mendoza Yero¹,
J. Lancis¹, G. Mínguez Vega¹ and J. E. Juliá²

Departamento de Química, CICECO, Universidade de Aveiro, 3810-193 Aveiro, Portugal

*Corresponding author: vpuerto@uji.es

Keywords: Nanotechnology, nanoparticles, laser ablation, femtosecond laser, absorption, optical properties

Introduction: Nowadays, solar energy extends over wide geographical areas and is becoming an essential means to keep up to the ever-increasing worldwide energy demand with minimal environmental impact. Traditionally, in conventional solar–thermal systems a heat transfer fluid is surrounded by a black surface absorber that convert the majority of the incoming solar radiation into heat that is subsequently transferred to the fluid. However, as the heat generation at the absorber is separated from the fluid, this causes radiative losses and the consequent lower in the efficiency. In 2009, solar nanofluids, an innovative type of nanofluids that are able to direct harvest solar radiation, were proposed for renewable solar thermal power applications [1]. The basic idea of a solar nanofluid is to use heat transfer fluids, which usually have low absorption in the visible and near infrared range in combination with nanoparticles. In this way, a volumetric absorption within the solar fluid itself is promoted, which increases the photothermal efficiency by at least 10% [2].

Discussion and Results: In this work, tin/ethylene glycol nanofluid samples were prepared by using pulsed laser ablation in liquids (PLAL) [3] techniques and the standard two-step method. The synthesis of PLAL's solar nanofluid was carried out using a Ti:Sapphire laser (Femtopower Compact Pro, Femtolasers), that emits pulses of 30 fs intensity full width at half maximum (FWHM) with a central wavelength of 800 nm and 1 kHz repetition rate. The thickness of the ethylene glycol (EG) layer above the tin was about 1 mm. The laser beam with a size of 6 mm diameter was focused by a lens of 75 mm with a mean power of 180 mW while moving the target perpendicular to the beam propagation axis at a constant velocity of 0.45 mm/s. The interaction of the pulsed laser radiation with the solid tin immersed in the ethylene glycol promotes the extraction of material from its surface in the form of an ablation plume. Tin nanoparticles (NPs) are formed from the ejected material and they are collected in the ethylene glycol as colloids creating the solar nanofluid.

For comparison, we also made a solar nanofluid with commercial tin nanoparticles by carefully mixing the nanoparticles with ethylene glycol at the same concentration. Commercial tin NPs were purchased from US Research Nanomaterials, Inc. NPs have a primary particle size of 60–80 nm and a density of 7310 kg/m³ according to the manufacturer. Nanofluids were prepared by

dispersing the corresponding amount of solid in ethylene glycol (EG; reagent grade, Scharlab S.L.). To break the agglomerates in the powder, the dispersion process was carried out by ultrasonic treatment with an ultrasonic probe UP400s (Hielscher Ultrasonics GmbH, Germany). The nanofluid was sonicated for 15 min immersed in an ice bath until the highest degree of dispersion was achieved.

To assure a good behaviour of the nanofluid through the time, it is important to characterize its stability for prolonged periods of time. A visual inspection of as-produced nanofluids over time was carried out. Figure 1 shows an image of PLAL nanofluid (top) and nanofluid synthesized by using the two-step method with commercial NPs (bottom) after 1, 4 and 10 days from its production. It was observed that a sedimentation of the heavier NPs at the base of the cuvette occurred. However, the stability of the nanofluid produced by PLAL was higher.

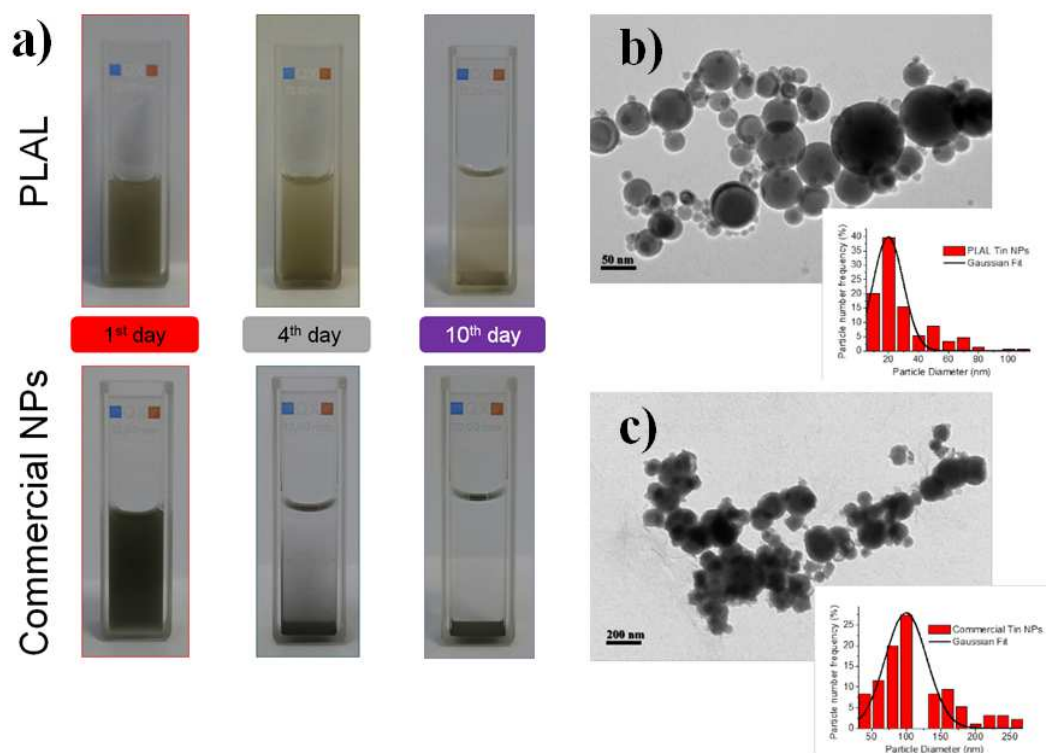


Figure 1. a) Picture of the solar nanofluids at the 1st, 4th and 10th day showing nanoparticle sedimentation over the time. Transmission electronic microscopy micrographs of b) nanofluid prepared by PLAL, c) nanofluid prepared by using commercial tin NPs. The inset of both micrographs represents a histogram showing the statistical size distribution of NPs contained in both nanofluids.

Micrographs of the NPs are shown in Figure 1. Nanoparticles produced by PLAL (Fig. 1 b)) show a higher sphericity and less aggregation than those synthesized by a chemical methods (Fig. 1 c)).

To evaluate the sunlight absorption capability of the nanofluid, which is directly related to the nanofluid efficiency, the transmission solar spectral irradiance through 1 cm of the nanofluid was calculated. For this purpose, the reference solar spectral irradiance, $I(\lambda)$, ASTM G-173 for a mass air of 1.5 (see Figure 2) was considered. The transmission solar spectral irradiance through the nanofluid is obtained by multiplication of the reference solar spectral irradiance by the transmittance spectra in 1 cm of nanofluid. In this way, we can qualitatively identify the transmission of our nanofluid related to the solar spectrum. Figure 2 shows the results for a) the PLAL nanofluid and b) the two-step nanofluid developed with commercial tin NPs. It is observed that for the first and second days both samples have a similar transmission behaviour. However, after the fourth day, the transmission of the PLAL sample is clearly lower. This can be attributed to its enhanced stability and is corroborated by visual inspection in Figure 1 a).

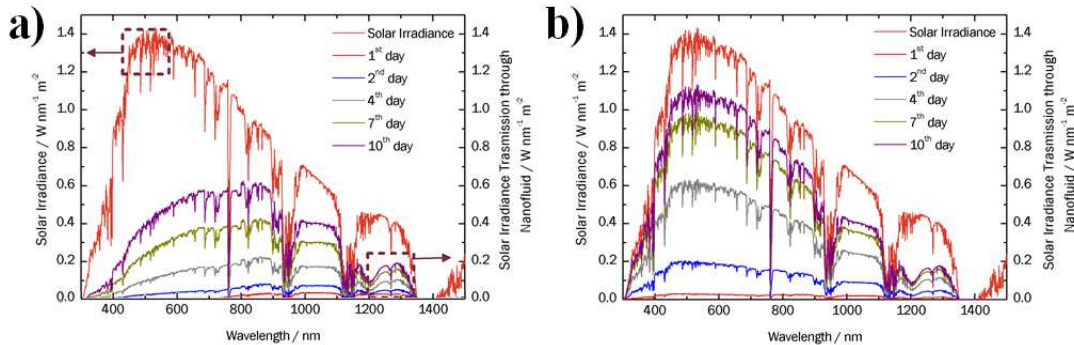


Figure 2. Reference solar spectral irradiance ASTM G-173 and the transmission of solar spectral irradiance through 1 cm of the nanofluid several days after formation: a) PLAL and b) commercial nanofluid.

In a first order approximation, calculations of the fraction of the incident power absorbed in the nanofluid after a path length of 1 cm have been done at the fourth, seventh and tenth days in order to study the temporal evolution of nanofluid performance. A detailed mathematical description of the methodology used can be found in Ref. [4]. In short, the experimental extinction coefficient of NPs decoupled from the base fluid contribution can be extracted from the transmission spectra. Then, the Rayleigh theory is used to calculate the scattering albedo which is required to calculate the spectral absorption coefficient, $\mu_{abs}(\lambda)$. Finally, to evaluate the sunlight absorption capability of nanofluid, the fraction F of the incident power absorbed in the fluid after a path length l within it is calculated from Equation [1]:

$$F(l) = 1 - \frac{\int_{\lambda_{\min}}^{\lambda_{\max}} I(\lambda) \cdot e^{-\mu_{abs}(\lambda) \cdot l} d\lambda}{\int_{\lambda_{\min}}^{\lambda_{\max}} I(\lambda) d\lambda} \quad [1]$$

where λ represents the wavelength, λ_{max} represents the maximum wavelength considered, λ_{min} the minimum wavelength considered, $\mu_{abs}(\lambda)$ the spectral absorption coefficient, and $I(\lambda)$ represents the solar spectra irradiance. In our calculations the sunlight absorption was calculated for the spectrum between 400–1500 nm and path length $l=1$ cm. This calculation considers ethylene glycol as base fluid and tin as the NPs. Under this circumstances, the simulation predicts that the absorbed sunlight fraction of the nanofluid synthesized by PLAL is at least the double than the commercial one as show in Table 1 [5].

Table 1. Absorbed sunlight fraction of the nanofluid for different days.

Day	PLAL nanofluid	Commercial nanofluid
4 th	67%	29%
7 th	57%	19%
10 th	48%	18%

Conclusions:

In this contribution, it was demonstrated that PLAL can be used to produce direct volumetric absorbers with remarkable thermal properties composed by tin and ethylene glycol for its exploitation in the harvesting of solar radiation field. By means of visual observation, DLS, the measurement of the thermal conductivity, and transmission spectra of the samples through the time, we show that the nanofluid produced by PLAL traps the electromagnetic radiation in a more convenient manner than nanofluids produced through conventional synthesis methods. Additionally, it shows a better stability against sedimentation.

References:

1. T. P. Otanicar, P. E. Phelan, and J. S. Golden, Optical properties of liquids for direct absorption solar thermal energy systems, *Sol. Energy* 83 (2009) 969-977.
2. A. Lenert and E. N. Wang, Optimization of nanofluid volumetric receivers for solar thermal energy conversion, *Sol. Energy* 86 (2012) 253-265.
3. V. Amendola and M. Meneghetti, Whats controls the composition and the structure of nanomaterials generated by laser ablation in liquids solutions, *Phys. Chem. Chem. Phys.* 15 (2013) 3027-3046.
4. R. Mondragón, R. Torres-Mendieta, M. Meucci, G. Mínguez Vega, E. Juliá, and E. Sani, Synthesis and characterization of gold/water nanofluids suitable for thermal applications produced by Femtosecond Laser Radiation, *J. Photonics Energy* 6 (2016) 034001.
5. R. Torres Mendieta, R. Mondragón, V. Puerto Belda, O. Mendoza Yero, J. Lancis, G. Mínguez Vega, and J. E. Juliá, Characterization of tin/ethylene glycol solar nanofluids synthesized by femtosecond laser radiation, *ChemPhysChem* 18 (2017) 1055-1060.

Abstracts

SESSION 7A: STABILITY, THERMAL CONDUCTIVITY AND OTHERS

AQUEOUS BASED BORON NITRIDE NANOFLUIDS FOR THERMAL MANAGEMENT APPLICATIONS: FORMULATION, STABILIZATION AND CHARACTERIZATION

G. Zhang, M.E. Navarro and Y. Ding*

School of Chemical Engineering, University of Birmingham, UK

*Corresponding author: y.ding@bham.ac.uk

Keywords: Boron nitride, aqueous nanofluids, thermal conductivity enhancement, stability.

Introduction: Thermal management (TM) is vital for many industrial sectors including computing, telecommunication and defense. Heat transfer intensification (HTI) is one of the key enabling technologies for the TM, which can be realized through the use of an efficient heat transfer fluids (HTF), an extended heat transfer surface, and the change of heat transfer fluid flow and path, to name but a few. This work concerns the use of nanofluids as a HTF. Such a type of fluids has been reported to be promising in numerous publications [1] [2]. However, no significant industrial applications of such fluids have occurred so far after more than two decades of research and development. An efficient HTF should lead to energy savings, reduction on the process time, increase of the lifespan of devices and improvement of the performance of the system. Clearly, nanofluids with all the expected advantages over traditional HTFs are yet to be formulated. As a result, considerable efforts are still made on the area around the world [3] [4].

Recently, attention has been paid to water based boron nitride (BN) nanofluids due to favorable thermal properties, chemical and physical stabilities and high electrical resistance [5] [6] [7]. . These properties make the BN nanofluids suitable for the cooling of electronic devices with little electromagnetic interference. However, these studies indicate contradictions in terms of the effects of the dispersants [5] [6] [7] and this provides the motivation for this work.

Here we report a recent study on deionized water based boron nitride nanofluids (BN/DI water). A two-step method was used to formulate the nanofluids with and/or without surfactants (Gum Arabic, Tween20 and Tween 80). The stability of the formulated nanofluids with different mass concentrations (0.05%-0.5% wt) was studied and their properties relevant to the cooling processes were characterized.

Materials and methods: Boron nitride nanoparticles (99% purity) with a nominal particle size smaller than ~150 nm were used to formulate the nanofluids of different concentrations: 0.05 % wt, 0.1 % wt and 0.5 wt. %. Gum Arabic (from acacia tree, Tween 20(polyoxyethylene-20-sorbitan monooleate) and Tween 80 (polyoxyethylene-20-sorbitan monooleate) were used as dispersants for the formulations. Boron nitride and surfactants were all purchased from Sigma-Aldrich and used without further purification. Deionized water was used as the base liquid.

The two-step method was used for the preparation of the nanofluids. The concentrations of the dispersants were the same as that of the BN nanoparticles. Ultrasonication was used to mix and homogenize the suspensions Fig. 1 illustrates the change of particle size as a function of the ultrasonic processing time. One can see a rapid decrease in size with time initially followed by a plateau after about 40min. Over the process, the average BN nanoparticle size reduced from 763 nm to ~360nm in 40min and 340nm in 60 min. A comparison of the measured size with the nominal size of BN nanoparticles from the provider (~150nm) suggest large aggregates of the BN nanoparticles as purchased; the ultra-sonication cannot completely disaggregate the agglomerates. In this work, a sonication time of 60 min was chosen for the preparation of all samples.

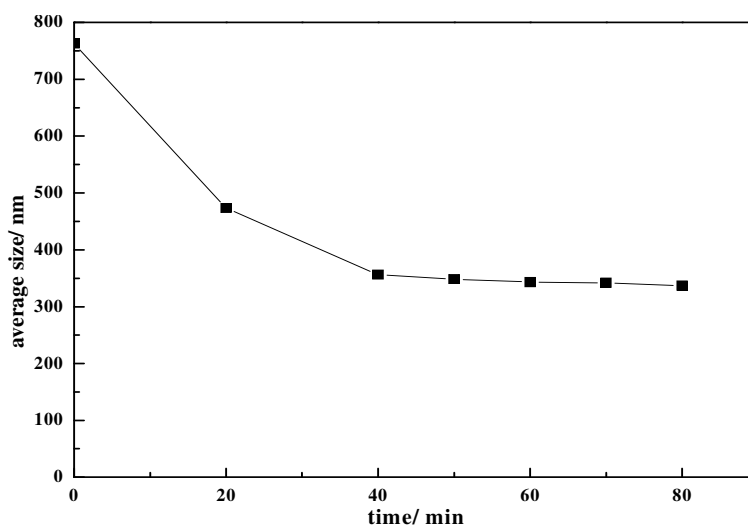


Fig. 1 The particle size with the ultrasonic time

Dynamic light scattering (DLS) analysis was used to measure the nanoparticles size distribution in DI water. Fig. 2 shows the particle size distribution (PSD) of 0.05% BN/DI water nanofluids without surfactant after being sonicated 60 minutes. The PSD varies from 130 nm to 720 nm with an average size of 336.8 nm after being sonicated for one hour. This size is larger than the claimed 150nm on BN nanoparticle label that proves the suspended nanoparticles agglomeration.

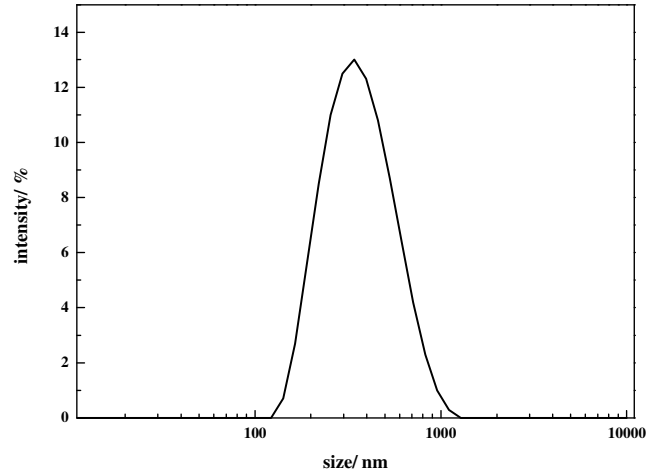


Fig. 2 PSD of 0.05% BN/DI water nanofluids without surfactant

Results and discussion

Effect of pH on stability

The pH has a great effect on the stability of the dispersion due to its effect on particle surface charge and hence the repulsive forces between NB particles in water. **Fig. 3** represents the variation of the zeta potential versus the pH. One can see that the isoelectric point (IEP) of BN nanoparticles in deionized water is around pH 2.4 and a pH value above 8 is expected to give a good stability where the zeta potential falls below -25mV .

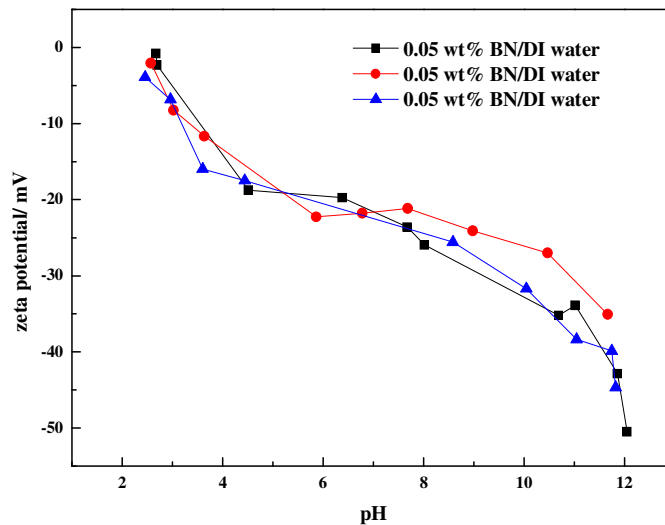


Fig. 3 Zeta potential as a function of pH for 0.05% BN/DI water without surfactant.

Effect of dispersants on stability

Fig. 4 shows the time evolution of the average particle size of 0.05% wt BN nanofluids with and without the use of dispersants. In the absence of dispersants, the average size increases from 336.8 nm to 380.5 nm after 8 days (**Fig. 4a**) and sedimentation can be clearly seen in the bottom of the vials. With the dispersants, the suspensions remain stable up to two weeks (**Fig. 4b**); the sizes with Gum Arabic, Tween 20 and Tween 80 increase respectively from 342 nm to 401 nm, 305 nm to 336 nm, and 321 nm to 332 nm. This shows that the use of the dispersants can increase the nanofluids stability with the Tween 20 and Tween 80 being more effective than with Gum Arabic.

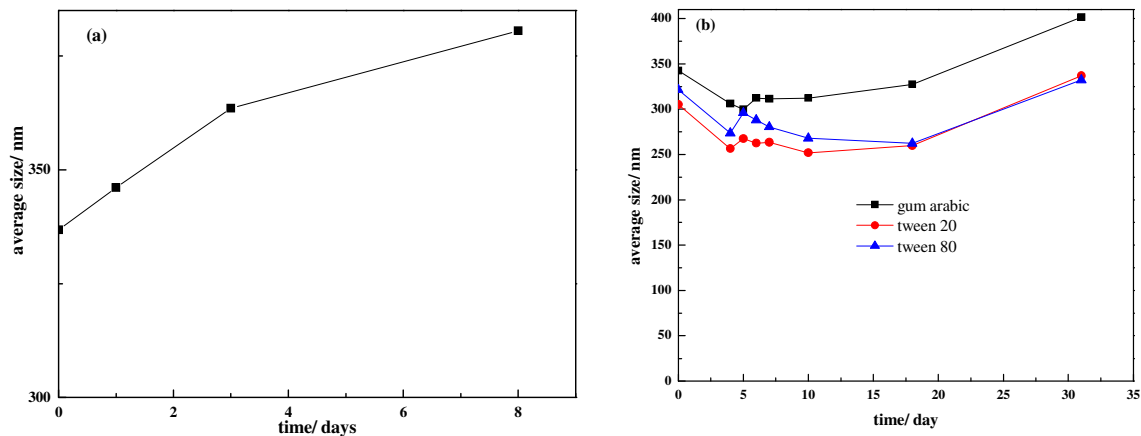


Fig. 4 Average particle size of 0.05% BN/DI water versus time of (a) without surfactant and (b) 3 different surfactants

Conclusions:

In the present study, the water based BN nanofluids have been formulated with and without the use of dispersants (Gum Arabic, Tween 20 and Tween 80). The main outcomes are listed below:

- (1) The isoelectric point of the aqueous based BN nanofluids is about 2.4. A pH higher than 8 gives a zeta potential greater than 25mV, which could stabilize the BN/DI water based nanofluids.
- (2) The use of dispersant enhances the nanofluids stability with Tween 80 and Tween 20 giving the best dispersion stability.

Acknowledgements

The authors acknowledge the finance support from Engineering and Physical Sciences Research (EPSRC) Council, UK – Integrated GaN-Diamond Microwave Electronics: From Materials, Transistors to MMICs (EP/P00945X/1).

References:

1. S. Sharma and S. Mital Gupta, Preparation and evaluation of stable nanofluids for heat transfer application: A review, *Experimental Thermal and Fluid Science* 79 (2016) 202-212.
2. M. Raja, R. Vijayan, P. Dineshkumar, and M. Venkatesan, Review on nanofluids characterization, heat transfer characteristics and applications, *Renewable and Sustainable Energy Reviews* 64 (2016) 163-173.
3. X. F. Li, D. S. Zhu, X. J. Wang, N. Wang, J. W. Gao, and H. Li, Thermal conductivity enhancement dependent pH and chemical surfactant for Cu-H₂O nanofluids, *Thermochimica Acta* 469 (2008) 98-103.
4. M. Mehrali, E. Sadeghinezhad, S. T. Latibari, S. N. Kazi, M. Mehrali, M. N. B. M. Zubir, and H. S. C. Metselaar, Investigation of thermal conductivity and rheological properties of nanofluids containing graphene nanoplatelets, *Nanoscale research letters*, 9 (2014) 1-12.
5. M. Krishnam, S. Bose, and C. Das, Boron nitride (BN) nanofluids as cooling agent in thermal management system (TMS), *Applied Thermal Engineering* 106 (2016) 951-958.
6. C. Zhi, Y. Xu, Y. Bando, and D. Golberg, Highly thermo-conductive fluid with boron nitride nanofillers, *ACS Nano*, 5 (2011) 6571-6577.
7. B. Ilhan, M. Kurt, and H. Ertürk, Experimental investigation of heat transfer enhancement and viscosity change of hBN nanofluids, *Experimental Thermal and Fluid Science* 77 (2016) 272-283.

EFFECTS OF AGITATION AND ULTRASONICATION ON DISPERSION AND THERMAL CONDUCTIVITY OF AQUEOUS TiO₂ NANOFUIDS

K. Cacia^{1,2}, F.E.B. Bioucas³, S.M.S. Murshed^{3*}, M.J.V. Lourenço³, F.J.V. Santos³, C.A. Nieto de Castro³

¹Universidad Nacional de Colombia, Advanced Material Science Group, Calle 59A 63-20, Medellín, Colombia

²Instituto Tecnológico Metropolitano, Faculty of Engineering, Advanced Material Science Group, Calle 54A No 30-01, Medellín, Colombia

³Centro de Química Estrutural, Faculdade de Ciências, Universidade de Lisboa
1749-016 Lisboa, Portugal

*Corresponding author: smmurshed@ciencias.ulisboa.pt

Keywords: Nanofluids, Thermal conductivity, Stability, Agitation, Ultrasonication, Nanoparticles

Introduction: In recent years, nanofluids have received huge interest from researchers and industrial people and thus extensive research works have been performed on various areas of these engineered fluids [1-3]. Despite some good developments in some areas, the real use of nanofluids in potential applications particularly in thermal management systems remain very challenging and beyond reach mainly due to not yet understanding the underlying mechanisms and also not able to have long-term stability of prepared nanofluids [1]. If nanoparticles are not well-dispersed and stable for long period in host fluids, nanofluids can neither exhibit desired high thermophysical properties nor can be used in real application particularly in close systems. Thus, it is of great importance to make sure that the added nanoparticles are properly (homogenously) dispersed in base fluids and nanofluids have as long stability. However, it is very challenging to achieve such long-term stability as many factors such as nanofluids preparation, nanoparticles types, size shapes, purity and degree of agglomerations as well as properties of base fluids are involved in this process. Various techniques, which include sonication, surfactant addition, agitation, and surface treatment of nanoparticles are commonly employed for better stability of sample nanofluids. However, most of the cases nanofluids are undergone sonication as well as having addition of various surfactants into them. Both of these means need to be carefully studied and understood before applying to sample nanofluids preparation for their better stability and properties without changing the chemistry of nanofluids and the original structures of nanoparticles [4-5]. On the one hand, addition of surfactant should be avoided as it can change the chemical composition and some properties of the nanofluids at different conditions (temperature and pressure) besides making nanofluids a three-phasic (nanoparticles, base fluids, surfactant) complex system. In case surfactant is to be used, its adverse effects due to adding wrong and excessive amount (must not exceed its critical

micelle concentration limit) need to be accounted for. On the other hand, though ultrasonication is most widely used in nanofluids studies, there is a lack of adequate knowledge on the effects of its various parameters and duration of use. For instance, the effects of amplitudes, frequency, power settings etc of (ultra) sonicator and its duration of use on the samples and their properties particularly on thermal conductivity are neither well understood nor carefully studied. Therefore, this study aims to identify the influence of sonication and agitation on the dispersion of TiO₂ nanoparticles and the thermal conductivity of their water-based nanofluids.

Samples and Experiments: Sample nanofluid was prepared with a very low concentration (0.1 w/w %) of TiO₂ nanoparticles of 20 nm and of spherical shape (from IoLiTec, Germany) in water (Milli-Q®). As-prepared nanofluid was then underwent ultra-sonication (Hielscher UP200Ht ultrasonic processor) at various amplitudes and different short time periods (0.5 to 6 mins using a pulse cycle of 0.5s on and 0.5s pause in order to avoid over heating of the sample) and the optimum ultrasonication amplitude (%) was obtained.

A schematic chart of the experimental methodology employed in this study is shown in Fig. 1. Besides visualization, UV-vis absorbance analysis was performed to identify the optimum dispersion and amplitude of the ultrasonicator. A double beam UV-Vis spectroscopy (Hitachi 100-40) was employed to determine the effects of added TiO₂ nanoparticles and sonication time on the dispersion behavior of nanofluids at $\lambda=520$ nm. It is known that the UV-Vis absorption spectroscopy provides useful information on the degree of dispersion of nanoparticles in nanofluids.

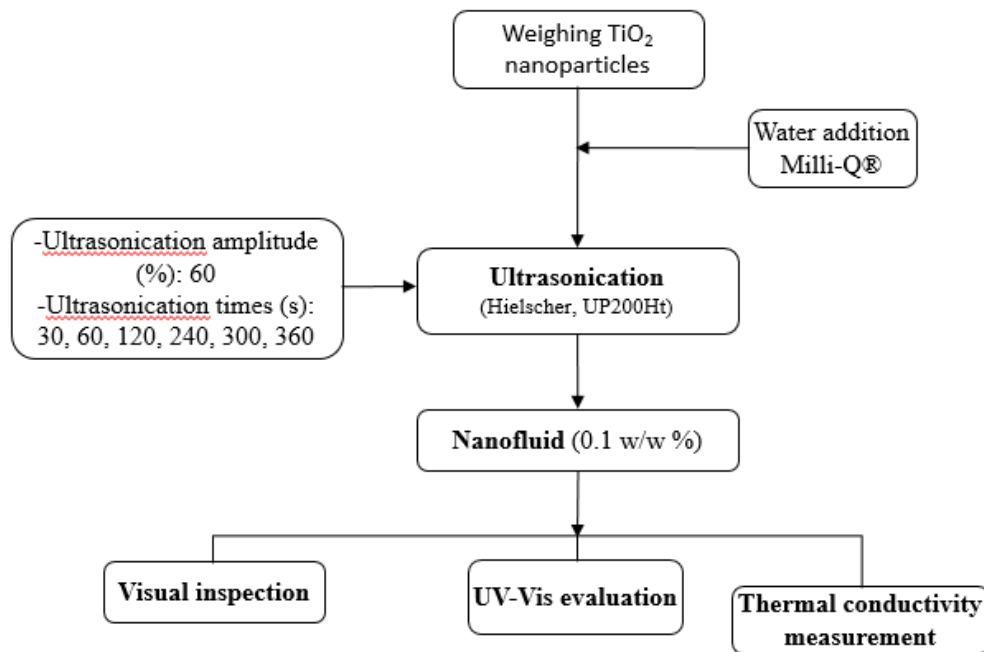


Figure 1. Schematic diagram of experimental methodology.

After sonication the thermal conductivity of sample nanofluids with agitation and without agitation was measured using a Hukseflux TPSYS08 device in conjunction with probe (non-steady-state thermal conductivity probe).

Results and discussion:

Ultrasonication amplitude effect: As mentioned before, employing sonication (ultra) during nanofluids sample preparation is the most effective and used technique. However, most of the studies failed to realize the importance of factors/parameters of the sonicator used and thus the values of these parameters are missing in most of published articles. One of such key parameters is the amplitude of ultrasonicator which mainly control the degree of dispersion and duration of sonication needed for particular samples. In this study, sample nanofluids were undergone ultrasonication at different amplitudes (20, 40 and 60%). Determination of UV-vis absorbance with respect to sample elapse time showed a minor variation in absorbance at 60% amplitude which indicates the best dispersion of nanoparticles as depicted in Fig. 2 with the sample and sonication information in the inset table. Thus an amplitude setting of 60% was used in this study.

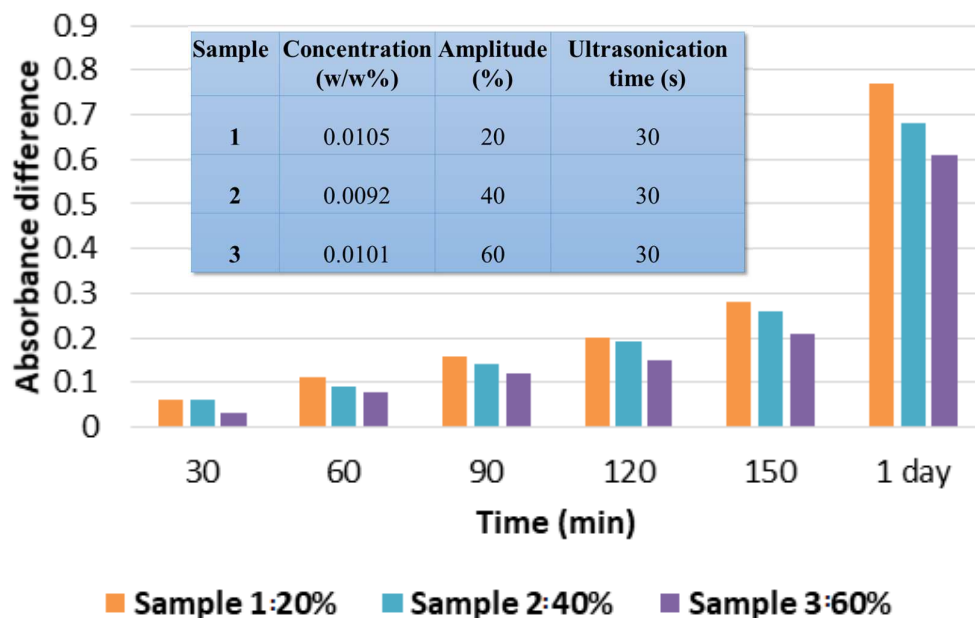


Figure 2. Absorbance variation of with respect to nanofluids elapse time at different amplitudes.

UV-vis absorbance and visual inspection: After completing each sonication the UV-vis absorbance of sample nanofluids was measured to evaluate the level of dispersion of nanoparticles. Table 1 shows magnitude of UV-Vis absorbance of a sample nanofluid on the

day of preparation and after 5 days at different sonication times. Table 1 indicates an increase in degree of agglomeration/sedimentation of this nanoparticle after 5 days. The increased sedimentation of nanoparticles can more clearly be evidenced from the visual inspection as shown in Fig. 3 which contains images of sample nanofluid at four different sonication times (s) at the day of preparation and after 5 days of preparation of the sample. As can be seen from Fig. 3 almost all nanoparticles are settled down at the bottom of the cuvettes within 5 days. This connotes that more measures to be taken in order to obtain better dispersion of nanoparticles and thus longer stability of nanofluids.

Table 1. UV-Vis absorbance of a fresh sample nanofluids and after 5 days at different ultrasonication times.

Sonication time (s)	Absorbance at day of preparation	Absorbance after five days
180	2.87	0.13
240	3.01	0.13
300	3.05	0.14
360	3.06	0.14

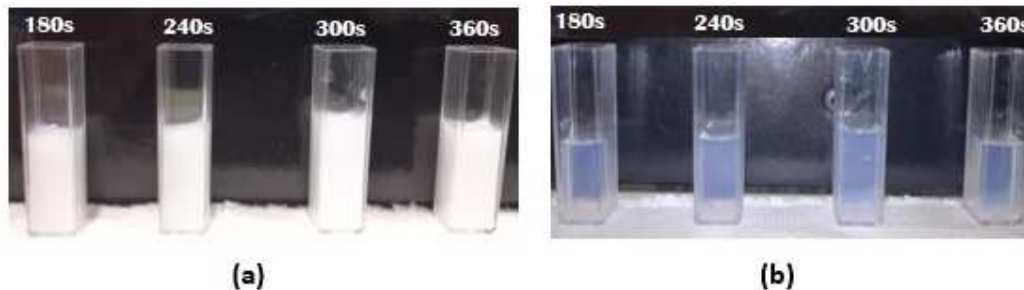


Figure 3. Visual evidence of sample nanofluids at 4 different times (s): (a) at the day of preparation and (b) 5 days after the preparation.

Agitation effect on thermal conductivity: Besides ultrasonication effect of agitation on the thermal conductivity was also studied. As commonly used, a magnetic stirring bar was employed in side the sample container used in Hukseflux (TPSYS08) device and thermal conductivity was measured while the sample underwent agitation. No noticeable effect of such agitation on the thermal conductivity of this nanofluids was observed as reported in Fig. 4. It can also be seen (Fig.4) that at the day of preparation (day 1) the thermal conductivity of nanofluid without agitation is slightly higher than that of nanofluids with agitation. Nonetheless, all these thermal

conductivity data fall within the measurement uncertainties. It was interesting to observe that during thermal conductivity measurement while agitating the nanofluids, nanoparticles were found adhering to the measurement probe as well as the wall of the cell container, which can be seen from the images shown in Fig. 4. This demonstrates that any kind of such agitation during the measurement will neither increase the stability nor can have any positive effect on the thermal conductivity of nanofluids.

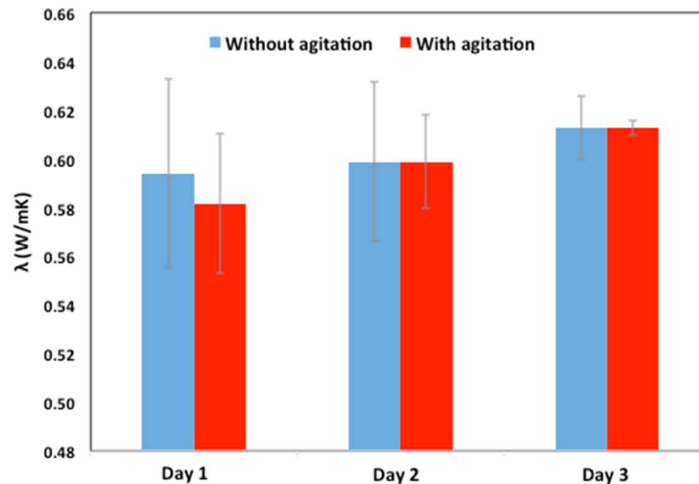


Figure 4. Thermal conductivities of TiO_2 /water nanofluids with and without agitation.



Figure 4. Visual inspection after thermal conductivity measurements with magnetic stirring (top left image showing the probe and all others showing the container).

Temperature effect on thermal conductivity: After performing ultrasonication, thermal conductivity of nanofluid was measured at different temperatures ranging from room temperature to 60°C. Figure 5 demonstrates that thermal conductivity of water increases due to addition of small concentration (0.1 w/w %) of this TiO₂ nanoparticles and it increases with increasing the temperature. It is also apparent that the enhancement of the thermal conductivity of nanofluids relative to base fluid (water) increases as the temperature increases. This is interesting as nanofluids can perform better heat transfer (like cooling) at high temperature conditions.

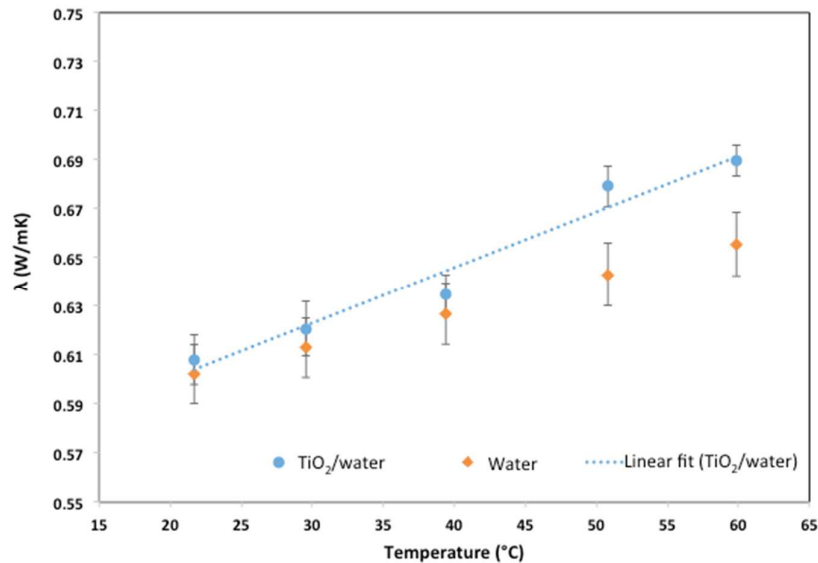


Figure 5. Thermal conductivity of water and TiO₂/water nanofluid as a function of temperature.

Conclusions: This study demonstrates that regardless of the brand of ultrasonication device used, the proper amplitude setting and sonication duration are very crucial for the better dispersion of nanoparticles without any adverse effect.

UV-vis absorbance determination with respect to time showed that the best dispersion of nanoparticles can be obtained at 60% amplitude setting of ultrasonicator for this nanofluid.

The agitation (by magnetic stirrer) was found to have no noticeable influence on the thermal conductivity of this nanofluid. In addition, due to using agitation to the sample nanofluids during the measurement of thermal conductivity nanoparticles were found to adhere to the measurement probe as well as the wall of the sample container.

Furthermore, the thermal conductivity of this nanofluid was observed to be higher than that of the pure water and the enhanced thermal conductivity increased noticeably with increasing temperature.

Nonetheless, more extensive and systematic studies on the dispersion of nanoparticles and stability of nanofluids as well as their impact on the thermal conductivity of nanofluids are to be performed.

References:

1. S.M.S. Murshed and C.A. Nieto de Castro, *Nanofluids: Synthesis, Properties and Applications*, Nova Science Publishers Inc., New York, 2014.
2. S.M.S. Murshed, C.A. Nieto de Castro, M.J.V. Lourenço, M.L.M. Lopes and F.J.V. Santos, A review of boiling and convective heat transfer with nanofluids, *Renewable and Sustainable Energy Review* 15 (2011) 2342-2354.
3. S.M.S. Murshed and C.A. Nieto de Castro, Conduction and convection heat transfer characteristics of ethylene glycol based nanofluids—A review, *Applied Energy* 184 (2016) 681-695.
4. M.J.V. Lourenço and S.I. Vieira, Nanofluids preparation methodology, in *Nanofluids: Synthesis, Properties and Applications*, Eds., Murshed SMS, Nieto de Castro CA, Ch. 1, pp.1-28, Nova Science Publishers Inc., New York, 2014.
5. C.A. Nieto de Castro, S.I. Vieira, M.J.V. Lourenço and S.M.S. Murshed, Understanding stability, measurements, and mechanisms of thermal conductivity of nanofluids, *Journal of Nanofluids* 6 (2017) 804-811.

RE-DISPERSION ABILITY OF MWCNT WITHIN OILS

A. Alasli¹ and A. Turgut^{2*}

¹Dokuz Eylul University, The Graduate School of Natural and Applied Sciences, Mechanical Engineering Department, Tinaztepe Campus, 35397, Buca, Izmir, Turkey

²Dokuz Eylul University, Engineering Faculty, Mechanical Engineering Department, Tinaztepe Campus, 35397, Buca, Izmir, Turkey

*Corresponding author: alpaslan.turgut@deu.edu.tr

Keywords: Nano-lubricant, MWCNT, 3ω method, Thermal Conductivity, Viscosity, Re-dispersion ability

Introduction: Among the various types of nano-lubricants, the suspension of carbon nanotube (CNT) has unique importance due to the enormous thermal conductivity of CNT (3000 W/mK MWCNTs [1]) and hence great potential for heat transfer enhancement compared to pure oil. Choi et al [2] and Yang [3] reported the highest achieved enhancement in thermal conductivity. 160% of (α -olefin) oil with the addition of MWCNT at 1 vol. % and 200% for poly (α -olefin) oil containing 0.35% (v/v) respectively. However, since these participations, no researcher was able to re-report such enhancement. Etefaghi et al. [4] investigated functionalized MWCNT with engine oil for four methods of dispersing. The authors suggested that, the sample prepared with planetary ball mill at 0.1 wt.%, which showed 18% thermal conductivity enhancement, is the most suitable sample for improving the properties of the engine oil. Liu et al. [5] also reported a thermal conductivity increment up to 30% at 2 vol.% for CNT/synthetic engine oil with N-hydroxysuccinimide as dispersant. Hwang et al. [6] found that for the case of CNT/synthetic engine oil with sodium dodecyl sulfate as surfactant, the thermal conductivity of 0.5 vol.% is increased to 8.7% compared to the base fluid. Beheshti et al. [7] investigated the effect of oxidized MWCNTs on thermophysical properties of transformer oil and reported 7.7% thermal conductivity enhancement at 0.01 wt.%. Recently, Ilyas et al. [8] provided a complete study that investigated the thermophysical and the rheological properties of MWCNT/engine oil at 0-1 wt.%.

Nevertheless, the main disadvantage of the CNTs is their poor dispersibility in the most of common liquids. Many approaches have been proposed to enhance their dispersibility. Chemical methods, which involves using surfactants or functionalization the tubes, improving their wetting characteristics and reducing their tendency to agglomerate in solvent [9]. In addition, mechanical methods, which collaborate mainly with adjusting grinding or sonication power and duration were also proposed. However, both methods can either seriously damage the CNTs, reshape their aspect ratio, or affect their surfaces resulting changes in the charlatanistic of their dispersions.

Apparently, there is notable number of researches which investigated CNTs. However, none of these studies has reported the re-dispersion ability of MWCNTs within oils, with which the

CNT is dispersible just by agitation. The main objective of this research is to focus the light on the recognized re-dispersion ability of the sonicated MWCNTs within several types of oil without adding any surfactant or using any special treatment to the tubes. Also, the viscosity and the thermal conductivity of the synthesized nano-lubricant were compared for both the freshly sonicated and the re-dispersed samples.

Discussion and Results: Pure MWCNTs, without any special treatment, were dispersed at 0.1 wt. % within five types of oils (low viscous compressor oil, sunflower oil, three types of engine oil (Helix, Star OPT and OPT)) without adding any surfactants. Two-steps method was selected for preparation with an ultrasonic liquid processor (Sonicator 3000, MISONIX Co, USA). The agglomerated tubes were dispersed with a power of 12 W at a frequency of 20 kHz. Mixing time of 40 min (with sequences of 3 sec on /1 sec off in order to prevent overheating) was enough to get homogenous samples.

Due to the effect of the gravitational force and Van der Waal's force, the sonicated MWCNTs starts to sediment and accumulate above each other at different rates according to the viscosity of the based oils. For full sedimentation, it takes between 48 h for the least viscous oil, as shown in Fig. 4 (a), and more than two months for the highest viscous one.

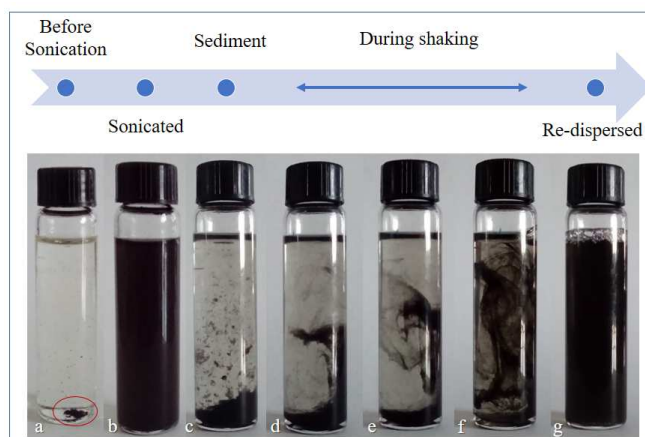


Fig.1. MWCNTs/Compressor oil sample at 0.1 wt.%; (a): before Sonication, (b): Sonicated, (c): Sediment, (d)(e)(f): floating MWCNTs during shaking, (g): Re-dispersed

Nevertheless, it was observed that with any minor motion, done to the agglomerated samples, the sediment carbon nano tubes start to float and hold within the oil, as Fig. 1 (d, e, and f) and Fig. 2 show. Moreover, after well shaking (manually), it seems that we were able to fully re-disperse the agglomerated MWCNTs in oil. The main reason behind this behaviour can be explained in two points. First, the CNTs were reported to be oleophilic (have high affinity to oil) [10]. Consequently, during sonication, the volume of the added MWCNTs was realized to be expanding, which means sonication not only separates and disperses MWCNTs, but also enhances their ability to absorb oil. This can be observed clearly from Fig. 1; notice the difference in the MWCNTs' volume between the case of fully sediment nano-lubricant (c) and

the one before sonication (a). Floating MWCNTs also supports this assumption because it indicates that the density of the sonicated tubes is almost equal to the density of the oil (817.8 kg/m³). In other words, even after agglomeration (sedimentation) the MWCNTs are still saturated and covered with oil since the density of the used MWCNTs in pure statue was reported to be 1911.3 kg/m³ [11]. Also, it is important to mention here that in each taken photo, the floating tubes are holding in oil also for hours. Second, Etefaghi et al. [4] and Beheshti et al [7] observed that adding MWCNTs to oil slightly lowers the nano-lubricant's viscosity comparing to the pure oil at low concentrations. As they concluded, when MWCNTs are dispersed in oil, they are placed between the oil layers which leads to ease the movement of the oil's layers on each other. From this we can also conclude that not only the MWCNTs ease the movement of oil layers on each other, but also the oil layers ease the movement of MWCNTs since these layers create barrier between tubes' surfaces that overcome Van der Waals force.

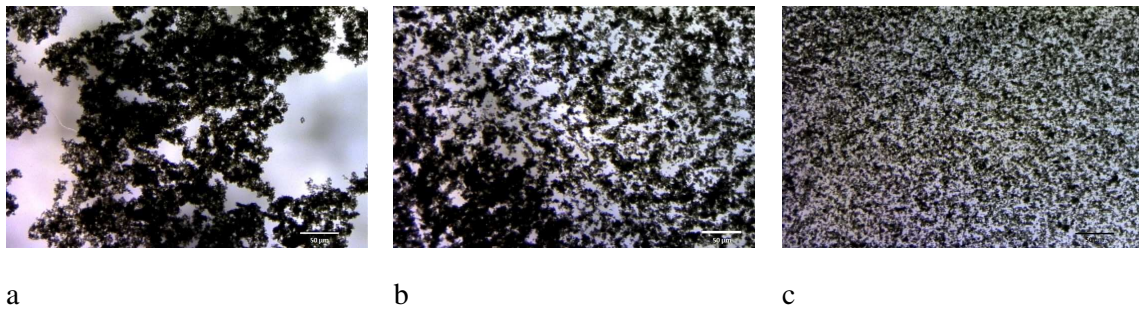


Fig. 2. Optical microscope images of re-dispersing MWCNTs within Oil; (a): Agglomerated, (b): Floating MWCNTs during agitation, (c): Re-dispersed.

A sine-wave Vibro Viscometer SV-10 (A&D, Japan) with a maximum deviation of 4% was employed for measuring the viscosity of the nano-lubricants. From the obtained results, it was noticed that the recently sonicated and re-dispersed samples give equal values within the uncertainty of measurements. Consequently, this indicates that MWCNTs are well re-dispersed within oil. The viscosity values of the studied nano-lubricants are given as a function of temperature in Fig. 3. The dynamic viscosity of the nano-lubricant highly depends on the viscosity of the pure based oil. However, the differences in dynamic viscosity between the nano-lubricant decreases dramatically with the increment of temperature. Also, it is noticed that the decrement trend is become greater with the increment of MWCNTs weight concentration.

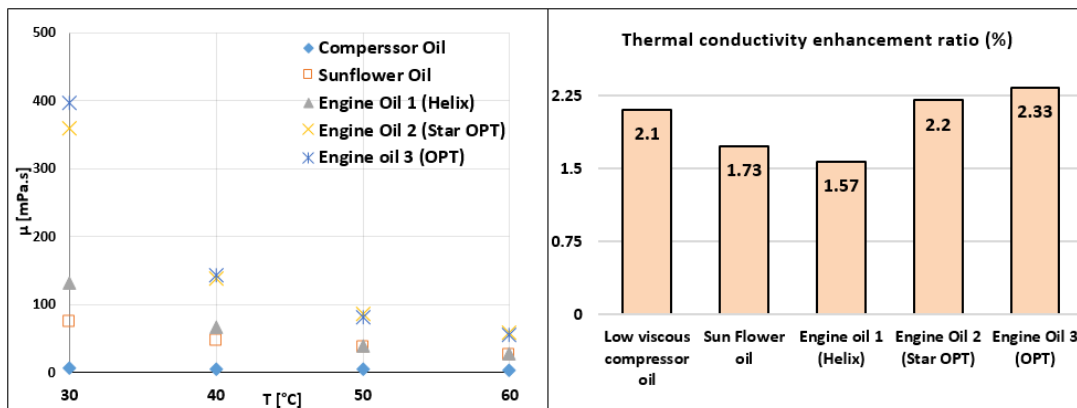


Fig. 3. Dynamic viscosity and thermal conductivity enhancement ratios of MWCNTs/oil with respect of different types of based oil.

Likewise viscosity, the thermal conductivity of recently sonicated and re-dispersed samples was also determined at room temperature with the help of by 3ω hot-wire technique [12]. As anticipated, identical enhancement in thermal conductivity for the both samples were obtained. The enhancement ratios, shown in Fig. 3, were close to the ones of Ilyas et al. [8]. The higher thermal conductivity and the larger specific surface area of CNT, as believed, are the main reason of this increment [5]. In addition, the recently dispersed and re-dispersed MWCNTs can form an extensive network with the same quality that facilitates thermal bridges within the base fluid as presented in Fig. 2. Nevertheless, the increment ratios are not only related to the properties of the chosen MWCNTs but it is also affected by the properties of the based oil, especially its viscosity and thermal conductivity. This is because, as mentioned above, MWCNTs are saturated and covered with thin layers of oil, which work relatively as a thermal isolation between the tubes; these two parameters (viscosity and thermal conductivity of oil) have a notable effect on the thickness of the layers and on the heat transfer rate between the MWCNTs. Also, this can explain why the enhancement in the nano-lubricants was not as high as expected comparing with other base fluids

Conclusions: The objective of the presented study is to investigate the re-dispersion ability of the sonicated MWCNTs within several types of oil. Untreated MWCNTs were dispersed by sonication without using any surfactant. It was observed that the sonicated nano tubes acquire the re-dispersion ability by agitation alone. The sonicated MWCNTs are separated, saturated, lubricated, and surrounded by oil layers, which ease its motion within the lubrication oil and create barriers between their surfaces that overcome Van der Waals force. Viscosity and thermal conductivity of both recently sonicated and re-dispersed samples were also investigated and equal values were obtained within the uncertainty of each measurements.

References:

1. P. Kim, L. Shi, A. Majumdar, P.L. McEuen, Thermal Transport Measurements of Individual Multiwalled Nanotubes, *Phys. Rev. Lett.* 87 (2001) 215502.

2. S.U.S. Choi, Z.G. Zhang, W. Yu, F.E. Lockwood, Anomalous thermal conductivity enhancement in nanotube suspensions, *Appl. Phys. Lett.* 79 (2001) 2252–2254.
3. S. Paolucci, G. Puliti, *Properties of Nanofluid*, CRC, 2015
4. E.-I. o llah Ettefaghi, H. Ahmadi, A. Rashidi, S.S. Mohtasebi, Preparation and thermal properties of oil-based nanofluid from multi-walled carbon nanotubes and engine oil as nano-lubricant, *Int. Commun. Heat Mass Transf.* 46 (2013) 142–147.
5. M.-S. Liu, M. Ching-Cheng Lin, I.-T. Huang, C.-C. Wang, Enhancement of thermal conductivity with carbon nanotube for nanofluids, *Int. Commun. Heat Mass Transf.* 32 (2005) 1202–1210.
6. Y. Hwang, J.K. Lee, C.H. Lee, Y.M. Jung, S.I. Cheong, C.G. Lee, Stability and thermal conductivity characteristics of nanofluids, *Thermochim. Acta.* 455 (2007) 70–74.
7. A. Beheshti, M. Shanbedi, S.Z. Heris, Heat transfer and rheological properties of transformer oil-oxidized MWCNT nanofluid, *J. Therm. Anal. Calorim.* 118 (2014) 1451–1460.
8. S.U. Ilyas, R. Pendyala, M. Narahari, Stability and thermal analysis of MWCNT-thermal oil-based nano fluids, *Colloids Surfaces A.* 527 (2017) 11–22.
9. K.E. Geckeler, T. Premkumar, Carbon nanotubes: Are they dispersed or dissolved in liquids?, *Nanoscale Res. Lett.* 6 (2011) 136–138.
10. T.-C. Huang, P. Li, H. Yao, H.-J. Sue, M. Kotaki, M.-H. Tsai, Highly efficient oil-water separators based on dual superhydrophobic and superoleophilic properties of multiwall-carbon nanotube filtration films, *RSC Adv.* 6 (2016) 12422–12425.
11. T. Evgin, H.D. Koca, N. Horny, A. Turgut, I.H. Tavman, M. Chirtoc, M. Omastová, I. Novak, Effect of aspect ratio on thermal conductivity of high density polyethylene/multi-walled carbon nanotubes nanocomposites, *Compos. Part A Appl. Sci. Manuf.* 82 (2016) 208–213.
12. A. Turgut, C. Sauter, M. Chirtoc, J.F. Henry, S. Tavman, I. Tavman, J. Pelzl, AC hot wire measurement of thermophysical properties of nanofluids with 3w method, *Eur. Phys. J. Spec. Top.* 153 (2008) 349–352.

THE PREPARATION OF Cu@Al₂O₃ NANOFIBER BY ORGANOMETALLIC TECHNIQUE AND ITS APPLICATION IN THE NANOFLUID SYSTEMS

A. Bulut, M Yurderi, I.E. Ertas and M. Zahmakiran*

¹Nanomaterials and Catalysis Research Group, Department of Chemistry, Yuzuncu Yil University, 65080, Van, Turkey

*Corresponding author: z Mehmet@yyu.edu.tr

Keywords: Nanofluid, Copper, Alumina, Nanoparticles

Introduction: Metal nanoparticles are particles that have at least one dimension in the nanometer scale (< 100 nm) [1] and have already found many fascinating applications in a wide variety of fields including nanofluid systems [2]. Metal nanoparticles are kinetically unstable against to bulk metal formation and the aggregation of metal nanoparticles during their use in nanofluid systems to the bulk metal despite using the best stabilizing agents [3] is still the most important problem that should be overcome in their nanofluid applications [2]. At this concern, the synthesis of metal nanoparticles in solid support materials seems to be one of the possible ways for preventing aggregation of small metal nanoparticles into bulk metal [4]. This study is aimed to organometallic synthesis of colloidally stable small sized copper nanoparticles and their decoration onto the Al₂O₃ nanofiber surface and the investigation of heat transfer parameters of nanofluid systems composed of the dispersion of Cu@Al₂O₃ nanofiber in water.

Discussion and Results: Firstly, the solid support matrix Al₂O₃ nanofibers were prepared by using hydrothermal synthesis approach in which aluminium nitrate nonahydrate (Al(NO₃)₃·9H₂O) was used aluminium precursor. Figure 1 shows scanning electron Microscopy (SEM) image of the resulting Al₂O₃ nanofibers and reveals that formation of well-dispersed and unagglomerated Al₂O₃ nanofibers. Colloidally stable copper nanoparticles were synthesized by using organometallic approach [5] through the dihydrogen (H₂) reduction of ([Cu(ⁱPr-Me-AMD)]₂: (N,N'-diisopropylacetamidinato) copper(I) complex in THF at room temperature. Transmission electron microscopy (TEM) image of as-prepared colloidal Cu nanoparticles is depicted in Figure 2, which shows the existence of highly dispersed and nearly monodispersed copper nanoparticles with an average size of 2.1 nm.

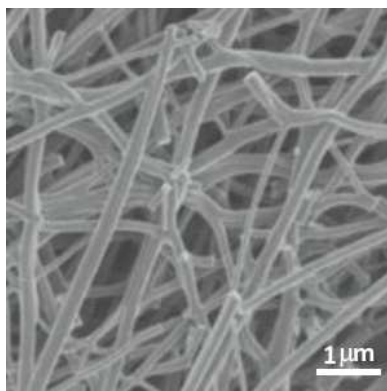


Figure 1. SEM image of Al_2O_3 nanofiber synthesized for solid matrix used in the stabilization of guest copper nanoparticles.

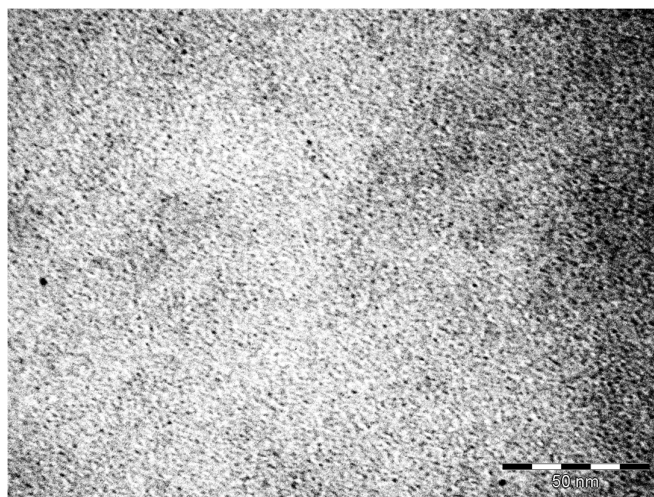


Figure 2. TEM image of colloidal stabilized copper nanoparticles by using organometallic approach through the dihydrogen (H_2) reduction of $([\text{Cu}(\text{iPr-Me-AMD})]_2)$: (N,N' -diisopropylacetamidinato) copper(I) complex in THF at room temperature.

The decoration of host Al_2O_3 nanofibers with guest copper nanoparticles ($\text{Cu}@ \text{Al}_2\text{O}_3$) was done by wet-impregnation technique. TEM image of the resulting $\text{Cu}@ \text{Al}_2\text{O}_3$ is given in Figure 3 and this TEM image is indicative of the formation of slightly clumped Cu nanoparticles on the surface of host Al_2O_3 nanofibers.

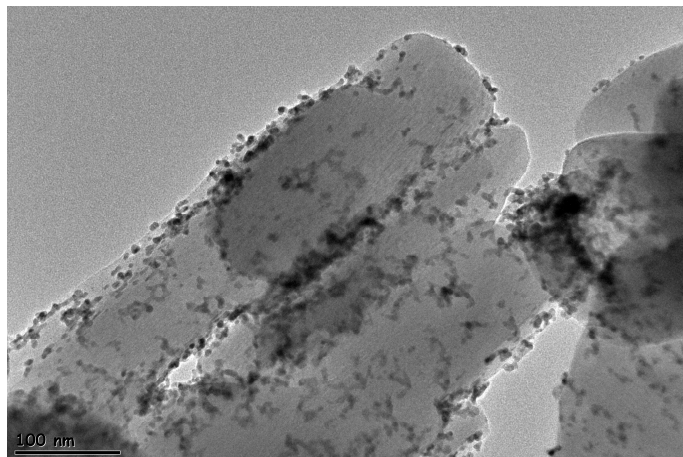


Figure 3. TEM image of colloidal copper nanoparticles by using organometallic approach through the dihydrogen (H_2) reduction of $([Cu^{(i)Pr-Me-AMD}]_2)$: (N,N' -diisopropylacetamidinato) copper(I) complex in THF at room temperature.

Then, the enhancement in convective heat transfer properties of a colloidal $Cu@Al_2O_3$ was studied with the base fluid water by following the methodology as described elsewhere [6]. Initial experiments started with determination of heat transfer coefficients of the nanofluid depending on the weight fraction of Cu nanoparticles in the nanofluid. Before starting to these experiments, the heat transfer coefficient value of the base fluid water was assessed to be $690 \text{ W/m}^2\text{K}$. The convective heat transfer coefficients for nanofluid with various percentage weight fractions of copper nanoparticles (wt % Cu: 0.20, 0.45, 0.71, 0.9 and 1.05) at Reynolds number (Re) of 2000 are given in Figure 4. As given in Figure 4, the heat transfer coefficient increases with an increase in concentration of copper nanoparticles and this value reached to maximum $880 \text{ W/m}^2\text{K}$ for 1.05 wt % of copper concentration, which corresponds to 22 % of enhancement in the heat transfer coefficient with respect to that of the pure base fluid water.

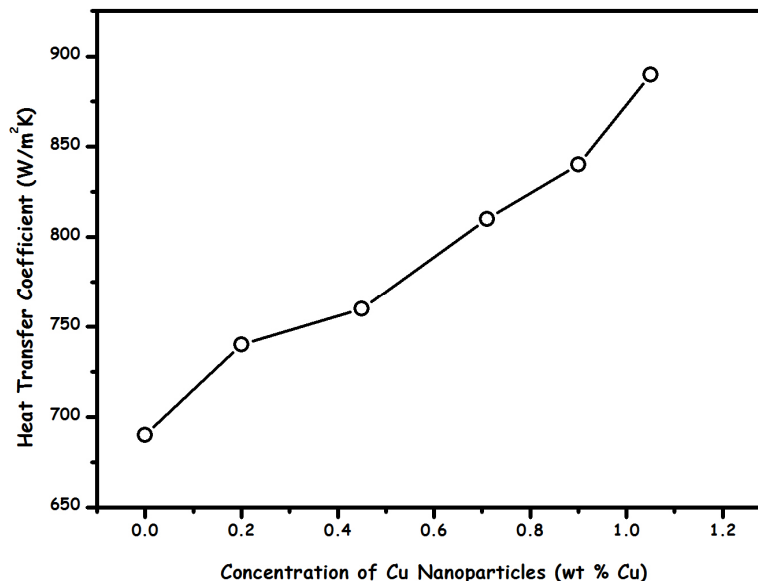


Figure 4. The graph of heat transfer coefficient (W/m²K) versus copper concentration (wt % Cu) for base fluid water at Re = 2000.

Conclusions: In this study, copper nanoparticles supported on Al₂O₃ nanofibers (Cu@Al₂O₃) were prepared and preliminary characterized by using several analytical techniques. The resulting Cu@Al₂O₃ was used in nanofluid system in which water was employed as the base fluid. The preliminary experiments showed that the heat transfer coefficient increases with an increase in concentration of copper nanoparticles exist in Cu@Al₂O₃ material. It is thought that the increase in concentration of copper nanoparticles enhances not only the collision of surface bound copper nanoparticles but also the effective diffusion rate and these two phenomena result in an improvement in the heat transfer coefficient [7]. More detailed experiments are still undergoing and will be announced soon.

References:

1. J. Shwarz, C. Contescu, K. Putyera, *Encyclopedia of Nanoscience and Nanotechnology*, 2nd Ed., Marcel-Dekker, New York (2004).
2. D. K. Devendiran, V. A. Amirtham, A review on preparation, characterization, properties and applications of nanofluids. *Renewable and Sustainable Energy Review* 60 (2016) 21-40.
3. S. Ozkar, R. G. Finke, Transition-Metal Nanocluster Stabilization Fundamental Studies: Hydrogen Phosphate as a Simple, Effective, Readily Available, Robust, and Previously Unappreciated Stabilizer for Well-Formed, Isolable, and Redissolvable Ir(0) and Other Transition-Metal Nanoclusters. *Langmuir*, 19 (2003) 6247-6259.
4. M. Zahmakiran, S. Ozkar, Metal nanoparticles in liquid phase catalysis; from recent advances to future goals. *Nanoscale*, 3 (2011) 3462-3481.

5. C. Pan, K. Pelzer, K. Philippot, B. Chaudret, F. Dassenoy, P. Lecante, M.-J. Casanove, Ligand-Stabilized Ruthenium Nanoparticles: Synthesis, Organization, and Dynamics. *Journal of American Chemical Society*, 123 (2001) 7584-7593.
6. P. Guray, S. Srinu Naik, K. Ansari, S. Srinath, K. A. Kishore, Stable colloidal copper nanoparticles for a nanofluid: Production and application in *Colloids and Surfaces A: Physicochemical and Engineering Aspects* 441 (2014) 589-597.
7. S.M.S. Murshed, C.A. Nieto de Castro, M.J.V. Lourenço, M.L.M. Lopes and F.J.V. Santos, A review of boiling and convective heat transfer with nanofluids, *Renewable and Sustainable Energy Review* 15 (2011) 2342-2354.

**EFFECT OF MANUFACTURING PROCESSES ON THERMOPHYSICAL
PROPERTIES AND CHARACTERISTICS OF WATER/ETHYLENE GLYCOL-BASED
Al₂O₃ NANOFLUIDS**

T.J. Choi, M.S. Park and S.P. Jang*

School of Aerospace and Mechanical Engineering, Korea Aerospace University, Korea

*Corresponding author: spjang@kau.ac.kr

Keywords: Nanofluids, Modified Two-step Method, Size Effect, Thermophysical Properties

Introduction: The nanofluids, stable suspension of nanoparticles in a conventional working fluid, have been highlighted as the working fluid of cooling systems. However, there are a lot of controversy results on the enhancement of thermal conductivity, viscosity and convective heat transfer coefficient. Also, many investigators have presented different results for thermophysical properties and characteristics of the nanofluids which were manufactured by the same nanoparticles using the two step method. We wonder why the nanofluids have different thermophysical properties and characteristics despite of the same manufacturing processes. So, in this paper, we experimentally observe the effect of the manufacturing processes on the thermal conductivity, viscosity and heat transfer coefficient of water/ethylene glycol-based Al₂O₃ nanofluids. Especially, to investigate effect of the manufacturing process systematically, we modify the conventional two-step method with the post-process including the RCF (Relative Centrifugal Force) of a high speed centrifuge. Using the modified two-step method, water/ethylene glycol-based Al₂O₃ nanofluids are manufactured according to the RCF. We measure the particles size suspended into nanofluids, the thermal conductivity and the heat transfer coefficient in laminar flow regime, respectively. Based on the results we clearly show why the nanofluids have different thermophysical properties and characteristics although the same nanoparticles are used.

Discussion and Results: To manufacture water/EG-based Al₂O₃ nanofluids, we used Al₂O₃ nanoparticles (D = 40-50nm, Nanophase Technologies Corp.), DI-water (J. T Baker) and ethylene glycol (Samchun Pure Chemical Co., LTD). We produced 4 cases of water/EG-based Al₂O₃ nanofluids with 1 vol.% using modified two-step method. In the process the high speed centrifuge which can control the RCF is employed. Figure 1 shows the relationship between Al₂O₃ nanoparticle size and RCF per unit time. Although the same nanoparticles manufactured by Nanophase Technologies Corp. were used, the average size of nanoparticles suspended in the nanofluids is different according to the RCF per unit time of the manufacturing processes as shown in Figure 2. The results using ZEN 1690 supplied by Malvern, indicate the manufacturing processes strongly affect the average size of nanoparticles suspended in nanofluids.

Also we measured the thermal conductivity of 4 cases using the transient hot wire apparatus in-house developed with operating range from -10°C to 80°C of 1% uncertainty. Figure 3 shows

the thermal conductivity of nanofluids in accordance with average particle size which strongly depends on the manufacturing processes. As the average particle size becomes small, the thermal conductivity of nanofluids is high as well as has a temperature dependency.

Figure 4 shows the viscosity of nanofluids in accordance with particle size using DV-III Ultra manufactured by Brookfield. The viscosity of the nanofluids tends to increase slightly as the particle size is decreased.

Figure 5 is the experimental apparatus for measuring the convective heat transfer coefficient at laminar flow regime. Using the apparatus with 4% uncertainty, we measure the heat transfer coefficient of nanofluids in a circular tube of fully developed regime of laminar flow under the constant heat flux condition. The convective heat transfer coefficient of the nanofluids is increased about 7.5% on average, which is higher than the increase of thermal conductivity of nanofluids.

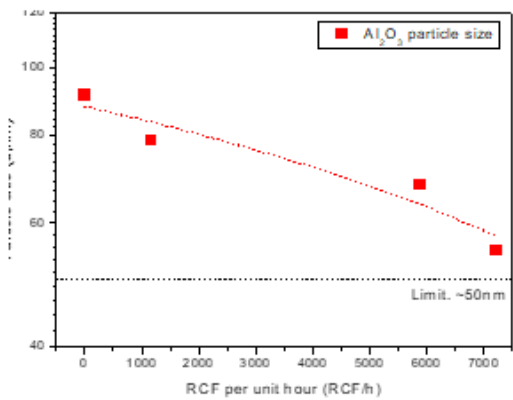


Fig. 1 Particle size of nanofluids

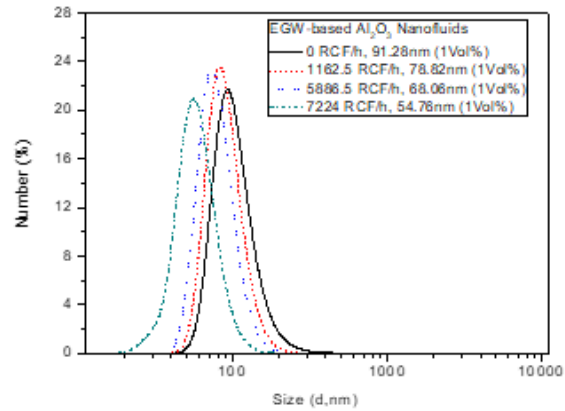


Fig. 2 PSA Results

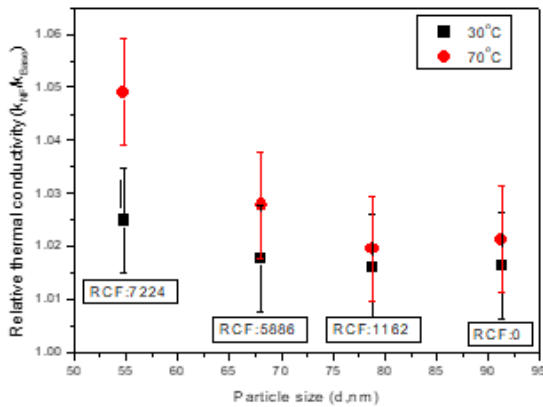


Fig. 3 Relative Thermal Conductivity

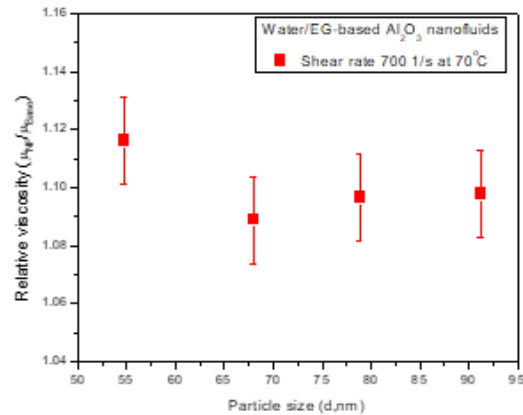


Fig.4 Relative Viscosity

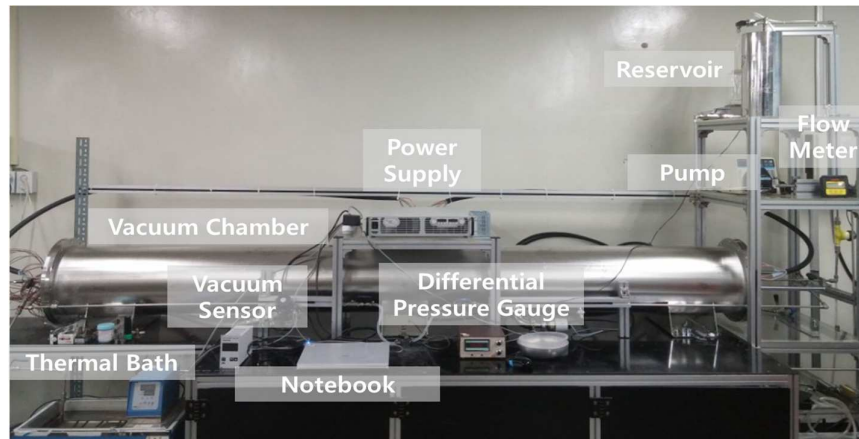


Fig.5 Experimental apparatus for measuring the convective heat transfer coefficient

Conclusions: We experimentally show the effect of the manufacturing processes on the thermal conductivity, viscosity and heat transfer coefficient of water/ethylene glycol-based Al_2O_3 nanofluids. Especially we present the manufacturing process strongly affects the average particle size of nanoparticles suspended in nanofluids although the same nanoparticles manufactured by Nanophase Technologies Corp. were used. Consequently, we strongly believed the average size of nanoparticles suspended in nanofluids is important to decide the thermophysical properties and characteristics of nanofluids.

References

1. D.J. Allen and M.P. Lasecki, Thermal management evolution and coolant flow, *SAE* (2001) 01-1732.
2. J.H Lee, T.Y. Ryu, S.Y. Shin and J.K. Choi, An experimental study on the metal surface temperature and heat transfer by improving gasoline engine cooling passages, *Korean Soc. Auto. Eng.* 10 (2002) 1-8.
3. D.K Kim, M.Y. Jung, J.Y. Lee and K.Y. Kim, A Study of improving of efficiency of power-train cooling system, *KSAE 2009 Annual Conference*, pp. 731-736.
4. S.K. Das, N. Putra and W. Roetzel, Temperature dependence of thermal conductivity enhancement for nanofluids, *ASME J. Heat Transfer*, 125 (2003) 567-574.
5. J.H. Lee, S.H. Lee and S.P. Jang, Do temperature and nanoparticle size affect the thermal conductivity of alumina nanofluids?, *Applied Physics Letters*, 104 (2014) 161908.

COMPARISON OF THERMAL CONDUCTIVITY MEASUREMENT TECHNIQUES OF METALLIC NANOCOLLOIDS

S. Puupponen^{1*}, S. Feja², M.H. Buschmann² and A. Seppälä¹

¹Department of Mechanical Engineering, Aalto University, P.O. Box 14400, FIN-00076 Aalto, Espoo, Finland.

²ILK Dresden gGmbH, Bertolt-Brecht-Allee 20, Dresden, 01309, Germany

*Corresponding author: salla.puupponen@aalto.fi

Keywords: Thermal conductivity, Nanofluid, Silver nanoparticles

Introduction: “Nanofluids” are new type of heat transfer fluid composed of nanoparticles (typically 10-100 nm in size) dispersed in a base fluid, such as water, oil or ethylene glycol. Addition of metal and metal oxide nanoparticles has been reported to increase substantially both the convective heat transfer performance [1,2] and thermal conductivity [3-7] of base fluids. However, there is no fundamental understanding on the heat transfer mechanisms in nanofluids, and the results are remarkably inconsistent among different research groups. Indeed, while many publications propose that nanoparticles give rise to substantially higher increment in the thermal conductivity of base fluid than predicted by the Maxwell’s classical theory for heterogeneous composites [8], several experiments show that the thermal conductivity of nanofluids follow the classical theory. Comparison of the measurement results is extremely demanding task, as thermal properties of nanofluids are influenced by particle size and shape, solution chemistry and surface charges just to name a few. Furthermore, nanofluids are often poorly characterized and the measurement apparatuses, protocols and analysis methods may differ substantially from each other, complicating the *situation* further. Heat conduction mechanisms of nanofluids have been attempted to explain e.g. by Brownian motion and liquid layering [3]. However, in many cases the high thermal conductivity of nanofluids can be explained by the Maxwell’s classical theory if the limiting bounds of nanoparticle configurations are taken into account. For the lower bound, the nanoparticles form the dispersed phase, whereas for the upper bound the nanoparticles form continuous linear or fractal configurations, in which the heat can be transferred efficiently [9,10]. Thus, the colloidal stability can be expected to play a major role in the heat conduction mechanisms of nanofluids. Naturally, the formation of large aggregates is not desirable feature for heat transfer purposes as large clusters are prone to sedimentation and increase substantially the viscosity of the fluid. In this work, thermal conductivity of silver nanocolloids is researched. The Ag nanocolloids are composed of well dispersed, ultrasmall (< 10 nm) nanoparticles (NPs). The nanocolloids are prepared by a new, modified chemical reduction method that utilizes Tollen’s reagent, $[\text{Ag}(\text{NH}_3)_2]^+$, as the silver source, strong NaBH_4 as the reducing agent and mixture of nonionic polysorbate20 and sorbitan trioleate with hydrophilic-lipophilic balance (HLB) of 12.5 as the surfactant [11]. The Ag concentration is varied between 1000 and 5000 ppm. Tested surfactant:

Ag molar ratios were 1:4, 1:6 and 1:8. The particle sizes, size distributions and colloidal stability of the nanocolloids are studied with scanning transmission electron microscopy (STEM) and dynamic light scattering (DLS). Thermal conductivity of the nanocolloids is studied with three measurement techniques: transient C-Therm thermal conductivity analyzer based on a modified transient source plane technique, transient laser flash apparatus (LFA) and static ring-gap apparatus (RGA) developed by ILK Dresden. Transient LFA and TCi measure thermal diffusivity and effusivity, respectively that are converted into thermal conductivity, whereas the steady-state RGA measurements are based on direct solution of the heat equation [9].

Discussion and Results: Stable silver nanocolloids were produced using Tollen's reagent as the silver source, strong NaBH_4 as the reducing agent and mixture of nonionic polysorbate 20 and sorbitan trioleate with hydrophilic-lipophilic balance (HLB) of 12.5 as the surfactant. The silver concentration was varied between 1000 and 5000 ppm. Tested surfactant: Ag molar ratios were 1:4, 1:6 and 1:8. The sample compositions, DLS and STEM particle sizes are presented in Table 1. The STEM images of Ag_3 and Ag_4 are presented in Figure 1. As expected, highest surfactant amount (surfactant: Ag = 1:4) produced the most monodisperse and smallest Ag NPs of ~ 4 nm (STEM particle size). The average particle size of the Ag nanocolloids did not increase much with decreasing surfactant concentration. However, the smaller surfactant amount caused increase in the polydispersity of the nanocolloids.

Table 1. Compositions and particle sizes of silver nanocolloids

Sample name	Ag_1	Ag_2	Ag_3	Ag_4	Ag_5
Ag concentration (ppm)	1000	2000	5000	2000	2000
Ag:surfactant molar ratio	1:4	1:4	1:4	1:6	1:8
Z-avg (nm)	32	28	17	17	22
PdI	0.48	0.45	0.51	0.63	0.56
Mean vol (nm)	0.8	0.7	1.2	1.2	3.8
STEM (nm)	-	-	4.1 (1.2-9.6)	5.5 (1.8-16)	-
D ($\mu\text{m}^2/\text{s}$)	15.3	17.7	29.2	27.8	22

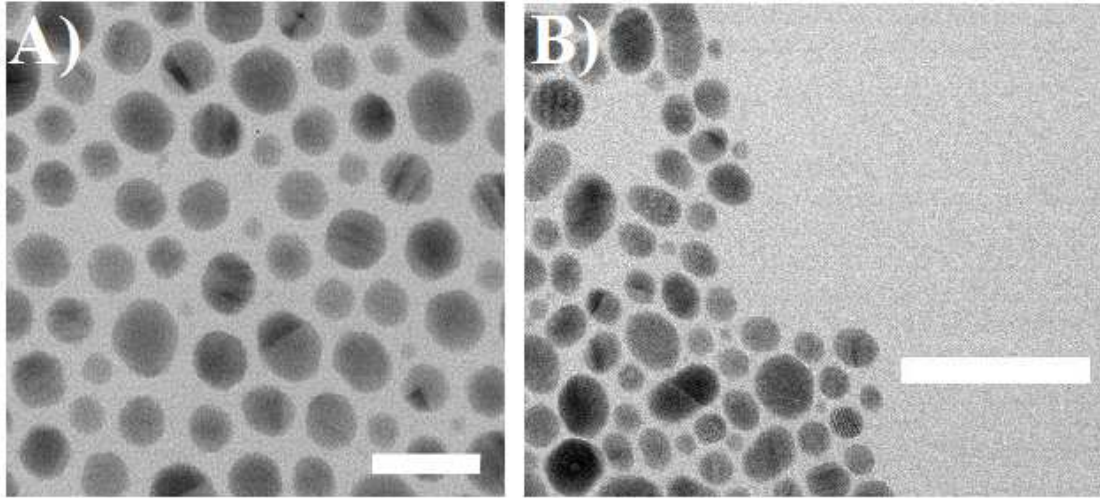


Figure 1. STEM images of A) Ag_3 (scale bar 15 nm) and B) Ag_4 nanocolloid (scale bar 50 nm)

Thermal conductivity (k) of the Ag nanocolloids were studied C-Therm TCi apparatus based on modified transient plane source method, Netzsch laser flash apparatus (LFA) and static ring-gap apparatus (RGA) developed by ILK Dresden [9]. The transient C-Therm TCi and LFA measurements were conducted at 20 °C and 60 °C, whereas the RGA measurement temperatures were 30 °C, 50 °C and 70 °C. Thermal conductivity of Ag nanocolloids are summarized in Table 2. Thermal conductivity of Ag_3 is also shown in Figure 2 together with k prediction of Ag_3 according to Maxwell's model ($\varphi = 0.0005$, values of pure Ag are taken as the density and thermal conductivity of Ag NPs: $\rho(\text{Ag}) = 10.5 \text{ g/cm}^3$, $k(\text{Ag}) = 420 \text{ W/mK}$ [12]). Figure 2 presents also the k value of water according to Huber *et al.* [13]. The measured k of RGA were corrected according to these literature values.

Table 2. Relative thermal conductivity ($k_{\text{rel.}}$) of Ag nanocolloids ($k_{\text{nf}}/k_{\text{H}_2\text{O}}$, where subscript *nf* refers to nanofluid). Abbreviations: $k_{\text{rel.}}(\text{TCi}) - k_{\text{NF}}/k_{\text{H}_2\text{O}}$ measured with C-Therm Tci, $k_{\text{rel.}}(\text{LFA}) - k_{\text{NF}}/k_{\text{H}_2\text{O}}$ measured with laser flash apparatus, $k_{\text{rel.}}(\text{RGA}) - k_{\text{NF}}/k_{\text{H}_2\text{O}}$ measured with RGA. Relative thermal conductivities of LFA and RGA are reported as averages over the measurement temperatures of 20 °C and 60 °C (LFA) and 30 °C, 50 °C and 70 °C (RGA). The $k_{\text{NF}}/k_{\text{H}_2\text{O}}$ measurement temperatures of TCi are reported in parenthesis.

Sample name	Ag_1	Ag_2	Ag_3	Ag_4	Ag_5
$k_{\text{rel.}}(\text{TCi})$	1.07 (20°C)	1.10(20°C), 1.33 (60°C)	1.20 (20°C), 1.38 (60°C)	1.25 (20°C)	-
$k_{\text{rel.}}(\text{LFA})$	-	0.999	0.991	-	-
$k_{\text{rel.}}(\text{RGA})$	1.004	-	1.002	1.004	1.012

According to Maxwell's classical theory, k of the Ag nanocolloids and water should be the same due to the absence of NP agglomerates (see Figure 1). Relative k of nanocolloids was roughly 1, whereas the k of nanocolloids measured with TCi was 7-38 % higher than k of water. The parallel k values of nanocolloids measured with TCi varied greatly from each other. For instance, the parallel measurements of Ag_3 measured with TCi varied $\pm 20\%$ and $\pm 30\%$ at 20 °C and 60 °C, respectively. Thus, the measurements of C-Therm TCi cannot be considered reliable. This result is somewhat surprising as we have not detected before such high k values for metal oxide nanofluids with TCi [14]. In addition, k of water, ethanol, ethylene glycol and glycerol measured with TCi were close to the literature values [15] (difference in the measured and literature values was on maximum $\pm 4\%$).

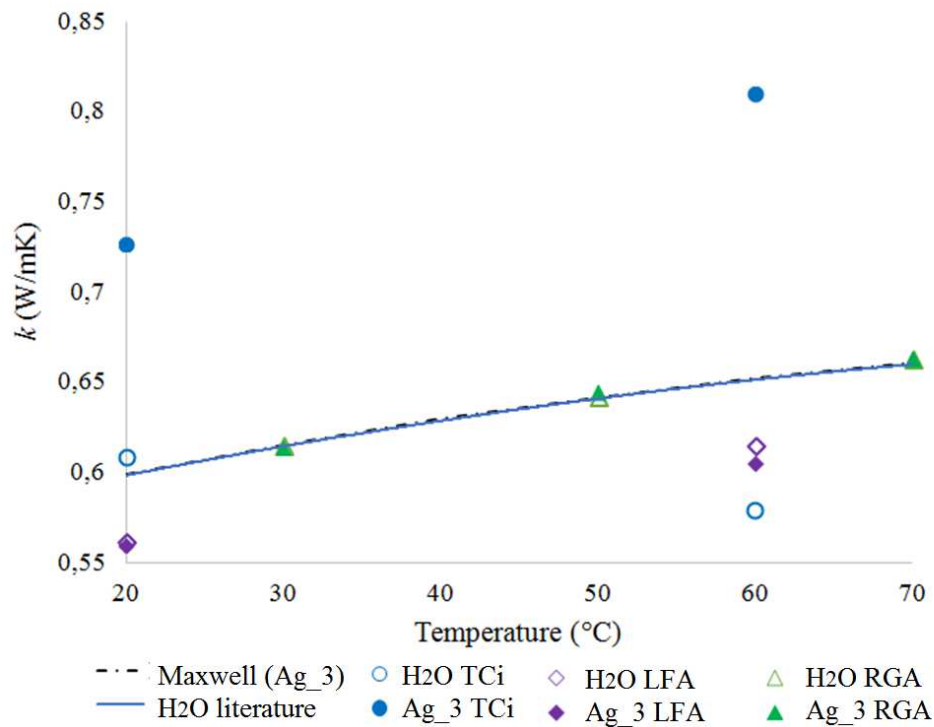


Figure 2. Thermal conductivity (k) of water and Ag_3 measured with C-Therm TCi thermal conductivity analyzer (TCi), laser flash apparatus (LFA) and ring-gap apparatus (RGA). Literature k values of water according to Huber *et al.* [13] and Maxwell's prediction of k for well-dispersed 5000 ppm Ag nanocolloid [8] are shown as solid and dashed curves, respectively.

One possible reason for the high k values of TCi may be the ultrasmall particle size and the metallicity of the Ag nanoparticles studied here. The electric field close to the sample/sensor interface may attract the metallic NPs, in which case the local concentration of small Ag NPs may be higher in the vicinity of the sensor surface. High concentration of Ag NPs close to the

sensor would cause erroneously high k values as the TCi determines the k primarily by the properties of the sample close to the sensor surface. Furthermore, TCi assumes the heat flow to be one-dimensional from the sensor/sample interface that may be incorrect if the Ag NPs are accumulated on the sensor surface. It can be concluded that the thermal conductivity measurement techniques of nanofluids should be always considered carefully and, if possible, compared with additional measurement apparatus.

Conclusions: Here, we presented comparison of thermal conductivity measurement techniques of silver nanocolloids. The silver nanocolloids were self-synthesized using novel, modified Tollen's process. The Ag concentration was varied between 1000 and 5000 ppm. The particle size and size distributions were studied with scanning transmission electron microscopy and dynamic light scattering. The particle sizes of the nanocolloids were < 10 nm, with average STEM particle size around 5 nm. The Ag NPs were well dispersed in water. Thermal conductivity (k) of Ag nanocolloids and water were measured with three different measurement techniques: transient laser flash apparatus (LFA), static ring-gap apparatus (RGA) and C-Therm TCi thermal conductivity analyzer based on modified transient plane source technology. Thermal conductivities of Ag nanocolloids followed the Maxwell's classical theory of heterogeneous composites' k according to LFA and RGA, whereas the k of Ag nanocolloids were 7-38 % higher than k of water measured with TCi. The parallel measurement results of TCi varied considerably from each other and thus, TCi cannot be considered to be reliable k measurement method of the Ag nanocolloids studied here. The reason for unusual high k measured with TCi may be caused by local high concentration of Ag NPs close to the sensor surface that would cause the assumption of one-dimensional heat flow of C-Therm TCi operation principle to fail.

References:

1. Meriläinen, A. Seppälä, K. Saari, J. Seitsonen, J. Ruokolainen, S. Puisto, N. Rostedt and T. Ala-Nissila, Influence of particle size and shape on turbulent heat transfer characteristics and pressure losses in water-based nanofluids, *International Journal of Heat and Mass Transfer*, 61 (2013) 439-448.
2. S. Kakac and A. Pramuanjaroenkij, Review of convective heat transfer enhancement with nanofluids, *International Journal of Heat and Mass Transfer* 52 (2009) 3187-3196.
3. P. Keblinski, S. R. Phillpot, S. U. S. Choi, and J. A. Eastman, Mechanisms of heat flow in suspensions of nano-sized particles (nanofluids), *International Journal of Heat and Mass Transfer*, 45 (2002) 855-863.0
4. J.A. Eastman, S.U.S. Choi, S. Li, W. Yu. and L.J. Thompson, Anomalously increased effective thermal conductivities of ethylene glycol-based nanofluids containing copper nanoparticles, *Applied Physics Letters*, 78 (2001) 718-720.
5. H.E. Patel, S.K. Das, T. Sundararajan, Thermal conductivities of naked and monolayer protected metal nanoparticle based nanofluids: manifestation of anomalous enhancement and chemical effects, *Applied Physics Letters* 83 (2003) 2931-2933.
6. H. Q. Xie, J.C. Wang, T. G. Xi, Y. Liu, F. Ai, and Q.R. Wu, Thermal Conductivity Enhancement of Suspensions Containing Nanosized Alumina Particles. *Journal of Applied Physics*, 91 (2002) 4568-4572.

7. L. Godson, B. Raja, D. Mohan Lal, S. Wongwises, Experimental investigation on the thermal conductivity and viscosity of silver-deionized water nanofluid, *Experimental Heat Transfer*, 23 (2010) 317-332.
8. J.C. Maxwell. *A Treatise on Electricity and Magnetism*, 1 (1873).
9. Ehle, S. Feja, M.H. Buschmann, Temperature dependency of ceramic nanofluids show classical behavior, *Journal of Thermophysics and Heat Transfer* 25(3) (2011) 378-385.
10. J. Eapen, E.R. Rusconi, R. Piazza, S. Yip, The classical nature of thermal conduction in nanofluids, *Journal of Heat Transfer*, 132 (2010) 102401-1-14.
11. S. Puupponen, H. Granbohm, E. Haimi, Y. Ge, T. Ala-Nissila and A. Seppälä, Facile preparation of concentrated silver and copper heat transfer nanocolloids, *Proceedings of HEFAT 2016- 12th International Conference on Heat Transfer, Fluid Mechanics and Thermodynamics*, July 11th-13th, Malaga, Spain 1700-1706.
12. D.R. Smith, F.R. Fickett, Low-temperature properties of silver, *Journal of Research of the National Institute of Standards and Technology*, 100(2) (1995) 119-171.
13. M.L. Huber, R.A. Perkins, D.G. Friend, J.V. Sengers, M.J. Assael, I.N. Metaxa, K. Miyagawa, R. Hellmann, and E. Vogel, New International for the Thermal Conductivity of H₂O, *Journal of Physical and Chemical Reference Data*, Vol. 41(3) (2012) 033102-1-23.
14. V. Mikkola, S. Puupponen, H. Granbohm, K. Saari, T. Ala-Nissilä, A. Seppälä, Convective heat transfer performance of polystyrene, SiO₂, Al₂O₃ and micelle nanofluids, *Proceedings of HEFAT 2016- 12th International Conference on Heat Transfer, Fluid Mechanics and Thermodynamics*, July 11th-13th, Malaga, Spain 1700-1706.
15. VDI Heat Atlas, *VDI-Gesellschaft Verfahrenstechnik und Chemieingenieurwesen (GVC) 2nd Edition*, Springer Reference.

Abstracts

SESSION 7B: NUMERICAL AND OTHERS

NANOROUND – A PROPOSAL FOR A NUMERICAL ROUND ROBIN TEST FOR SIMULATION OF NANOFLUIDS

A. A. Minea¹, A. Huminic², G. Huminic², J. Tibaut³ and J. Ravnik^{3,*}

¹Faculty of Materials Science and Engineering, Technical University "Gheorghe Asachi" from Iasi, Iasi, Romania

²Transilvania University of Brasov, Brasov, Romania

³Faculty of Mechanical Engineering, University of Maribor, Slovenia

*Corresponding author: jure.ravnik@um.si

Keywords: Round robin test, Nanofluid models, Laminar flow in a pipe

Introduction: Heat transfer in straight tubes and channels was the subject of numerous researches for the last century [1, 2]. The development of new applications stimulated a great interest to study flow and heat transfer in micro-channels [3, 4]. A number of theoretical and experimental investigations devoted to this problem were performed during last years [5–8] and data on heat transfer in laminar and turbulent flows in micro/macro channels with different geometry were obtained. Several special problems related to heat transfer in channels were extensively discussed in the literature: effect of axial conduction in the wall, viscous dissipation effect [8-14] and comprehensive surveys may be found in [13-16].

Nanofluids (i.e. suspensions nanometre-sized particles in a base liquid) have been a subject of tremendous efforts during last years. Researchers have been focusing on the production procedures, on measuring nanofluid properties as well as on numerical modelling of nanofluids. Several models and numerical approaches as well have been proposed [17]. The models differ in terms of the used limitations and assumptions, which were taken into account as well as in terms of the description of the nanofluid. Single-phase approaches with effective properties have been used as well as two phase Euler – Lagrange and other approaches were considered. Researchers have proposed the use of an additional convection-diffusion equation for nanoparticle concentration and have been determining nanofluid properties based on the spatially and temporarily varying concentration [17]. A vast amount of literature on the subject exists, where different models have been proposed and tested on different flow and heat transfer configurations to a varying degree of success against other numerical or experimental test cases. However, the models and computational approaches have not been tested on an equal footing in order to establish the optimal modelling approach. Thus, based on the available literature, it is still not clear, which is the best way of modelling nanofluids in numerical simulations in order to provide as accurate as possible results and facilitate engineers in the design process of devices, which use nanofluid as a working fluid. Thus, we propose to start the *NANOROUND* project – a numerical round robin test aimed at comparing numerical nanofluid models.

Round robin test: With this paper, we intent to set a base to invite research groups to participate in a numerical round robin test for simulation of nanofluids. Commercial, open-source or in-house computational fluid dynamics codes may be used based on any numerical method. The groups are invited to use their preferred nanofluid model and simulate the one of the two test cases described below. Each group should make their own grid sensitivity and time step analyses. A document describing the boundary conditions in detail will be made available on the *NANOROUND* project website.

Test cases: Test cases were selected based on the existing literature and also by checking the details inserted by each groups. Finally, for preliminary readings we have chosen two experimental studies [18, 19] with a simple geometry and well defined initial and boundary conditions. Both have considered laminar flow of nanofluids in a pipe with constantly heated walls. They both have considered water based nanofluids with different particle concentrations as well as pure water for comparison. When a nanofluid enters the heated test section, it is heated up and the temperature at the wall was measured in several locations along the pipe.

The boundary and initial conditions of the two test cases can be summarized as follows: a constant temperature nanofluid enters the test section. At the inlet, the flow is laminar (Reynolds number is around 1000), fully developed and steady. As it travels through the pipe it is heated by a prescribed heat flux on the walls. The pipe is straight and at the outlet an outlet boundary condition may be prescribed. At the walls a no-slip boundary condition may be applied.

By this time, the authors of this paper worked most on test case A that is explained further on. Test case A is based on Colla et al. [19]. In Figure 1 a scheme of the experiment is shown. Results of measurement for test case A are given in Table 1, were placement of temperature sensors is shown and all measurements are in mm. Pipe length is 2m and the pipe diameter is $d = 8\text{mm}$.

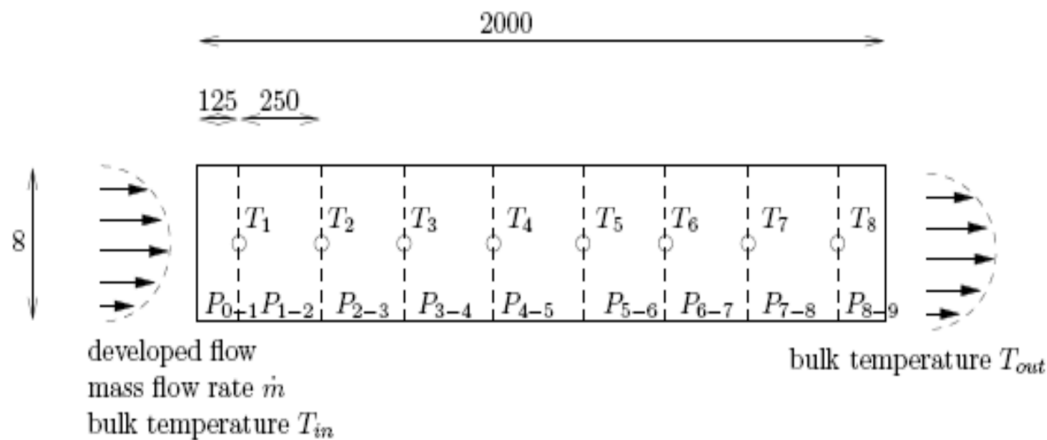


Figure 1: A sketch of the test case.

Table 1: Experimental values for test case A [19].

inlet								
mass flux, $\dot{m} = 0.0061151 \text{ kg/s}$								
bulk temperature at inlet, $T_{in} = 19.57^\circ\text{C}$								
water properties at inlet: $\rho = 998.295 \text{ kg/m}^3$, $k = 0.597685 \text{ W/mK}$,								
$c_p = 4184.36 \text{ J/kgK}$, $\mu = 1.012429 \cdot 10^{-3} \text{ Pa}\cdot\text{s}$								
Reynolds number at inlet, $Re = \frac{\dot{m}}{\pi d \mu} = 961.4$								
outlet								
bulk temperature at outlet, $T_{out} = 27.38^\circ\text{C}$								
wall temperature [°C]								
T_1	T_2	T_3	T_4	T_5	T_6	T_7	T_8	
25.6	28.0	28.7	29.5	30.2	30.9	31.8	32.7	
power [W]								
P0-1	P1-2	P2-3	P3-4	P4-5	P5-6	P6-7	P7-8	P8-9
12.6	25.2	25.2	25.2	25.0	24.9	24.9	24.8	12.4

Based on Colla et al. [19] experimental conditions we fixed the initial and boundary conditions as seen in Table 1.

Temperature dependent water properties to be taken into account for simulation are in Table 2. All expressions should be used with temperature expressed in °C.

Table 2. Water properties

Density:
$\rho(T) [\text{kg/m}^3] = 1.31839028583 \cdot 10^{-9} \cdot T^5 - 4.1415691320879 \cdot 10^{-7} \cdot T^4$
$+ 0.0000627465524729587 \cdot T^3 - 0.00812457260548172 \cdot T^2$
$+ 0.0554068116720146 \cdot T + 999.90837195736$
Thermal conductivity:
$k(T) [\text{W/mK}] = -0.0000000000074354379 \cdot T^5$

$$+2.43717635743 \cdot 10^{-9} \cdot T^4 - 0.0000002889967610567 \cdot T^3$$

$$+5.15309471096903 \cdot 10^{-6} \cdot T^2 + 0.00185267131276284 \cdot T + 0.561293060017584$$

Specific heat at constant pressure:

$$c_p(T) [J/kgK] = -4.088550653591 \cdot 10^{-8} \cdot T^5$$

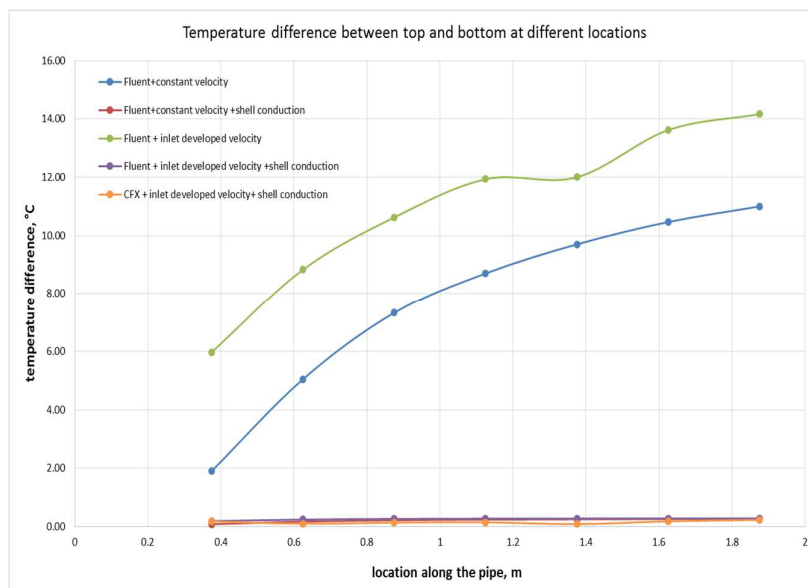
$$+0.0000117146192195605 \cdot T^4 - 0.00137712095636289 \cdot T^3$$

$$+0.0902711920148249 \cdot T^2 - 2.99500832260219 \cdot T + 4217.11488982432$$

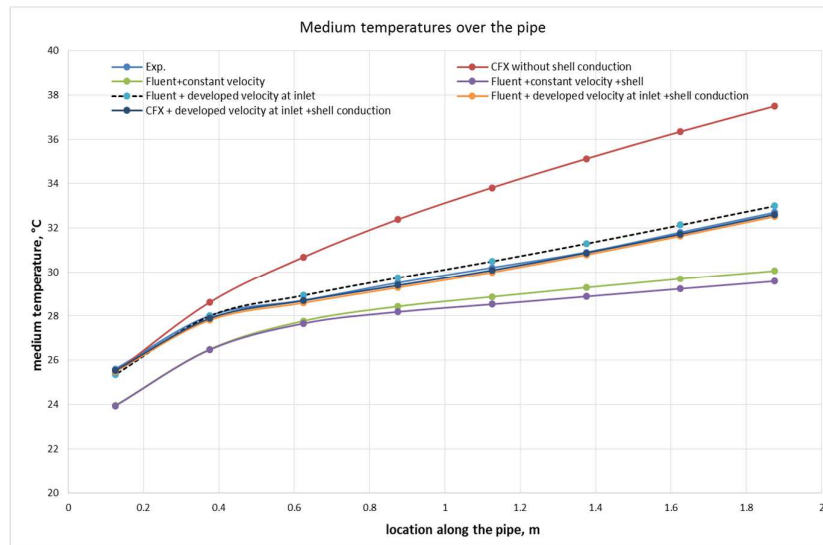
Viscosity:

$$\mu(T) [Pas] = 2.414 \cdot 10^{-5} \times 10^{247.8/(T+133.15)}$$

Using the above mentioned properties, preliminary results were obtained in Ansys Fluent and CFX [20] solvers using different settings (studying also the influence of gravity), profiles for inlet velocity and also considering conduction in the copper tube. Some of the preliminary results are summarized in Figure 2.



a.



b.

Figure 2. Preliminary results: a. difference in temperature between top and bottom of the pipe at different locations along the pipe; b. medium temperature at a certain point.

Also, by performing our calculus both in Fluent and CFX we noticed strong influence of gravity, which change the classical (Hagen-Poiseuille) velocity profile and generate also a rotational flow, which clearly influence the heat transfer.

The aim of the *NANOROUND* numerical simulations will be to predict measured wall temperatures as well as to export results in a prescribed and organized manner to facilitate comparison between different groups, nanofluid models and computational approaches.

Summary: Efforts were done to validate the experimental results obtained by Colla et al [18] since the performed experiment was very detailed and we worked on every point validation and not on an overall one in order to attain extremely accurate results and to establish a very well defined base for the numerical study. A lot of possible scenarios were considered as one can see from preliminary results inserted. This technique was not applied until now, as far as the authors are aware.

In conclusion, we propose to start the *NANOROUND* project – a numerical round robin test aimed at establishing the advantages and disadvantages of nanofluid models. Research groups with expertise in computational fluid dynamics and nanofluid modelling are welcome to participate. The project dissemination activities will include a website to publish the results and findings as well as a scientific paper reporting on the results. Presentation at the next European Symposium on Nanofluids is also planned.

References:

1. Petukhov B.S. (1967) Heat transfer and drag of laminar flow of liquid in pipes. Energy, Moscow.
2. Kays W.M., Crawford M.E. (1993) Convective Heat and Mass Transfer, McGraw-Hill, New York.
3. Ho, C.M. Tai, Y.-C. (1998) Micro-electronic mechanic systems (MEMS) and fluid flows, *Ann. Rev. Fluid Mech.* 30, pp 5–33.
4. Gad-el-Hak, M. (1999) The fluid mechanics of micro-devices. The Freeman Scholar Lecture, *J. Fluid Eng.* 12, pp1 5–33.
5. Reynaud S., Debray F., Frans J.-P., Maitre, T. (2005) Hydrodynamics and heat transfer in two-dimensional mini-channels, *Int. J. Heat Mass Transfer* 48 3197–3211.
6. Wang B.X., Peng, X.F. (1994) Experimental investigation on liquid forced- convection heat transfer through microchannels, *Int. J. Heat Mass Transfer* 37 (1) 73– 82.
7. Peng X.F., Peterson G.P. (1995) The effect of thermofluid and geometric parameters on convection of liquid through rectangular micro-channels, *Int. J. Heat Mass Transfer* 38, 755–758.
8. Peng X.F., Peterson, G.P. (1996) Convective heat transfer and flow friction for water flow in micro-channel structures, *Int. J. Heat Mass Transfer* 39, 2599–2608.
9. Maranzana G., Perry, I. Maillet D. (2004) Mini- and microchannels: influence of axial conduction in the walls, *Int. J. Heat Mass Transfer* 47 3993–4004.
10. Tunc, G. Bayazitoglu, Y. (2001) Heat transfer in micro-tubes with viscous dissipation, *Int. J. Heat Mass Transfer* 44, 2395–2403.
11. Koo J., Kleinstreuer, C. (2004) Viscous dissipation effects in micro-tubes and micro-channels, *Int. J. Heat Mass Transfer* 47, 3159–3169.
12. Sobhan, C.B., Garimella, S.V. (2001) A comparative analysis of studies on heat transfer and fluid flow in micro-channels, *Microscale Thermophys. Eng.* 5, 293–311.
13. Hassan, I. Phuttavong P., Abdelgawad, M (2004) Micro-channel heat sinks: an overview of the state of the art, *Microscale Thermophys. Eng.* 8, 183–204.
14. Morini, G.L. (2004) Single-phase convective heat transfer in micro-channels: overview of experimental results, *Int. J. Thermal Sci.* 43, 631–651.
15. Garimella S.V., Sobhan, C.B. (2003) Transport in micro-channels- a critical review, *Ann. Rev. Heat Transfer* 13, 1– 50.
16. Minea, AA. (2017) *Advances in New Heat Transfer Fluids: From Numerical to Experimental Techniques*, CRC Press.
17. Wen, D. & Ding, Y. Experimental investigation into convective heat transfer of nanofluids at the entrance region under laminar flow conditions, *International Journal of Heat and Mass Transfer*, 47 pp. 5181–5188, 2004.
18. Colla, L., Fedele, L., & Buschmann, M. H. (2015). Laminar mixed convection of TiO₂-water nanofluid in horizontal uniformly heated pipe flow. *International Journal of Thermal Sciences*, 97, 26–40.
19. Ansys commercial code

DEVELOPMENT OF THE BOUNDARY ELEMENT METHOD FOR SIMULATION OF NANOFUIDS

J. Ravnik* and J. Taibaut

Faculty of Mechanical Engineering, University of Maribor, Slovenia

*Corresponding author: jure.ravnik@um.si

Keywords: Boundary element method, Variable material properties, Nanofluids

Introduction: Many natural phenomena involve energy transfer, which is governed by the diffusion and convection transport processes. In nature and for most engineering purposes, heat transfer occurs in environments, where the velocity of the fluid changes within the domain in question. Fluid properties, such as density, specific heat and heat conductivity are usually considered as constant. However, there are examples, where changes in fluid material properties must be considered. One example is a case, where large temperature differences are present in the simulation domain. Since material properties are temperature dependent, these must be considered. Another example are nanofluids [1]. These are suspensions of nanometre-sized particles in a base liquid. The properties of the suspension (when modelled as a single phase liquid with modified properties) depend on the concentration of the particles, which in turn depends on the flow field.

Transport phenomena, such as momentum, mass and heat transferred are governed by the diffusion-convection partial differential equations. Numerical solution of these is a challenging task. Many numerical algorithms have been proposed. In this paper, we develop the boundary element method for simulation of nanofluids with variable material properties.

Numerical method: Fluid flow and heat transfer are governed by systems of nonlinear partial differential equations. When nanofluids are considered in a single-phase Eulerian framework the fluid material properties also vary with location and time due to the changes in temperature and nanoparticle distribution. We developed a boundary element based method for simulation of such systems. The method is based on the use of the fundamental solution of the underlying partial differential equation to write an integral representation of the governing equations. We implemented it on the velocity-vorticity formulation of Navier-Stokes equations and solved it by a domain decomposition approach. Treatment of variable material properties has implemented by a careful derivation of the integral formulation of the governing equations to give a field gradient free representation. The employed domain decomposition approach leads to sparse over-determined systems of linear equations, which are solved in a least-squares manner.

Validation: The developed fluid flow and heat transfer solver has been validated using several benchmark test cases. The standard lid driven cavity and natural convection in a cavity cases were used to establish the validity of the method and assess the solution convergence properties on different mesh designs. We found that the developed method is second order accurate and is,

due to the used of the fundamental solution of the governing PDE, able to capture the physics of flows using relatively coarse meshes.

Discussion and Results: The developed numerical method was used to simulate enhancement of free convection in several configurations, [2-4]. In Figure 1 geometry and boundary conditions of the simulation cases are presented. An example of results is shown in Figure 2. The main conclusion drawn from the analysis was that the use of a nanofluid as compared to base fluid enhances heat transfer the most when conduction is the dominant heat transfer mechanism. In convection-dominated flows, the enhancement achieved by nanofluid is lower.

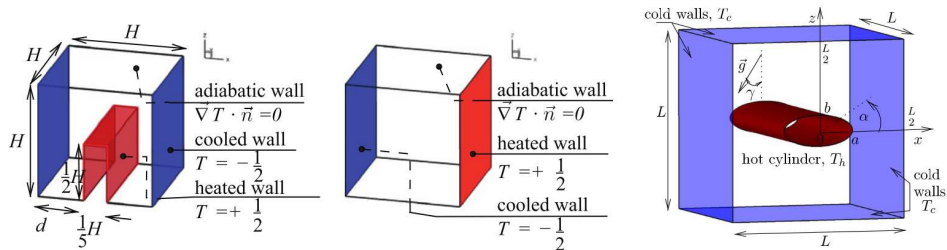


Figure 1: Geometry and boundary conditions of the simulation cases.

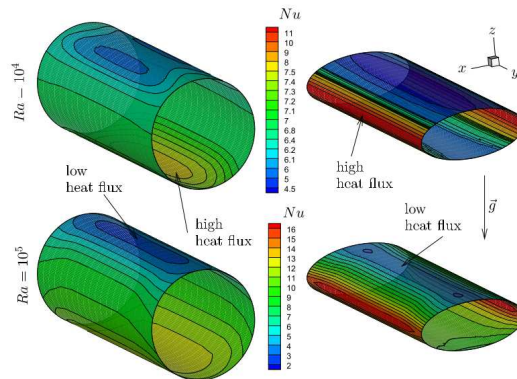


Figure 2: Example analysis of heat flux distribution for one of the simulation cases.

Summary: We developed a boundary element based numerical technique, which is able to simulate flow and heat transfer of fluid with variable material properties. The developed technique was validated and tested by simulating free convection of a nanofluid.

References:

1. Choi, S. U. S. Enhancing thermal conductivity of fluids with nanoparticles. *Develop. Appl. Non Newtonian Flows*, 66 (1995) 99–106

2. Ravnik, J., Škerget, L., and Hribersek, M. Analysis of three-dimensional natural convection of nanofluids by BEM. *Engineering Analysis with Boundary Elements*, 34 (2010), 1018–1030.
3. Ravnik, J., & Škerget, L. A numerical study of nanofluid natural convection in a cubic enclosure with a circular and an ellipsoidal cylinder. *International Journal of Heat and Mass Transfer*, 89 (2015) 596–605.
4. Kramer Stajniko, J., Jecl, R., and Ravnik, J. Numerical simulation of convective flow in a non-Darcy porous cavity filled with nanofluid. *International Journal of Computational Methods and Experimental Measurements*, 4 (2016) 454–463.

NANOFLUID THERMAL BOUNDARY LAYER

J.T.C. Liu*, D. Hopper, D. Jaganathan, J.L. Orr, J. Shi, F. Simeski and M. Yin

School of Engineering EN2760 and the Centre for Fluid Mechanics, Brown University,
Providence, Rhode Island 02912, USA

*Corresponding author: joseph_liu@brown.edu

Keywords: Nanofluids, Convective Heat Transfer, Heat Transfer Enhancement, Adiabatic temperature

Introduction: Application of nanofluids in heat transfer enhancement involves flowing nanofluids in, for instance, forced convective heat transfer situation, as in the experiments of Wen and Ding [1] and of Jung, et al. [2] in microchannels. They showed that the leading edge region of the microchannels gave significant heat transfer enhancement as function of increasing nanofluid volume fraction. In this case, it is of theoretical importance to understand the convective thermal boundary layer behaviour that resembles the channel leading edge over a large streamwise distance before the boundary layers merge, whereas the downstream fully developed region has much less spectacular heat transfer behaviour.

The continuum description [3] of the nanofluid boundary layer is in general in compressible form, even though the base fluid is incompressible. This is because of the dependence of the nanofluid thermophysical properties on the nanoparticle concentration, which in turn, is subjected to nanoparticle diffusion through possible Brownian diffusion and thermal diffusion effects. On the basis that nanofluid heat transfer experiments are carried out at very dilute nanofluid volume fractions, a series of papers [4-6] devised a perturbation scheme for small volume concentrations. This reduced the problem into perturbation about the base fluid; the nanofluid effect becomes linear and separable nanofluid momentum, diffusion and thermal boundary layer equations.

The Basic Equations for Nanofluid Boundary Layer Flow: Because of the dependence of the nanofluid thermophysical properties on the concentration of nanoparticle volume fraction, the fundamental equations are necessarily in the form for a compressible fluid, even though the individual constituents, such as the base fluid and the dispersed nanoparticles, are individually incompressible. The continuum description is synthesized by Buongiorno [3]. Use is made of the two-dimensional flat plate as an approximation for the leading edge of a semi-infinite micro channel in the developing region prior to the merging influence of the upper and lower walls. The two-dimensional boundary layer continuity and momentum equations for steady flow are given in [5,6]; we state the energy equation that is augmented from that used in [5,6] to include the effect of viscous dissipation. It is presented first in dimensional form for discussion purposes

Thermal energy:
$$\rho \left(u \frac{\partial h}{\partial x} + v \frac{\partial h}{\partial y} \right) = - \frac{\partial q}{\partial y} + \mu \left(\frac{\partial u}{\partial y} \right)^2$$

where the nanofluid static enthalpy is $h = \int c dT$, $c = dh / dT$ is the nanofluid heat capacity and T is the absolute temperature, The work done by the pressure gradients is not present for the zero streamwise and normal pressure gradients in this case. The normal component of the heat flux vector is q and includes the mechanisms of conduction and thermal energy transport owing to nanoparticle concentration diffusion

$$q = - \left(k \frac{\partial T}{\partial y} \right) - \left(\rho_p D \frac{\partial \phi}{\partial y} h_p \right)$$

where k is the nanofluid thermal conductivity, ρ_p is the nanoparticle density, D is the Brownian diffusion coefficient [7], ϕ is the nanoparticle phase volume fraction, $h_p = c_p T$ is the static enthalpy of the nanoparticle phase, c_p is it's heat capacity. Thermal equilibrium is assumed between the base fluid and the nanoparticle phase [3]. The rate of viscous dissipation is the last term in the thermal energy equation, to include this effect, it will be shown that it is convenient to let the nanofluid temperature remain dimensional. Thu the nanofluid energy equation in boundary layer form becomes

$$\rho^* c^* \left(u^* \frac{\partial T}{\partial x^*} + v^* \frac{\partial T}{\partial y^*} \right) = \frac{1}{\text{Re Pr}_f} \frac{\partial}{\partial y^*} \left(k^* \frac{\partial T}{\partial y^*} \right) + \frac{\phi_\infty}{\text{Re Sc}_f} \frac{\partial}{\partial y^*} \left((\rho c)^* D^* \frac{\partial \Phi}{\partial y^*} T \right) + \frac{U^2 / c_f}{\text{Re}} \mu^* \left(\frac{\partial u^*}{\partial y^*} \right)^2$$

subscript ∞ denote conditions in the free stream, the Prandtl number is $\text{Pr}_f = \nu_f / \kappa_f$, where the subscript f pertains to the base fluid, the kinematic viscosity and thermal diffusivity are $\nu_f = \mu_f / \rho_f$, $\kappa_f = k_f / \rho_f c_f$, respectively. The Schmidt number is $\text{Sc}_f = \nu_f / D_{ref}$, the dimensionless nanoparticle density heat capacity product is $(\rho_p c_p)^* = \rho_p c_p / \rho_f c_f$, $D^* = D / D_{ref}$, $D_{ref} = k_B T_{ave} / 6\pi\mu_f r_d$. The Brownian diffusion coefficient is evaluated at the average temperature T_{ave} , so that $D^* = 1$, k_B is the Boltzmann constant, r_d is the average nanoparticle radius.

While the heat transfer problem in absence of viscous dissipation is thoroughly discussed in [5,6], the present work discusses the adiabatic wall problem, which completes the overall study of the nanofluid thermal boundary layer. The dependency of the nanofluid density, heat capacity, thermal conductivity and viscosity upon the nanofluid concentration necessitates the computation of the volume concentration according to the diffusion equation for $\Phi = \phi / \phi_\infty$, it is derivable from continuity equation for the nanoparticle species in terms of its mass fraction and then related to the volume fraction for dilute concentration [5,6]. Thermal diffusion is neglected.

Thermophysical Properties: The continuum description [7] requires input from separate considerations of the thermophysical properties, and are represented in terms of the volume fraction. To first order in the volume fraction, in dimensionless form normalized by the corresponding quantity of the base fluid,

$$\begin{aligned}\rho^* &= 1 + \phi_\infty (\rho^*)'_{\phi=0} \Phi + \vartheta(\phi_\infty^2) \\ \rho^* c^* &= 1 + \phi_\infty (\rho^* c^*)'_{\phi=0} \Phi + \vartheta(\phi_\infty^2) \\ \mu^* &= 1 + \phi_\infty (\mu^*)'_{\phi=0} \Phi + \vartheta(\phi_\infty^2) \\ k^* &= 1 + \phi_\infty (k^*)'_{\phi=0} \Phi + \vartheta(\phi_\infty^2)\end{aligned}$$

where $(\chi^*)'_{\phi=0}$ is the slope of $\chi^*(\phi)$ at the origin. The representations are in “general form” in that they could be obtained from various separate considerations discussed in [5,6] and will not be elaborated here. The preference is to use properties recently obtained from molecular dynamics simulations [9-11], although this is performed only for gold-water nanofluids. Denoting by subscript MD for molecular dynamics, the properties extracted from [9-11] by [5] are $(\rho^*)'_{\phi=0,MD} \cong 18.7$, $(\rho^* c^*)'_{\phi=0,MD} \cong -2.37$, whereas results for viscosity and thermal conductivity are only available in [9] and subject to interpretation [5], are $(\mu^*)'_{\phi=0,MD} \cong 10$, $(k^*)'_{\phi=0,MD} \cong 20$.

Dilute

Nanoparticle Concentration-Perturbation for $\phi_\infty \ll 1$: In general, nanofluid heat transfer experiments (e.g., [1,2]) are performed for dilute nanoparticle concentration. In this case, simplifications result from a perturbation analysis for $\phi_\infty \ll 1$. The perturbation expansion is first applied to the partial differential equations, incorporating the thermophysical properties (which are already in perturbation form), the results are subjected to the similarity transformation of the Blasius-Pohlhausen type [12] for both perturbation orders: $\eta = y^* / \sqrt{x^* / \text{Re}}$ with streamfunction $\psi^* = \psi / UL = f(\eta) \sqrt{x^* / \text{Re}}$ and transformed velocity components $u^* = f'(\eta)$, $v^* = (\eta f' - f) / 2\sqrt{x^* / \text{Re}}$, where primes denote differential with respect to η . The small volume fraction perturbation reduces the boundary layer equation to an incompressible form, in which only the zeroth order momentum equation is nonlinear. The momentum and diffusion problems remain unchanged for the present problem and we refer to [5,6] for details of the similar solutions. The perturbation for the thermal boundary layer is stated more explicitly $\theta_H = \theta_{H,0} + \phi_\infty \theta_{H,1} + \vartheta(\phi_\infty^2)$ and $\theta_P = \theta_{P,0} + \phi_\infty \theta_{P,1} + \vartheta(\phi_\infty^2)$. The zeroth order ($\theta_{H,0}$) and first order ($\theta_{H,1}$) heat transfer problems are identical to that discussed in [5,6]. The viscous dissipation effect enters through the particular solutions $\theta_{P,0}$ for the base fluid for an insulated wall [12], the the first order nanofluid thermal boundary layer equation obtained is

$$\begin{aligned} \theta_{P,1}'' + (\text{Pr}_f/2)(f_0\theta_{P,1}' + f_1\theta_{P,0}') &= -[(k^*)'_{\phi=0} - (\rho^*c^*)'_{\phi=0}]\Phi\theta_{P,0}'' - (k^*)'_{\phi=0}\Phi'\theta_{P,0}' - \text{Pr}_f[(\rho_p c_p)^*/Sc_f](\Phi'\theta_{P,0})' \\ &- 2\text{Pr}_f[(\mu^*)'_{\phi=0}\Phi(f_0'')^2 + 2f_0''f_1'] \\ \theta_{P,1}(0) &= 0, \quad \theta_{P,0}(\infty) = 0 \end{aligned}$$

The numerical integration results for gold-water nanofluid using molecular dynamics properties is shown in Figure 1. The diffusion layer for $\Phi(\eta)$ is much thinner than that of the thermal boundary layer owing to the large Schmidt number for which $Sc_f = 2 \times 10^4$ (for nanoparticle radius of 10nm) and $\text{Pr}_f = 7$. Referring to Figure 1, the $\Phi_w = 1$ case is equivalent to a solid wall for which there is no nanoparticle flux at the wall, $\Phi'(0) = 0$. The $\Phi_w = 0$ case is one in which the wall is porous and nanoparticles are removed by a magnitude equal to the free stream concentration ϕ_∞ , resulting in a lowered adiabatic wall temperature. The $\Phi_w = 2$ case is one in which nanoparticles are injected at the wall by a magnitude equal to the free stream concentration ϕ_∞ , resulting in increased adiabatic wall temperature. The effect is mainly due to the dependence of transport properties dependent on the volume concentration near the wall. The bulge of the temperature profiles $\theta_{P,1}(\eta)$ is due to the maximum of the viscous dissipation in the interior of the boundary layer.

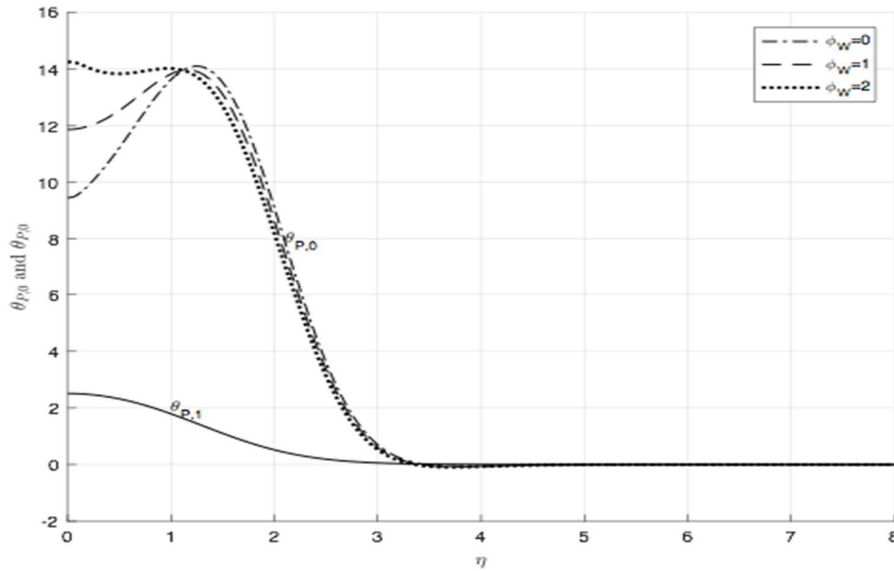


Figure 1. Dimensionless temperature profiles $\theta_{P,0}$ (solid line) and $\theta_{P,1}$ (dashed lines) vs. η . Adiabatic wall temperatures $\theta_{P,1}(0; \Phi_w)$: $\theta_{P,1}(0;0) = 9.46$, $\theta_{P,1}(0;1) = 11.87$, $\theta_{P,1}(0;2) = 14.86$.

Concluding Remarks: The present particular solution $\theta_{p,1}(\eta)$ can always be combined with the heat transfer solution θ_H obtained in [6] to form the general solution for the heat transfer with viscous dissipation. The possibilities of applying the continuum framework to estimate heat transfer capabilities, relative to skin friction rise, depends on the availability of nanofluid properties. This could be obtained through further applications of molecular dynamics to other combination of nanoparticles and base fluids, or, via experimentally obtained properties.

References:

1. D. Wen and Y. Ding, Experimental investigation of nanofluids of the entrance region under laminar flow conditions, *International Journal of Heat and Mass Transfer* 47 (2004) 5181-5188.
2. J.-Y. Jung, H.-S. Oh, H.-Y. Kwak, Forced convective heat transfer of nanofluids in micro channels, *International Journal of Heat and Mass Transfer* 52 (2009) 466-472.
3. J. Buongiorno, Convective transport in nanofluids, *ASME Journal of Heat Transfer* 128 (2006) 240-250.
4. J.T.C. Liu, On the anomalous laminar heat transfer intensification in developing region of nanofluid flow in channels or tubes, *Proc. of the Royal Society A* 408 (2012) 2383-2398.
5. J.T.C. Liu, M.E. Fuller, K.L. Wu, A. Czulak, A.G. Kithes and C.J. Felten, Nanofluid flow and heat transfer in boundary layers at small nanoparticle volume fraction: zero nanoparticle flux at solid wall, *Archives of Mechanics* 69 (Warszawa 2017) 75-100.
6. C.J.B. de Castilho, M.E. Fuller, A. Same and J.T.C. Liu, Nanofluid flow and heat transfer in boundary layers: the influence of concentration diffusion on heat transfer enhancement, *Journal of Heat Transfer Engineering* (accepted for publication, 2017).
7. P.A. Lagerstrom, *Laminar Flow Theory*, Princeton University Press, Princeton, N.J., 1996.
8. A. Einstein, On the motion of small particles suspended in liquids at rest required by the molecular-kinetic theory of heat, *Annalen der Physik* 17 (1905) 549-560.
9. G. Puliti, *Properties of Gold-Water Nanofluids Using Molecular Dynamics*, Ph.D. Thesis, Univ. Notre Dame, 2012.
10. G. Puliti, S. Paolucci and M. Sen, Thermodynamics of gold-water nanofluids using molecular dynamics, *J. Nanoparticle Research* 14 (2012), article no. 1296.
11. S. Paolucci and G. Puliti, Properties of nanofluids, in *Heat Transfer Enhancement with Nanofluids*, Eds., Bianco, V., Manca, O., Nardini, S. and Vafai, K., pp.1-44, CRC Press, New York, 2015.
12. H. Schlichting, *Boundary Layer Theory*, 7th edition (Translated by J. Kestin), McGraw-Hill, New York, 1979.

TAILORING THE PROPERTIES OF NANOPARTICLES BY ALD NANOCOATINGS

D. Valdesueiro*, A. Goulas and B. van Limpt

Delft IMP B.V., Molengraaffsingel 10, 2629 JD, Delft, The Netherlands

*Corresponding author: d.valdesueiro@delft-imp.nl

Keywords: Atomic layer deposition, nanoencapsulation, nanoparticles, nanocoatings

Introduction: In this paper we present a gas-phase coating technology, atomic layer deposition (ALD), that allows the deposition of nanometer-thin conformal coatings on a wide variety of particles. The versatility of ALD covers both the nature and size of the particles, as well as to the chemistry of the coating. For example, particles ranging from nanoparticles to particles of several hundreds of micrometers can be coated with this technique. Additionally, the nature of the substrate can be ceramic (e.g. Al_2O_3 , TiO_2 , SiO_2), metallic (Ti), and polymeric (powder coating paints), amongst many others. The nature of the coating can be also selected from metal oxides (Al_2O_3) or nitrides (e.g. AlN), pure metals (e.g. Pt), organic coatings and even inorganic-organic hybrid coatings [1]. These thin films can be also used for nanofluid applications, achieving an encapsulation of the nanoparticles comprising the nanofluids without interfering with their intrinsic heat properties.

ALD is a coating process that relies on a layer-by-layer growth mechanism in which the coating chemistry is split into two half-reactions. Each of these reactions is self-limiting, such that at most a monolayer of a compound can be deposited per cycle (Figure 1). In this way, we have full control over the coating thickness: the number of times that the alternating feed of the two precursors is repeated determines the thickness of the achieved coating [2].

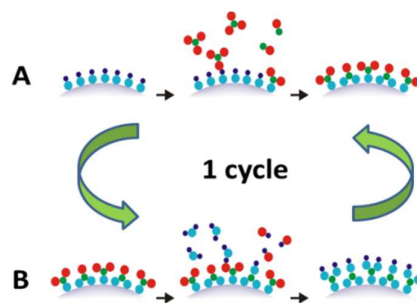


Figure 1. Reaction mechanism of one cycle of atomic layer deposition.

In recent years, atomic layer deposition (ALD) has become a standard tool to apply ultrathin and conformal coatings on substrates of complex geometries, mostly driven by an interest from semiconductor industry applications. The intrinsic advantages of controlling the structure growth at the (sub)nanometer level, while coating complex surfaces – either for providing

protection to the substrate or boosting its activity – are also relevant for other industrial applications related to particle technology, such as nanofluids.

In a nutshell, in this presentation we will also show two examples of the influence of nanometer-thin aluminium oxide films on two different applications that can be relevant in the development of nanofluids. One example shows the encapsulation of a polymer-based powder with nanometer-thin films, which confined the softened core material without altering the thermal properties. That can be of use with nanofluids based on phase change materials. The second example consisted of using an alumina layer to improve the affinity between an inert core and a radioactive isotope, to be used as tracer in hydrodynamic studies of concentrated solar plants. This application can be interesting in order to investigate the coating performance at elevated temperatures. A more detailed description is given below, aiming at incorporate this coating process as a potential technique to boost the industrial application of nanofluids.

Discussion and Results: The first example is the tuning of the surface finish of a standard polyester-based powder coating paint, from gloss to matt (Figure 2, left), by depositing ultrathin films of Al_2O_3 on the powder coating particles [3]. The coating experiments were performed in a fluidized bed reactor at 1 bar and 27 °C, using an alternating exposure of the particles to the two precursors (trimethylaluminium and water). By varying the number of coating cycles from 1 to 9, we deposited alumina films ranging from 1 to 30 nm. When the average alumina shell was thicker than 6 nm, the shell prevented the flow of the core particles, even though the powder particles did soften above their glass transition temperature. With the particles morphology intact, this resulted in a rough and matte surface finish of the coating after curing. Additionally, the alumina coating acted as a barrier able to encapsulate the softened powder coating above the glass transition temperature, without altering other thermal properties as such as the glass transition temperature (Figure 2, right). This type of application can be extended to the encapsulation of phase change materials with thin alumina films, that would contain a molten core without modifying the thermal properties, which is of crucial importance in the development of efficient nanofluids.

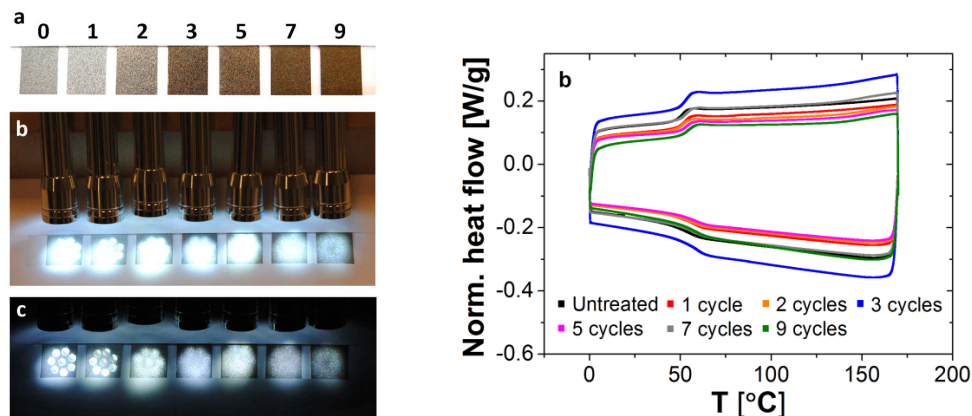


Figure 2. (left) Tuning of the surface finish of the paint from gloss to matte depending

on the thickness of the deposited aluminium oxide film. (right) Differential scanning calorimetry profiles of the uncoated and coated powder coating samples.

The other example that we will show in the presentation is the enhanced radio-activation efficiency of SiC (silicon carbide) particles to be employed as tracers in studies using PEPT (Positron Emission Particle Tracking) for the development of concentrated solar plants [4].

SiC particles have by nature a poor affinity towards ^{18}F ions, normally used as radio-active ion. To overcome that, $\gamma\text{-Al}_2\text{O}_3$ particles are used as tracers due to their good activation efficiency. However, using a different particle as tracer might induce a change in the hydrodynamic behaviour of the tracer due to mismatches in geometry, density or particle size with the particles used as heat transfer fluid. To overcome that, we coated SiC particles with aluminium oxide. The resulting SiC- Al_2O_3 core-shell structure shows a good labelling efficiency, comparable to $\gamma\text{-Al}_2\text{O}_3$ tracer particles (Figure 3, left).

The thickness of the alumina films, which ranged from 5 to 500 nm, was measured by elemental analysis and confirmed with FIB-TEM (focus ion beam – transmission electron microscope), obtaining consistent results from both techniques. By depositing such a thin film of alumina, properties that influence the hydrodynamic behaviour of the SiC particles, such as size, shape and density, are hardly altered, ensuring that the tracer particle shows the same flow behaviour as the other particles (Figure 3, right). The thin alumina coatings applied to study a heat transfer fluid used in concentrated solar plants can be also used within a similar context in nanofluids that have to resist elevated temperatures. This example of a coated SiC opens the possibility to investigate how these materials can perform at more demanding temperatures.

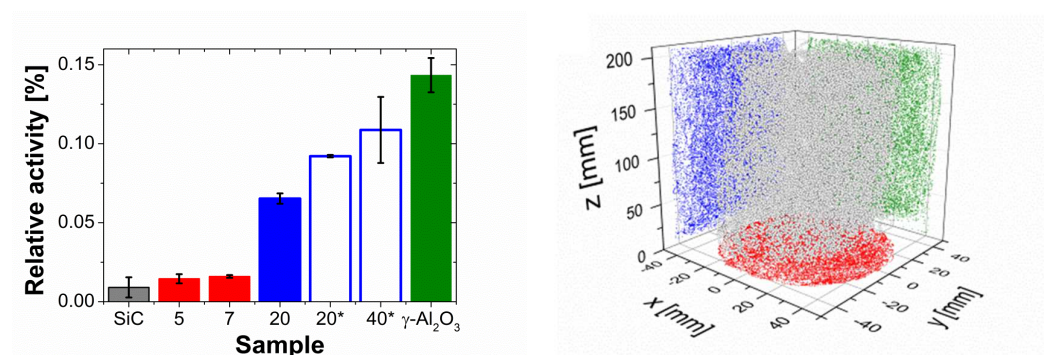


Figure 3. (left) Activation efficiency of the uncoated and alumina-coated SiC particles, and $\gamma\text{-Al}_2\text{O}_3$ particles, normally used as tracers. (right) Trajectory of the alumina coated-SiC tracer during a PEPT experiment.

Conclusions: In this presentation we will show the process of depositing ultrathin films on particles with the coating technique atomic layer deposition, and will present two examples on how the performance of a material can be tuned without altering other physical properties such

as density, heat capacity, shape or size. Additionally, we will explain how the coating process works, and what can be further done with this versatile technique, aiming at a scaled up process able to produce coated particles at industrially relevant volumes. Finally, we will discuss how this technique could contribute to the development of new nanofluids. This technique can be interesting for this emerging application, since from other fields it has been proven that ultrathin films can enhance the performance of other materials, perhaps applications for nanofluids being the next one.

References.

1. Miikkulainen, V., et al., Crystallinity of inorganic films grown by atomic layer deposition: Overview and general trends. *Journal of Applied Physics*, 2013. 113(2): p. 1-101.
2. George, S.M., Atomic layer deposition: An overview. *Chemical Reviews*, 2010. 110(1): p. 111-131.
3. Valdesueiro, D.H., H, et al., Tuning roughness and gloss of powder coating paint by encapsulating the coating particles with thin Al₂O₃ films. Submitted for publication, 2017.
4. Valdesueiro, D., et al., Enhancing the activation of silicon carbide tracer particles for PEPT applications using gas-phase deposition of alumina at room temperature and atmospheric pressure. *Nuclear Instruments and Methods in Physics Research, Section A: Accelerators, Spectrometers, Detectors and Associated Equipment*, 2016. 807: p. 108-113.

ENVIRONMENTAL ASSESSMENT OF ADVANCED HEAT MANAGEMENT SOLUTIONS

J. Krupanek^{1*}, B. Michaliszyn¹, Ł. Lelek² and J. Kulczycka²

¹Instytut Ekologii Terenów Uprzemysłowych, Kossutha 6 st., 40-844 Katowice, Poland

²Instytut Gospodarki Surowcami Mineralnymi i Energią PAN, ul. Wybickiego 7A, 31-261 Kraków, Poland

*Corresponding author: j.krupanek@ietu.pl

Keywords: Life Cycle Perspective, environmental assessment, heat evacuation, Metal Matrix Composites, carbon materials

Introduction:

For heat management there are used many solutions in the electronic and automotive industries, based on metal materials including copper and aluminium. To improve the performance a wide range of solutions based on nanomaterials is researched including Metal Matrix Composites and Nanofluids.

It is expected that improved thermal management can give new technological opportunities and environmental benefits. Higher utilization of advanced materials can improve performance without increasing the costs. At the same time consumption of raw materials and energy can decrease and waste generation during processing, manufacturing and/or dismantling phases can be reduced. To explore a full potential of the novelty solutions they should be developed with respect to Life Cycle environmental performance of their final applications taking into consideration their environmental efficiency, impacts, risks and waste management issues.

Approaches of integrating various aspects of environmental assessment of innovative heat management solutions are being advanced in relevant research projects [1,2]. As an example an integrative approach to environmental assessment was applied in the project Smart Thermal conductive Al MMCs by casting – THERMACO funded by the European Union 7th Framework Program which aim was to develop Metal Matrix Composites based on metal structures (aluminium) and carbon crystalline forms (Thermal Pyrolytic Graphite, Graphene, diamonds) characterised with high heat conductivity.

Discussion and Results:

Life Cycle Assessment - LCA was the key method used in the study accompanied by Environmental Impact Assessment including assessment of health risk and analysis of waste management requirements. LCA is a tool quantifying impact on the environment in a holistic an established procedure [3], standardised according to PN-EN ISO 14040:2009 LCA [4].

Purpose of the LCA study in the Thermaco project was to assess the environmental performance of the new Al-MMC materials with respect to current heat evacuation solutions based on copper and to analyse various production paths to find those having the lowest environmental impact. It took into consideration all the aspects, direct and indirect, that could potentially affect the environment and are associated with the innovative heat management options.

The analysis of innovative solutions in the Life Cycle Perspective was performed in a tiered approach:

- Screening of predefined composite material combinations in Life Cycle perspective including assessment of the production processes of basic (aluminium, copper) and carbon materials. It was accompanied with assessment of environmental impact and health risks related to releases to the environment of the carbon materials during their life cycle,
- Comparative assessment in Life Cycle perspective of the designed functional materials and component demonstrators taking into account real data from the technical experiments carried out in the project and considering technologies of their production. It was accompanied with assessment of environmental impacts generated in the production of the MMC materials and components with identification and quantification of emissions to the environment, analysis of abatement measures, wastes generation and their appropriate utilisation and analysis of occupational health hazards,
- Comparative assessment of the designed demonstrators of functional components intended for energy and automotive industries and prospected basic scenarios of their application in final products. They were assessed in the full Life Cycle perspective with identification and evaluation of potential environmental benefits such as: reduced weight of the components, reduced waste generation or energy savings. It included evaluation of their potential environmental performance during consumption phase. Moreover an extensive prognosis of the waste management requirements in post-consumption phase with analysis of utilisation options was performed and the results were integrated in the LCA assessment.

A data set of inputs and outputs LCI (Life Cycle Inventory) was prepared with preparation of the balance sheet, identification and calculation for functional units representing the analysed system, the elements coming out from the environment and the elements going out of the system to environment (e.g. CO₂ emissions to air, emissions to water etc.) [5]. It was done basing on technical expert knowledge, literature data, analyses and simplified modelling of the technological processes, and using of EcoInvent 2.2 database. Life Cycle perspective of the functional components is presented in figure 1.

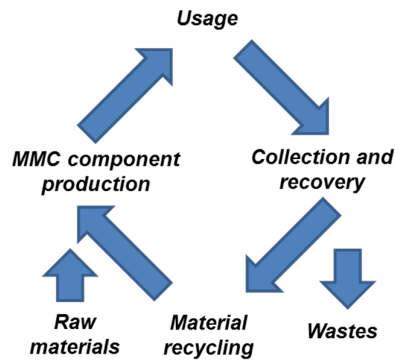


Figure 1. Life Cycle Perspective of Al-MMC materials

In the final stage of the LCA, the impact categories and characterizing models were defined. The aggregate potential impact on the environment was estimated and quantified taking into account the impact on all components of the environment (i.e. output: emissions to water, air, waste, etc.) and also the consumption of resources (i.e. inputs: materials and energy) throughout the life cycle. The environmental performance of the innovative solutions was compared based on cumulated eco-indicator (Figure 2). It referred to the results of current state or a fixed level (benchmarking) resulting from the currently used criteria of assessing the efficiency of environmental performance.

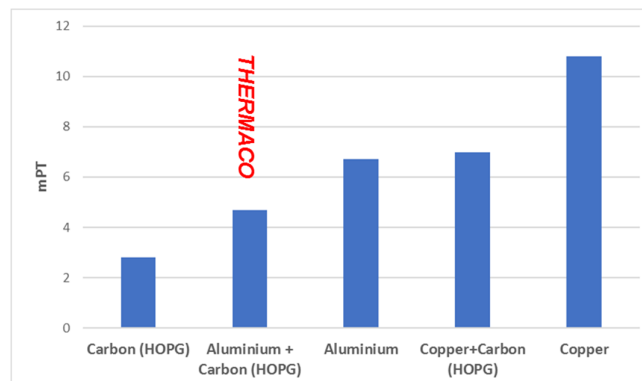


Figure 2. Examples of Life Cycle environmental impact of heat management materials

Summary:

Results of the overall Environmental Assessment of the materials and functional components studied in the project were used as the base for the decision process in field of development and application of new technology solution or modernization of existing products.

It was found out that environmental impacts are related predominantly to production of basic materials (especially carbon materials) used in manufacturing of Thermaco composites. Thus, it is very important to well account for environmental benefits during the use phase of the materials

which can outbalance environmental costs of manufacturing processes: less material used for production, lighter vehicles.

The main achievements of the study in the scope of assessing environmental aspects of the innovative heat management solutions were:

- New knowledge and competences developed by research and industrial partners,
- Recommendations for design of the materials and their applications in products
- Tailoring and optimisation of production processes,
- Recommendations for raising benefits in consumption phase,
- Defining requirements for dismantling of products and processing of waste material in post-consumption phase.
- Directions of future research regarding heat evacuation solutions.

References:

1. A. Jovanovic, M. Cordella, *Life cycle assessment (LCA)&Risk Analysis in nanomaterials related NMP projects*, Information booklet, Specialist Brainstroming and Coordination Meeting March 2, Brussels (Belgium), 2011
2. G. Barbiero, S. Scalbi, P. Buttol, P. Masoni, S. Righi, *Combining life cycle assessment and qualitative risk assessment: The case study of alumina nanofluid production*, Science of The Total Environment, Vol. 496, 2014 pp 122-131.
3. Z. Kowalski, J. Kulczycka, M. Góralczyk, *Ekologiczna ocena cyklu życia procesów wytwórczych*, PWN, Warszawa 2007.
4. JB Guinée, M. Gorrée, R. Heijungs, G. Huppes, R. Kleijn, L. van Oers, A. Wegener Sleswijk, S. Suh, U. de Haes, H. de Bruijn, R. van Duin and MAJ. Huijbregts *Life Cycle Assessment: An Operational Guide to the ISO Standards*. Kluwer Academic Publishers, Dordrecht, The Netherlands, 2002.
5. O. Jolliet, A. Brent, M. Goedkoop, N. Itsubo, R. Mueller-Wenk, C. Peña, R. Schenk, M. Stewart, B. Weidema: *LCIA Definition Study of the SETAC-UNEP Life Cycle Initiative*. UNEP, 2003.

GRAPHENE NANOFLUIDS – NEW AND INTERESTING RESULTS IN A SOLAR THERMAL COLLECTOR

F.E.B. Bioucas, S. Vieira, M.J.V. Lourenço*, F.J.V. Santos and C.A. Nieto de Castro

Centro de Química Estrutural, Faculdade de Ciências da Universidade de Lisboa

Campo Grande, 1749-016 Lisboa, Portugal

*Corresponding author: mjlourenco@ciencias.ulisboa.pt

Keywords: Nanofluid, Heat Transfer Fluid, Solar Thermal Collector, Graphene

Introduction: A solar thermal collector can be optimized in different aspects, such as the use of a better insulation material to reduce the heat losses, a better absorber with a better specific coating (2), or a better heat transfer fluid. Heat transfer fluids based on water and ethyleneglicol are widely known and used in typical solar collectors. Our intention is to improve the heat transfer efficiency of a heat transfer fluid composed of water and ethyleneglicol with graphene, creating a pumpable nanofluid which could be used industrially. A second purpose is to achieve equilibrium between cost/efficiency without retrofitting.

Experimental/Theoretical Study:

Solar collector: The solar collector was bought from PHYWE company, but several modifications were made. In Figure 1 the schematic of our solar. In this work, we measured the temperature at four different points: cold current entering the collector (A), hot outlet current leaving the collector (B), the temperature of the water bath (C) and the ambient temperature. We also used a gear pump, a magnetic flow meter to measure the flow velocity, and a flow regulator valve to adjust the flow.

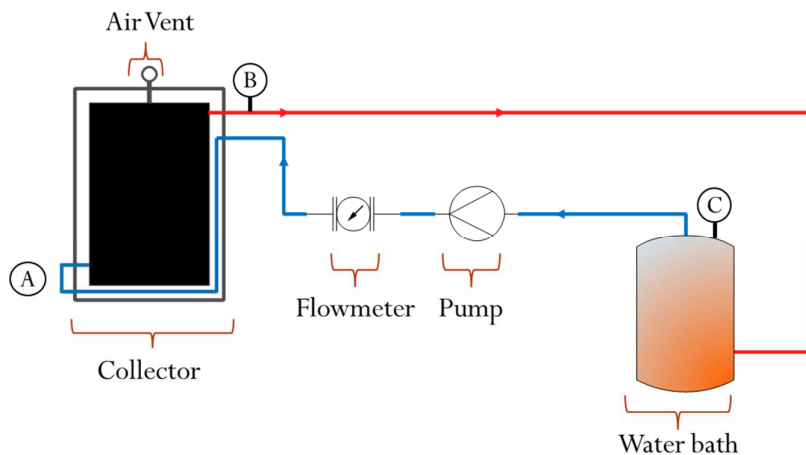


Figure 1: Schematic of the solar collector unit.

Heat transfer fluid: The nanofluids were prepared in a two-step process: first the base fluid was prepared and then the graphene was added to the base fluid and sonicated with Hielscher UP200HT with a probe S26d40 at amplitude of 50%, a pulse cycle of 50% and a frequency of 25 ± 1 Hz for three minutes.

The graphene used in this experiment was obtained from Skyspring Nanopowder and Nanoparticles (US), the graphene has a thickness of 6 – 8 nm and an average particle diameter of 15 μm .

Tests: In this work two different tests were performed and the parameters of each tests are present in table I. In Test I, the base fluid and the three nanofluids were tested inside our laboratory using a halogen lamp with 1000 W of power to simulate the sun radiation. This test was performed in order to have the same exact conditions for each fluid, and in fact we were able to have the same ambient temperature, we didn't have the influence of the atmospheric conditions (wind, clouds, variation of the ambient temperature) and we were also able to start all the experiments at the same temperature. The projector was only turned on when the difference between the inlet and outlet temperature was below 0.2 °C.

In the second test, Test II, we used the heat transfer fluid that showed the best and worst performance and tested them in a real situation: outside with the solar radiation and the influence of the atmospheric conditions. Two tests were performed for each HTF at similar atmospheric conditions; the results present in this paper are the average of these values. The solar collector was covered with an insulation blanket, when the difference between the temperature of the inlet and outlet were below 1.0°C the blanket was removed.

Table 1: Experimental parameters of Test I and Test II.

	Test I - Halogen Lamp	Test II – Solar radiation
Radiation Source	Halogen lamp (1000 W)	Sun (800 – 950 W)
Distance to light source	0.65 m	-
Tilt	90 °	30 °
Flow velocity	100±10 ml/min	
Water heater volume	1,8 l	
Test duration	200 min	120 min
Influence of atmospheric conditions	None	Wind, Clouds and $\Delta T_{\text{exterior}}$

Discussion and Results:

Test I: From figure 2, which shows the outlet temperature of the heat transfer fluid, it is possible to conclude that with the higher concentration of graphene one can achieve a higher temperature than the base fluid (with a difference of 1.8°C). Identical results were observed for the inlet current (3.0°C), and for the water bath (1.2°C).

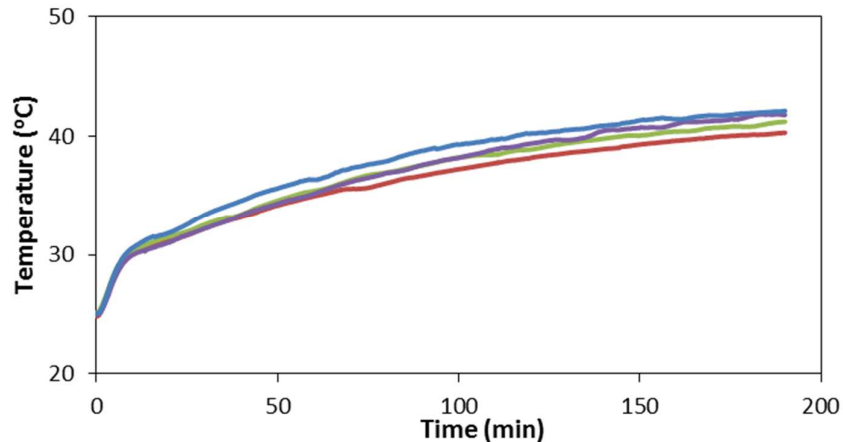


Figure 2: Temperature of the outlet current in function of time, — base fluid, — base fluid with 0.05 wt% graphene, — base fluid with 0.08 wt% of graphene and — base fluid with 0,10 wt% of graphene.

Test II: The second test was performed outside and thus all the measurements were influenced by the atmospheric conditions such wind, clouds and the variation of the ambient temperature, oscillating between 30 and 38°C . The base fluid and the base fluid with 0.10 wt% of graphene were tested, two tests were performed for each heat transfer fluid in similar atmospheric conditions. In figure 3 the efficiency of the two fluids is presented. It is possible to see that there is an oscillation in the data, which derive from the influence of the atmospheric conditions. From the figure 3 it is also visible that the base fluid with 0.10 wt% of graphene has a higher efficiency than the base fluid, as the base fluid has average efficiency of 54.66% and the nanofluid has an efficiency of $60,56\%$.

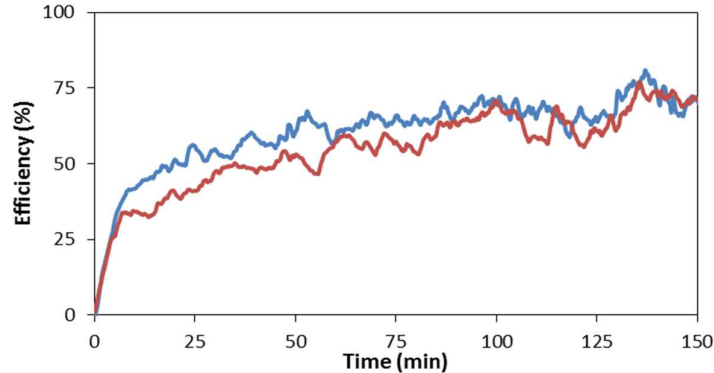


Figure 3: Efficiency of the solar collector, — base fluid and — base fluid with 0.10 wt% of graphene.

Conclusions: The current work shows that graphene can be used on a solar collector in order to improve the efficiency. In a controlled environment, the heat transfer fluid with graphene achieved a higher temperature in the outlet and inlet currents as well as in the water bath. An increase of 5.9% in efficiency is achieved in comparison with the base fluid.. Although these results show a possible use of graphene in a commercial solar thermal collector further studies are necessary. In this paper the experiment was performed in short periods of time (maximum of 3h), in the future these periods should be increased to a week in order to understand the full behavior of this system. Furthermore, we intend to integrate a dynamic light scattering technique in order to know the real concentration of the graphene in the heat transfer fluid, since it becomes attached to the wall, lowering the initial concentration flowing in the solar collector.

References:

1. S.M.S. Murshed and C.A. Nieto de Castro, Conduction and convection heat transfer characteristics of ethylene glycol based nanofluids – A reviews, *Applied Energy* 184(2016) 681–695.
2. S. Vieira, *PhD Thesis*, Universidade de Lisboa (2015).

Magnetic nanofluids for electric power engineering applications

M. Rajnak^{1,3}, M. Timko^{1*}, P. Kopcansky¹, T. Tobias¹, K. Paulovicova¹, J. Kuchta², M. Franko², J. Kurimsky³, B. Dolnik³, R. Cimbala³

¹Institute of Experimental Physics SAS, Watsonova 47, 04001 Košice, Slovakia

²Electrotechnical research and projecting company, Trenčianska 19
018 51 Nová Dubnica, Slovakia

³Faculty of Electrical Engineering and Informatics, Technical University of Košice, Letná 9,
04200 Košice, Slovakia

*Corresponding author: timko@saske.sk

Keywords: transformer oil, iron oxide nanoparticles, transformer, cooling.

Introduction/Background: The increasing global electric power consumption and related demands on reliability and performance of insulating and cooling materials have stimulated intensive research on novel cooling and insulating media in power systems. In the process of electric power transmission and distribution, the transformers play a key role. On the other hand, these electrical devices have been statistically found as the most critical part of an electric power network [1]. The regions of intense temperature between the transformer's core and windings and between the windings cause degradation of the winding insulation as well as the conductive components of the transformer. One of the important materials providing the proper function, reliability and protection of the transformers is transformer oil which is often based on mineral oil [2]. The primary function of the transformer oil is to insulate and cool a transformer. It must therefore have high dielectric strength, thermal conductivity, and chemical stability. However, to cope with the increasing demand of future high voltage networks and small size of transformers, the development of more effective cooling and insulating liquid medium is extensively required. In the last years, the transformer oil based nanofluids have been produced to meet the necessary attributes [1].

One of the dielectric and cooling nanofluids intensively investigated as a potential replacement of the transformer oil is the magnetic nanofluid (ferrofluid) based on transformer oil [3–5]. Besides the increased thermal conductivity, the cooling by magnetic nanofluid relies on thermomagnetic convection [6]. This refers to a convective heat transfer that makes use of the spatial gradient in the magnetic susceptibility of the nanofluid that is produced in the presence of a temperature gradient. When a magnetic fluid is exposed to a non-uniform magnetic field in the presence of a temperature field, besides convectional gravitational body force, the varying susceptibilities result in a non-uniform magnetic body force. In other words, as the heat load increases, the magnetization of the magnetic nanofluid decreases, leading to the increase in the nanofluid flow velocity and consequently, faster heat transfer from the heat

source [7]. The thermomagnetic convection in various magnetic nanofluids and under different conditions was reported in numerous papers [8–10].

Surprisingly, the presence of magnetic nanoparticles in transformer oils can enhance not only the thermal transport properties of the oil, but have a positive impact on the dielectric breakdown field strength of the oil. This peculiar finding was reported for the first time in [4]. Moreover, it was also highlighted that the propagation velocity of the streamer is reduced due to the presence of the nanoparticles. Theoretical modeling demonstrated that this velocity reduction is a crucial phenomenon leading to the understanding of the higher breakdown field strength of the magnetic nanofluid [11]. However, complete comprehension of the breakdown mechanism requires further experimental and theoretical study.

In this paper, we report on the experimentally tested cooling effectiveness of a magnetic nanofluid applied in a specially designed transformer. The localized temperatures in various regions in the transformer are compared for two cases, when the cooling medium is the transformer oil and the magnetic nanofluid.

Discussion and Results: For the purpose of our investigation, we have designed a small model transformer T1N-5-400/230. When designing the transformer, the attention was paid to providing good conditions for the expected thermomagnetic convection in the magnetic nanofluid. Thus, in order to increase the stray magnetic field and create more space for the convection, the transformer with a gap between the primary and secondary winding and between the winding and the core was constructed. The model of the transformer is depicted in Fig. 1.

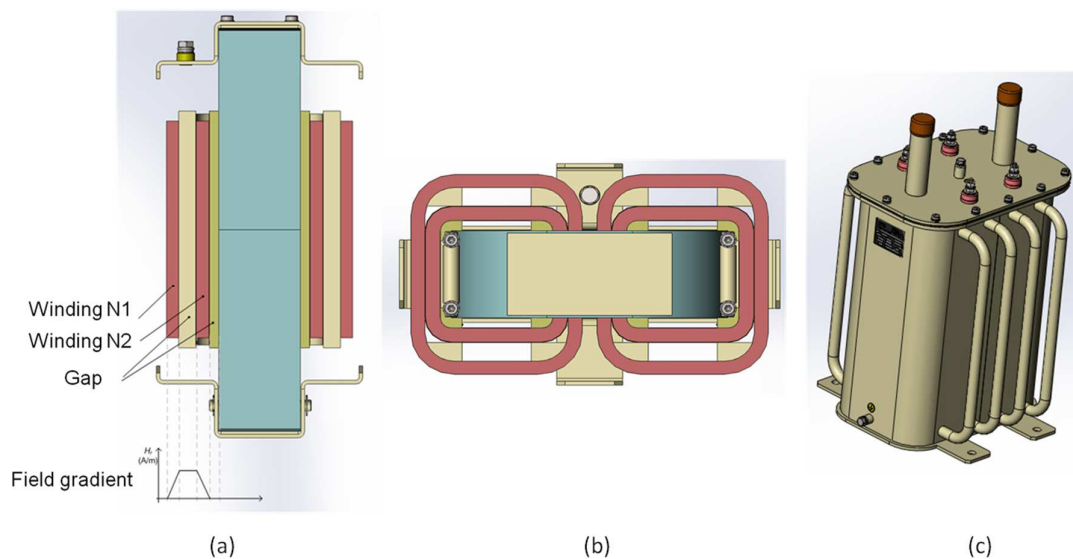


Fig. 1 The scheme of the model transformer used to test the cooling effectiveness of the magnetic nanofluid. (a) front view cross-section, (b) top view cross-section, (c) transformer tank.

The transformer was filled firstly with a commercial transformer oil Mogul Trafo CZ-A, and then with a magnetic nanofluid based on this oil and iron oxide nanoparticles. The basic physical parameters of the oil are as follows: the pour point of the oil is $-42\text{ }^{\circ}\text{C}$, the flash point is greater than $150\text{ }^{\circ}\text{C}$, the relative density is 870 kg/m^3 , and the viscosity at $40\text{ }^{\circ}\text{C}$ is $11\text{ mm}^2/\text{s}$, as provided by the manufacturer. The magnetic nanoparticles for the nanofluid were synthesized by the well-known chemical co-precipitation method [14] from aqueous solution of Fe^{2+} and Fe^{3+} ions in the presence of NH_4OH at $80\text{-}82\text{ }^{\circ}\text{C}$. The synthesized magnetite nanoparticles were covered with a single surfactant layer (vegetal oleic acid, $\text{C}_{18}\text{H}_{34}\text{O}_2$, 65-88%, Merk). The chemisorption was followed by the washing with distilled water with magnetic decantation to remove residual unreacted salts, followed by flocculation (acetone) to remove free surfactant. The purified magnetite nanoparticles were dispersed in the transformer oil. Finally, 6 liters of magnetic nanofluid were prepared for the experiment. The magnetic mass fraction (particle concentration) in the nanofluid was 2.85 %, as determined from magnetic measurements.

In order to compare the cooling ability of the transformer oil and the magnetic nanofluid, we performed the heating tests of the loaded transformer with an apparent power of 4.3 kVA. The temperature sensors monitoring the temperature evolution were located at various places within the transformer. In Table 1, the saturated temperature values are presented for the transformer filled with the pure oil and the nanofluid. The values were taken at the time when the transformer was 10 hours under the load.

	Lower shell	Upper shell	Core down	Core up	Winding down	Winding up	Coolant down	Coolant up
Pure oil, T ($^{\circ}\text{C}$)	70.2	71.58	53.12	56.07	56.35	34.71	48.6	68.15
Nanofluid T ($^{\circ}\text{C}$)	69.06	71.02	52.71	55.75	56.03	34.15	43.82	67.39
ΔT ($^{\circ}\text{C}$)	1.14	0.56	0.41	0.32	0.32	0.57	4.78	0.78

Table 1 Comparison of the cooling effect of the transformer oil and the magnetic nanofluid in the model transformer T1N-5-400/230.

As one can see from Table 1, the temperature of the loaded transformer at various locations is lower when the transformer is filled with the magnetic nanofluid. The greatest temperature difference was found when measuring the coolant temperature at the bottom of the transformer shell. The average transformer temperature difference is $1.05\text{ }^{\circ}\text{C}$ in favour of the magnetic nanofluid. This cooling enhancement is associated with the increased thermal conductivity of the

transformer oil due to the presence of the nanoparticles. It is known that the large surface area of the nanoparticles allows for more heat transfer. Besides the effective thermal interaction of the nanoparticles, the high mobility of the nanoparticles, attributable to the nanosize, leads to the enhanced thermal transport properties too. The particle movement may bring about micro-convection of the magnetic nanofluid and hence increase the heat transfer. Moreover, owing to the created gaps between the windings and the core, the stray magnetic field and temperature gradients give rise to the thermomagnetic convection of the nanofluid, intensifying so the heat transfer. It is worth to notice that according to the laws of insulation aging it is clear that the lower the temperature, the slower the insulation deterioration. Thus, lowering the operating temperature of the transformer by using the magnetic nanofluid can result in the higher loadability and longer service life of the transformer.

Summary/Conclusions: In this study we have tested the cooling effect of a magnetic nanofluid based on transformer oil and iron oxide nanoparticles. The tests were carried out in a model transformer with the apparent power of 4.3 kVA. It was found that the transformer temperature is lower in the case when filled with the magnetic nanofluid instead of the transformer oil. The average temperature difference is 1.05 °C. This effect stems from the enhanced thermal transport properties of the transformer oil due to the presence of magnetic nanoparticles and induced thermomagnetic convection in the gap between the transformer windings and the core.

This work was supported by the Slovak Academy of Sciences and Ministry of Education in the framework of projects VEGA Nos. 2/0141/16, 2/0016/17 and 1/0311/15, Ministry of Education Agency for structural funds of EU Project Nos. 26220120033 and 26220120003, COST CA15119NANOUP TAKE, ITMS: 313011D232, and Slovak Research and Development Agency under the Contract No. APVV-15-0438 and APVV-15-0453 (M-Vision).

References:

- [1] M. Rafiq, Y. Lv, C. Li, M. Rafiq, Y. Lv, and C. Li, "A Review on Properties, Opportunities, and Challenges of Transformer Oil-Based Nanofluids, A Review on Properties, Opportunities, and Challenges of Transformer Oil-Based Nanofluids," *J. Nanomater. J. Nanomater.*, vol. 2016, 2016, p. e8371560, Jul. 2016.
- [2] R. Bartnikas, *Electrical Insulating Liquids*. Philadelphia, PA: Astm Intl, 1994.
- [3] J.-C. Lee, H.-S. Seo, and Y.-J. Kim, "The increased dielectric breakdown voltage of transformer oil-based nanofluids by an external magnetic field," *Int. J. Therm. Sci.*, vol. 62, pp. 29–33, Dec. 2012.
- [4] V. Segal, A. Hjortsberg, A. Rabinovich, D. Nattrass, and K. Raj, "AC (60 Hz) and impulse breakdown strength of a colloidal fluid based on transformer oil and magnetite nanoparticles," in *Conference Record of the 1998 IEEE International Symposium on Electrical Insulation, 1998*, 1998, vol. 2, pp. 619–622 vol.2.

- [5] K. Raj and R. Moskowitz, "Ferrofluid-cooled electromagnetic device and improved cooling method," US5462685 A, 31-Oct-1995.
- [6] I. Nkurikiyimfura, Y. Wang, and Z. Pan, "Heat transfer enhancement by magnetic nanofluids—A review," *Renew. Sustain. Energy Rev.*, vol. 21, pp. 548–561, May 2013.
- [7] V. Chaudhary, Z. Wang, A. Ray, I. Sridhar, and R. V. Ramanujan, "Self pumping magnetic cooling," *J. Phys. Appl. Phys.*, vol. 50, no. 3, p. 03LT03, 2017.
- [8] A. Lange, "Thermomagnetic convection of magnetic fluids in a cylindrical geometry," *Phys. Fluids*, vol. 14, no. 7, pp. 2059–2064, May 2002.
- [9] H. Rahman and S. A. Suslov, "Thermomagnetic convection in a layer of ferrofluid placed in a uniform oblique external magnetic field," *J. Fluid Mech.*, vol. 764, pp. 316–348, Feb. 2015.
- [10] A. Lange and S. Odenbach, "Patterns of thermomagnetic convection in magnetic fluids subjected to spatially modulated magnetic fields," *Phys. Rev. E*, vol. 83, no. 6, p. 066305, Jun. 2011.
- [11] J. G. Hwang, M. Zahn, F. M. O'Sullivan, L. A. A. Pettersson, O. Hjortstam, and R. Liu, "Effects of nanoparticle charging on streamer development in transformer oil-based nanofluids," *J. Appl. Phys.*, vol. 107, no. 1, p. 014310, Jan. 2010.
- [12] L. Vékás, M. V. Avdeev, and D. Bica, "Magnetic Nanofluids: Synthesis and Structure," in *NanoScience in Biomedicine*, D. Shi, Ed. Berlin, Heidelberg: Springer Berlin Heidelberg, 2009, pp. 650–728.

END